Technical Memorandum 104822

Advanced Active Thermal Control Systems Architecture Study

A. J. Hanford, Ph.D., and M. K. Ewert

October 1996

Advanced Active Thermal Control Systems Architecture Study

A. J. Hanford, Ph.D.
Lockheed Martin Engineering and Science Services
Houston, Texas 77058

and

M. K. Ewert
Lyndon B. Johnson Space Center
National Aeronautics and Space Administration
Houston, Texas 77058

October 1996

ACKNOWLEDGMENTS

TABLE OF CONTENTS

NOMENCLATURE

Item	Definition
ABS	ammonia boiler subsystem
ATCS	active thermal control system (ITCS plus ETCS)
COP	coefficient of performance
DCSU	dc switching unit
DDCU	dc-to-dc converter unit
DDCU-E	external DDCU
ETCS	external thermal control system
FCA	flow control assembly
FES	flash evaporator subsystem
FLO	First Lunar Outpost
GSE	ground support equipment
GSE HX	ground support equipment heat exchanger
H_2O	water
ISS	International Space Station
ITCS	internal thermal control system
low alpha	low solar absorptivity
LP	low-power
LTL	low temperature loop
LVS	Loral Vought Systems
MBSU	main bus switching unit
ML	Mars Lander
MP/S	mechanical pump/separator
MTL	moderate temperature loop
N_2	nitrogen (elemental)
NASA	National Aeronautics and Space Administration
NH_3	ammonia (R717)
O_2	oxygen (elemental)
ORU	orbital replacement unit
P0	a proposed segment to be added to ISS as part of the baseline ISS evolution mission to support additional radiator ORUs
PCM	phase-change material
PLB	Permanent Lunar Base

Item	Definition
PV-TCS	thermal control system for photovoltaic power arrays
radiating area	the total surface area of a radiator through which heat is rejected, equal to the plan or projected area for a single-sided radiator (for example, a horizontal radiator mounted on a planetary surface), and equal to twice the plan or projected area for a two-sided radiator (for example, the ATCS radiator panels on ISS's radiator ORUs or a vertical radiator)
S0	base truss segment for U.S.-led portion of ISS
S1, P1	Truss segments outboard to either side of Segment S0 on ISS, to which the TRRJs and the structure supporting the radiator ORUs attach directly. "S" designates a starboard segment while "P" designates a port segment.
S4, S6, P4, P6	segments outboard of the solar alpha rotary joints (Segments S3 and P3) on ISS which support the solar photovoltaic power arrays
Shuttle	an alternate name for Space Transportation System
SINDA/FLUINT	Systems Improved Numerical Differencing Analyzer and Fluid Integrator, a thermal and fluid analysis package which uses a network analysis approach. This program was prepared under a contract from NASA Lyndon B. Johnson Space Center. Cullimore and Ring Technologies, Inc., continues to distribute and support this product.
STS	Space Transportation System (which is often called "Shuttle")
STS-41	Space Transportation System Mission 41 (Discovery, October 6 to 10, 1990)
TCS	thermal control system
TRL	technology readiness level
TRRJ	thermal radiator rotary joint
TSS	Thermal Synthesizer System, a thermal analysis package for space systems. This program was developed by Lockheed Missiles and Space Company, Inc. of Sunnyvale, California under a contract from NASA Lyndon B. Johnson Space Center. Currently TSS is maintained and supported by Lockheed Martin Engineering and Science Services of Houston, Texas.
VPGC	Variable Pressure Growth Chamber, also known as the Johnson Space Center 10-foot Regenerative Life Support Systems Test Chamber
Z-93	a radiator surface coating

ADVANCED ACTIVE THERMAL CONTROL SYSTEMS ARCHITECTURE STUDY

SUMMARY

STUDY OBJECTIVE

The study which follows quantifies potential mass savings offered by various technologies and identifies promising development initiatives for advanced thermal control systems. This, in turn, provides a common basis to compare many diverse technologies.

Assessments are presented for five reference missions considered to be likely candidates for major human space flight initiatives beyond the assembly of International Space Station. These include:

- International Space Station Evolution
- Space Transportation System Upgrade
- First Lunar Outpost Lander
- Permanent Lunar Base
- Mars Lander

The objective of this study is to estimate potential benefits for various proposed and under-development thermal control technologies for possible human missions early in the next century. Twenty advanced thermal technologies currently under various stages of development by the National Aeronautics and Space Administration (NASA) were applied to the reference missions. These technologies represent a host of potential advanced thermal control system architectures. As research and development progress and mission planning and equipment mature, this study can be revised and extended to include new data as well as additional technologies and mission scenarios.

STUDY METHODOLOGY

The study format compares all technologies to baseline missions using mass as a basis. Power consumption is included directly by converting it to an equivalent mass using a mission appropriate power mass penalty. Qualitative ratings are presented for each advanced thermal control technology. The qualitative ratings allow other considerations, besides mass, to be included in the technology assessments. The qualitative rating process is fully described in Section 1.0 and the qualitative ratings are presented in Section 2.0.

Primary Assessments:

- equipment mass savings
- power savings
- power converted to mass
- overall mass savings
  (including equipment and power)

Qualitative Assessments:

- volume
- ease of deployment or installation
- reliability
- development cost
- terrestrial use potential

Table 5.1 within this report gives a complete summary of mass savings while Table 2.1 provides a summary of qualitative ratings for each advanced thermal control technology.

Each baseline architecture uses single-phase flow loops to transport waste heat from collection sites to rejection devices. More specifically, the baseline architecture assumes:

- Heat exchangers collect heat and transfer it to flow loops.

- The internal thermal control system collects heat from the cabin occupied by humans. This heat is rejected to the external thermal control system. The internal thermal control system working fluid is single-phase water.

- The external thermal control system collects heat from the internal thermal control system and other payloads outside the cabin. This heat load is rejected to the environment. The external thermal control system working fluid is a single-phase refrigerant. For redundancy, there are at least two external thermal control system flow loops in each architecture.

- The heat-rejection devices assumed in the baseline architecture are aluminum, flow-through radiators.

This configuration is common to spacecraft currently in service. Advanced technologies are defined as "not used on previous or current human vehicles." The technologies considered as advanced include:

- two-phase thermal control systems
- lightweight radiators
- phase-change thermal storage
- rotary fluid coupler
- carbon brush heat exchanger
- heat pipes
- heat pumps
- radiator shades
- plant chamber cooling improvements

These technologies, including several variations, were all compared to the baseline system for each mission individually without combining them. It is expected that combining some technologies with others will yield additional savings. Such combinations, however, were not considered in this initial study. The criteria used to pare the advanced technology list for each mission were availability of information, practicality and mission suitability, and engineering judgment. Certain technologies apply to only certain environments or missions, while other technologies are more generally applicable over a wider range of missions.

Because the study format compares various architectures with a commonly defined baseline, it is versatile and expandable. When better information becomes available, the affected portions of the study can be readily updated without redoing the entire effort. Further, missions and technologies, including combinations of technologies, can also be added without disrupting the overall study.

BASELINE MISSION DEFINITION

- **International Space Station Evolution**

This study assumes that the current International Space Station thermal control system orbital replacement units will need replacement and augmentation after project year 20, with an overall project design life of 30 years. The current external thermal control

system design uses six flow-through radiator orbital replacement units in two clusters. Due to micrometeoroid impacts, optical property degradation, and other failures, it is assumed that all six radiator orbital replacement units will be replaced. Further, it is assumed in year 20 International Space Station will be augmented with two solar dynamic power modules, increasing the onboard power supply of the U.S.-led portion to provide an additional 20 kW of user power. This does not include additional power which might be added for the thermal control system.

The baseline mission adds two additional radiator orbital replacement units to handle the increased heat load. Therefore, the baseline International Space Station evolution configuration would replace the original six radiator orbital replacement units mounted in two clusters of three units with new equipment and add one new cluster of two units. To mount the third cluster of two units, a hypothetical third truss segment is added in some unspecified manner.

- **Space Transportation System Upgrade**

This mission addresses upgrading the current Space Transportation System, or Shuttle, with new thermal control system components of the same or improved capabilities as those currently available. Alternatively, one might replace the current vehicles with new vehicles of similar capabilities. The external thermal control system working fluid is Freon 21. In addition to flow-through radiators, Shuttle uses evaporative cooling in both primary and secondary cooling equipment. On orbit, the radiators provide primary cooling while a flash evaporator provides secondary cooling by evaporating water and then rejecting the steam. On orbit, Shuttle rejects up to 39.5 kW of heat from its radiators and flash evaporator. A vehicle life of 140 missions (seven flights per year for 20 years) following upgrades is assumed. This basis of 140 missions could also refer to the total number of flights a fleet of vehicles might make over the life of the program. The mass savings are considered cumulative for the life of the vehicle(s).

- **First Lunar Outpost Lander**

The baseline First Lunar Outpost Lander thermal control system uses a low solar absorptivity, horizontal radiator with single-phase liquid ammonia as the working fluid. No additional cooling devices are presumed for surface operations. The radiator upper surface coating is silver Teflon, while the lower radiator surface is insulated to reduce heating by the lunar surface. The user heat load for the thermal control system is 16.0 kW with a mission length of up to 45 days. Two First Lunar Outpost Landers are assumed. The mass savings are considered cumulative for both vehicles.

- **Permanent Lunar Base**

One proposal for a Permanent Lunar Base would bury three modified Space Station modules beneath the lunar surface to provide living and working space continually for a crew of three or four. The base elements would include a habitation module, a laboratory module, and a plant growth module. The plant growth module would be an integral part of the base environmental control and life support system by replenishing atmospheric oxygen, removing carbon dioxide, and providing some food for the crew.

Power for the base would be supplied by solar photovoltaic power arrays with regenerative fuel cells for energy storage. Baseline thermal control system heat rejection would be accomplished through horizontal radiators with low solar absorptivity surface coatings. The thermal control working fluid is single-phase liquid ammonia. The overall thermal user load is 50 kW. Assessments for a single base at the equator with a project life of 15 years are presented.

- **Mars Lander**

This study concentrates on Mars Lander while it is situated on the martian surface for a 30-day stay. The vehicle will have both habitation and laboratory space for a crew of four. The baseline Mars Lander thermal control system uses low solar absorptivity, vertical radiators with single-phase liquid ammonia as the working fluid. The vehicle will land at the martian equator and generate an overall user heat load of 30 kW continuously. One mission is assumed.

ADVANCED TECHNOLOGIES

The advanced thermal control technologies may be grouped into several general categories based on functionality. Additionally, some of the technologies considered here can not be grouped with other technologies. These technologies are placed at the end of the list.

- Two-Phase Thermal Control Systems:
  - Two-Phase Thermal Control System With Mechanical Pump/Separator
  - Low-Power Two-Phase Thermal Control System
  - Two-Phase Thermal Control System With Electrohydrodynamic Pumping
  - Capillary Pumped Loops

- Heat Pumps:
  - Vapor Compression Heat Pump
  - Solar Vapor Compression Heat Pump [1]
  - Complex Compound Heat Pump
  - Zeolite Heat Pump

- Heat Pipe Radiators:
  - Arterial Heat Pipe Radiators
  - Arterial Heat Pipe Radiators With Electrohydrodynamic Pumping
  - Axial-Groove Heat Pipe Radiators

- Lightweight Radiators:
  - Composite Flow-Through Radiators
  - Composite Reflux Boiler Tube Radiators
  - Composite Heat Pipe Radiators
  - Unfurlable Radiators

---

[1]   This is also referred to as a vapor compression heat pump with a dedicated solar photovoltaic power array.

- Other Heat Rejection Technologies:
  - Phase-Change Thermal Storage
  - Parabolic Radiator Shade
- Additional Technologies:
  - Rotary Fluid Coupler
  - Plant Chamber Cooling Improvements
  - Carbon Brush Heat Exchanger

Two-phase thermal control systems utilize a vapor and liquid mixture, as opposed to a liquid, within the thermal control system flow loop. Upon returning from the heat-rejection device, the working fluid is a liquid. Upon collecting heat at various sites along the flow loop, the working fluid vaporizes. At the end of the flow loop the working fluid passes to the heat-rejection device and reliquefies. Thus, by using the latent heat of the working fluid more heat can be carried per mass of working fluid circulated.

Heat pumps increase the heat-rejection temperature, and thereby the rate of radiant heat rejection, at the expense of energy input. For mechanically driven heat pumps, the energy input is usually in the form of electricity to drive the compressor. For heat-driven heat pumps, the cycle requires an input of high temperature heat which can come as a by product of another process or may be generated specifically to drive the heat pump.

Heat pipes are passive, two-phase heat transfer devices. Heat is collected by evaporating the internal working fluid within the evaporator. The heat pipe rejects heat by condensing its working fluid in the condenser. The working fluid is pumped back to the evaporator by capillary forces acting along an internal slit or groove.

Lightweight radiators use composites and advanced material processing techniques to produced less massive radiator units. These technologies are unified through their dependence on common materials and processing techniques. The actual heat-rejection mechanisms vary among the different technologies. In this study, however, lightweight radiators were assessed a mass savings as a category rather than individually. The different technologies presented are examples of actual lightweight radiators.

Phase-change thermal storage melts a phase-change material to absorb and store heat. The stored heat may be rejected at a later time when the primary heat-rejection device is operating below its capacity.

A radiator shade reduces the effective temperature of the environment to which a heat-rejection device radiates. In particular, the parabolic radiator shade reflects direct solar irradiation away from a protected heat-rejection device and blocks infrared radiation from the planetary surface.

Several additional technologies are unrelated to those in the other categories. The rotary fluid coupler is a device which passes the thermal control system working fluid from a habitat or vehicle which is fixed to a radiator which rotates to maintain a particular thermal environment. Plant chamber cooling improvements include ideas to reduce the mass of the thermal control equipment within a plant growth chamber. Carbon brush heat exchangers use numerous carbon fibers to improve conductivity across evacuated gaps.

RESULTS

- ### International Space Station Evolution

The solar vapor compression heat pump displayed a mass savings of 32% compared with the baseline architecture. This option may be potentially the least disruptive to implement once International Space Station is fully operational. Lightweight radiators also offer significant mass savings. For this mission, composite flow-through radiators or composite heat pipe radiators may be appropriate. The two-phase thermal control systems appear to offer savings of almost 10% for this mission, but that may be within the range of uncertainty for this type of preliminary analysis. The other technologies, due to the uncertainty in the estimation procedures, produce systems which, in terms of mass, are probably similar to the baseline configuration. The enhancing technologies, listed here as additional technologies, can provide mass savings in their area of application regardless of the thermal control system architecture selected. Though these technologies yield small mass savings, they may offer other benefits which improve system reliability or overall operations.

Thermal Control System Mass Savings for International Space Station Evolution
Basis = 1 Upgrade:

	Mass [kg]	
Baseline External Thermal Control System [2]	15,600	
	Savings [kg]	Percent Savings
Heat Pumps		
Solar Vapor Compression	5,021	32
Vapor Compression	-250	-2
Lightweight Radiators	1,661	11
Two-Phase Thermal Control Systems		
Capillary Pumped Loops	1,535	10
Low-Power	1,366	9
With a Mechanical Pump/Separator	1,203	8
Additional Technologies		
Rotary Fluid Coupler	444	3
Carbon Brush Heat Exchanger	118	1
Heat Pipe Radiators		
Arterial with Electrohydrodynamic Pumps	427	3
Arterial Heat Pipes	-238	-2
Axial-Groove Heat Pipes	-309	-2

---

[2] This value does not represent the entire thermal control system mass for International Space Station. However, the omitted items, including the line masses, the line working fluid, and the pump masses, are similar for both the baseline architecture and each of the advanced technologies.

- ## Space Transportation System Upgrade

The Space Transportation System has a relatively small thermal control system mass. Each vehicle, however, is launched numerous times throughout its life. Thus, even small savings can be beneficial over the life of a vehicle. Reducing the mass of the radiators by using lightweight components may reduce overall thermal control system mass by 11%. Composite flow-through radiators appear to be most appropriate here. A low-power two-phase thermal control system or a phase-change thermal storage system will provide thermal control systems with masses similar to that of the baseline architecture. The phase-change thermal storage system, however, is an enhancing technology which can be added regardless of other improvements to the thermal control system.

Thermal Control System Mass Savings for Space Transportation System Upgrade
Basis = 140 Flights:

	Cumulative Mass [kg]	
Baseline External Thermal Control System [3]	201,000	
	Savings [kg]	Percent Savings
Lightweight Radiators	22,904	11
Phase-Change Thermal Storage	11,875	6
Low-Power Two-Phase Thermal Control System	8,176	4

---

[3]　This value does not represent the entire thermal control system mass for Space Transportation System. However, the omitted items are equivalent for both the baseline architecture and each of the advanced technologies.

- ### First Lunar Outpost Lander

For First Lunar Outpost Lander, the parabolic radiator shade displayed a mass savings of roughly 30% over the baseline architecture. Assuming that a lightweight, remotely-activated deployment scheme is developed, this technology is ideally suited for the lunar environment near the equator. Lightweight radiators yield a mass savings of about 28%. Any of the lightweight radiator technologies may be used, although those which require a vertical configuration may require shading or heat pumping to operate. Capillary pumped loops also provide a mass savings close to 20%. Both the low-power two-phase thermal control system and the solar vapor compression heat pump offer mass reductions of slightly more than 10%.

Thermal Control System Mass Savings for First Lunar Outpost Lander
Basis = 2 Missions:

	Cumulative Mass [kg]	
Baseline External Thermal Control System [4]	2,100	
	Savings [kg]	Percent Savings
Parabolic Radiator Shade	642	31
Lightweight Radiators	584	28
Capillary Pumped Loops	370	18
Low-Power Two-Phase Thermal Control System	286	14
Solar Vapor Compression Heat Pump	259	12

---

[4]   This value does not represent the entire thermal control system mass for First Lunar Outpost Lander. However, the omitted items are equivalent for the baseline architecture and each of the advanced technologies.

- **Permanent Lunar Base**

For Permanent Lunar Base, the parabolic radiator shade and the solar vapor compression heat pump are the most promising technologies. Both individually offer mass savings greater than 65%. These large reductions in thermal control system mass are possible here because radiator shades and heat pumps both allow large reductions in radiator surface area during the middle of the lunar day. In fact, shades and heat pumps are often designated as "enabling technologies" for long-term lunar missions. The heat-driven heat pumps, specifically complex compound and zeolite heat pumps, provide mass savings between 35 and 40%. Lightweight radiators give a mass savings of 30% for this mission, while the two-phase thermal control systems yield overall masses similar to the baseline configuration. Any of the lightweight radiator technologies may be used, although those which require a vertical configuration may require shading or heat pumping to operate. The additional technologies are all enhancing technologies which may be utilized regardless of the thermal control system architecture. Plant chamber cooling improvements are a collection of ideas which, if implemented in the assumed plant growth chamber, offer a significant mass savings.

Thermal Control System Mass Savings for Permanent Lunar Base
Basis = 1 Installation:

	Mass [kg]	
Baseline External Thermal Control System [5]	10,900	
	Savings [kg]	Percent Savings
Parabolic Radiator Shade	7,416	68
Heat Pumps		
Solar Vapor Compression	7,321	67
Vapor Compression	7,017	64
Complex Compound	4,241	39
Zeolite	3,818	35
Lightweight Radiators	3,306	30
Additional Technologies		
Plant Chamber Cooling Improvements	2,867	26
Carbon Brush Heat Exchanger	154	1
Two-Phase Thermal Control Systems		
Capillary Pumped Loops	917	8
Low-Power	751	7
With a Mechanical Pump/Separator	456	4

---

[5]   This value does not represent the entire thermal control system mass for Permanent Lunar Base. However, the omitted items are similar for both the baseline architecture and each of the advanced technologies.

- **Mars Lander**

For Mars Lander, lightweight radiators offer the greatest individual mass savings for any of the technologies considered. Any of the lightweight radiator technologies may be used. The projected mass savings from the solar vapor compression heat pump indicate the resulting system mass will be comparable to the baseline architecture. However, the heat pump will add flexibility to the thermal control system which is beneficial considering the uncertain climate on the surface of Mars.

Thermal Control System Mass Savings for Mars Lander
Basis = 1 Mission:

	Mass [kg]	
Baseline External Thermal Control System [6]	2,170	
	Savings [kg]	Percent Savings
Lightweight Radiators	416	19
Heat Pumps		
Solar Vapor Compression	127	6
Vapor Compression	-425	-20
Two-Phase Thermal Control Systems		
Capillary Pumped Loops	58	3
Low-Power	45	2

---

[6] This value does not represent the entire thermal control system mass for Mars Lander. However, the omitted items are equivalent for the baseline architecture and each of the advanced technologies.

CONCLUSIONS

The solar vapor compression heat pump and lightweight radiators show the greatest promise as general advanced thermal technologies which can be applied across a range of missions.

- The vapor compression heat pump suffers from high power requirements. However, the entire system compares favorably to baseline architectures when the heat pump is integrated with a dedicated solar photovoltaic power array and operated only while the vehicle or habitat is in sunlight.

- Lightweight radiators, although not rigorously defined here, offer the hope of directly reducing the radiator mass, which is the single greatest mass within the external thermal control system. In this initial study, four lightweight radiator concepts are considered, allowing this technology to be applied across a wide range of missions and environments.

- The qualitative assessments, which are separate from the quantifiable mass savings, additionally identify the rotary fluid coupler, the carbon brush heat exchanger, and electrohydrodynamic pumping as promising technologies. Even though these technologies do not yield large reductions in the total thermal control system mass, they offer other benefits which may warrent consideration.

For certain missions, several other technologies deserve consideration:

- Parabolic radiator shades have great utility on the lunar surface. In this airless planetary environment, they offer the greatest potential mass savings for missions at low latitudes assuming the shade surface can be maintained free of dust.

- Phase-change thermal storage is useful for orbital missions where the time during which the vehicle must endure its maximum heat load is less than the orbital period.

- Two-phase thermal control systems offer greater promise for larger systems with long flow lines. With the exception of International Space Station and Permanent Lunar Base, the vehicles here are too small to make adequate use of this technology. For Permanent Lunar Base, however, a two-phase thermal control system may be a wise investment, especially if the base will be expanded sometime in the future. As flow lines lengthen and heat loads increase, the pump power saved by a two-phase thermal control system will be significant. Capillary pumped loops may provide a mass savings even for smaller vehicles assuming the thermal control system is not expected to operate under high accelerations.

- Due to their extra mass, metallic heat pipes appear to be justified for human missions only when thermal control system flow loop punctures from external debris are expected to be a serious problem. When a mission flies in such an environment, mass savings become secondary to the reliability of the heat-rejection system. Current debris predictions for the missions here do not consider this to be a problem except possibly for International Space Station evolution, which flies in low Earth orbit where the debris problem is expected to be greatest. Further, longer arterial heat pipes are lighter per unit of radiant surface area. Combining longer units with lighter thermal interfaces and/or electrohydrodynamic pumps also improves the mass savings.

- Heat-driven heat pumps offer mass savings for Permanent Lunar Base compared with the baseline architecture. Coupled with a source of high-temperature waste heat, such as from an industrial process, they may provide economical cooling. However, heat-driven cycles are not as efficient as mechanically driven cycles and, therefore, heat-driven heat pumps weigh more than mechanically-driven heat pumps.

- Several enhancing technologies appear in this study. These include the rotary fluid coupler, plant chamber cooling improvements, and the carbon brush heat exchanger. Alone, they do not offer large mass savings. However, they also do not require a particular thermal control system architecture and, therefore, can be implemented individually or with other technologies.

This initial study identifies several promising advanced thermal control technologies which offer both mass savings and other benefits compared to traditional thermal control systems. Future research and development is expected to more accurately and precisely define these mass savings as various programs proceed to develop flight-ready hardware. Future technical developments and additional knowledge may change current understanding on which these results are based. Therefore, this study is expected to be an ongoing effort which will be updated as needed to allow a common basis for future programmatic decisions. Subsequent work in this area is currently planned to include a wider range of technologies as well as architectures which combine various technologies at the system level.

1.0   INTRODUCTION

This study presents advanced active thermal control system (ATCS) architectures for five proposed National Aeronautics and Space Administration (NASA) vehicles and habitats. The objective is to define possible alternate thermal control systems using new or proposed technologies for these vehicles and habitats and determine what mass savings and other benefits might be available. Non-mass savings are converted to mass using an appropriate penalty. For example, a power savings is converted to mass using a power mass penalty. However, many benefits are considered only qualitatively. Because this is preliminary work, many details of various vehicles and technologies are either assumed or neglected entirely. To aid the reader, the significant assumptions are listed.

The five reference missions considered below are:

- International Space Station (ISS) Evolution
- Space Transportation System (STS or Shuttle) Upgrade
- First Lunar Outpost (FLO) Lander
- Permanent Lunar Base (PLB)
- Mars Lander (ML)

Twenty different advanced technologies in various stages of maturity are considered for this study. The main areas collectively addressed by these technologies include thermal transport systems, heat pumps, and radiators. However, several additional options, such as the rotary fluid coupler and the carbon brush heat exchanger, fall into categories by themselves. Because each of the advanced technologies either does not apply to all of the vehicles or habitats examined, or it is expected that the given technology would not yield a benefit, the technology list was pared as appropriate for each reference mission. The advanced technologies considered for each vehicle or habitat are addressed in Table 1.1.

Table 1.1 Advanced Technologies Applied to Reference Missions

Advanced Technologies	Reference Vehicles and Habitats				
	ISS	STS	FLO	PLB	ML
Two Phase Thermal Control Systems:					
1. Two-Phase TCS With Mechanical Pump/Separator	X			X	
2. Low-Power Two-Phase TCS	X	X	X	X	X
3. Two-Phase TCS with Electrohydrodynamic Pumping			X	X	X
4. Capillary Pumped Loops	X		X	X	X
Heat Pumps:					
5. Vapor Compression Heat Pump	X			X	X
6. Solar Vapor Compression Heat Pump	X		X	X	X
7. Complex Compound Heat Pump				X	
8. Zeolite Heat Pump				X	
Heat Pipe Radiators:					
9. Arterial Heat Pipe Radiators	X				
10. Axial-Groove Heat Pipe Radiators	X				
11. Arterial Heat Pipes With Electrohydrodynamic Pumping	X				
Lightweight Radiators [7]:	X	X	X	X	X
12. Composite Flow-Through Radiators	x	x	x	x	x
13. Composite Heat Pipe Radiators	x		x	x	x
14. Composite Reflux Boiler Tube Radiators			x	x	x
15. Unfurlable Radiators			x	x	x
Other Heat Rejection Technologies:					
16. Phase-Change Thermal Storage		X			
17. Parabolic Radiator Shade			X	X	
Additional Technologies:					
18. Rotary Fluid Coupler	X				
19. Plant Chamber Cooling Improvements				X	
20. Carbon Brush Heat Exchanger	X			X	
Total Number of Applicable Technologies	10	3	5	11	5

It should be noted that the various advanced technologies were assumed to operate as theorized. Because some technologies are currently not well-developed, the analysis which follows may seem speculative. However, as stated earlier, the purpose here is to estimate what mass savings and other benefits might accrue from pursuing various ideas for active thermal control systems which may be available in the near future.

Each of the technologies considered has desirable and undesirable attributes. To reduce the time spent on unproductive exercises, the technology list was pared to examine only technologies which were likely to offer an advantage for a particular mission. Further, technologies were not combined with each other to optimize the use of a particular technology in this initial work. In other words, each technology was considered individually to determine its benefits.

---

7   This study evaluates lightweight radiators as a class. The other architectures mentioned in this category are possible implementations of a lightweight radiator. Those which are possibilities for each mission are marked with an 'x' (small x) but they are not evaluated separately as a technology.

Two-phase thermal control systems, according to Ungar (1995), are most likely to lower pumping requirements for larger systems with larger heat loads. Further, electrohydrodynamic pumping appears appropriate only for systems not operating while the vehicle is accelerating rapidly, such as during launch or landing. Capillary pumped loops employ two-phase heat acquisition and rejection for the thermal control system flow loop. However, unlike the other two-phase architectures mentioned above, capillary pumped loops do not use any moving parts. Their main disadvantage is a reliance on capillary pumping, which typically generates a low pumping head, so that such a system will not operate under launch or landing accelerations.

Heat pumps are a versatile technology which can be applied to most vehicles and missions. Their major detracting attribute is the need for a relatively large power source or a high-temperature heat source. Further, the study here considered heat-pumping for the entire thermal control system load, and not just for partial loads. Under these conditions, the vapor compression cycles were deemed feasible for all missions except Space Transportation System upgrade, and the heat-driven cycles were considered only for Permanent Lunar Base.

Heat pipes, which are generally heavier than flow-through radiators, are attractive for environments where high concentrations of debris may strike and puncture the radiators. Of the missions considered here, only International Space Station evolution is projected to possibly operate in a high debris environment for long periods of time.

Lightweight radiators represent a general category where the radiators are constructed using lighter and stronger materials. Due to this category's broad nature, the implementation of this option for each of the missions is expected to differ. Some initial speculative calculations are presented which presume lighter components based upon using flow-through radiator architecture. Specific examples of lightweight radiators include composite flow-through radiators, composite heat pipe radiators, composite reflux boiler tube radiators, and unfurlable radiators. Of these examples, composite reflux boiler tube radiators and unfurlable radiators are restricted to vertical deployments on planetary surfaces. Further, the composite heat pipe radiator is also deployed vertically when on a planetary surface, but they may also operate in a microgravity environment. These technologies are mentioned for each mission when appropriate.

Phase-change thermal storage utilizes the heat of fusion for a homogeneous material to store cooling or heating capacity. Here such a material is used in conjunction with flow-through radiators to supplement the radiators' heat-rejection capability by melting the phase-change material while the vehicle is in a relatively hot thermal environment. This technology appears to be most attractive for situations where a vehicle is operated continuously in its hottest environment for short periods of time, such as for atmospheric braking and on-orbit mission elements.

The parabolic radiator shade requires large surface areas for deployment and absence of an atmosphere which might allow wind to deposit dust on the shade.

The rotary fluid coupler is appropriate for situations when a tracking radiator is necessary and less complicated radiator systems would be inadequate. This is a consideration for orbiting vehicles. On a planetary surface it is generally impossible to avoid all significant sources of solar radiation on the radiator using selective radiator positioning.

Plant chamber cooling improvements are applicable only for missions which contain plant growth chambers. In the current study only Permanent Lunar Base is projected to use a plant chamber.

Carbon brush heat exchangers have utility where ever a coldplate exists. Here they were restricted to coldplates for dc-to-dc converter units for International Space Station evolution and Permanent Lunar Base.

At the end of each advanced technology assessment, a composite qualitative assessment is given in addition to the overall mass savings. Assessments are made in five areas. These assessments rate volume, ease of deployment or installation, reliability, remaining development cost to bring the technology to a readiness level of at least 6, and potential for terrestrial applications. In situations where the advanced technology is expected to have similar performance to the base reference mission, the qualitative assessment used is "average." In situations where the advanced technology is expected to differ significantly from the reference architecture, one of the two extreme assessments are assigned. The development cost is assigned a value of "low" for estimated remaining development program costs up to one million dollars, "average" for costs between one and three million dollars, and "high" for costs in excess of three million dollars. More specifically, the qualitative grading assessments are described in Table 1.2.

Table 1.2 Qualitative Scores for Assessment Areas

Assessment Area	Qualitative Score		
	-1	0	+1
Volume	large	average	compact
Deployment (or Installation)	difficult	average	easy
Reliability	degraded	average	improved
Development Cost	high	average	low
Terrestrial Use Potential	none	possible	good

Details of the qualitative assessments are given in Section 2.0 for each advanced technology.

To aid in assessing the development cost, each advanced technology was assigned a technology readiness level rating based on NASA (1991) for each reference mission. In the most basic terms, these technology readiness level ratings are defined as:

Rating	Technology Readiness Level Description
1	Basic principles observed and reported
2	Technology concept and/or application formulated
3	Analytical and experimental critical function / characteristic proof-of-concept
4	Component / breadboard validation in laboratory environment
5	Component / breadboard validation in relevant environment
6	System/subsystem model or prototype demonstration in relevant environment
7	System prototype demonstration in a simulated environment
8	System completed and flight qualified through test and demonstration
9	System "Flight proven"

2.0   ADVANCED THERMAL CONTROL TECHNOLOGIES

This section presents the various advanced thermal control technologies considered in this study. The technologies are applied to each baseline mission individually to assess their benefits compared with the baseline architecture. The baseline architecture is either the present configuration for a vehicle or habitat, if known, or a defined baseline configuration. The defined baseline configurations assume a thermal control system (TCS) with fluid flow loops to collect heat loads and flow-through radiators to reject the heat load to space. More specifically, the defined baseline configurations use an internal thermal control system (ITCS) flow loop with water as the working fluid and an external thermal control system (ETCS) flow loop with single-phase, liquid ammonia as the working fluid. Heat exchange from the ITCS to the ETCS is by way of interface heat exchangers.

2.1   Two-Phase Thermal Control Systems

A two-phase TCS takes advantage of the working fluid's latent heat of vaporization to store and release thermal energy. When heat is collected by the ETCS flow loop, the working fluid vaporizes. The working fluid liquefies when it rejects the collected heat load to a rejection device. Compared with a single-phase system, the two-phase system should use smaller piping, less working fluid, and correspondingly less pumping power, especially for larger vehicles or habitats with longer ETCS fluid lines.

Ungar (1995) compares single- and two-phase TCSs for space stations of several sizes. His results indicate that two-phase TCSs are advantageous for larger vehicles, comparable for medium-sized vehicles, and less efficient for smaller vehicles. In this initial section on technologies, a larger vehicle, such as ISS after evolution or PLB are assumed for the qualitative assessments.

2.1.1   Two-Phase Thermal Control System With Mechanical Pump/Separator

The mechanical pump/separator (MP/S) uses centrifugal forces to separate a two-phase stream into liquid and vapor before pumping the fluid to the heat exchangers and radiators. The liquid is extracted from the periphery of the device by a pitot pump and delivered to the ITCS/ETCS interface heat exchangers while the vapor in the center flows to the radiators (Figure 2.1). While in the radiators, the vapor condenses, liberating heat to space, and exits the radiators as a subcooled liquid.

To simplify the analysis for this study, several assumptions are helpful. First, the masses for two-phase plumbing, fittings, and interface heat exchangers are approximately the same as the masses of the corresponding single-phase equipment. Second, changes in the fluid inventory between this two-phase system and the baseline single-phase system are not considered.

Radiator Orbital Replacement Units
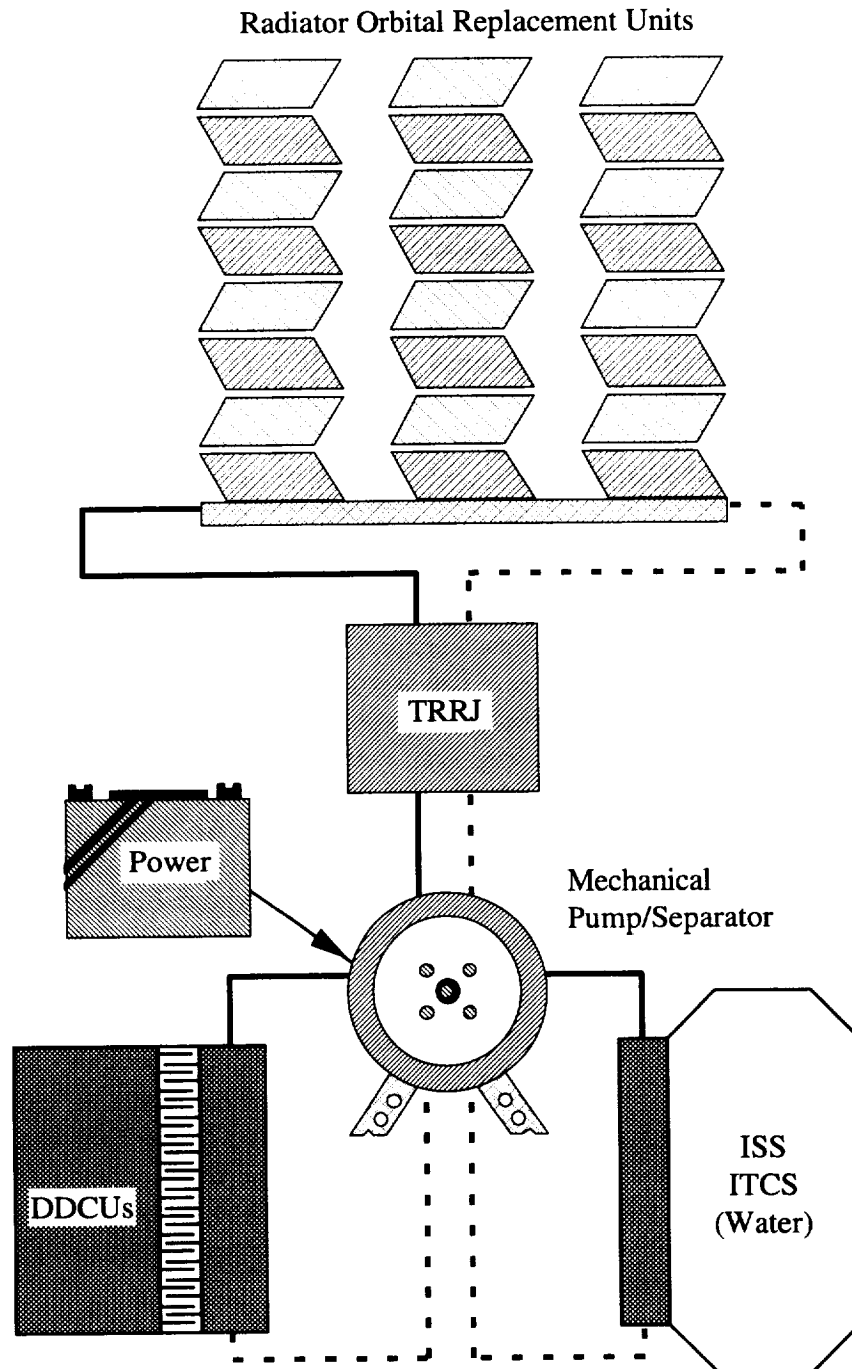
Figure 2.1 An external thermal control system using a two-phase thermal control system with mechanical pump/separator. The lines through which two-phase fluid flows are dashed and the single-phase lines are solid. The example here presents the configuration for International Space Station.

Because a two-phase TCS with MP/S was originally proposed for Space Station, much of the developmental and design work has already been completed for a larger TCS. For ISS evolution, this option has a technology readiness level (TRL) of 7. For other reference missions the TRL would be 6. Flight testing is not considered necessary to complete a system design. Thus, the development cost is expected to be low. The reliability and deployment of such a TCS should be comparable to current equipment once development is completed. It is also expected that, due to the high heat-transfer rates and low power consumption associated with evaporative cooling and condensation in a two-phase system, this technology may be attractive to terrestrial users. However, a flash tank [8] in an environment with gravity is a proven method which requires no input power to separate liquid and vapor streams.

General Qualitative Assessments:

Technology Readiness Level [9]	6
Volume	average
Deployment	average
Reliability	average
Development Cost	low
Terrestrial Use Potential	none
Composite Qualitative Score	0

2.1.2 Low-Power Two-Phase Thermal Control System

The low-power (LP) two-phase TCS is similar to the two-phase TCS with MP/S with the added benefit that only liquid is pumped. Like the two-phase TCS with MP/S, the ETCS stream vaporizes while extracting heat from the ITCS. Here a two-phase liquid/vapor mixture is delivered to the radiators. However, the pump is placed downstream of the radiators where the fluid is always sub-cooled. This approach reduces the necessary pumping power requirements and avoids the technical complexities associated with specialized equipment such as a MP/S. For the study here, the quantifiable difference between a two-phase TCS with MP/S and a LP two-phase TCS is an additional reduction in pumping power associated with the latter option.

As with the previous two-phase system, the LP two-phase TCS is still in the developmental stage. However, because the LP two-phase TCS uses standard components in an innovative arrangement, the developmental work should be primarily at the system level. To simplify the analysis for this study, several assumptions are helpful. First, the masses of two-phase plumbing, fittings, and interface heat exchangers are similar to the masses of the corresponding single-phase equipment. Second, changes in the fluid inventory between this two-phase system and the baseline single-phase system are not considered.

---

[8] A flash tank is a chemical, or flow, processing unit with at least one inlet and two outlets. The tank itself is typically at a lower pressure than its upstream components, so the process stream "flashes" or separates into vapor and liquid components using gravity as the driving potential for the separation.

[9] For ISS evolution this technology would have a TRL of 7.

Technically, this option should be easier to implement than the two-phase TCS with MP/S. However, the LP two-phase TCS has a lower TRL of 3. Thus, an average development cost is anticipated. Terrestrial uses for this technology are not expected even though several possibilities initially suggest themselves. One suggestion would replace a building's air conditioning cycle with a LP two-phase TCS. However, the coefficient of performance of this technology is expected to be significantly lower than a standard heat pump cycle at temperatures common to residential and commercial building cooling applications. Further, to avoid pumping a two-phase mixture against gravity, the condenser, which is in contact with a cooler environment, must be located above the evaporator (cooling unit) in the building [10]. Thus, this technology is probably impractical for cooling buildings. For higher temperature applications, such as industrial process cooling, liquid sprays or tanks are often used. The additional equipment, such as coldplates and piping, for a LP two-phase TCS cooling cycle would be a more expensive alternative as long as the current technology is acceptable. Further, the petrochemical and other industries already use something similar to the LP two-phase TCS. For transporting two-phase streams a flash tank is used to separate the components which may then be pumped individually. When applicable, this approach is generally less expensive than subcooling a process stream. Thus, while innovative, the LP two-phase TCS and its associated technology are not expected to inspire terrestrial uses.

General Qualitative Assessments:

Technology Readiness Level	3
Volume	average
Deployment	average
Reliability	average
Development Cost	average
Terrestrial Use Potential	none
Composite Qualitative Score	-1

2.1.3　Two-Phase Thermal Control System With Electrohydrodynamic Pumping

To use a two-phase TCS, the difficulty of transporting a mixture of liquid and vapor must be addressed. The LP two-phase TCS sub-cools the ETCS working fluid in the radiators, allowing only liquid to enter the ETCS pumps. Electrohydrodynamic pumping would pump the entire fluid stream, regardless of its phase, by using a distributed network of electrohydrodynamic pumps. This technology would be appropriate for thermal control loops which were not subjected to large accelerations. Thus,

---

[10]　Radiators, for commercial and residential cooling, are inappropriate because the terrestrial environmental temperatures are too high when cooling is necessary. However, a cooling tower could be placed on a building's roof to provide an appropriate sink for a LP two-phase TCS cooling system. However, cooling towers are, by necessity, extremely heavy. Thus, a LP two-phase TCS cooling system could probably not be economically installed in an older building. Further, the additional structural support necessary to implement a LP two-phase TCS in a new building is expected to be prohibitive.

electrohydrodynamic pumping would be appropriate for missions in microgravity and on planetary surfaces but not for vehicles subjected to launch loads.

Electrohydrodynamic pumping should have several advantages for a two-phase TCS (Bryan, 1995). The mass of any phase separation device could be eliminated. The standard single-phase pumps could also be removed, but the mass gain associated with the electrohydrodynamic pumps will mostly offset this benefit. The power for an electrohydrodynamic pumping system is expected to be similar to that associated with mechanical pumping. The volume will be comparable to other two-phase TCSs. The deployment should be comparable to other TCSs. Electrohydrodynamic pumping would be significantly more reliable because this technology utilizes a greater number of smaller pumps. Thus, losing a single pump is less damaging than losing a mechanical pump in a standard TCS. In this application, electrohydrodynamic pumping is immature with a TRL of 2. Because this technology generates low pumping pressures, a test on orbit is needed to assess its behavior in a microgravity environment. However, terrestrial testing should be sufficient for systems deployed on a planetary surface. Thus, the development cost for a two-phase TCS with electrohydrodynamic pumping is expected to be high for orbital applications and average for planetary missions. Electrohydrodynamic pumping may have applications in the medical field and in the petrochemical industry. Medical flows often contain more than one phase, such as blood or a suspension of bacteria, and electrohydrodynamic pumps would, in cases where the pumping process does not alter the fluid in the flow, provide an excellent method of transporting these mixtures. Further, electrohydrodynamic pumping moves flows over long distances by using numerous electrohydrodynamic pumps. This pumping configuration avoids introducing extreme stresses into the flow unlike conventional mechanical pumping. For flows with shear sensitive components, electrohydrodynamic pumping would be preferable to traditional mechanical pumping. Unlike the LP two-phase TCS, electrohydrodynamic pumping can transport two-phase flows without separating them into their components. Thus, in some industrial applications, electrohydrodynamic pumping may be a more expedient approach than traditional techniques which separate the flow for transport.

General Qualitative Assessments:

Technology Readiness Level	2
Volume	average
Deployment	average
Reliability	improved
Development Cost	average
Terrestrial Use Potential	good
Composite Qualitative Score [11]	+2

2.1.4 Capillary Pumped Loops

Capillary pumped loops are two-phase thermal control loops which use capillary forces to drive the flow. More specifically, as illustrated in Figure 2.2, the capillary

---

[11]   This assessment is for missions on a planetary surface. For orbital missions the development cost is "high" and the overall score is +1.

pumped loop acquires heat by vaporizing the working fluid at the evaporator and rejects heat to the environment or a heat-rejection interface when the working fluid condenses at the condenser. The wick, which in American and European implementations [12] is typically porous high-molecular-weight polyethylene, is normally saturated with liquid. When heat is applied to the evaporator, the liquid on the outer diameter of the wick evaporates and moves as a pure vapor to the condenser, where it condenses and is subcooled. The pumping action of the wick returns the liquid to the evaporator. The reservoir contains saturated working fluid, liquid and vapor, at the desired loop pressure and, therefore, temperature. Thus, capillary pumped loops, in their standard mode of operation, are variable conductance devices [13] which transfer heat proportional to the rate of vapor formation at the evaporator and operate at some temperature determined by the set-point pressure of the loop.

Cullimore (1993) provides a broad overview of capillary pumped loop operating characteristics and traits supported by an extensive literature survey. Several observations from this work are applicable here. Of greatest importance for rejecting heat from human vehicles and habitats is the overall capacity of the capillary pumped loop. Studies (see Cullimore, 1993) demonstrate that capillary pumped loops can be designed to transfer from 5 W up to 25 kW per loop using aluminum and ammonia systems [14]. Further, the heat load may be acquired using numerous parallel evaporators and rejected from numerous parallel condensers. Correspondence between the number of evaporators and the number of condensers is not required. Using multiple evaporators and condensers allows the capillary pumped loop to function as a thermostat for the loads it services by heating those loads which are cooler than the loop set-point and cooling only the loads which are warmer than the loop set-point. However, to prevent the capillary pumped loop from shutting down [15], the overall sum of the loads serviced by the loop requires cooling.

A capillary pumped loop is not constrained by a fixed geometry but is rather a combination of components arranged to give a specific TCS architecture [16]. Further, they can pump working fluid 0.3 m to 3.0 m against terrestrial gravity, depending on the chosen wick structure and flow geometry. Thus, assuming care is taken in the system design, capillary pumped loops could be used on a planetary surface as well as in space. The only situation where capillary pumped loops would be completely inappropriate are

---

[12] The experiences from the former Soviet Union, and now Russia, differ in some significant ways. Cullimore (1993) mentions some of these differences for the interested reader. The remainder of this description assumes American or European heritage equipment and practice.

[13] If the reservoir ever becomes completely filled with liquid, the capillary pumped loop becomes a constant conductance heat transport device. Traditional practice dictates that capillary pumped loops are designed and charged so that this cannot occur.

[14] Flight-rated hardware so far has concentrated on cooling robotic probes with multiple capillary pumped loops which transfer no more than hundreds of Watts each. An example of such a vehicle is the Earth Observing System (EOS), which has three instruments. Each of the instruments, which have maximum heat loads up to 250 W, uses one of two redundant capillary pumped loops to transfer those loads to constant conductivity heat pipes (Ku, 1996).

[15] A capillary pumped loop functions as a diode with respect to heat transfer. If the heat load to be rejected by the loop is cooler than the condenser environment, the liquid line will boil, allowing the evaporators to deprime and shut down the loop. The capillary pumped loop may be restarted later (Cullimore, 1993).

[16] As such, they are placed here with the two-phase TCSs and not with the heat pipes.

for systems which must function while enduring high accelerations, such as during launch or re-entry.
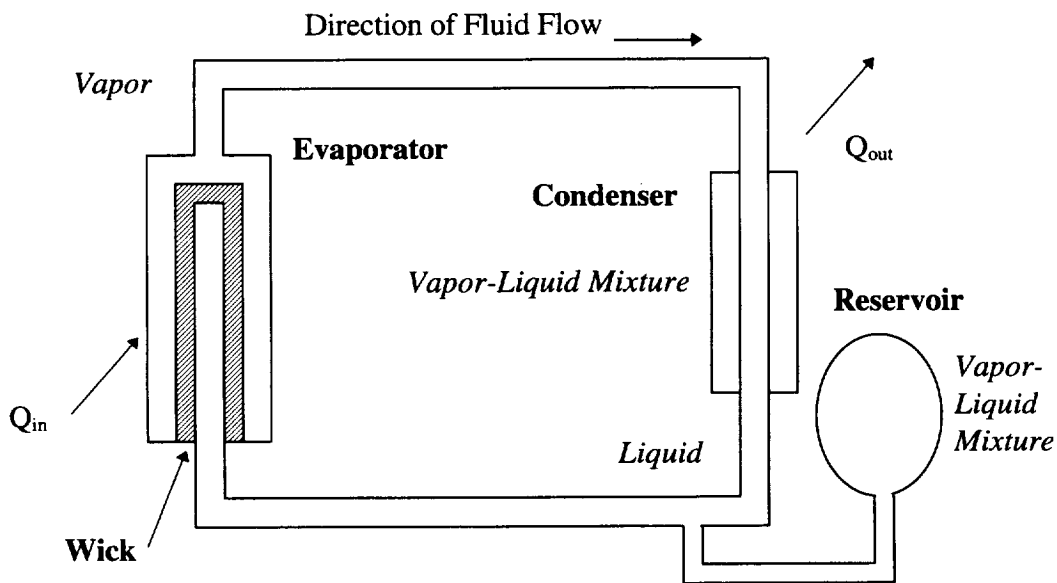
Figure 2.2 A simple implementation of a capillary pumped loop (Cullimore, 1993). The capillary pumped loop acquires heat by vaporizing the working fluid at the evaporator and rejecting heat to the environment by condensing working fluid at the condenser. The wick pulls liquid into its pores by capillary action from the liquid volume at its inner diameter. As the evaporator acquires heat, the liquid on the outer diameter of the wick evaporates and moves as a slightly superheated vapor to the condenser. The reservoir contains saturated working fluid liquid and vapor at the desired loop pressure and, therefore, temperature. Thus, capillary pumped loops, in their standard mode of operation, are variable conductance devices which transfer heat proportional to the rate of vapor formation at the evaporator and operate at some temperature determined by the set-point pressure of the loop. (Capillary pumped loop components are denoted by bold text while working fluid states are given by italic text.)

As presented in this study, capillary pumped loops are rated assuming they require no external pumping power and in turn require no additional equipment mass beyond that for the baseline single-phase TCS architecture. Assuming the capillary pumped loop is properly sized, this TCS does not require any mechanical pumping except possibly for starting the system and/or recovering from depriming. The only power input is that for maintaining the temperature of the reservoir which sets the capillary pumped loop set-point. This power expenditure is a small fraction of the total heat load carried by the capillary pumped loop. The actual capillary pumped loop equipment may be significantly different than that for a comparable single-phase TCS because capillary pumped loop designs must use components with low flow resistance to minimize the overall loop

pressure drop [17]. However, these components are not necessarily more massive than the corresponding single-phase components.

Qualitatively, capillary pumped loops integrated into new vehicles and habitats should have a volume and ease of deployment comparable to the baseline architecture [18]. The system reliability should be improved relative to the baseline architecture because the capillary pumped loop has no moving parts and can operate with little external power input. The development cost for piloted vehicles on orbital missions will be high because a capillary pumped loop of sufficient capacity with multiple evaporators/condensers has yet to be tested on orbit. For systems placed on a planetary surface, terrestrial testing should suffice so an average development cost is anticipated. The TRL for piloted vehicles is 5. Applications are currently unknown for capillary pumped loops, so no terrestrial uses are anticipated.

General Qualitative Assessments:

Technology Readiness Level	5
Volume	average
Deployment	average
Reliability	improved
Development Cost	average
Terrestrial Use Potential	none
Composite Qualitative Score [19]	0

2.2　Heat Pumps

Assuming the radiating area is fixed, a greater heat load may be rejected by either lowering the effective environmental, or sink, temperature or by increasing the radiator surface temperature [20]. Heat pumps, as presented in this study for space applications, effectively cool a vehicle or habitat using a refrigeration cycle and reject the work load and the original heat load at a higher temperature. Two general classes of heat pumps are presented. Vapor compression heat pumps use a mechanically driven cycle built around a

---

[17]　Ungar (1996) recommends that the overall loop pressure drop not exceed 3,447 N/m^2 (0.5 lb$_f$/in^2) based on the limited capillary pumping head available from current high-molecular-weight polyethylene wicks.

[18]　Retrofitting a vehicle using a single-phase TCS with a capillary pumped loop may be difficult, if not impossible. Thus, for installation on a pre-existing vehicle, the rating for deployment should be "difficult."

[19]　This assessment is for missions on a planetary surface. For orbital missions the development cost is "high" and the overall score is -1.

[20]　Heat rejection in a vacuum between a radiator and its environment, q, may be defined as:

$$q = \eta A \varepsilon F_{ij} \sigma \left[T_{radiator}^4 - T_{sink}^4 \right]$$

where A is the actual radiating surface area, η is the fin efficiency, ε is the surface emissivity, F_{ij} is the view factor between the radiator surface and the environment, σ is the Stefan-Boltzmann constant, and $T_{radiator}$ and T_{sink} are the radiator surface and environmental temperatures, respectively.

compressor [21]. The primary utility for a vapor compression cycle is a source of electricity to run the compressor. Heat-driven heat pumps are built around a chemical or physical absorption-desorption cycle over a range of temperatures. Here the cycles considered use solid/vapor adsorption systems with a fixed refrigerant carrier (Yerushalmi, 1992). The primary utility necessary for heat-driven cycles is a source of high temperature heat. Ideally, this could be obtained as waste heat from some other process such as a nuclear power plant or other industrial process. However, solar concentrators can also provide a high-temperature heat source to operate a heat-driven cycle. The results here for heat-driven heat pumps are based on Ewert (1993) and assume solar concentrators for the heat source.

Generally, the systems here are sized so that heat pumping is only necessary while the vehicle or habitat is receiving solar irradiation. Orbital vehicles, however, may receive continuous heat pumping because their sunlight/shade cycles are relatively short. For example, ISS will have roughly a 90-minute orbital cycle with about 30 minutes in shade for a beta angle of 0 degrees. The heat pumping here is also assumed to be centralized as opposed to distributed.

2.2.1 Vapor Compression Heat Pump

With respect to an active thermal control system (ATCS), heat pumps could be used to increase the radiator fluid temperature, thereby increasing radiator heat rejection and reducing the necessary radiator surface area. A typical single-stage heat pump for this application would accept heat from the ITCS, which is at the cycle's cold temperature, by evaporating a working fluid. The resulting stream, usually a superheated vapor, is compressed and passed to the condenser. Within the condenser, which is the cycle's hot working temperature, the fluid condenses and rejects heat to the ETCS radiators at an elevated temperature. Upon leaving the condenser, the working fluid flows through an expansion valve before returning to the evaporator (Figure 2.3). Generally more efficient high-lift heat pumps use more than a single stage.

The main disadvantage of the vapor compression heat pump is its high power requirement relative to the baseline TCS architecture using only metal flow-through radiators. The overall TRL for a vapor compression heat pump is 5. For application on a planetary surface, the development cost is expected to be low. For orbital applications, the influence of microgravity on lubricant circulation within the heat pump must be resolved and tested on orbit. Thus, for orbital applications the development cost is high. The deployment in general should be comparable to baseline architectures, or average. Directly, heat pumps can be used for heating or cooling of terrestrial habitats or industrial equipment. Further, coupled with non-chlorofluorocarbon refrigerants, this technology may pay commercial dividends. Some work has already been completed for a high-lift, multistage heat pump designed for use with lunar habitations. This design has fewer components which are susceptible to micrometeoroid punctures and optical degradation than the baseline TCS architecture. The vulnerable radiator flow loops are shorter and the

---

[21] Another mechanical heat pump uses the Stirling cycle. The Stirling cycle has many of the same attributes as a vapor compression cycle. However, to date, Stirling heat pumps have not been applied to high load or high temperature applications. Thus, they were not considered here.

heat pump itself is compact enough to take advantage of local shielding. Additional components with moving parts, however, will degrade the reliability of this technology.

General Qualitative Assessments:

Technology Readiness Level	5
Volume	average
Deployment	average
Reliability	degraded
Development Cost	low
Terrestrial Use Potential	good
Composite Qualitative Score [22]	+1

2.2.2 Solar Vapor Compression Heat Pump

A solar heat pump uses the same equipment as the heat pump presented in Section 2.2.1 except that input power is provided by a dedicated solar photovoltaic power array instead of from the general habitat or vehicle power grid [23]. To further reduce mass, only minimal power conditioning equipment is provided. This is expected to significantly reduce the mass of the power plant and distribution net for the heat pump. (See Ewert, Keller, and Hughes, 1996) Further, a bypass line for the heat pump will allow the ETCS to use the radiators directly when the heat pump is not in use, such as when the base is not in sunlight. Therefore, a solar heat pump does not require any electrical storage (Figure 2.4).

The solar heat pump has the same advantages as the standard vapor compression heat pump presented in the previous section. However, the mass of the required supporting power systems for the solar heat pump is significantly less. Because the power system can account for over 90% of the mass added for the vapor compression heat pump, reducing this mass is highly advantageous.

General Qualitative Assessments:

Technology Readiness Level	5
Volume	compact
Deployment	average
Reliability	degraded
Development Cost	low
Terrestrial Use Potential	good
Composite Qualitative Score [24]	+2

---

[22] For orbital applications, the development cost is "high" for an overall score of -1.

[23] This option is more correctly called a vapor compression heat pump with a dedicated solar photovoltaic power array.

[24] As with the vapor compression heat pump, this option has a "high" development cost for orbital applications. The overall score for orbital applications is 0.
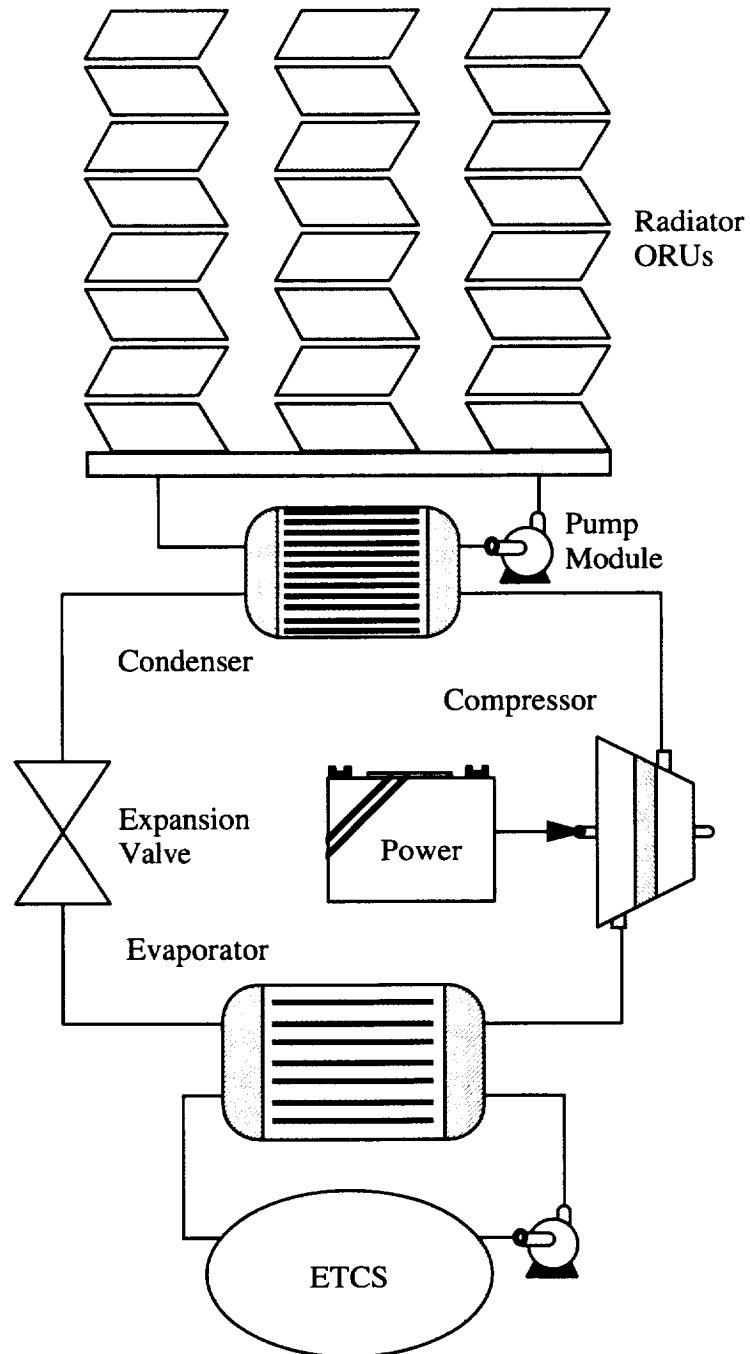
Figure 2.3 An external thermal control system using a vapor compression heat pump. The example here presents the configuration for International Space Station.

2.2.3   Complex Compound Heat Pump

Heat-driven heat pumps use cycles requiring a source of extremely high temperature heat to operate. For a complex compound heat pump, the high heat source requires a temperature of 500 K (Yerushalmi, 1992). Commonly, this heat is transported to a heat-driven heat cycle using an appropriate working fluid.

In the baseline missions studied here, no sources of waste heat are present. In order to generate heat to drive a heat-driven heat pump, at least two other methods are available. One method would generate heat from electricity generated by solar photovoltaic power arrays through resistive heating. A second method would use a collector to focus solar radiation on a tube containing a working fluid. This is a more efficient technique and is assumed for the heat-driven cycles in this study.

The TCS with complex compound heat pumps is similar to the baseline technology in many areas. This heat pump will allow for more compact radiators, compared with the baseline TCS, but this benefit will be partially offset by the addition of the heat pumps. The deployment should be comparable to the baseline mission. The system reliability will probably be the same as the baseline mission because heat-driven heat pumps contain fewer components with moving parts than vapor compression heat pumps. The heat pump itself has few moving parts but the collector system to supply high temperature heat to the cycle will have a reliability comparable to other technologies. Because current heat pump research is directed toward an application for space, the development cost for this system is expected to be average. While orbital missions are not proposed for this heat pump, the microgravity environment is not expected to affect it. The TRL is assessed at 4. Terrestrial uses could exist for complex compound heat pumps as cooling devices in heavy industries where a source of high temperature heat is readily available. Examples might include power generation, metal processing and forging, or possibly use in arid regions where an uninterrupted source of solar energy can be readily collected.

General Qualitative Assessments:

Technology Readiness Level	4
Volume	compact
Deployment	average
Reliability	average
Development Cost	average
Terrestrial Use Potential	possible
Composite Qualitative Score	+1

2.2.4   Zeolite Heat Pump

Zeolite heat pumps also use a heat-driven cycle and require a high heat source at a temperature of 700 K (Yerushalmi, 1992). From the perspective of this report, zeolite heat pumps have many of the same attributes as complex compound heat pumps. Therefore, the same overall approach as for the preceding technology is employed here.
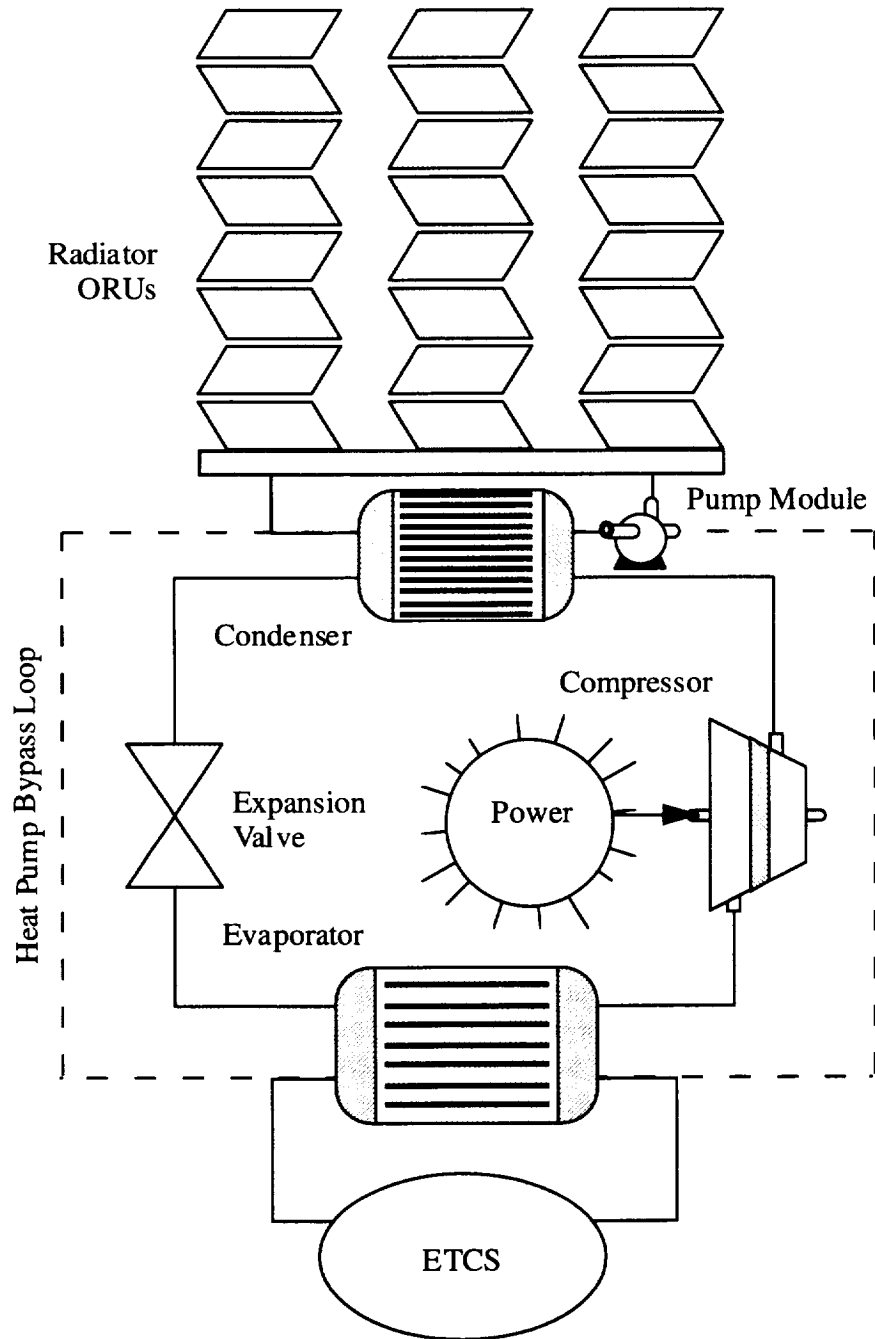
Figure 2.4 An external thermal control system using a solar vapor compression heat pump (a vapor compression heat pump with a dedicated solar photovoltaic power array). The example here presents the configuration for International Space Station.

The TCS with zeolite heat pumps is similar to the baseline technology in many areas. This heat pump will allow for more compact radiators, compared with the baseline TCS, but again this benefit will be partially offset by the addition of the heat pumps which are more massive than the complex compound equipment. The deployment should be comparable to the baseline mission and the system reliability will probably be the same as the baseline mission. Again, the zeolite heat pump itself has few moving parts but the collector system to supply high temperature heat to the cycle will have a reliability comparable to the baseline technologies. Because current heat pump research is directed toward an application for space, the development cost for this system is expected to again be average. The zeolite heat pump is slightly behind the complex compound heat pump, so the TRL is 3. As above, terrestrial uses could exist for the zeolite heat pumps as cooling devices in heavy industries with a source of waste high-temperature heat.

General Qualitative Assessments:

Technology Readiness Level	3
Volume	compact
Deployment	average
Reliability	average
Development Cost	average
Terrestrial Use Potential	possible
Composite Qualitative Score	+1

2.3   Heat Pipe Radiators

Heat pipes are self-contained, two-phase devices which transfer heat from a hot source to a cold source. The heat pipe evaporator vaporizes the internal working fluid to acquire the heat load. The vapor travels out into the condenser and liquefies the working fluid as the heat pipe rejects the heat load to the cold source. For missions in this study, the cold source is the environment. The working fluid travels back to the evaporator by capillary forces, which provide the primary pumping within heat pipes. For a given heat pipe, the heat transport is limited by the available capillary pumping capability. When the transport limit is exceeded, the working fluid may collect in the heat pipe's condenser, rendering the unit unusable. One technique for working around this tendency is to add extra heat pipe capacity to ensure that the system transport limit is not exceeded. Another option is to add individual pumps to each heat pipe to increase each unit's transport limit.

The primary advantage of arterial heat pipes, even though equivalent metallic arterial heat pipe systems are often heavier than corresponding metallic flow-through radiator systems, is their redundancy which provides added reliability in environments with micrometeoroids and on-orbit debris. If an ETCS flow line is punctured by a micrometeoroid, the working fluid is expected to drain quickly to space. Spacecraft and bases with flow-through radiators are most susceptible to this because their main ETCS flow lines pass through the exposed and lightly protected radiators. In a similar scenario with arterial heat pipes, the ETCS flow lines would be protected with only the heat pipe condensers exposed to on-orbit debris punctures. In this second situation only the

working fluid and capacity of a single heat pipe would be lost to a single puncture, not that of an entire ETCS flow loop. Axial-groove heat pipes replace just the flow-through tubes within radiator panels (Nguyen, 1992) so they do not yield a significantly more robust system for applications where micrometeoroid and on-orbit debris are a significant concern.

2.3.1 Arterial Heat Pipe Radiators

Arterial heat pipe radiators are somewhat different from the current state-of-the-art heat pipe [25]. In this concept, the current radiators are replaced with a heat exchanger to which a number of long heat pipes are mounted. The heat exchanger collects thermal energy from the ETCS loop and passes it to the heat pipe radiators. The heat pipes are much longer than the axial-groove heat pipes presented in Section 2.3.3 [26]. As such, the arterial heat pipes extend individually from the heat exchanger into space to reject heat. The portion of the heat pipe in contact with the heat exchanger, a base section about 0.91 m (3.0 ft) long on 13.11-m heat pipes, is the evaporator, while the remaining section, which is connected to a fin and rejects heat to space, is the condenser. Internally, the heat pipe uses channels shaped liked barbells to convey the fluid. The vapor travels due to a pressure gradient within the larger channel while the liquid travels in the opposite direction by a pressure gradient within the liquid channel. The pressure gradients within both channels are supplied by capillary forces acting along a slit passage which connects the two channels and runs the length of the heat pipe (Figure 2.5).

Originally Space Station planned to use arterial heat pipes with a two-phase TCS. In that configuration, the ETCS heat exchangers mentioned above were ETCS condensers. These ETCS condensers were to be attached to Space Station while the heat pipes were all individual orbital replacement units (ORUs). The arterial heat pipes could be individually replaced without disturbing the flow. Because the condensers were relatively small they could be shielded from projectile impacts. Thus, this design offered effective resistance to micrometeoroid and orbital debris. However, a major disadvantage of this design was the relatively heavy interface or clamping mechanism used to attach the individual heat pipe ORUs to the ETCS condensers.

---

[25] Generally the phase "heat pipe," when applied to spacecraft, refers to axial-groove heat pipes or similar equipment.

[26] Arterial heat pipes of at least four different length specifications have been considered or tested by NASA. These include a 6.71-m (22-ft) unit [tested on orbit in SHARE II], a 13.11-m (43-ft) unit [not tested], a 14.63-m (48-ft) unit [tested on the ground in SERS], and a 15.24-m (50-ft) unit [tested on orbit in SHARE]. Additionally, the internal designs of these different arterial heat pipes varied both due to the manufacturer and the time period. In general, the longer design specifications preceded the shorter design specifications.

ETCS Heat Exchanger

Six Arterial Heat Pipes
Plugged into One
ETCS Heat Exchanger

Heat Pipes

An Arterial Heat Pipe ORU

Heat Pipe Evaporator Cross Section

Heat Pipe Condenser Cross Section
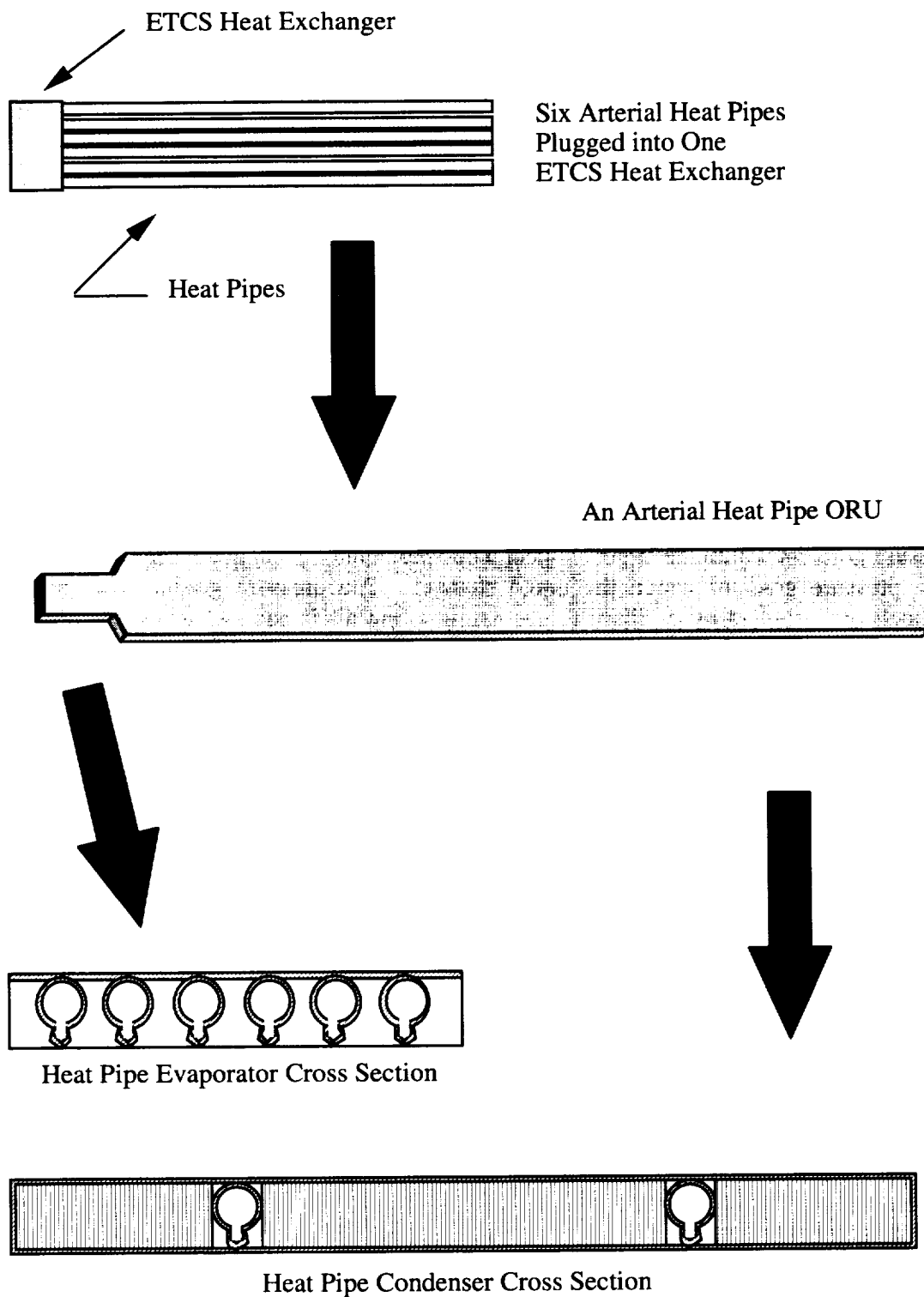
Figure 2.5 An overview of arterial heat pipes installed in a heat exchanger interface.

The previous comments apply to both of the heat pipe configurations considered below. The first configuration presented is an installation using 13.11-m (43-ft) long heat pipes [27]. Longer heat pipes during ground testing demonstrated the best heat rejection per unit mass (Chambliss and Ewert, 1990). Thus, the 13.11-m heat pipes were originally selected as part of the Space Station baseline ATCS. Tests on orbit using a 15.24-m heat pipe [28] were less than satisfactory. A shorter heat pipe, 6.71-m (22-ft) long, functioned well when tested on orbit (Brown, Ungar, and Cornwell, 1992) [29].

13.11-meter (43-foot) Long Arterial Heat Pipe Panels

The components for the arterial heat pipe radiator installation using 13.11-m panels are:

Arterial Heat Pipe Radiator Components (Chambliss and Ewert, 1990, Kantara, 1989, and LTV, 1990)	Mass [kg]	[lb$_m$]	Radiating Area [m^2]
ETCS Condenser (per ORU panel) [30]	22.90	50.49	--
Arterial Heat Pipe ORU Panel (dry) [31]	39.01	86.00	7.43
Heat Pipe Working Fluid (ammonia)	1.87	4.13	--
Radiator Beam Truss (per ORU panel)	1.59	3.50	--
Total Mass and Area (per ORU panel)	65.37	144.12	7.43

The component masses, based on Kantara (1989), for the 13.11-m arterial heat pipes are:

	Study Panel
Overall Length [m]	13.11
Evaporator Section: Length [m]	0.91
Mass [kg]	5.20
Condenser Section: Length [m]	12.19
Mass [kg]	33.81
Total Dry Panel Mass [kg]	39.01

The mass per radiating area is 8.80 kg/m^2. Unfortunately, longer heat pipes using a similar internal configuration to the 13.11-m units did not function properly during the on-orbit SHARE test. If this design were modified to incorporate the knowledge gained from the

---

[27]   This length is the longest which will fit in the payload bay of a Shuttle (STS) vehicle.

[28]   This is the SHARE test.

[29]   This is the SHARE II test. Besides the length, the heat pipe tested during SHARE II used a different internal arrangement than the heat pipe tested during SHARE.

[30]   Chambliss and Ewert (1990) mention that the ETCS condenser mass per ORU panel includes 14.0 kg (30.9 lb$_m$) for the interfacial clamping mechanism in the LTV design.

[31]   These values are for a 13.11-m (43.0-ft) LTV arterial heat pipe. The condenser is 0.30 m (12.0 in.) wide. The evaporator is 0.91 m (36.0 in.) long and 0.23 m (9.0 in.) wide. The panel is 0.0279 m (1.10 in.) thick (Oren, 1995). Depending on the thickness, the LTV 13.11-m panels vary in mass from 32.91 kg to 40.88 kg. The corresponding Grumman panels vary in mass from 41.19 kg to 49.41 kg. The ETCS condenser masses per panel are 22.90 kg and 19.05 kg for the LTV and Grumman panels, respectively (Kantara, 1989).

SHARE II test, it is expected that this heat pipe should operate properly (Ungar, 1996). However, additional testing on orbit would still be needed to flight certify this design.

6.71-meter (22-foot) Long Arterial Heat Pipe Panels

The components for the arterial heat pipe radiator installation using 6.71-m panels are:

Arterial Heat Pipe Radiator Components (LTV, 1990)	Mass		Radiating Area [m^2]
	[kg]	[lb$_m$]	
ETCS Condenser (per ORU panel) [32]	19.73	43.50	--
Arterial Heat Pipe ORU Panel (wet) [33]	45.05	99.32	6.94
Radiator Beam Truss (per ORU panel)	3.81	8.39	--
Total Mass and Area (per ORU panel)	68.59	151.21	6.94

The mass per radiating area is 9.88 kg/m^2.

The arterial heat pipes will have high reliability due to using numerous individually sealed elements and their ease of replacement. Loss of a single heat pipe ORU will have negligible effect on the overall ATCS heat rejection. Further, any one heat pipe can be replaced much more easily than a flow-through radiator panel. The overall volume for either installation of arterial heat pipe radiators is similar to the baseline flow-through radiators. The development cost of this option is low for the 6.71-m units because previous work moved them to a TRL of 8. The 13.11-m units have a TRL of 6 but still require a test on orbit to verify proper internal circulation due to the available capillary forces. Thus, they will have a high development cost. Arterial heat pipes are flexible to deploy. They can be individually replaced by astronauts on an extravehicular activity. Arterial heat pipes can also be manufactured as larger panels by joining several individual heat pipes together. On a planetary body, arterial heat pipes must be installed level to the surface so that the local gravity does not supplant the intended working fluid circulation path with another flow path. However, a horizontal orientation exposes an arterial heat pipe to full solar irradiation at local noon, which seriously degrades this system's ability to reject heat. Thus, no terrestrial uses are expected for this technology.

---

[32] The condenser has a mass of 6.80 kg (15.0 lb$_m$) and the interface mechanism and socket have a total mass of 12.93 kg (28.5 lb$_m$).

[33] These values are for a 6.71-m (22.0-ft) LTV arterial heat pipe. The condenser is 0.61 m (24.0 in.) wide and 5.69 m (224.0 in.) long. The evaporator is 0.23 m (9.0 in.) wide. The transition zone between the evaporator and condenser is 0.33 m (13 in.) long.

General Qualitative Assessments:

Technology Readiness Level [34]	8
Volume	average
Deployment	average
Reliability	improved
Development Cost	low
Terrestrial Use Potential	none
Composite Qualitative Score [35]	+1

2.3.2   Arterial Heat Pipe Radiators With Electrohydrodynamic Pumping

In general, heat pipes depend upon capillary forces to keep the working fluid circulating. When the transport limit is exceeded, the working fluid may collect in the heat pipe condenser and render the affected unit unusable. To maintain the capacity of a heat pipe system, designers add extra units so that the heat transport capacity of all heat pipes is sufficient for the anticipated load. To augment the heat transfer capacity of individual heat pipes, Bryan (1995) proposes applying electrohydrodynamic pumping to each individual unit. This arrangement would guard against the working fluid collecting in the condenser and ensure that each unit would be able to continually reject its applied heat load. For the arterial heat pipes presented in Section 2.3.1, Bryan proposes that one of two condenser extrusions be removed. The fin efficiency is expected to decrease from 0.925 to 0.763. The added mass for electrohydrodynamic pumps is assumed equivalent to an additional two extrusions in the evaporator section. Currently arterial heat pipes have two condenser extrusions and six evaporator extrusions. Additionally, the electrohydrodynamic pumps would require 2 W of power per heat pipe. Further, it is assumed that electrohydrodynamic pumping will allow the 13.11-m heat pipes to function as envisioned so they form the basis for the analysis here. Thus, using electrohydrodynamic pumping for arterial heat pipes:

---

[34]   The TRL for the 6.71-m units is 8, while the TRL for the 13.11-m units is only 6.

[35]   This applies to the 6.71-m units. The 13.11-m units have a "high" development cost and an overall score of -1.

	Arterial Heat Pipe Without Electrohydrodynamic Pumping	Arterial Heat Pipe With Electrohydrodynamic Pumping [36]
Evaporator Section Mass [kg]	5.20	6.93
Condenser Section Mass [kg]	33.81	22.54
Heat Pipe Working Fluid Mass [kg]	1.87	1.87
Electrohydrodynamic Pumping Power [kW]	--	0.002
Electrohydrodynamic Pumping Power as Mass [kg]	--	0.95
Total Panel Mass [kg]	40.88	32.29

The overall mass, including the ETCS interface, per radiating area is 7.64 kg/m^2.

The overall volume for the arterial heat pipe radiators is slightly larger than the current baseline radiator architecture due to the lower fin efficiency. However, this difference may not be significant. Like arterial heat pipes, this radiator configuration should have high reliability. While significant work and some prototype testing have been completed for arterial heat pipes, a reasonable amount of work is needed to develop working electrohydrodynamic pumps. Thus, the TRL is currently 4. The development cost for this option is expected to be high because this assessment is based on the unproven 13.11-m units which still require on-orbit testing. Finally, there may be some terrestrial uses for these technologies. (See Sections 2.1.3 and 2.3.1.) However, because this is an integrated package, no assessment for terrestrial use potential is offered here.

General Qualitative Assessments:

Technology Readiness Level	4
Volume	average
Deployment	average
Reliability	improved
Development Cost	high
Terrestrial Use Potential	--
Composite Qualitative Score	(0)

2.3.3 Axial-Groove Heat Pipe Radiators

Axial-groove heat pipe radiators take advantage of capillary forces to transfer heat between hot and cold reservoirs. In practice, axial-groove heat pipes are long tubes with longitudinal fins around the inner wall. Each heat pipe is filled with an appropriate working fluid and sealed on both ends. Each end is placed in thermal contact with either

---

[36] For purposes of this estimate, the heat pipe with electrohydrodynamic pumping uses an evaporator mass multiplier of 8/6 and a condenser mass multiplier of 2/3 times the values for the panel without electrohydrodynamic pumping. The condenser mass multiplier is not one half because the facesheets are the same for each heat pipe.

the hot or cold reservoir. At the hot end of the heat pipe, the working fluid absorbs heat by evaporating. At the cold end of the heat pipe, the working fluid releases heat by condensing to the periphery. Physically, axial-groove heat pipes operate similarly to arterial heat pipes. In axial-groove heat pipes, the vapor flows through a central core while the liquid returns in grooves between internal longitudinal fins running the length of the heat pipe on the periphery. The grooves also provide the wicking, or the capillary driving force, that the slit provides in an arterial heat pipe (Figure 2.6).

Heat pipe radiator panels could be used to replace the existing flow-through radiator panels for active thermal control (Nguyen, 1992). In this application, heat pipes replace the flow-through tubes which join the fluid manifolds on either edge of the radiator panels. The hot end of each heat pipe is placed in thermal contact with working fluid from the ETCS as it enters the radiator assembly while the cold end is placed in contact with the radiator face sheet. In practice, heat pipes are placed between two separate manifolds which each contain an entering and returning line for the ETCS working fluid

Heat-pipe panels are expected to be more reliable than conventional flow-through radiators. A micrometeoroid puncturing any radiator ORU panel destroys only a single heat pipe. However, because axial-groove heat pipes only replace the flow-through panel flow tubes, which have a fairly low probability of puncture compared with the overall probability of a loop puncture, this is not a significant consideration for this technology (Christiansen, 1992). Finally, axial-groove heat pipes are a proven technology with a TRL of 9. Axial-groove heat pipes have been used successfully to reject heat on robotic spacecraft (Nguyen, 1992). However, the TRL for an integrated radiator using axial-groove heat pipes in place of flow-through tubes is only 6. Thus, the developmental cost for such a system is low. Finally, there may be some terrestrial uses for this technology. These units resemble reflux boilers or other similar devices.

General Qualitative Assessments:

Technology Readiness Level	6
Volume	average
Deployment	average
Reliability	average
Development Cost	low
Terrestrial Use Potential	possible
Composite Qualitative Score	+1

2.4　Lightweight Radiators

Lightweight radiators replace conventional materials within radiator units with lighter, high-strength substitutes. The strength and efficiency of the radiator units which are critical to specific missions are maintained while the overall mass is reduced. Further, by tailoring the system specifically to its final environment, such as on a planetary surface versus on orbit, newer radiator designs are optimized for the intended mission.

Radiator Manifolds

Radiator
ORUs

Radiator Panel

Heat Extracted from
Manifolds (Fluid Evaporates
Inside of Heat Pipe)

A

A

Heat Pipe

Heat Rejected
to Space (Fluid
Condenses Inside
of Heat Pipe)

Liquid Travels by Capillary
Action Between the Fins

Vapor Travels by Pressure
Difference in the Pipe Core

Crosssection A-A
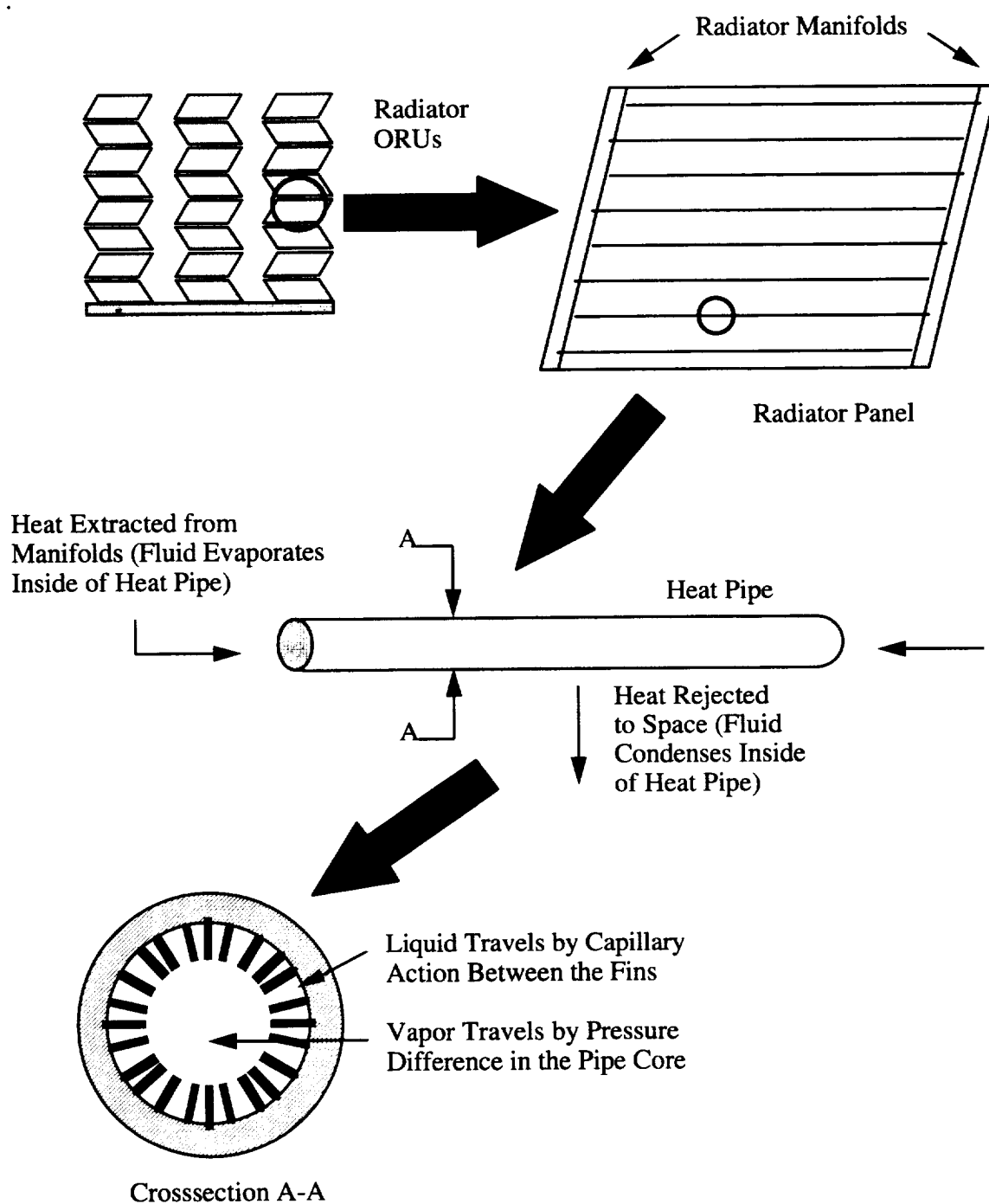
Figure 2.6   An overview of axial-groove heat pipes installed in a radiator orbital
replacement unit.

Several concepts which are lighter versions of other radiators are examined here. Thus, this section's uniting technologies are the composites and fabrication techniques employed to produce each of these radiators rather than a specific heat transfer mechanism or similar equipment as in other sections. Initially, each radiator is evaluated to determine its relative mass per surface area. These estimates provide guidance for generic estimates of the mass savings expected for a particular mission when using lightweight radiators. Such generic mass savings are employed throughout this study for lightweight radiators. Once further details for specific lightweight radiator concepts become available, those concepts might be assessed individually for the various reference missions.

2.4.1 Composite Flow-Through Radiators

This lightweight radiator concept applies composite materials to the traditional flow-through radiator architecture. This concept is under development to possibly replace or supplement the water sublimator currently used to reject heat from the portable life support system of the extravehicular mobility unit (Cross, 1996). The heart of this design employs flow-through radiator panels utilizing flow passages of rectangular cross section formed from sheets of carbon composite material. Above the sheet of flow passages is placed another sheet of carbon composite material separated by a thin gap. The gap is either evacuated or filled with low-pressure nitrogen gas (10 torr). While the gap is filled with gas, it will provide conduction paths between the sheet of flow tubes and the separated sheet. When the gap is evacuated, the only heat exchange mechanism between the sheet of flow passages and the separated sheet is radiation. In other words, the evacuated gap effectively acts as insulation for the sheet of flow passages. This prevents the working fluid from freezing (Figure 2.7). The mass per radiating area for single-sided heat rejection using this design is 8.21 kg/m^2. This value includes mass for the manifolds and assumes ammonia as the working fluid. For a double-sided radiator panel, the mass per radiating area is 4.67 kg/m^2 after accounting for an additional gas gap cover sheet.

There are several issues about this concept which require more work. The most ingenious aspect of this concept is the use of a gap, which may use either conductive or radiant heat transfer, to control the rate of heat loss from the radiating surface. This, in turn, allows the user to protect the radiator from cold environments while making full use of the radiating surface for hot environments. This is an extremely useful development. The current design, which is under development for possible use in an extravehicular mobility unit, is too heavy to be applied directly to vehicle or habitat thermal control architectures. However, this design for an extravehicular mobility unit uses flow passages which are spaced so close to each other as to render the radiator fin efficiency as almost unity. As such, a composite flow-through radiator could possibly have a much lighter mass per area when optimized for a base or habitat. Further, though the radiator itself is fairly rigid, work to date has not addressed the structure or deployment necessary to integrate this technology into a large TCS. Thus, this concept is presented here because of its general utility even though it is not ready to be applied to a vehicle or habitat TCS.

The composite flow-through radiator is in many ways identical to the baseline metal flow-through radiators. As such, the volume and deployment for this concept are expected to be average. The reliability will also be average although the method of protecting the radiator from episodes of frozen working fluid within the flow passages differs from that of the baseline architecture. Even though the TRL is 4, the development

cost for this technology is expected to be average because all remaining testing may be completed in terrestrial facilities. Terrestrial uses for this technology, or at least for the material processing techniques used to develop these components, is highly likely.

General Qualitative Assessments:

Technology Readiness Level	4
Volume	average
Deployment	average
Reliability	average
Development Cost	average
Terrestrial Use Potential	good
Composite Qualitative Score	+1

2.4.2 Composite Reflux Boiler Tube Radiators

Composite reflux boiler tube radiators [37] utilize thin-walled reflux tubes encased in an epoxy sleeve as radiator elements. As such, these devices require a gravitational field to operate efficiently. The units currently under development have a circular cross-section with a diameter of 0.02395 m and a length of 1.143 m. The condenser section length is 1.067 m, which implies a radiating surface area of 0.08027 m^2 per unit. Because these units are not finned, the effective fin efficiency is 1.0. This radiator, however, will "see" other portions of itself so its view factor to space will not be 1.0 as it is for a planer radiator. The exact view factor to space will depend upon the selected tube configuration. Each unit includes a thin-walled titanium tube surrounded by an outer sleeve of epoxy composite. The composite outer sleeve provides burst support for the titanium tube. Each unit has a mass of 0.165 kg including 0.020 kg of water which is the working fluid (Thermacore, 1995 b). An ETCS interface for 320 tubes for a similar deployment has an estimated mass of 35.62 kg (Blades, 1996) [38].

Composite Reflux Boiler Tube Unit Components	Component [kg]
Titanium Liner / Epoxy Sleeve	0.145
Working Fluid (water)	0.020
ETCS Interface per Tube	0.111
Mass per Tube	0.276

---

[37] An earlier reflux boiler tube radiator concept is the ultralight fabric reflux tube radiator (Hurlbert, Ewert, Graf, Keller, Pauley, Guenther, and Antoniak, 1996). While the composite reflux boiler tube is a descendent of the previous project, it does not share the shortcomings associated with the ultralight fabric reflux tube units.

[38] The estimate here for the ETCS interface is based on the ultralight fabric reflux tube which is similar in dimensions to other reflux boiler tube designs.
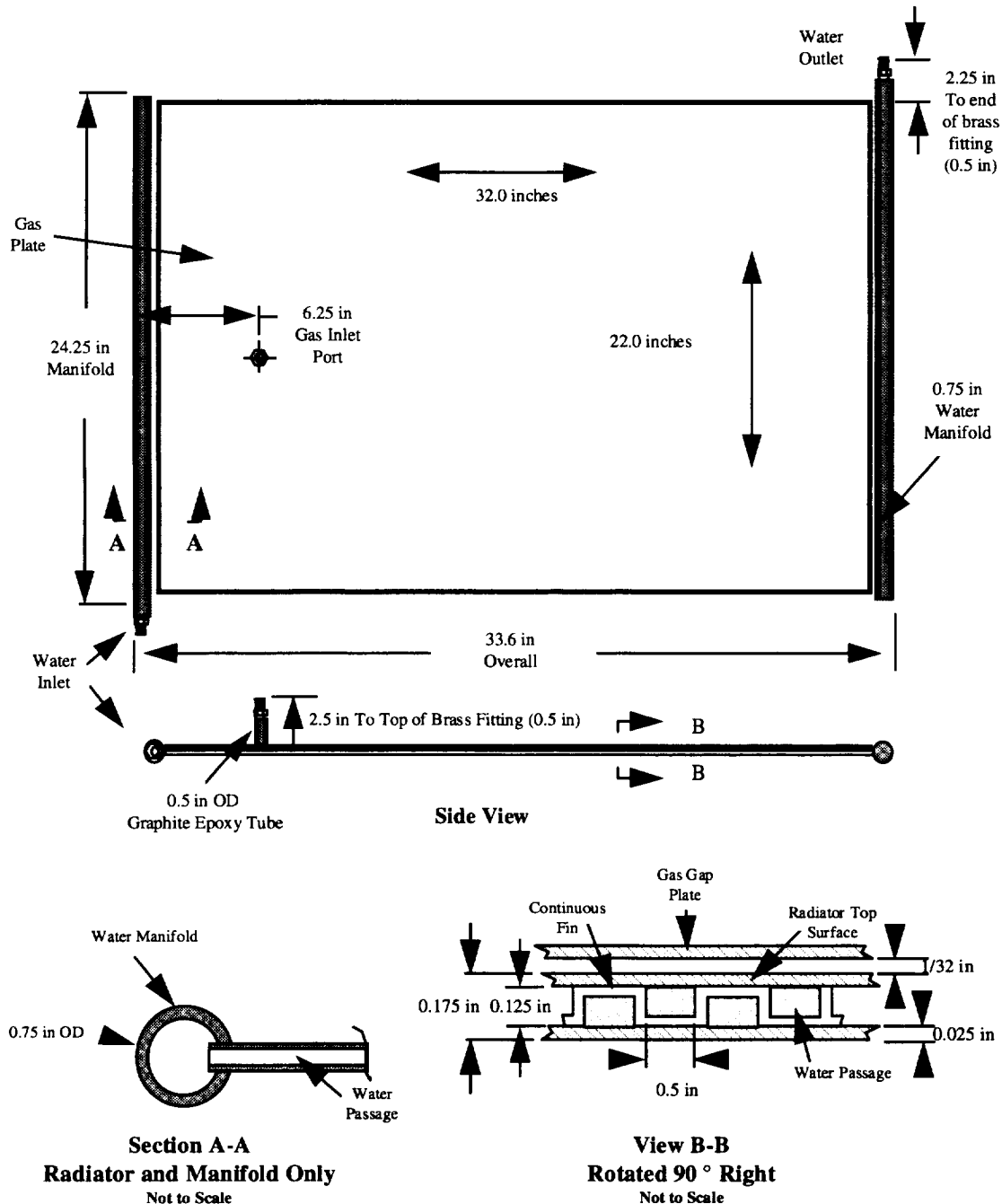
Figure 2.7 The configuration for the extravehicular activity composite radiator test article from Cross (1996). This concept is based on the traditional single-phase, flow-through radiator architecture. The carbon composites form the unit instead of aluminum as in the baseline architecture. Additionally, this radiator features a gas gap which insulates the flow passages when evacuated. The portable life support system for which this concept is under consideration will use water as its working fluid. However, a thermal control system radiator using this approach will probably circulate ammonia or another fluid besides water.

The overall mass per surface area for composite reflux boiler tube radiators is 3.44 kg/m². While planetary surface missions are not expected to operate in high debris fields, composite reflux boiler tube radiators are very similar, with regard to redundancy, to arterial heat pipe radiators. If necessary, the ETCS interface could be shielded from debris punctures while the composite reflux boiler tube radiator units remain exposed to the environment. A puncture in one or even a few units would not significantly reduce the heat-rejection ability of the overall system. Based on their architecture, composite reflux boiler tube radiators have improved reliability. The deployment of the overall system is also expected to be comparable to the baseline architecture, although the vertical geometry of the reflux tube units may be advantageous in some cases. The volume should be no more than that of the baseline architecture. The development cost for this technology is low because the TRL is already 5 and any remaining testing may be completed in terrestrial facilities. From this application, both the lightweight reflux boiler tubes and the associated material processing techniques could have terrestrial uses.

General Qualitative Assessments:

Technology Readiness Level	5
Volume	average
Deployment	average
Reliability	improved
Development Cost	low
Terrestrial Use Potential	good
Composite Qualitative Score	+3

2.4.3   Composite Heat Pipe Radiators

Composite heat pipe radiators are a lightweight variation on the heat pipes presented in Section 2.3.3. Based here on the work of Juhasz and Bloomfield (1994) and Juhasz and Rovang (1995), the composite heat pipe is constructed from a thin niobium-zirconium alloy foil liner covered by a carbon-carbon composite outer shell. The foil liner has a wall thickness of 0.064 millimeters which is furnace brazed to the composite outer shell. The evaporator section, which extends 0.076 m beyond the composite liner on one end of the unit, has a thicker wall of 0.4 millimeters. The heat pipe itself has a circular cross section with a diameter of 0.025 m. The composite shell, with two opposing 0.05 m wide fins, surrounds the foil liner for the length of the condenser section, 0.914 m [39]. The composite has a thermal conductivity of roughly 0.575 kW/(m*K) at 300 K [40]. The overall test unit is about a meter in length.

---

[39]   The view factor to the environment and the fin efficiency of this radiator are unknown but both are less than unity. To avoid this problem, numerical analysis, correlation, or experiment are useful.

[40]   This heat pipe research was funded by NASA Lewis Research Center to develop radiators to reject high temperature heat from power systems in space. This information is provided by Juhasz (1996).

The components for the composite heat pipe radiator installation are:

Composite Heat Pipe Radiator Components (Based on Juhasz and Bloomfield, 1994, and Juhasz and Rovang, 1995)	Mass [kg]	Radiating Area [m^2]
ETCS Interface (per composite heat pipe) [41]	0.111	--
Composite Heat Pipe Panel (dry)	0.322	0.2335
Working Fluid (per composite heat pipe)	0.014	--
Total Mass and Area (per composite heat pipe)	0.447	0.2335

The component masses for the composite heat pipes are (Juhasz and Rovang, 1995):

Masses of 0.99 m Test Panel Components	Component Mass [grams]
Carbon-Carbon Composite Shell	214.0
Liner Including Evaporator	41.2
End Caps	13.1
Fill Tubes	7.2
Braze	22.5
Wick	24.0
Working Fluid (liquid metal) [42]	13.5
Mass per Panel	335.5

The overall mass per surface area for composite heat pipe radiators is 1.91 kg/m^2. This unit is designed to operate vertically on a planetary surface. Because the composite heat pipe already contains an integral wick, slight modifications should allow them to function under microgravity also (Juhasz, 1996). The volume for this installation will probably be comparable to that of the baseline architecture. Significant work and prototype testing have been completed for composite heat pipes, although flight-testing is still required for any on-orbit applications. The current TRL is 5. Thus, the development cost is expected to be low for planetary applications and high for orbital applications. Like the arterial heat pipes presented in Section 2.3.1, the composite heat pipes detailed here should provide a high level of radiator redundancy and therefore have high reliability. Terrestrial uses from this technology include advances in materials processing plus those presented for axial-groove heat pipes in Section 2.3.3.

---

[41]　The ETCS interface is assumed to be similar to the unit given by Blades (1996). See Section 2.4.2.

[42]　The high temperature (800 K) application investigated by NASA Lewis Research Center required liquid metal as a working fluid. However, Juhasz and Rovang (1995) note that this technology has been demonstrated for the 400 K to 450 K range using a stainless steel foil liner and demineralized water as the working fluid. Both the high temperature panel and this low temperature panel have roughly the same mass (Juhasz, 1996).

General Qualitative Assessments:

Technology Readiness Level	5
Volume	average
Deployment	average
Reliability	improved
Development Cost	low
Terrestrial Use Potential	good
Composite Qualitative Score [43]	+3

2.4.4 Unfurlable Radiators

Unfurlable radiators and composite reflux boiler tube radiators both utilize reflux boiler tubes as their base heat-rejection element. Unfurlable radiators differ from the previous concept in that the boiler tube condenser is flexible instead of rigid. In fact, the condenser wall is manufactured from a metal and plastic laminate which collapses under terrestrial atmospheric pressures when the unit is not operating (Gernert and Donovan, 1994). When the unit is operating, the internal working fluid vapor is sufficient to inflate the condenser. As with other reflux boiler tube devices, unfurlable radiators require a gravitational field to operate properly. To package this concept, the unfurlable radiator tubes would be affixed to an interface module. Upon activating the TCS, working fluid vapor would inflate the radiator unit condensers.

The prototype test units have a circular cross-section with a diameter of 0.01905 m and an overall length of 1.000 m. The condenser section length is 0.951 m which implies a radiating surface area of 0.05694 m^2 per unit (Thermacore, 1995 a). These prototype units are not finned, so their effective fin efficiency is 1.0. Again, this radiator will "see" other portions of itself so its view factor to space will not be unity as it is for a planer radiator. The exact view factor to space will depend upon the selected unit configuration. Each unit includes a thin-walled polymeric film and metal laminate condenser attached to a rigid evaporator base. In the completed radiator, the evaporator units sit in an ETCS interface assembly which supplies the heat load. An ETCS interface for 320 reflux boiler tubes has an estimated mass of 35.62 kg (Blades, 1996) [44].

Composite Reflux Boiler Tube Unit Components (Thermacore, 1996)	Component [kg]
Condenser With Fiber and Cap	0.051
Evaporator, Epoxy, and Cap	0.089
Working Fluid (water)	0.012
ETCS Interface per Tube	0.111
Mass per Tube	0.263

---

[43] This is for planetary missions. For orbital missions, the development cost is "high" and the overall score is +1.

[44] The estimate here for the ETCS interface is based on the ultralight fabric reflux tube which is similar in dimensions to other reflux boiler tube designs.

The overall mass per surface area for unfurlable radiators is 4.62 kg/m². While planetary surface missions are not expected to operate in high debris fields, unfurlable radiators are very similar, with regard to redundancy, to arterial heat pipe radiators. If necessary, the ETCS interface could be shielded from debris punctures while the radiator units remain exposed to the environment. A puncture in one or even a few units would not significantly reduce the heat-rejection ability of the overall system. The deployment of the overall system should be easy because little setup is required for this radiator. The vertical geometry of the reflux tube units may be advantageous in some cases. The stored volume should be less than that of the baseline architecture. The development cost for this technology is expected to be average because prototype testing is in progress and the current TRL is 4. As with other lightweight radiators, the primary terrestrial use from this program will probably be advances in processing composite materials.

General Qualitative Assessments:

Technology Readiness Level	4
Volume	compact
Deployment	easy
Reliability	improved
Development Cost	average
Terrestrial Use Potential	good
Composite Qualitative Score	+4

2.5   Other Heat Rejection Technologies

Several other radiator-related technologies are under consideration for near-term missions. These include using phase-change materials (PCMs), to provide supplemental cooling for short periods requiring higher than average heat rejection, and radiator shades, which shield a radiator from strong irradiation sources.

2.5.1   Phase-Change Thermal Storage

To implement phase-change thermal storage within an ETCS, a portion of the empty volume within the radiator panels could be filled with packages of PCM, or wax [45]. These packages would be positioned around the current flow-through tubes within the radiator panels. When the vehicle experiences high heat loads, the hot ETCS working fluid could pass through these radiator panels and melt the previously solidified PCM, effectively increasing the rate of heat removal from the working fluid while the PCM melted. When the vehicle experiences low heat loads, the tubes surrounded by PCM could be bypassed, allowing the PCM to solidify. At least two scenarios are possible to size a phase-change thermal storage device.

---

[45]   A PCM for an application is a solid at the minimum operating temperature, but the material melts at some temperature below the maximum system operating temperature. Thus, they mimic candle wax, which is solid at room temperature, but melts easily near a source of flame. In fact, long-chain alkanes, which are a class of compounds including waxes, are useful as PCMs.

One case would presume to replace a heat-rejection system which uses expendable materials with phase-change thermal storage. A system using expendables is sized to handle an expected heat load for some finite length of time, such as that experienced by a vehicle during aero-braking. An example of a heat-rejection device using expendable materials is the ammonia boiler subsystem on STS.

A second case assumes that phase-change thermal storage is used to provide auxiliary cooling in conjunction with other heat-rejection systems such as radiators and heat-rejection devices using expendable materials. In particular, phase-change thermal storage could reduce usage of the expendable heat-rejection device, thereby reducing the mass consumed by the vehicle [46]. The PCM packages are solidified while the radiator rejects heat above the average orbital value and the PCM is allowed to melt to provide additional cooling while the radiator is rejecting heat below the average orbital value. Because the radiator heat load varies around an orbit, even when a vehicle is entirely in full sun at high beta angles, this approach is generally applicable. Figure 2.8 schematically illustrates the assumed implementation of phase-change thermal storage for Shuttle. The PCM packages could be integrated within the aft radiator panels around the existing tube bundle and panel honeycomb [47] or in a separate unit placed either upstream or downstream of the radiator panels [48].

For this study, two materials were considered. Water has a thermal density [49] of 10.0 kg/kW*h for phase-change applications, or 18.0 kg/kW*h including packaging [50]. Water solidifies at 273.2 K under standard atmospheric pressure. Further, water also expands upon solidifying. A long-chain alkane, or wax, such as n-dodecane, has a thermal density of 16.8 kg/kW*h for phase-change applications, or an assumed value of 30.2 kg/kW*h including packaging. n-Dodecane solidifies at 263.6 K under standard atmospheric pressure. While water is the preferred material, n-dodecane is assumed to be representative of a range of alkanes which, taken collectively, could be tailored to handle phase-change loads over a wide range of temperatures [51]. Water, however, is restricted to applications near 273.2 K.

From a qualitative perspective, phase-change thermal storage offers some advantages. The volume consumed by this system could be negligible because it could fill volume already set aside for radiators. Installation for this system should be relatively easy because the proposed components should readily fit in available volume. The reliability should be comparable to the current systems. This technology uses the passive technology

---

[46] For example, as designed, Shuttle uses water generated by the production of electricity in its fuel cells as feedwater for the flash evaporator subsystem. Early in the next century, however, that water generated by Shuttle's fuel cells may be tapped as a source of potable water to be delivered to ISS or for the crew on extended-duration Shuttle missions. Use of phase-change thermal storage would save some water which currently is consumed by the flash evaporator subsystem.

[47] The panel honeycomb is aluminum and provides additional conduction pathways for heat transport from the radiator tubes to the radiator surface sheet, which is a fin. Thus, the honeycomb is effectively an extension of the surface fin.

[48] The thermal densities used in this study for estimating the mass of the phase-change thermal storage device include packaging mass and do not assume an in-panel installation.

[49] Thermal density is defined here as 1/(heat of fusion).

[50] Packaging mass is assumed to be 80% of the mass of the PCM.

[51] The actual melting points of the various alkanes differ, but their overall thermal densities are assumed to be roughly similar to that of n-dodecane.

of phase-change cooling but requires sensor units and automatically controlled valves, so reliability is expected to be average. Even though phase-change thermal storage has been tested on orbit historically, the TRL for missions here is 5. Thus, the cost to integrate this technology into other missions should be no more than average. Terrestrial applications may exist for the PCMs when packaged within personal protection suits for high temperature applications. Applications may also exist for cooling equipment, such as machinery for cutting or forming of hard materials, which can experience extremely high heat loads for short intervals. PCMs might also be incorporated as packaging materials for any item which is to be maintained at a temperature other than that of its environment.

Current Shuttle Cooling Schematic
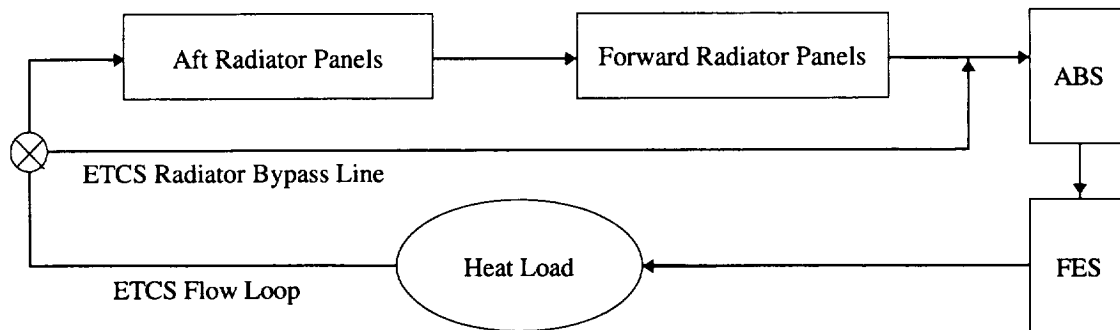
Revised Shuttle Cooling Schematic with Phase-Change Material Packages
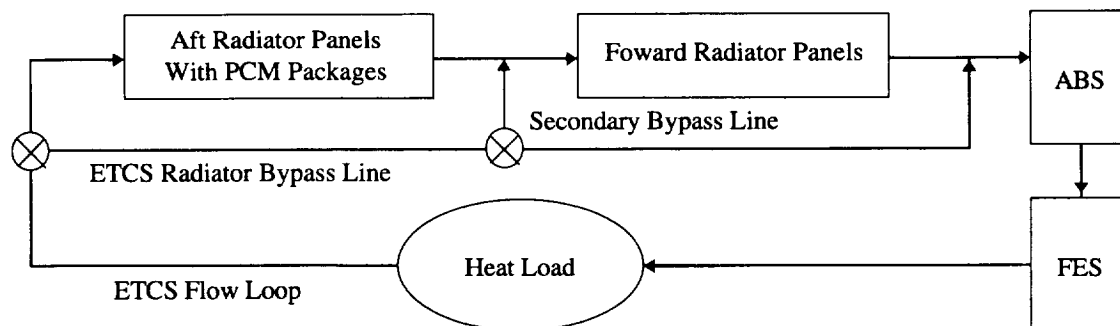
Figure 2.8 To integrate phase-change thermal storage into Shuttle, the phase-change material packages could be placed within the aft radiator panels or in units outside of the radiators. To solidify the phase-change material while the radiators are facing a relatively cold environment, the ETCS flow loop, which is warmer than the melting point of the phase-change material, bypasses the phase-change material packages by means of the secondary bypass line. While the vehicle is in a hot environment, the ETCS flow loop can receive additional cooling by melting the previously solidified phase-change material.

General Qualitative Assessments:

Technology Readiness Level	5
Volume	compact
Deployment	average
Reliability	average
Development Cost	average
Terrestrial Use Potential	good
Composite Qualitative Score	+2

2.5.2 Parabolic Radiator Shade

Parabolic radiator shades provide a means of lowering the effective sink temperature around a radiator to allow heat rejection at temperatures associated with waste heat from environmental control and life support systems for human beings. The shade, which has a specular upper surface and gray under surface, is designed to redirect incident solar radiation back to space while directly blocking diffusely scattered and infrared radiation from the lunar surface (Ewert and Clark, 1991, Keller, 1994, and Ewert, Graf, and Keller, 1995). More specifically, the shade's parabolic shape focuses the incoming solar radiation along a line above a radiator placed in the shade's trough. The surface coatings on the lower side of the shade reflect thermal energy from the planetary surface (Figure 2.9). The shade must be aligned such that the incident solar vector is parallel to the radiator throughout the day. Otherwise, the shade itself will direct solar radiation on to the radiator in addition to any energy directly striking the side of the radiator. Because Luna only tilts 1.53 degrees on its axis from the orbital plane, a parabolic radiator shade is ideal at the lunar equator and can be readily adapted for other lunar sites.

The overall volume is expected to be similar or slightly more compact than a standard radiator. For a long term mission, deployment of a radiator shade should be comparable to deployment of a larger flow-through radiator system. For a lander vehicle, an extravehicular activity may be required to align the shade system properly and this would be more difficult than deploying radiators mounted on the vehicle. The reliability is expected to be the same as standard equipment for the short duration mission. For longer missions, the issue of dust accumulation on the radiator shade, which degrades the shade's effectiveness, is more significant. Occasional replacement of the shade for longer missions should alleviate this problem. The program TRL is 5. Some additional testing is needed, but the development cost remaining is average. Currently, no terrestrial uses are expected for the parabolic radiator shade.
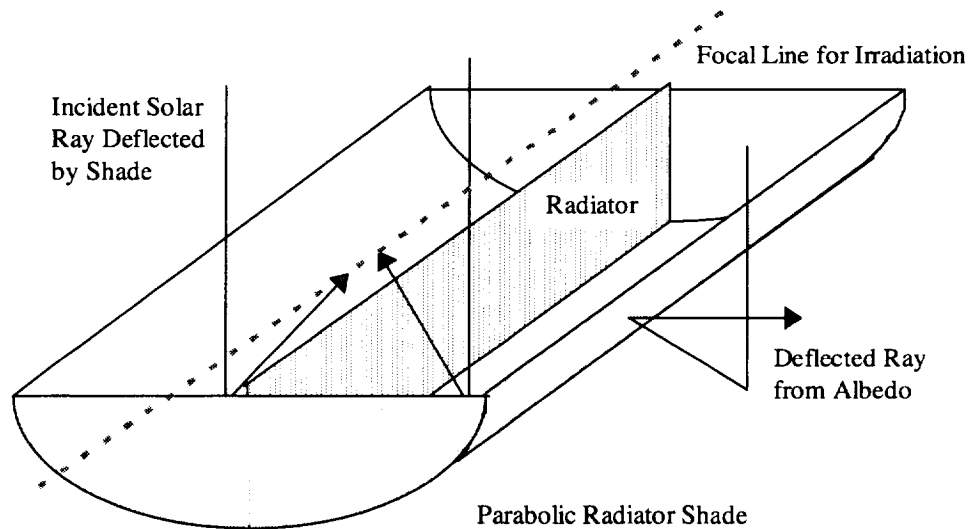
Figure 2.9 A parabolic radiator shade around a vertical radiator. The incident solar irradiation hitting the upper shade surface is reflected to a focal line above the radiator, while irradiation from the planetary surface is deflected away by the underside of the shade. Endsheets guard the radiator from radiation enterting through the ends of the shade.

General Qualitative Assessments:

Technology Readiness Level	5
Volume	average
Deployment [52]	average
Reliability	average
Development Cost	average
Terrestrial Use Potential	none
Composite Qualitative Score	-1

2.6   Additional Technologies

The heat transfer technologies presented below are unlike other technologies presented in this study.

2.6.1   Rotary Fluid Coupler

In the ISS TCS, the radiator ORUs are clustered in two sets of three ORUs each. Each cluster is fixed to a truss which rotates on a thermal radiator rotary joint (TRRJ) to maintain the radiator panel faces parallel to the local solar vector. This arrangement

---

[52]   For missions where a vehicle mounted system is preferable, the deployment for this option would be "difficult" yielding a Composite Qualitative Score of "-2" for this technology.

minimizes solar absorption by the radiators. To allow ATCS fluids to pass from within ISS to the ETCS radiators, a rotary coupler is part of each TRRJ.

A rotary fluid coupler is a fully rotating device which uses liquid seals to contain and separate the internal fluid flow channels (Harwell, 1992). A fully rotating device allows the radiators to always be aligned with the panel faces parallel to the solar vector. The projected rotary fluid coupler mass is 10.9 kg (24 lb_m) with an approximate volume of 0.0127 m^3 (0.45 ft^3). Further, the rotary fluid coupler is expected to be more reliable than the baseline coupler because its components have longer service lives and its smaller size makes it less susceptible to micrometeoroid puncture. Also because of its size, the rotary fluid coupler is easier to replace. The rotary fluid coupler is similar in size and mass to a pump allowing it to be readily handled by an individual astronaut. The rotary fluid coupler also displays some disadvantages. The liquid seals between flow channels permit low amounts of leakage between channels when they wear, but this is not a significant problem. Further, the rotary fluid coupler is geometrically different from the current coupler. As such, it may be expensive to retrofit ISS to accept rotary fluid couplers.

Even though the previous rotary fluid coupler program was discontinued, significant work has been completed. The TRL is 7. Therefore, the developmental costs should be low. This technology provides a generic, low-leakage rotary coupler. However, the rate of rotation is limited to 45 degrees per minute. Therefore, terrestrial uses may be possible in some large industrial machines.

General Qualitative Assessments:

Technology Readiness Level	7
Volume	compact
Deployment	easy
Reliability	average
Development Cost	low
Terrestrial Use Potential	possible
Composite Qualitative Score	+3

2.6.2 Plant Chamber Cooling Improvements

Regenerative life support systems are of great importance as an enabling technology for extended-duration missions with crews. In particular, plant growth chambers promise to provide future space explorers with both food and oxygen replenishment. The practical aspect of this system then becomes optimizing the edible biomass (food) produced by a plant growth module as a function of mass. This study concentrates on improving an assumed baseline chamber by adding more reliable/less massive equipment in place of the baseline materials.

The baseline plant growth module for this study is patterned after a test chamber at the Lyndon B. Johnson Space Center in Houston, Texas, built by the NASA Crew and Thermal Systems Division. Jerng (1991) and Barta, Dominick, and Kallberg (1995) provide descriptions of this chamber which is known as the Johnson Space Center 10-foot Regenerative Life Support System Test Chamber or, more recently, as the Variable

Pressure Growth Chamber (VPGC). The relevant overall parameters of the plant chamber assumed here are (Jerng, 1991) [53]:

Physical Dimensions:

Chamber Volume	13.7 m^3
Crop Tray Growing Area (per tray)	1.43 m^2
Number of Crop Trays	4
Number of Lamps	32
Total Growing Area	5.72 m^2
Biomass (wheat, *Triticum aestivum*) [54]	21.7 kg

Maximum Power/Heat Loads [55]:

Atmospheric Circulation Fan/Blower [56]	1.9 kW
Lighting:	
Lamps (high pressure sodium)	12.8 kW
Ballasts	2.3 kW
Reheat [57]	3.0 kW
Total Power/Heat Load	20.0 kW
Assumed Power Usage	Continuous
Power as Mass	15,000.0 kg

Figure 2.10 provides a general illustration of a portion of the plant growth chamber. Overall, the redesigned plant growth chamber will be similar to the baseline configuration. Because the bulk of the chamber volume is dictated by the volume requirements of the crop, the volume of the redesigned chamber is expected to be similar to the baseline. Further, the deployment is expected to be similar to the baseline chamber. The reliability is expected to be slightly higher due to equipment improvements. The overall TRL is 5 because some testing and development has been completed. The development cost for any additional work is expected to be low. Terrestrial uses for these technologies are less obvious. As applied to plant growth, there may be some interest within agricultural products companies and research labs, especially for small, high-value crops which require closely controlled growing conditions. Thus, because few terrestrial users will, in the foreseeable future, require completely isolated chambers for growing plants, there is little anticipated terrestrial use for this technology. However, terrestrial uses for individual components of the plant chamber assembly are possible.

---

[53] The dimensions listed here correspond to one half of those for the overall VPGC.

[54] Actual data from the VPGC using high-pressure sodium lamps.

[55] Actually, these are power inputs for the listed systems. However, all input power is assumed to eventually require rejection as heat, so these are also heat loads associated with this equipment.

[56] Estimated for 45 Hertz.

[57] Paul (1995). The reheat increases the temperature of the air stream before it returns to the plant growth volume. In some cases, to control humidity within the growing volume of the chamber, the air is cooled below the return air stream set-point temperature. After removing the excess water vapor, the reheat increases the air temperature before the stream returns to the growing volume.

General Qualitative Assessments:

Technology Readiness Level	5
Volume	average
Deployment	average
Reliability	average
Development Cost	low
Terrestrial Use Potential	possible
Composite Qualitative Score	+1

2.6.3   Carbon Brush Heat Exchanger

Heat exchange across an evacuated gap between two flat plates is a common problem. The gap effectively adds a resistance to heat transfer which, in some cases when a vacuum fills the gap, is the controlling resistance. One solution, when an extravehicular activity compatible interface is required, is to mount fins extending perpendicularly from each surface bounding the gap. When the two fin sets are intermeshed, a radiant fin interface is formed and heat is transferred primarily by radiation. Knowles (1995) gives the interfacial conductivity as 60 $W/(m^2*K)$ for this arrangement.

Another solution to transfer heat across the gap is to mount fine carbon fibers extending perpendicularly from the gap boundaries. Heat is again transferred by radiation but also by contact conductance when the fibers are allowed to intermesh. This arrangement is a carbon brush interface. Though this arrangement is similar to the radiant fin interface, the interfacial conductivity increases to 2500 $W/(m^2*K)$ (Knowles, 1995) due to increased area for radiant transfer and the numerous physical contact points for conductive transfer (Figure 2.11).

Currently the dc-to-dc converter units (DDCUs) are affixed to coldplates transferring heat using radiant fin interface. The fins, which are made of aluminum, are 0.0508 m tall by 762 micrometers thick and run the length of the DDCU coldplate [58]. In order to save mass and improve DDCU cooling efficiency, the radiant fin interfaces could be replaced by carbon brush interfaces. A quick one-dimensional heat transfer analysis reveals that this change will increase the interfacial conductivity by almost two orders of magnitude. This, in turn, yields more efficient cooling of the DDCUs. What further advantage or savings this imparts is dependent on the cooling needs of other units on the ETCS loop.

---

[58]   These dimensions apply to units designed for use on ISS. Other units are assumed to be comparable.
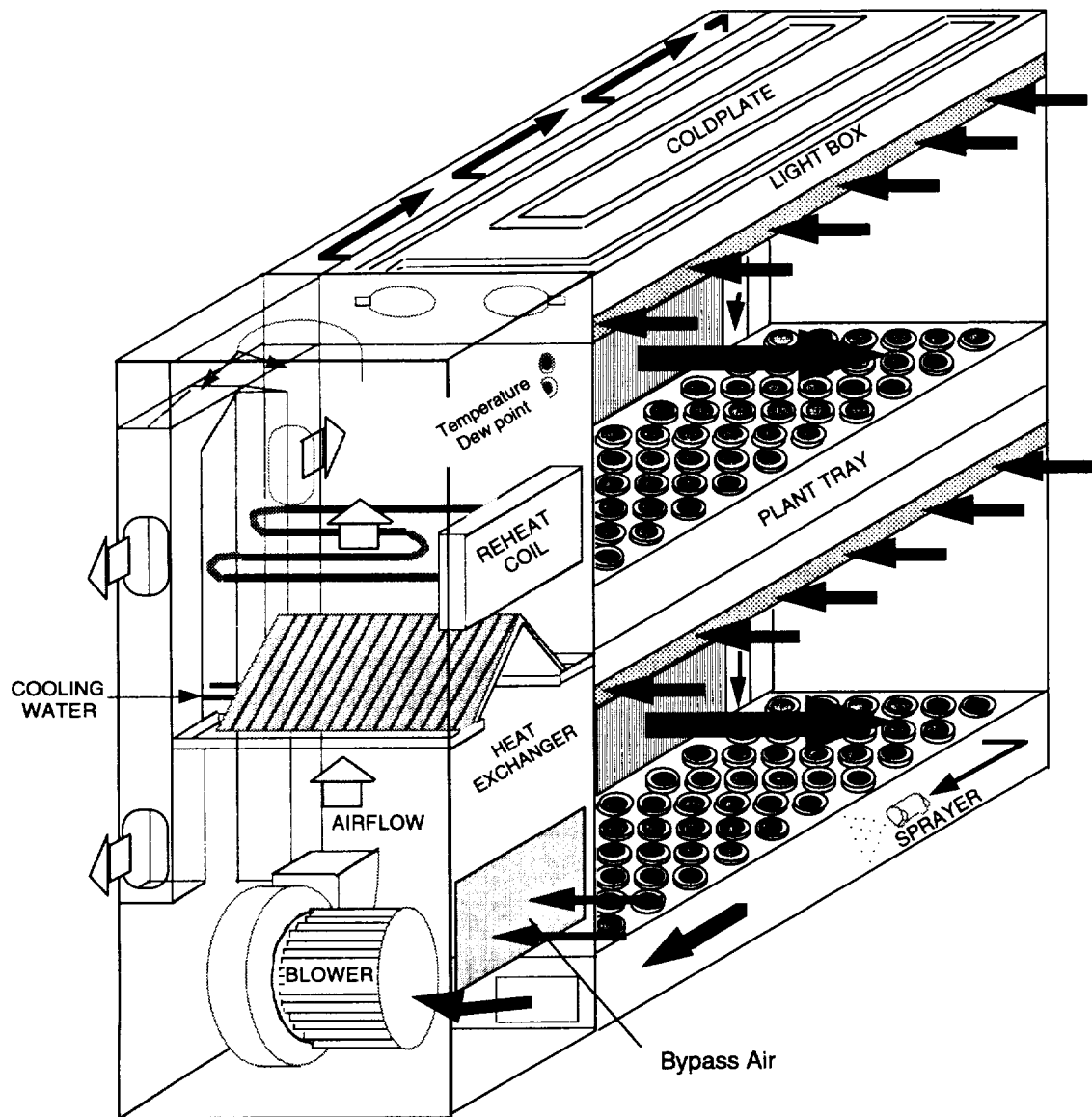
Figure 2.10 An overall drawing of the Variable Pressure Growth Chamber used by Ewert, Paul, and Barta (1995). This view shows two of eight plant growth trays plus the chamber environmental control equipment. The coldplate and heat exchanger use liquid water as the working fluid while the reheat coil is a resistance heating device. The arrows indicate the mean airflow pattern within the chamber.

Overall, the carbon brush heat exchanger has excellent properties. The volume of the carbon brush interface is slightly smaller than a radiant fin interface. Units using a carbon brush interface should be as easy to deploy as the current design. The carbon brush should be very reliable and inexpensive. Because the theoretical basis for this idea is well developed at a TRL of 5, the development cost is low. For terrestrial applications, this technology could be used to cool high temperature electronics. The major disadvantage of the carbon brush heat exchanger is the possible generation of small particle debris as individual fibers detach or break upon handling (Knowles, 1995). This may be unacceptable near electronic devices such as DDCUs because the particles may float into the electronics. Depending on other considerations, such as component packaging, the hazard of such particle debris may be reduced.

General Qualitative Assessments:

Technology Readiness Level	5
Volume	average
Deployment	average
Reliability	improved
Development Cost	low
Terrestrial Use Potential	good
Composite Qualitative Score	+3

DDCU Coldplate

Radiant Fin
Interface

Coldplate Socket

Coldplate Socket
with Carbon Fibers
(for illustrative
purposes only)

DDCU Coldplate

Carbon Brush
Interface

Coldplate Socket
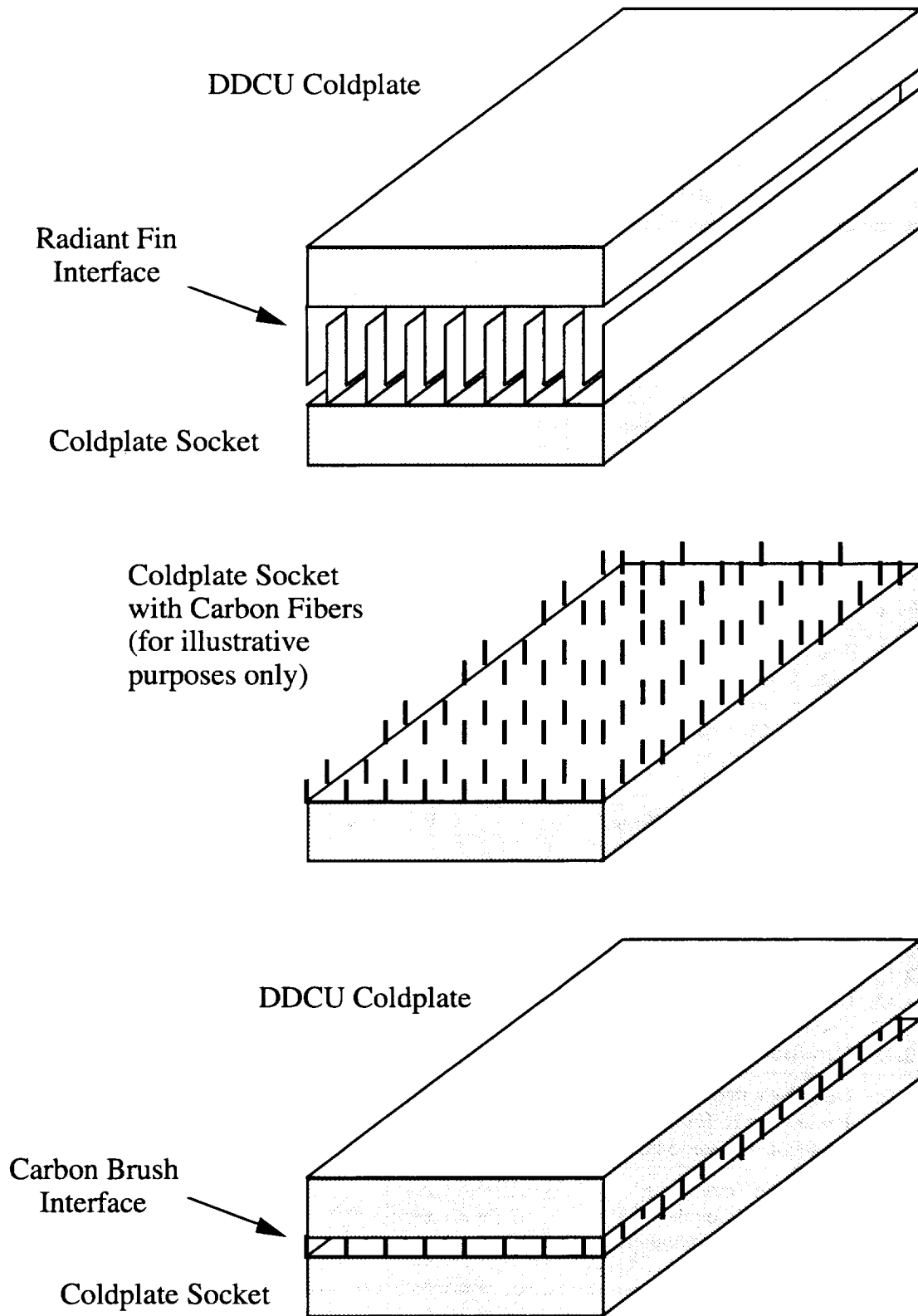
Figure 2.11 The radiant fin and carbon brush heat exchangers. (This figure is not drawn to scale.)

2.7   Summary

Overall, the qualitative assessments of the various technologies may be summarized in the following table:

Table 2.1 Summary of Qualitative Assessments for Advanced ATCS Architecture Technologies

	Volume	Deployment	Reliability	Development Cost	Terrestrial Use Potential	Total
2.1 Two-Phase Thermal Control Systems						
2.1.1 Two-Phase Thermal Control System With Mechanical Pump/Separator	0	0	0	+1	-1	0
2.1.2 Low-Power Two-Phase Thermal Control System	0	0	0	0	-1	-1
2.1.3 Two-Phase Thermal Control System With Electrohydrodynamic Pumping	0	0	+1	0	+1	+2
2.1.4 Capillary Pumped Loops	0	0	+1	0	-1	0
2.2 Heat Pumps						
2.2.1 Vapor Compression Heat Pump	0	0	-1	+1	+1	+1
2.2.2 Solar Vapor Compression Heat Pump	+1	0	-1	+1	+1	+2
2.2.3 Complex Compound Heat Pump	+1	0	0	0	0	+1
2.2.4 Zeolite Heat Pump	+1	0	0	0	0	+1
2.3 Heat Pipe Radiators						
2.3.1 Arterial Heat Pipe Radiators	0	0	+1	+1	-1	+1
2.3.2 Arterial Heat Pipe Radiators With Electrohydrodynamic Pumping [59]	0	0	+1	-1	--	(0)
2.3.3 Axial-Groove Heat Pipe Radiators	0	0	0	+1	0	+1
2.4 Lightweight Radiators						
2.4.1 Composite Flow-Through Radiators	0	0	0	0	+1	+1
2.4.2 Composite Reflux Boiler Tube Radiators	0	0	+1	+1	+1	+3
2.4.3 Composite Heat Pipe Radiators	0	0	+1	+1	+1	+3
2.4.4 Unfurlable Radiators	+1	+1	+1	0	+1	+4
2.5 Other Heat Rejection Technologies						
2.5.1 Phase-Change Thermal Storage	+1	0	0	0	+1	+2
2.5.2 Parabolic Radiator Shade	0	0	0	0	-1	-1
2.6 Additional Technologies						
2.6.1 Rotary Fluid Coupler	+1	+1	0	+1	0	+3
2.6.2 Plant Chamber Cooling Improvements	0	0	0	+1	0	+1
2.6.3 Carbon Brush Heat Exchanger	0	0	+1	+1	+1	+3

Above the header row: *Qualitative Assessments*

---

[59]   This is a combination of technologies, so no assessment is provided for terrestrial use potential. Such assessments are provided under the individual component technologies.

Advanced technology radiators exhibit a wide range of masses per radiating area. The baseline heat-rejection devices for the reference missions below assume flow-through radiators constructed from aluminum alloys using single-phase working fluids. For the vehicles and habitats examined, the mass per radiating area, excluding the fin efficiency, falls between 5.0 kg/m^2 and 8.5 kg/m^2. The table below summarizes the masses per radiating area for the various radiators presented as advanced technologies. These masses per radiating area are based on the total radiator mass, including any working fluid, divided by the radiating surface area.

Table 2.2 Summary of Masses per Radiating Area
for Advanced Technology Radiators

		Mass per Radiating Area [kg/m^2]	Fin Efficiency	Effective Mass per Radiating Area [60] [kg/m^2]
2.3	Heat Pipe Radiators			
2.3.1	13.11-m Arterial Heat Pipe Radiators	8.80	0.925	9.51
	6.71-m Arterial Heat Pipe Radiators	9.88	0.925	10.68
2.3.2	Arterial Heat Pipe Radiators			
	With Electrohydrodynamic Pumping	7.64	0.763	10.01
2.4	Lightweight Radiators			
2.4.1	Composite Flow-Through Radiators			
	(Single-Sided Rejection)	8.21	~1.00	8.21
	Composite Flow-Through Radiators			
	(Double-Sided Rejection)	4.67	~1.00	4.67
2.4.2	Composite Reflux Boiler Tube Radiators	3.44	1.00	3.44
2.4.3	Composite Heat Pipe Radiators [61]	1.91	0.97	1.96
2.4.4	Unfurlable Radiators	4.62	1.00	4.62

---

[60]　The effective mass per radiating area is the mass per radiating area divided by the fin efficiency.

[61]　The fin efficiency listed for the composite heat pipe radiator is estimated based on an analysis using the Thermal Synthesizer System (TSS) and SINDA/FLUINT. The actual value is unknown.

3.0   ORBITAL MISSIONS

Several aspects of orbital operations are unique. Microgravity, generated by the motion of the vehicle itself, is the only body force which applies to orbital operations. The time constant associated with an orbital cycle is on the order of a couple of hours or less for a low altitude orbit. This allows a frequent transition between sunlight and shade. Finally, by the nature of the environment itself, there are few additional natural resources or atmosphere of any type associated with an orbital mission.

3.1   INTERNATIONAL SPACE STATION EVOLUTION

3.1.1   Reference Mission

This study assumes that the current International Space Station (ISS) TCS ORUs will need replacement and augmentation after year 20 (year 2017, assuming a project genesis in 1997). The current radiator configuration is six flow-through radiator ORUs in two clusters. Due to micrometeoroid impacts, optical property degradation, and other failures, it is assumed that all six radiator ORUs will be replaced. Further, it is assumed in year 20 ISS will be augmented with two solar dynamic power modules increasing the onboard power supply of the U.S.-led portion of ISS from 75 kW to 95 kW. This will require an additional 20 kW of heat-rejection capability. An alternate reference mission for the advanced thermal technologies below would be to construct an entirely new space station.

3.1.2   Baseline Case

ATCS requirements for ISS (Howell, *et al.*, 1994):

- Loop A and Loop B are independent flow passages with Loop A on segment S1 and Loop B on segment P1. Each loop will use liquid ammonia (NH_3) to carry heat from the ITCS to the heat-rejection devices in the ETCS. (See Figure 3.1 for a schematic of the ISS ATCS.)
- Steady-state heat rejection must be greater than or equal to 11.67 kW per radiator ORU for flowrates of 0.1591 kg/s (1263 lb_m/hr) per loop with an entrance temperature T_{in} of 283.3 K (50.2 °F). The set-point temperature T_{sp} is 275.4 K (36 °F). This assumes an equal heat load on each ETCS loop.
- The temperature for ammonia leaving the ETCS heat-rejection device should fall between 199.8 K (-100 °F) and 273.7 K (33 °F), inclusive.
- The temperature of ammonia entering the ETCS heat-rejection device falls between 280.8 K (45.8 °F) and 285.9 K (54.9 °F), inclusive.
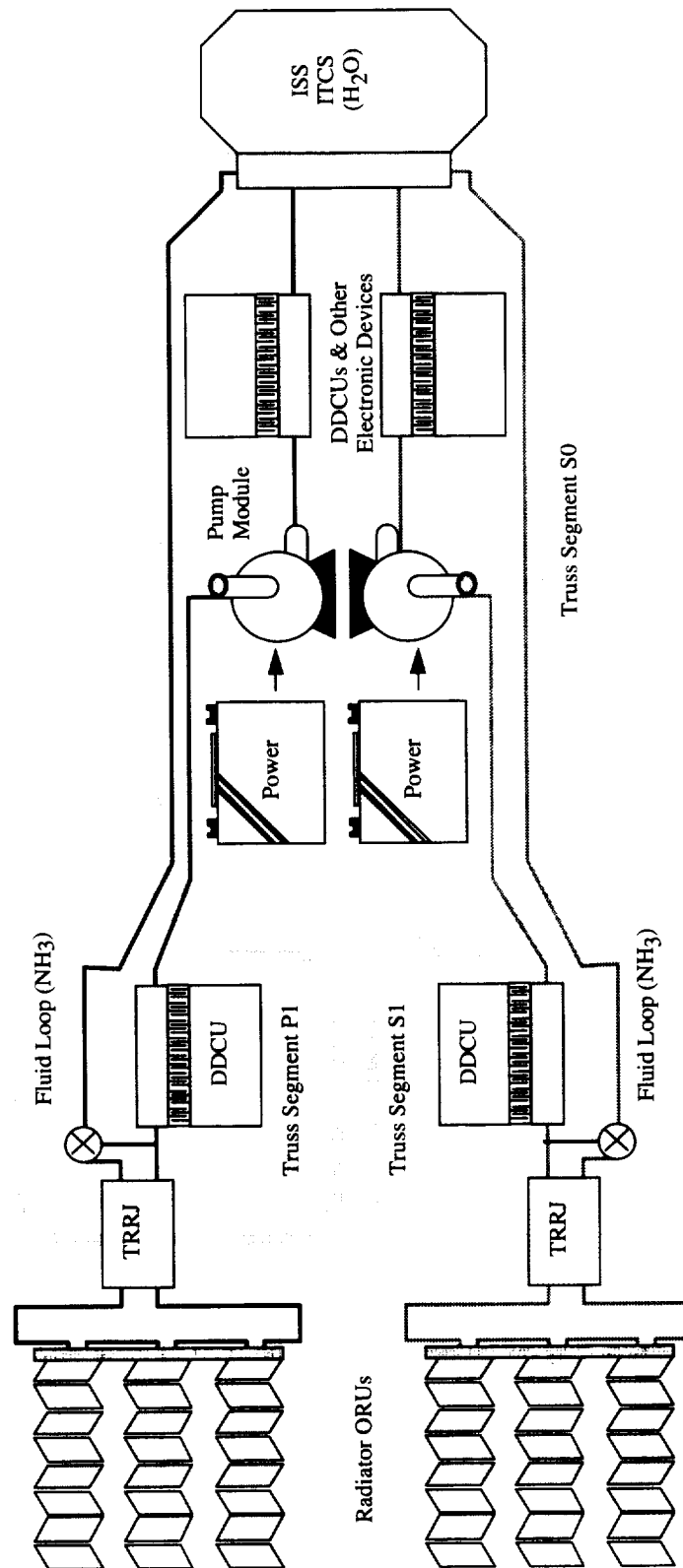
Figure 3.1   International Space Station external thermal control system baseline configuration.

- Total mass for each of the six ETCS radiator ORUs on ISS should be no more than 1,080 kg (2,380 lb$_m$) per ORU. With fluids, the current radiator ORU mass is 1,104.9 kg (2,435.9 lb$_m$) [62].

- Each radiator ORU has 129.8 m^2 (1397.2 ft^2) of radiating surface area for heat transfer. The radiator mass per radiating area is 8.51 kg/m^2.

- The two ammonia loops have mass flowrates of 1.121 kg/s (8,900 lb$_m$/hr) and 0.958 kg/s (7,600 lb$_m$/hr). The corresponding total pressure drops for each loop are 386,100 N/m^2 (56 lb$_f$/in^2) and 296,500 N/m^2 (43 lb$_f$/in^2), respectively. Assuming a fluid density of 635.9 kg/m^3 (which is for saturated liquid ammonia at 275.4 K or 36 °F), the necessary power delivered to the fluid is 1.130 kW. The total power set aside for both pumps, which are identical, is 2.650 kW. Therefore, the overall efficiency of the pumping system must be at least 42.6%.

- The pressure drop across any ORU radiator panel set is at least 34,470 N/m^2 (5.0 lb$_f$/in^2) and not more than 48,260 N/m^2 (7.0 lb$_f$/in^2). Assuming a fluid temperature equal to the loop temperature, 275.4 K (36 °F), and maximum mass flowrate through the radiators, 0.9546 kg/s (7578 lb$_m$/hr), the mechanical power dissipated within the radiator panel flow passages is 72.5 W. Thus, assuming a pump efficiency of 0.45, 161.1 W of pumping power must be available for flow through the radiators in addition to other needs.

The above criteria apply when the heat load is split evenly between Loop A and Loop B.

As of March 30, 1994, Loral Vought Systems, the prime ETCS radiator sub-contractor, presented the following design information (Howell, *et al.*, 1994):

- Current Radiator Design: Each radiator ORU will use eight radiator panels. Each radiator panel has 22 tubes in spread-spacing. In spread-spacing, the effective tube fin area at the panel center is less than for the tubes at the extremities. Based on analysis, the estimated maximum steady-state heat rejection is 11.67 kW per ORU for a flowrate of 0.1591 kg/s (1263 lb$_m$/hr) per path with an entrance temperature T_{in} of 283.3 K (50.2 °F). The ORU design has a mass of 1,088.38 kg (2,399.49 lb$_m$) dry and 1,123.25 kg (2,476.35 lb$_m$) with all fluids. The mass breakdown is:

---

[62]   See Table 3.1 for details.

Table 3.1 ATCS Radiator ORU Hardware for ISS

Radiator ORU Hardware	Quantity per ORU	Total Item Mass kg	lb_m
Base Structure	(1)	200.81	442.72
Scissors Beam and Hinges	(1)	92.76	204.50
Torque Panels and Arms	(1)	47.26	104.20
Cinching Mechanism	(6)	23.26	51.27
Deployment Mechanism	(1)	34.40	75.85
Deployment Motor	(1)	11.39	25.12
Flex Hose and Manifold Set	(8)	246.68	543.84
Radiator Panel Set	(7)	358.37	790.07
Radiator Panel Set	(1)	50.83	112.06
Electrical	(1)	9.71	21.40
Assembly Hardware	(1)	8.92	19.66
Boeing Furnished Equipment	(1)	3.99	8.80
Total Dry Mass as of 29-Mar-94 (per ORU radiator)		1088.38	2399.49
Total Dry Mass as of 28-Sep-94 (per ORU radiator) (NASA, 1994)		1070.0	2359.0
Fluids - NH_3 (estimated)	--	34.86	76.86

Single-phase ammonia (NH_3) is the working fluid. This is the baseline radiator ORU design.

• Table 3.2 through Table 3.8 show the overall ISS ITCS and ETCS hardware masses (NASA, 1994).

Table 3.2 Significant Structural ATCS Hardware per ORU Cluster

Significant Structural ATCS Hardware Masses per Radiator ORU Cluster	Total Item Mass kg	lb_m
Attachment Hardware	552.9	1219.0
Keel Structure	95.3	210.0
Primary Truss Structure	3286.2	7244.8
Radiator Beam	1210.0	2667.6
Tank and Pump Structures	298.0	657.0
TCS Structural Support	68.0	150.0
Thermal Radiator Rotary Joint:		
TRRJ	306.0	674.6
Flex Hose Coupler	158.8	350.0
TRRJ Torque Box	138.3	305.0
Total Structural TCS Hardware per Radiator ORU Cluster	6113.5	13478.0

Table 3.3 Total Active ETCS Mass in ISS Segments

Total Active ETCS Hardware Mass in each Module (excluding structural members, and wiring)	Total Item Mass kg	lb$_m$
Integrated Truss Segment P1		
DDCU Coldplate	51.1	112.6
Fluids (NH$_3$ and N$_2$)	322.0	710.0
Instruments and Sensors	352.2	776.4
Pump Module	332.0	731.9
Radiator Beam Valves	104.2	229.8
Radiator ORUs (3)	3210.1	7077.0
Other	570.5	1257.8
Integrated Truss Segment S0		
Coldplates	469.9	1036.0
Plumbing and Instruments	249.7	550.6
Integrated Truss Segment S1		
DDCU Coldplate	51.1	112.6
Fluids (NH$_3$ and N$_2$)	322.0	710.0
Instruments and Sensors	352.2	776.4
Pump Module	332.0	731.9
Radiator Beam Valves	104.2	229.8
Radiator ORUs (3)	3210.1	7077.0
Other	581.9	1282.8
Node 2		
Heat Exchangers	209.6	462.0
Heaters	12.5	27.5
U. S. Habitation Module		
Heat Exchangers	45.4	100.0
Other	25.9	57.1
U. S. Laboratory		
Heat Exchangers	55.5	122.3
Other	4.8	10.5
Total	**10968.9**	**24182.0**

Table 3.4 Other Significant ATCS Mass in ISS

Other Significant ATCS Hardware Masses	Total Item Mass kg	lb$_m$
Piping and Plumbing [63]	3363.2	7414.6
Ammonia per ETCS Loop [64]	191.8	422.9
Science Power Platform Radiator [65]	1000.2	2205.0

---

[63] Estimated from Ungar (1995).

[64] From Wuestling (1994).

[65] Russian hardware.

Table 3.5 Total Active ITCS Mass in ISS Segments

Total Active ITCS Hardware Mass in each Module (excluding structural members)	Total Item Mass kg	lb$_m$
Common US/RSA Airlock	169.4	373.5
Node 1	269.0	593.1
Node 2	416.9	919.1
U. S. Habitation Module	849.4	1872.7
U. S. Laboratory	1037.0	2286.1
Total	2741.7	6044.5

Table 3.6 Percentage of ISS ETCS Mass as a Function of Category Excluding Structural Elements

Category	Percentage of ETCS Mass
1. Coldplates	4.1
2. Heat Exchangers	2.5
3. Radiator ORUs	50.8
4. Pump Modules	5.3
5. Instruments and Sensors	6.1
6. Fluids (NH$_3$ and N$_2$)	5.1
7. Plumbing	16.5
8. TRRJ Assemblies	9.6

Table 3.7 Percentage of ISS ETCS Mass as a Function of Category

Category	Percentage of ETCS Mass
1. Coldplates	2.1
2. Heat Exchangers	1.3
3. Radiator ORUs	25.9
4. Pump Modules	2.7
5. Instruments and Sensors	3.1
6. Fluids (NH$_3$ and N$_2$)	2.6
7. Plumbing	8.4
8. Primary Structure	31.6
9. TRRJ Assemblies	4.9
10. Radiator Beams	9.7
11. Other TCS Structure	2.9
12. Other	4.8

Table 3.8 Breakdown of Mass for ISS Truss Segment P1

Total Mass for Segment P1 Module (including structural members)	Total Item Mass	
	kg	lb_m
Additional Mechanical Equipment	112.9	248.9
Additional Wiring	1283.7	2830.1
Antennas and Cameras	375.3	827.4
Attachment Hardware	552.9	1219.0
Crew Equip. Trans. Assembly Cart B	319.8	705.1
Command and Data Handling	289.7	638.6
DDCU and Connector Box	129.2	284.9
Dedicated ETCS Equipment		
DDCU Coldplate	51.1	112.6
Fluids (NH_3 and N_2)	322.0	710.0
Instruments and Sensors	352.2	776.4
Pump Module	332.0	731.9
Radiator Beam Valves	104.2	229.8
Radiator ORUs (3)	3210.1	7077.0
Other	570.5	1257.8
Handholds and Worksites	253.6	559.1
P1 Keel Structure	95.3	210.0
P1 Primary Truss Structure	3286.2	7244.8
Passive TCS Equipment	129.0	284.3
Radiator Beam	1210.0	2667.6
Remote Power Controller Modules	72.2	159.2
RJMC	70.9	156.2
Support Radiator	4.5	10.0
Tank and Pump Structures	298.0	657.0
TCS Structural Support	68.0	150.0
Thermal Radiator Rotary Joint, Torque Box, and Coupler	679.9	1498.9
Utility Distribution System Support Structure	428.2	944.0
Total	14601.4	32190.6

Elements listed as structural or mechanical members are included in the listings for truss P1 for reference purposes. These, after all, are not designed to be easily replaced once ISS is actually on orbit.

- The photovoltaic power array thermal control system (PV-TCS), though separate from the central ATCS, is very similar. It is therefore appropriate to examine mass savings for this system should replacement be necessary. When fully operational, ISS will derive electricity from four solar power modules. Each module mounts two external dc-to-dc converter units (DDCU-E) and a PV-TCS radiator ORU. The PV-TCS radiator ORUs are smaller versions of the flow-through radiator ORUs used in the ATCS. This study will briefly examine replacing the PV-TCS radiators and the DDCU-E interfaces. Table 3.9 presents the relevant baseline masses.

Table 3.9 Masses of Photovoltaic Power Array Thermal Control System Members

Masses for Some PV-TCS Equipment (Found on Segments S4, S6, P4, and P6)	Quantity per Segment	Item Mass kg	lb_m
dc-to-dc Converter Unit-External	(2)	63.5	139.9
PV-TCS Radiator ORU	(1)	618.0	1362.5

3.1.3 Implementing the Reference Mission

If one replaces and augments the ISS TCS with additional flow-through radiator ORUs, the TCS configuration following year 20 would include eight radiator ORUs. These replacement radiators would be mounted in two clusters of three ORUs each and one cluster of two ORUs. In addition to the two radiator ORU clusters on segments S1 and P1, a hypothetical third truss segment, designated here as P0, would be added to ISS to support the radiator cluster with two ORUs. Table 3.10 shows the assumed configuration for P0.

Table 3.10 Breakdown of Mass for Proposed Truss Segment P0

Total Mass for Segment P0 Module (including structural members) [66]	Total Item Mass kg	lb_m
Attachment Hardware	414.7	914.2
DDCU, Coldplate, and Connector Box	180.3	397.5
Dedicated ETCS Equipment for Two Radiator ORUs	3260.7	7188.6
P0 Primary Truss & Keel Structure	2254.3	4970.0
Passive TCS Equipment	129.0	284.3
Radiator Beam	806.7	1778.4
Tank and Pump Structures	198.7	438.0
TCS Structural Support	45.4	100.0
Thermal Radiator Rotary Joint, Torque Box, and Coupler	679.9	1498.9
Other	2408.1	5309.0
Total	10377.8	22878.9

---

[66] This construction for segment P0 is based primarily on the values given in Table 3.8 for segment P1. Some of the component masses for segment P0 are lower to reflect attachment of only two radiator ORUs instead of three. Specifically, the masses for "Attachment Hardware" and "Other" are three-quarters of the corresponding masses listed for segment P1, which are more conservative estimates to account for equipment which must be installed regardless of the number of ORUs included. The masses for "Primary Truss & Keel Structure," "Radiator Beam," "Tank and Pump Structures," and "TCS Structural Support" are two-thirds of the corresponding masses listed for segment P1.

Table 3.11 Summary of Active ETCS Mass to be Added in Year 20

Total Active ETCS Hardware Mass Added in Year 20 (excluding structural members)	Total Item Mass kg	lb$_m$
Integrated Truss Segment P0		
DDCU Coldplate	51.1	112.6
Fluids (NH$_3$ and N$_2$)	214.7	473.3
Instruments and Sensors	234.8	517.6
Pump Module	221.3	487.9
Radiator Beam Valves	69.5	153.2
Radiator ORUs (2)	2140.0	4718.0
Other	380.4	838.5
Total	3311.8	7301.1

This would lead to an overall ETCS equipment mass in year 20, excluding structural components and piping, of 14,280.7 kg (31,483.7 lb$_m$) for the reference ISS evolution mission. (See Table 3.3 and Table 3.11) Overall, this vehicle would circulate 453.3 kg (999.5 lb$_m$) of ammonia, or 226.7 kg (499.7 lb$_m$) per ETCS loop [67]. It is presumed that clusters with four radiator ORUs in the present radiator locations are not feasible for dynamic or structural reasons. Assuming a pump efficiency of 0.45, the power necessary just to pump ammonia through the eight radiator ORUs is 215 W. Thus, the total pumping power will be 2,704 W. The assumed power mass penalty is 476 kg/kW while using continuous power. Thus, the power as mass is 1,287.1 kg (2,837.6 lb$_m$). The power mass penalty (Table 3.12) may be broken down as:

Table 3.12 Breakdown of ISS Power Mass Penalty

Source	Mass Penalty [kg/kW$_{supplied}$]
Photovoltaic Array (generation)	50
Storage	
Batteries	157
Thermal Control System	80
Power Management and Distribution	54
Structure	135
Total for Continuous Power	476

Thus, the overall baseline ETCS mass for ISS evolution is 15,567.8 kg (34,321.3 lb$_m$).

A major disadvantage of this reference mission is the need to add additional truss segments to accommodate the additional radiator ORUs. Because these additional trusses need to be fixed with respect to the S0 truss segment, they need to eventually be located in

---

[67] Actually, the total working fluid mass will probably be greater than the values listed here because the ETCS fluid mass in the lines to and from the two additional radiator ORUs has not been included. If any additional habitable segments are added in the evolution, the ETCS fluid mass will further increase.

board of the solar alpha rotary joints on segments S3 and P3. It is presumed that this augmentation operation would require major reconstruction of the baseline ISS structure to properly locate the additional radiator ORUs. This would probably require lengthy and unacceptable periods during which ISS is not fully available for use.

3.1.4 Parametric Study Using the Baseline Case

Parametric studies are often used to determine the sensitivity of a design to a set of prescribed variables. For those variables to which the design shows the greatest sensitivity, the greatest care must be exercised to accurately determine these values. This study provides bounds on the extent of ISS ETCS heat-rejection variation based on some of the more common ETCS parameters.

A simple model for the Baseline Case can be developed by considering an overall heat balance for a single radiator ORU. Basically, the heat lost by the ammonia flowing through the radiator tubes must be equal to the net emission by the radiator panels. Thus:

$$\frac{dE}{dt} = \dot{E}_{generated} + \dot{E}_{in} - \dot{E}_{out}$$

Assumptions and Restrictions:

- The heat transfer for a radiator panel is steady without internal generation.
- The difference between the simple average temperature of the panel surface, $\overline{T}_p$, and the simple average temperature of the ammonia, $\overline{T}$, is a known linear function of the sink temperature, T_e. Here:

$$\overline{T} - \overline{T}_p = -0.0500\, T_e + 13.88\ K$$

The base values for this model (Andish, 1995) are:

T_e		$\overline{T} - \overline{T}_p$	
K	°F	K	°F
244.3	-20	1.7	3
210.9	-80	3.3	6

- The radiator ORU fin efficiency, $\eta\ (T_e)$, is a linear function of the sink temperature, T_e. Here:

$$\eta(T_e) = 0.00204\frac{1}{K}T_e + 0.380$$

The base values for this model (Farner, 1995, and Ungar, 1995) are:

T_e		η
K	°F	
240.0	-27.7	0.87
249.8	-10.0	0.89

- An average specific heat, computed at the simple average temperature of the ammonia, $\bar{c}_p(\bar{T})$, may be used for the fluid side heat transfer. Here:

$$\bar{c}_p(\bar{T}) = 0.008286 \frac{kW * s}{kg * K^2} \bar{T} + 2.424 \frac{kW * s}{kg * K}$$

The parametric study computes the heat rejection for a radiator ORU containing eight individual panels. Six radiator ORUs are present for the TCS on ISS. The LVS Base Case presented below uses the values presented by Loral Vought Systems (LVS) (Howell, *et al.*, 1994). They report a heat rejection of 11.67 kW which the current simple model reproduces at a sink temperature of 245.4 K (-18.0 °F).

Input study constants:

Stefan-Boltzmann Constant	5.670×10^{-11} kW/(m²*K⁴)
Radiating Area	129.8 m²
Infrared Emissivity [68]	0.90
Calculation Tolerance	0.0001

The initial cases examine the LVS Case (design case) and combinations of the minimum and maximum allowable ammonia mass flowrates and inlet temperatures. These cases provide bounds on the current abilities of the radiator ORU design.

	LVS Case	Case A11	Case A12
Mass Flowrate of Ammonia [kg/s]	0.1591	0.1591	0.0031
Ammonia Inlet Temperature [K]	283.3	283.3	283.3
Sink Temperature [K]	245.4	249.8	249.8
Fin Efficiency	0.88	0.89	0.89
Average Ammonia Temperature [K] [69]	275.5	276.2	253.4
Average Panel Surface Temperature [K]	273.9	274.8	252.1
Average Ammonia Specific Heat [kW*s/kg*K]	4.71	4.71	4.52
Outlet Temperature of Ammonia [K]	267.7	269.1	223.6
Total Heat Rejection per Radiator ORU [kW]	11.68	10.66	0.84
Heat Rejection per Unit Area [kW/m²]	0.0900	0.0821	6.45×10^{-3}

	Case B11	Case B12	Case C11	Case C12
Mass Flowrate of Ammonia [kg/s]	0.1591	0.0031	0.1591	0.0031
Ammonia Inlet Temperature [K]	280.8	280.8	285.9	285.9
Sink Temperature [K]	249.8	249.8	249.8	249.8
Fin Efficiency	0.89	0.89	0.89	0.89
Average Ammonia Temperature [K]	274.3	253.3	278.2	253.6
Average Panel Surface Temperature [K]	272.9	251.9	276.7	252.2
Average Ammonia Specific Heat [kW*s/kg*K]	4.70	4.52	4.73	4.53
Outlet Temperature of Ammonia [K]	267.7	225.7	270.4	221.3
Total Heat Rejection per Radiator ORU [kW]	9.74	0.77	11.64	0.91
Heat Rejection per Unit Area [kW/m²]	0.0750	5.95×10^{-3}	0.0897	6.98×10^{-3}

---

[68] This value was suggested by Keller (1995 a) and is consistent with other sources for ISS.

[69] This is the simple arithmetic average of ammonia inlet and outlet temperatures.

	Case A21	Case A22
Mass Flowrate of Ammonia [kg/s]	0.1591	0.0031
Ammonia Inlet Temperature [K]	283.3	283.3
Sink Temperature [K]	238.7	238.7
Fin Efficiency	0.87	0.87
Average Ammonia Temperature [K]	274.6	244.0
Average Panel Surface Temperature [K]	272.6	242.1
Average Ammonia Specific Heat [kW*s/kg*K]	4.70	4.45
Outlet Temperature of Ammonia [K]	265.8	204.8
Total Heat Rejection per Radiator ORU [kW]	13.08	1.08
Heat Rejection per Unit Area [kW/m^2]	0.101	8.34×10^{-3}

	Case B21	Case B22	Case C21	Case C22
Mass Flowrate of Ammonia [kg/s]	0.1591	0.0031	0.1591	0.0031
Ammonia Inlet Temperature [K]	280.8	280.8	285.9	285.9
Sink Temperature [K]	238.7	238.7	238.7	238.7
Fin Efficiency	0.87	0.87	0.87	0.87
Average Ammonia Temperature [K]	272.6	243.9	276.6	244.3
Average Panel Surface Temperature [K]	270.7	241.9	274.6	242.3
Average Ammonia Specific Heat [kW*s/kg*K]	4.68	4.44	4.72	4.45
Outlet Temperature of Ammonia [K]	264.4	206.9	267.2	202.6
Total Heat Rejection per Radiator ORU [kW]	12.19	1.02	14.02	1.15
Heat Rejection per Unit Area [kW/m^2]	0.0939	7.84×10^{-3}	0.108	8.85×10^{-3}

The following studies increased the inlet ammonia temperature and varied the sink temperature while holding the mass flowrate constant. The purpose here was to observe how an increased thermal bus temperature affected heat rejection.

	Case D11	Case D21	Case D31	Case D41
Mass Flowrate of Ammonia [kg/s]	0.1591	0.1591	0.1591	0.1591
Ammonia Inlet Temperature [K]	290.9	290.9	290.9	290.9
Sink Temperature [K]	249.8	238.7	227.6	210.9
Fin Efficiency	0.89	0.87	0.84	0.81
Average Ammonia Temperature [K]	281.9	280.4	279.1	277.7
Average Panel Surface Temperature [K]	280.6	278.4	276.6	274.4
Average Ammonia Specific Heat [kW*s/kg*K]	4.76	4.75	4.74	4.73
Outlet Temperature of Ammonia [K]	273.0	269.9	267.4	264.5
Total Heat Rejection per Radiator ORU [kW]	13.57	15.88	17.75	19.81
Heat Rejection per Unit Area [kW/m^2]	0.105	0.122	0.137	0.153

	Case D12	Case D22	Case D32
Mass Flowrate of Ammonia [kg/s]	0.0031	0.0031	0.0031
Ammonia Inlet Temperature [K]	290.9	290.9	290.9
Sink Temperature [K]	249.8	238.7	227.6
Fin Efficiency	0.89	0.87	0.84
Average Ammonia Temperature [K]	254.0	244.6	235.6
Average Panel Surface Temperature [K]	252.6	242.7	233.1
Average Ammonia Specific Heat [kW*s/kg*K]	4.53	4.45	4.38
Outlet Temperature of Ammonia [K]	217.0	198.4	180.3
Total Heat Rejection per Radiator ORU [kW]	1.04	1.28	1.51
Heat Rejection per Unit Area [kW/m^2]	7.99×10^{-3}	9.84×10^{-3}	0.0116

The final studies are similar to the previous set except that the inlet ammonia temperature was varied until the outlet ammonia temperature reached either the maximum or minimum set-point temperature [273.7 K (33 °F) or 199.8 K (-100 °F)].

	Case E11	Case F21	Case G31	Case H41
Mass Flowrate of Ammonia [kg/s]	0.1591	0.1591	0.1591	0.1591
Ammonia Inlet Temperature [K]	292.3	298.3	302.8	307.5
Sink Temperature [K]	249.8	238.7	227.6	210.9
Fin Efficiency	0.89	0.87	0.84	0.81
Average Ammonia Temperature [K]	283.0	286.0	288.3	290.6
Average Panel Surface Temperature [K]	281.6	284.1	285.8	287.3
Average Ammonia Specific Heat [kW*s/kg*K]	4.77	4.79	4.81	4.83
Outlet Temperature of Ammonia [K]	273.7	273.7	273.7	273.7
Total Heat Rejection per Radiator ORU [kW]	14.12	18.75	22.30	25.94
Heat Rejection per Unit Area [kW/m^2]	0.109	0.144	0.172	0.200

	Case I12	Case J22
Mass Flowrate of Ammonia [kg/s]	0.0031	0.0031
Ammonia Inlet Temperature [K]	310.9	289.2
Sink Temperature [K]	249.8	238.7
Fin Efficiency	0.89	0.87
Average Ammonia Temperature [K]	255.3	244.5
Average Panel Surface Temperature [K]	254.0	242.6
Average Ammonia Specific Heat [kW*s/kg*K]	4.54	4.45
Outlet Temperature of Ammonia [K]	199.8	199.8
Total Heat Rejection per Radiator ORU [kW]	1.56	1.23
Heat Rejection per Unit Area [kW/m^2]	0.0120	9.50×10^{-3}

These results are summarized graphically by Figure 3.2 through Figure 3.7.
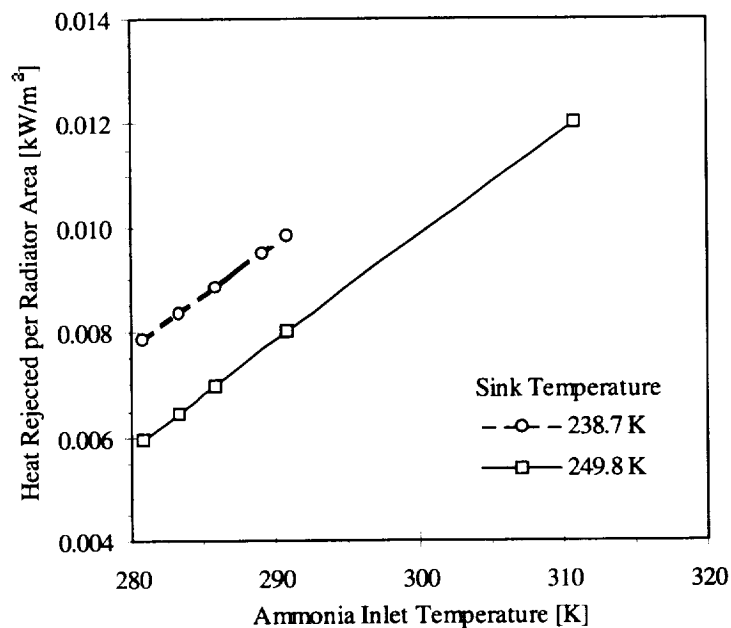
Figure 3.2 Baseline Case Parameter Study Results: Heat rejected per unit radiator area as a function of ammonia inlet temperature for a flowrate of 0.0031 kg/s, which is the minimum radiator flowrate.
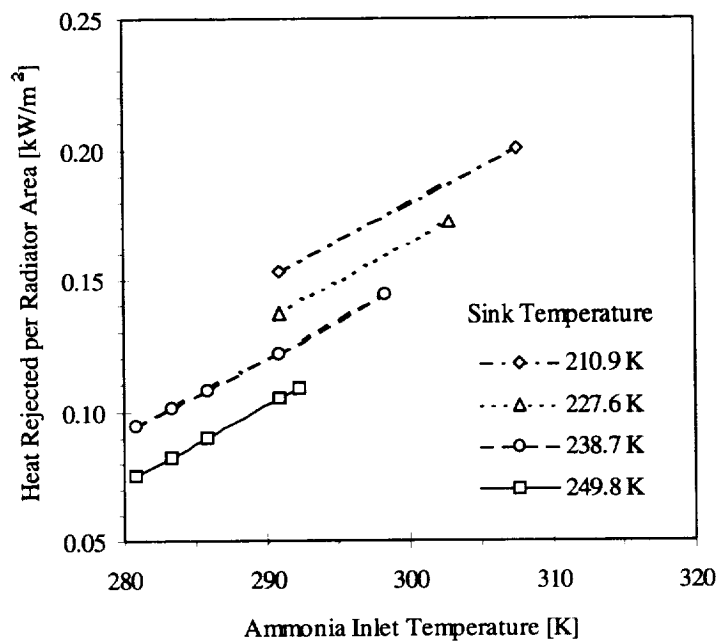
Figure 3.3 Baseline Case Parameter Study Results: Heat rejected per unit radiator area as a function of ammonia inlet temperature for a flowrate of 0.1591 kg/s, which is the maximum radiator flowrate.
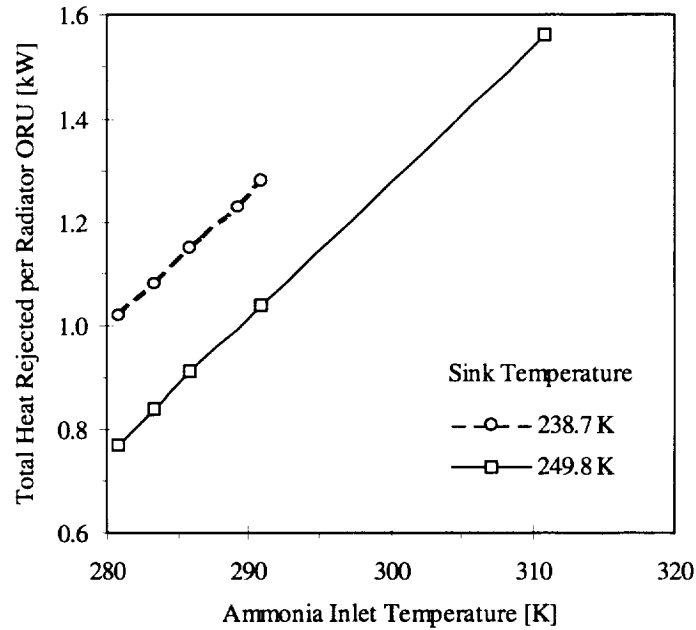
Figure 3.4 Baseline Case Parameter Study Results: Total heat rejected per radiator orbital replacement unit as a function of ammonia inlet temperature for a flowrate of 0.0031 kg/s, which is the minimum radiator flowrate.
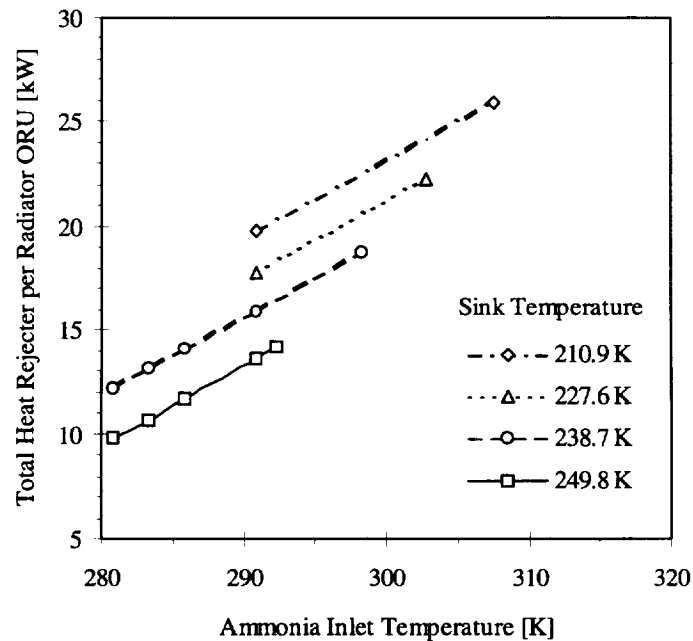
Figure 3.5 Baseline Case Parameter Study Results: Total heat rejected per radiator orbital replacement unit as a function of ammonia inlet temperature for a flowrate of 0.1591 kg/s, which is the maximum radiator flowrate. The LVS Case has a sink temperature of 245.4 K and an ammonia inlet temperature of 283.3 K.
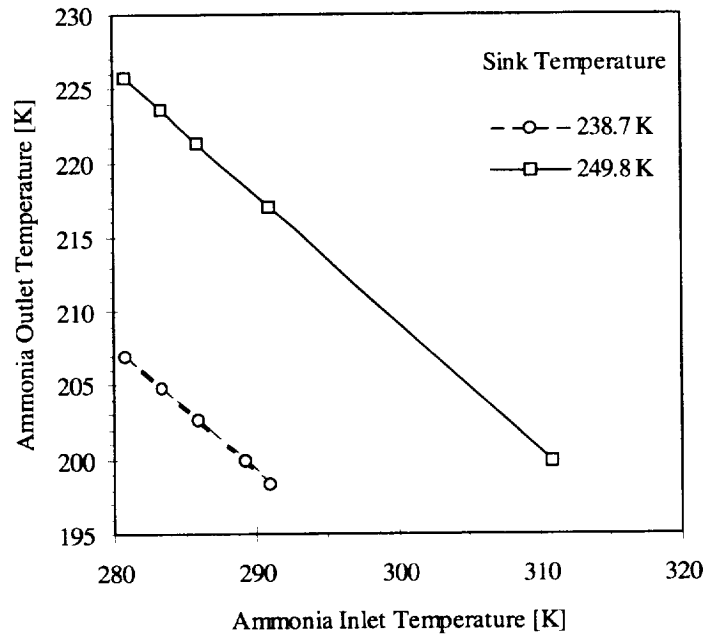
Figure 3.6 Baseline Case Parameter Study Results: Radiator ammonia outlet temperature as a function of ammonia inlet temperature for a flowrate of 0.0031 kg/s, which is the minimum radiator flowrate.
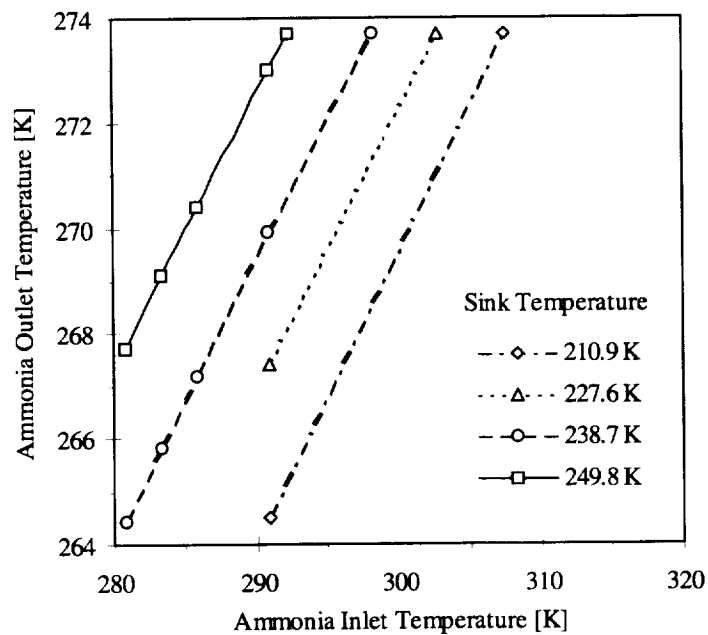
Figure 3.7 Baseline Case Parameter Study Results: Radiator ammonia outlet temperature as a function of ammonia inlet temperature for a flowrate of 0.1591 kg/s, which is the maximum radiator flowrate.

3.1.5 Advanced ATCS Architecture for International Space Station Evolution

Currently, the assumed ISS project life is 30 years from the date construction begins on orbit. As noted above, the TCS radiator ORUs are assumed to need replacement in year 20. Because the original architecture and the advanced architectures which follow have service lives in excess of 10 years, the computed mass savings is for a single radiator-ORU replacement. Qualitative assessments for these advanced technologies are presented in Section 2.0.

3.1.5.1 Two-Phase Thermal Control System With Mechanical Pump/Separator

For the specific ISS evolution to a two-phase TCS with MP/S [70], several assumptions are helpful. Overall, the current single-phase plumbing and lines will not be removed. The single-phase radiator and heat exchanger ORUs will be replaced with an equivalent number of two-phase units. Therefore, changes in the ORU mass, fluid mass, and pumping power need to be considered.

Ungar (1995) presents a study comparing single-phase and two-phase TCS designs for space stations of differing sizes. His example for a large station is the previous U.S.-led Space Station which contained two more crew modules than the current ISS design. However, with the additional power modules in year 20, ISS may add some additional modules for human activities leaving it to closely resemble Ungar's large station. Ungar (1995) gives the pumping power for the large station with a two-phase TCS with MP/S [71] as 0.697 kW. In year 20, ISS will use 2.7 kW for its single-phase cascade system. From Ungar (1995), the projected radiator areas are roughly equivalent for the two-phase TCS with MP/S design and the corresponding single-phase cascade design for the large station. (The two-phase TCS with MP/S design uses 9% less radiator area.) Assuming the two TCSs use the same radiating area, the mass for a comparable two-phase radiator is available. Howell, *et al.* (1994), presents the final two-phase radiator ORU design before the ISS TCS evolved from a two-phase system to a single-phase cascade system. This two-phase radiator ORU design (designated Revision K) uses the same surface area and roughly the same tube arrangement as the current ISS single-phase radiator ORUs.

Thermal Control System	Dry ORU Mass [kg]	ORU Fluids Mass [kg]	Pumping Power [kW]	Power as Mass [kg]
Single-Phase Cascade	1070.0 kg	34.9 kg	2.700	1285.2 kg
Two-Phase With Mechanical Pump/Seperator	1051.0 kg	22.7 kg	0.697	331.8 kg
Total Mass Savings	19.0 kg	12.2 kg	2.00	953.4 kg

For a system of eight radiator ORUs, the total mass savings is 249.6 kg (550.3 lb$_m$) for hardware deleted and 953.4 kg (2101.9 lb$_m$) for the reduction in required pumping power.

---

[70] See Section 2.1.1 for details of a two-phase TCS with MP/S.

[71] Ungar (1995) designates this TCS as a rotary fluid management device (RFMD) type two-phase TCS.

Specific Assessments:

Equipment Mass Savings	250 kg
Power Savings	2.00 kW
Power Savings as Mass	953 kg
Overall Mass Savings	1,203 kg
Composite Qualitative Score	0

3.1.5.2 Low-Power Two-Phase Thermal Control System

As in the previous section, several assumptions are necessary to analyze a LP two-phase TCS [72] for ISS evolution. Overall, the current single-phase plumbing and lines will not be removed. The single-phase radiator and heat exchanger ORUs will be replaced with an equivalent number of two-phase units. Therefore, changes in the ORU mass, fluid mass, and pumping power need to be considered. These are identical to the assumptions in the previous section. Thus, with respect to the analysis here, the only quantifiable difference between a two-phase TCS with MP/S and a LP two-phase TCS is the additional savings in pumping power associated with the latter option. Ungar (1995) presents a pumping power value of 355 W for the LP two-phase TCS on a large space station. Thus:

Thermal Control System	Dry ORU Mass [kg]	ORU Fluids Mass [kg]	Pumping Power [kW]	Power as Mass [kg]
Single-Phase Cascade	1070.0 kg	34.9 kg	2.700	1285.2 kg
Low-Power Two-Phase	1051.0 kg	22.7 kg	0.355	169.0 kg
Total Mass Savings	19.0 kg	12.2 kg	2.35	1116.2 kg

For a system of eight radiator ORUs, the total mass savings is 249.6 kg (550.3 lb$_m$) for lighter hardware and 1116.2 kg (2460.8 lb$_m$) for the reduction in required pumping power.

Specific Assessments:

Equipment Mass Savings	250 kg
Power Savings	2.35 kW
Power Savings as Mass	1,116 kg
Overall Mass Savings	1,366 kg
Composite Qualitative Score	-1

3.1.5.3 Capillary Pumped Loops

Based on Section 3.1.3, capillary pumped loops [73] will save 2.7 kW, which is the estimated ETCS pumping power following ISS evolution. Upon converting this to an

---

[72] See Section 2.1.2 for details of a LP two-phase TCS.
[73] See Section 2.1.4 for background on capillary pumped loops.

equivalent mass, the savings in power is 1,285.2 kg (2,833.4 lb$_m$). As above, most of the capillary pumped loop equipment mass is assumed to be similar to the corresponding mass of the equipment for the single-phase TCS with mechanical pumps. However, the capillary pumped loop will use the two-phase radiator panels which yield a savings of 249.6 kg (550.3 lb$_m$) in lighter hardware for a system of eight radiator ORUs. Thus, the overall savings for this option is 1,534.8 kg (3,383.7 lb$_m$).

Specific Assessments:

Equipment Mass Savings	250 kg
Power Savings	2.70 kW
Power Savings as Mass	1,285 kg
Overall Mass Savings	1,535 kg
Composite Qualitative Score [74]	-2

3.1.5.4   Vapor Compression Heat Pump

To incorporate a vapor compression heat pump [75] system for ISS evolution several assumptions apply. The heat pump is generic and ammonia is the working fluid within the radiators. The NASA specification used by LVS to size the radiator ORUs, given above by the LVS Case in the parametric study, is the sizing criterion for the heat pump. Finally, the design here is assumed to have six radiator ORUs like the current ISS ATCS configuration.

Cold Source Temperature, T_C (average ETCS temperature)	275.5 K
Temperature Lift, $T_H - T_C$	30.6 K
Hot Source Temperature, T_H (condenser temperature)	306.1 K
Radiator Inlet Temperature, T_{in}	302.0 K
Environmental Temperature, T_{sink}	245.4 K
Total Cooling Load, Q_C	93.36 kW
(which is equivalent to the load from 8 LVS Case ORUs)	

For a Carnot efficient heat pump, the coefficient of performance (COP) may be expressed as:

$$COP_{Carnot} = \frac{Q_C}{W} = \frac{T_C}{T_H - T_C}$$

---

[74] Because ISS evolution assumes that an existing vehicle would be retrofit to use a capillary pumped loop, the assessment for deployment for this mission is "difficult." Further, because this is an orbital mission, the development cost is "high."

[75] See Section 2.2.1 for details of vapor compression heat pumps.

For a nonideal heat pump, the required work input is:

$$W_{real} = \frac{Q_C}{\eta \, COP_{Carnot}}$$

From these equations,

Ideal Coefficient of Performance, COP_{Carnot}	9.00
Heat Pump Efficiency, η [76] (Ewert, 1991)	0.50
Necessary Input Power, W_{real}	20.7 kW

The ETCS radiators are modeled by the model developed for the parametric study.

Radiating Area per radiator ORU	129.8 m^2
Fin Efficiency	0.88
Emissivity	0.90
Radiator Mass Flowrate of Ammonia per Radiator ORU	0.1591 kg/s
Average Panel Surface Temperature	288.1 K
Heat Rejection per Unit Area	0.147 kW/m^2

By the first law of thermodynamics for a heat pump,

$$Q_{H,real} = W_{real} + Q_C$$

Total Heat Rejected by the Radiators, $Q_{H,real}$	114.1 kW
Necessary Radiator Surface Area	778.0 m^2
Number of Radiator ORUs Required	6

To check that this configuration was indeed a minimum, a parametric study was conducted using the model developed above (Figure 3.8). From this study, the mass for the heat pump power requirements increases more quickly than the mass of the radiator ORUs decreases. Therefore, the heat pump saves mass overall because the truss segment P0 may be deleted once a sufficiently high temperature lift is used. In this case that temperature lift is 30.6 K.

To account for pumping fluid through the heat pump condenser and the heat pump evaporator, pumping power equal to 150% of that required for the radiators is added. After deducting the radiator pumping power for the baseline case, this results in a net pumping power increase of 187.1 W. However, this heat pump will save mass in other areas because the truss segment P0 may be deleted entirely.

---

[76] Percentage of Carnot coefficient of performance (COP).
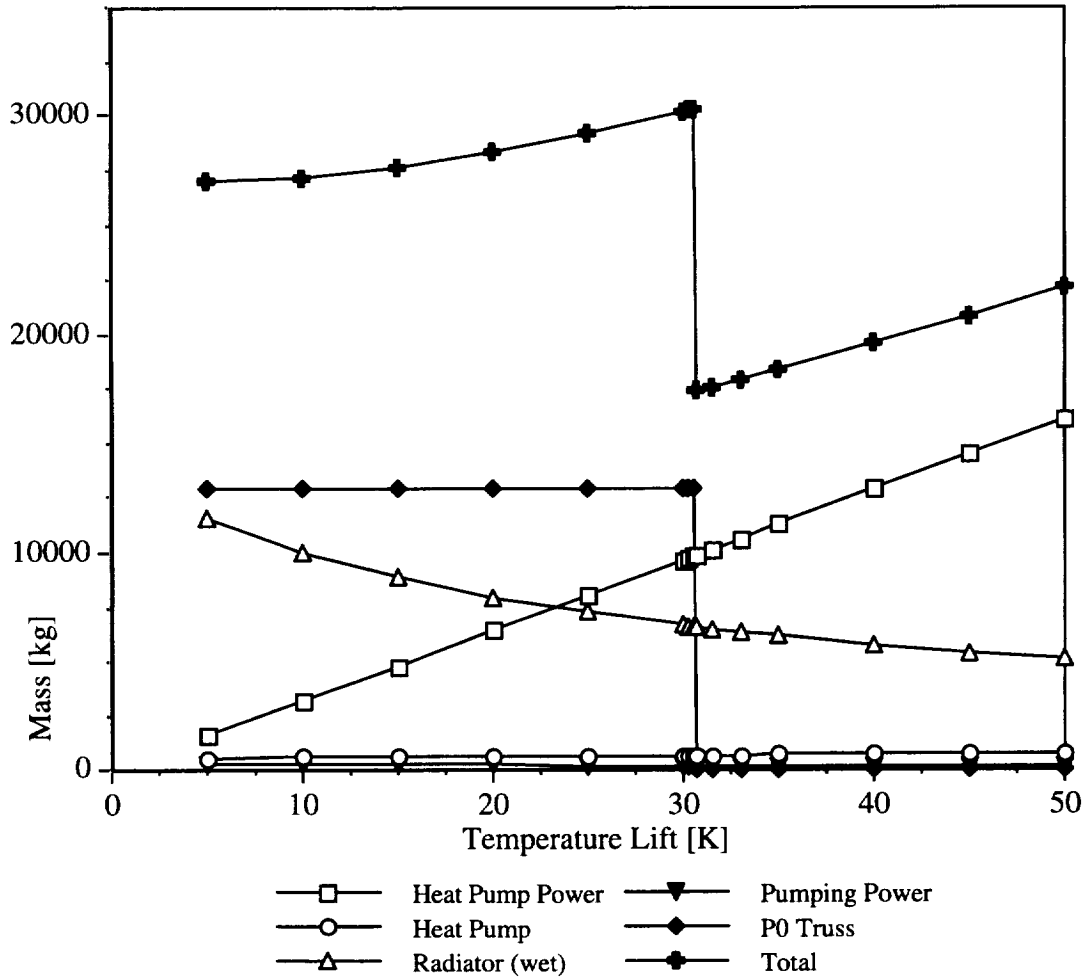
Figure 3.8 Variation of the ISS ETCS mass as a function of heat pump temperature lift for the LVS Case.

Net Mass Decrease Due to Vapor Compression Heat Pump Installation	Total Item Mass [kg]
Heat Pump [77]	-699.1
Segment P0 [78]	10,377.8
Mass of Power for Heat Pump, 20.7 kW	-9839.6
Mass of Pump Power Due to Added Equipment, 0.1871 kW	-89.1
Total	-250.0

[77] The heat pump mass is the sum of its component masses. The evaporator and condenser masses are 2.72 kg per kW of heat exchanger capacity (Swanson, Sridhar, and Gottman, 1993). The total of the heat pump compressor and driving motor masses is taken as 31.83 $(\text{Input Work})^{0.476}$ (Green, 1991).

[78] See Table 3.10 for details.

This heat pump's main disadvantage is an extremely high power requirement [79] but this option does not require adding additional truss segments for radiator ORUs. If the heat pump supports could be affixed to existing structures, this would minimize disruptions to ISS operations.

Specific Assessments:

Equipment Mass Savings	9,679 kg
Power Savings	-20.9 kW
Power Savings as Mass	-9,929 kg
Overall Mass Savings	-250 kg
Composite Qualitative Score [80]	0

3.1.5.5   Solar Vapor Compression Heat Pump

A solar vapor compression heat pump [81] uses the same equipment as the heat pump presented in Section 3.1.5.4 except that input power is provided by a dedicated solar photovoltaic array instead of by the general station resources. Further, a bypass for the heat pump will allow the ETCS to use the radiators directly when the heat pump is not in use on the dark side of the orbit. Therefore, a solar heat pump does not require any electrical storage. Using the assumption that the power management and distribution system mass can be cut by a third and the power storage mass can be entirely eliminated, the appropriate power mass penalty from Table 3.12 becomes 221 kg/kW. The pumping power is computed using a penalty factor of 476 kg/kW because continuous use is assumed. The net mass decrease for a solar vapor compression heat pump is:

Net Mass Decrease Due to Solar Vapor Compression Heat Pump Installation	Total Item Mass [kg]
Heat Pump [82]	-699.1
Segment P0 [83]	10,377.8
Mass of Power for Heat Pump, 20.7 kW	-4568.4
Mass of Pump Power Due to Added Equipment, 0.1871 kW	-89.1
Total	5021.2

---

[79]   The power consumption here is equivalent to the entire output of the solar power modules added as part of the upgrade to ISS in year 20. While additional power modules may be added to offset usage by the heat pump, and this is the assumed scenario, this comparison hopefully puts some perspective on the heat pump's power consumption.

[80]   The deployment for this option is "easy" because this technology does not require additional supporting trusses. However, the development cost is "high" because this is an orbital mission.

[81]   See Section 2.2.2 for details on solar vapor compression heat pumps.

[82]   See the footnotes for Section 3.1.5.4 for the heat pump sizing correlation.

[83]   See Table 3.10 for details.

The solar heat pump has the same advantages as the standard heat pump presented in the previous section. However, the mass of the required supporting power systems for the solar heat pump is about half of the corresponding power mass for the standard heat pump. Because the power system accounts for over 90% of the mass added for the vapor compression heat pump, reducing this mass by over half is highly advantageous.

Specific Assessments:

Equipment Mass Savings	9,679 kg
Power Savings	-20.9 kW
Power Savings as Mass	-4,658 kg
Overall Mass Savings	5,021 kg
Composite Qualitative Score [84]	+1

3.1.5.6   Arterial Heat Pipe Radiators

For the mission of ISS evolution, the first arterial heat pipe [85] configuration presented uses 13.11-m (43-ft) units. These units are the longest that will fit in the payload bay of a Shuttle vehicle. Longer heat pipes during ground testing demonstrated the best heat rejection per unit system mass (Chambliss and Ewert, 1990). Thus, the 13.11-m heat pipes were originally selected as part of the Space Station baseline ATCS. Tests on orbit using 15.24-m heat pipes [86] were less than satisfactory. A shorter heat pipe, 6.71-m (22-ft) long, functioned well when tested on orbit (Brown, Ungar, and Cornwell, 1992) [87]. The second configuration presented employs this shorter heat pipe.

13.11-meter (43-foot) Long Arterial Heat Pipe Panels

After the ISS evolution mission in year 20, the total load rejected by the eight ETCS flow-through radiator ORUs at a sink temperature of 245.4 K would be 93.39 kW. Assuming an equivalent load for arterial heat pipes, analysis yields:

Heat Load Rejected	93.36 kW
Average ETCS Ammonia Temperature	275.5 K
Fin Efficiency (Pekrul, *et al.*, 1989)	0.925
Surface Emissivity	0.90
Temperature Drop Between the ETCS Heat Exchanger and the Arterial Heat Pipe (Chambliss and Ewert, 1990)	2.4 K
Average Radiator Temperature	273.1 K
Sink Temperature	245.4 K

---

[84]   The deployment for this option is "easy" because this technology does not require additional supporting trusses. However, the development cost is "high" because this is an orbital mission.

[85]   See Section 2.3.1 for a description of arterial heat pipes.

[86]   This is the SHARE test.

[87]   This is the SHARE II test. Besides the length, the heat pipe tested during SHARE II used a different internal arrangement than the heat pipe tested during SHARE.

Arterial Heat Pipe ORU Surface Area	7.43 m²
Total Heat Pipe Radiating Area	1,021.55 m²
Total Number of Heat Pipe ORUs	137.45

In terms of actual hardware, it is assumed that each ETCS heat exchanger will hold six arterial heat pipe ORUs. The ETCS heat exchangers are affixed to the radiator beam truss in a line with the arterial heat pipes extending from one side. The center of the radiator beam truss attaches to the TRRJ interface.

Rounding the previous estimate upward, the final configuration will use 138 heat pipe ORUs and 23 ETCS heat exchangers. They will be deployed in two clusters of eight ETCS heat exchangers plus one cluster of seven ETCS heat exchangers, to remain consistent with the assumed ISS reference mission. Further, the mass for the ETCS condenser in the original two-phase system given in Section 2.3.1 will be assumed for the ETCS heat exchangers. The power for pumping flow through the ETCS heat exchangers is assumed to equal the power required for pumping fluid through the current ISS flow-through radiator ORUs. Additionally, to install the 13.11-m arterial heat pipe radiators on ISS, new radiator beam trusses will be needed. The baseline radiator beam trusses will be removed and the radiator beam truss for segment P0 [88] will be omitted. Thus, for the 13.11-m arterial heat pipes:

Mass Savings Using 13.11-m Arterial Heat Pipes	Item Mass [kg]	Quantity in Year 20	Total Mass [kg]
Arterial Heat Pipe ORU	-40.88	(138)	-5641.4
ETCS Heat Exchanger and Interfacial Mechanism	-137.40	(23)	-3160.2
Radiator Beam Truss (per ORU panel)	-1.59	(138)	-219.4
Total Mass for Arterial Heat Pipe Radiators			-9021.0
ISS Flow-Through Radiator ORU With Fluids (28-Sep-94)	1104.9	(8)	8838.9
Segment P0 Radiator Beam	806.7	(1)	806.7
Total Baseline Configuration Mass			9645.6
Equipment Mass Savings			624.6

The 13.11-m arterial heat pipe radiators will yield a mass savings of 624.6 kg (1,377.0 lb_m) in hardware compared with the ISS reference mission using flow-through radiator ORUs.

6.71-meter (22-foot) Long Arterial Heat Pipe Panels

After the ISS evolution mission in year 20, the total load rejected by the eight ETCS flow-through radiator ORUs at a sink temperature of 245.4 K would be 93.39 kW. Assuming an equivalent load for arterial heat pipes, analysis yields:

---

[88]   See Table 3.10 for a listing of truss segment P0.

Heat Load Rejected	93.36 kW
Average ETCS Ammonia Temperature	275.5 K
Fin Efficiency [89]	0.925
Surface Emissivity	0.90
Temperature Drop Between the ETCS Heat Exchanger and the Arterial Heat Pipe (Chambliss and Ewert, 1990)	2.4 K
Average Radiator Temperature	273.1 K
Sink Temperature	245.4 K
Arterial Heat Pipe ORU Surface Area	6.94 m^2
Total Heat Pipe Radiating Area	1021.55 m^2
Total Number of Heat Pipe ORUs	147.20

In terms of actual hardware, it is assumed that each ETCS heat exchanger will hold four arterial heat pipe ORUs. The ETCS heat exchangers are affixed to the radiator beam truss in a line with the arterial heat pipes extending from both sides. In fact, each ETCS heat exchanger has two sockets on each side. The end of the radiator beam truss attaches to the TRRJ interface.

Rounding the previous estimate upward, the final configuration will use 148 heat pipe ORUs and 37 ETCS heat exchangers. They will be deployed in two clusters of 13 ETCS heat exchangers plus one cluster of ten ETCS heat exchangers, to remain consistent with the assumed ISS reference mission. Further, the mass for the ETCS condenser in the original two-phase system given in Section 2.3.1 will be assumed for the ETCS heat exchangers. The power for pumping flow through the ETCS heat exchangers is assumed to equal the power required for pumping fluid through the current ISS flow-through radiator ORUs. Additionally, to install the 6.71-m arterial heat pipe radiators on ISS, new radiator beam trusses will be needed. Again, the baseline radiator beam trusses will be removed and the radiator beam truss for segment P0 will be deleted. Thus:

Mass Savings Using 6.71-m Arterial Heat Pipes	Item Mass [kg]	Quantity in Year 20	Total Mass [kg]
Arterial Heat Pipe ORU	-45.05	(148)	-6667.4
ETCS Heat Exchanger and Interfacial Mechanism	-78.92	(37)	-2920.0
Radiator Beam Truss (per ORU panel)	-3.81	(148)	-563.9
Total Mass for Arterial Heat Pipe Radiators			-10151.3
ISS Flow-Through Radiator ORU With Fluids (28-Sep-94)	1104.9	(8)	8838.9
Segment P0 Radiator Beam	806.7	(1)	806.7
Total Baseline Configuration Mass			9645.6
Equipment Mass Savings			-505.7

---

[89]　Internally, 6.71-m arterial heat pipes have four extrusions in their evaporators and condensers. Thus, even though these panels are wider, they have the same fin efficiency as the 13.11-m heat pipes. The fin efficiency for the 13.11-m heat pipes is given by Pekrul, *et al.* (1989).

The 6.71-m arterial heat pipe radiators will require 505.7 kg (1,114.9 lb$_m$) more in hardware compared with the ISS reference mission using flow-through radiator ORUs.

Arterial Heat Pipe Reliability

The arterial heat pipes will have high reliability due to using numerous individually sealed elements and their ease of replacement. Loss of a single heat pipe ORU will have negligible effect on ISS's overall heat rejection. Further, any one heat pipe ORU can be replaced much more easily than the flow-through ORUs. Christiansen (1992) predicts that micrometeoroids and orbital debris will puncture the flow-through radiator ORUs 1.55 times during the final ten years of the original 30-year ISS project life. His results are presented below and graphically in Figure 3.9. Here the arterial heat pipe installation using 6.71-m heat pipes is selected. While the 13.11-m option is less massive, the shorter heat pipes are already proven on orbit.

	Time [Years]		
	10	20	30
Cumulative Number of Flow-Through Radiator Perforations Due to On-Orbit Debris [90]	0.616	1.6	3.15

It is assumed that any debris puncture to the ISS ETCS will drain the corresponding flow loop in about two hours (Keller, 1995 a). After the hole is patched, or the damaged section of the radiator is closed off from the rest of the flow loop, the appropriate ETCS flow loop can be refilled using new ammonia, 226.7 kg [91], brought on a resupply flight. Further, this process will be acutely necessary because one loop represents half of the heat-rejection capability of the U.S.-led portion of ISS. In contrast, assuming the ETCS heat exchangers for the arterial heat pipes are well shielded such that an ETCS loop puncture is unlikely, puncturing debris will render only a single heat pipe unusable. Because a single arterial heat pipe represents only 1/148th of the ATCS capacity for the U.S.-led portion of ISS, replacing this loss is not immediately critical. Assuming:

- Any puncture of an ETCS flow-through radiator for the U.S.-led portion of ISS will be repaired or closed off from the rest of the flow loop. (It is assumed the radiator ORU itself will not require complete replacement.)
- The ETCS heat exchangers for the arterial heat pipes are well shielded from impacting space debris.
- Any punctured arterial heat pipe ORU will also not be replaced. (Its loss will be considered insignificant.)

Then, a mass savings for the arterial heat pipe ORUs compared with the baseline flow-through radiator ORUs is equal to the mass of ammonia lost using the flow-through panels over the final ten years of the original life of ISS.

---

[90] From Christiansen (1992). The value for 20 years is estimated using the curve fit to the data found in Figure 3.9.

[91] This value assumes that the ISS ATCS grows to include eight flow-through radiator ORUs. There is 191.8 kg of ammonia per ETCS loop when using six flow-through radiator ORUs (Wuestling, 1994).
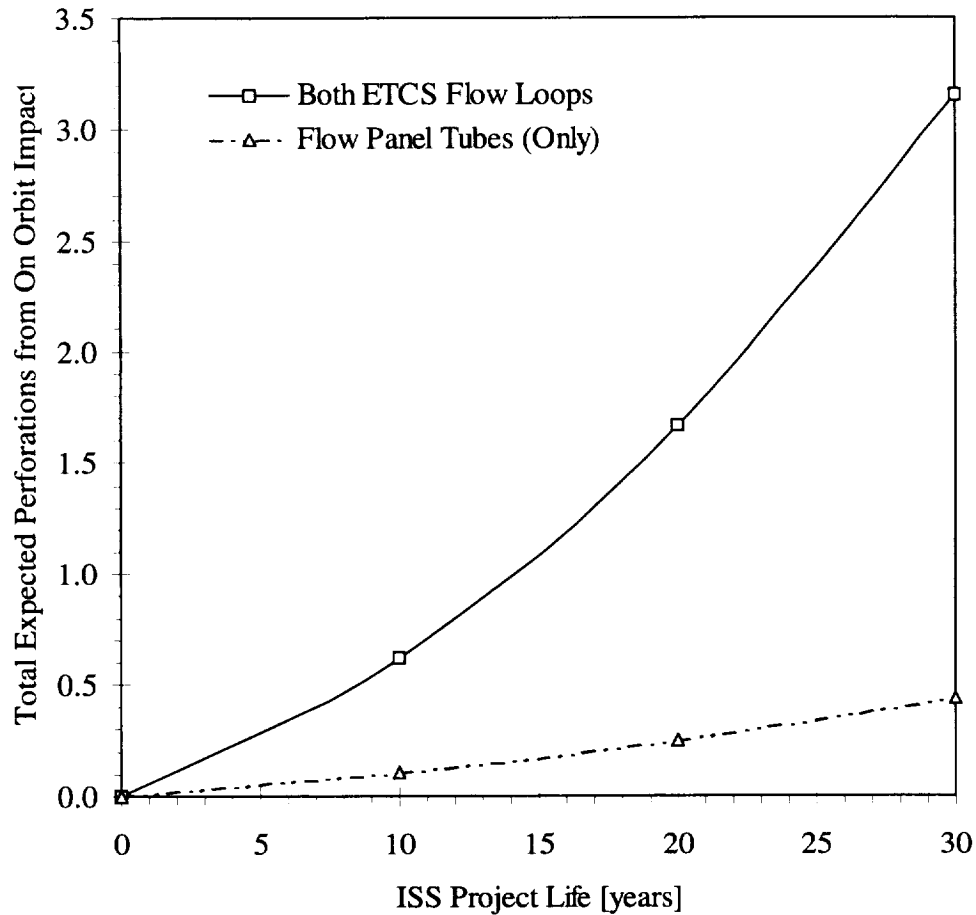
Figure 3.9 Perforations in the ISS radiator ORUs as a function of time. The flow loop segments within the remainder of ISS are sufficiently well-shielded that punctures due to on-orbit debris are not expected during the life of the project. The data points are from Christiansen (1992) while the curves are second-order polynomial fits to the data. The upper curve represents the number of ETCS loop punctures as a function of time for the flow-through radiator ORUs. The lower curve gives the number of punctures expected for just the panel flow tubes, which corresponds to the number of punctures expected in axial-groove heat pipes.

Mass of Ammonia per ETCS Loop	226.7 kg
Number of Flow-Through Radiator ORU Punctures Expected in the Final 10 Years	× 1.55
Mass of Ammonia Lost in the Final 10 Years Using Flow-Through Radiators	351.3 kg

Thus, any arterial heat pipe installation will yield a mass savings of 351.3 kg over ten years by saving ETCS loop ammonia which might be lost to space.

The 6.71-m arterial heat pipes require 505.7 kg more for hardware while saving 351.3 kg in ETCS working fluid when compared with the baseline ETCS. Overall, this option is 154 kg heavier than the baseline ETCS.

Specific Assessments:

Equipment Mass Savings	-505 kg
Replacement Mass Savings	351 kg
Power Savings as Mass	negligible
Overall Mass Savings	-154 kg
Composite Qualitative Score	+1

3.1.5.7 Axial-Groove Heat Pipe Radiators

The table below presents axial-groove heat pipe [92] and flow-through tube radiator panels to reject comparable quantities of heat for ISS evolution. Both radiator ORUs have the same surface area and use all the same equipment, including manifolds and radiator panels, except for the flow tubes/heat pipes themselves. The first design, by OAO Corporation (Nguyen, 1982, and Swerdling, 1993), employs 18 heat pipes (outside diameter of 0.015 m or 0.59 inch) spaced evenly in each radiator panel. The second design, by Loral Vought Systems (Howell, *et al.*, 1994) uses 22 flow-through tubes in spread-spacing. The overall fin efficiencies are similar.

Radiator ORU Hardware	Mass of Flow Tubes / Heat Pipes [kg]	Tubes per Panel	Fin Efficiency
OAO Corporation Heat Pipe ORU Radiator Panel Set [93]	143.92	18	0.872
Loral Vought Systems Flow-Through ORU Radiator Panel Set [94]	105.27	22	0.88

The radiator ORU mass increase using axial-groove heat pipes is 38.65 kg (85.21 lb_m). This translates to an equipment mass increase of 309.2 kg (681.7 lb_m) overall in year 20. Because the volume devoted to the ammonia circulating within the ETCS will decrease, a mass savings can be obtained by deleting some ammonia. The necessary power for pumping ammonia through the radiator manifolds will increase slightly (Nguyen, 1992) which will roughly offset the mass savings associated with using less ammonia.

A similar mass increase will apply to the PV-TCS radiator ORUs. Assuming the panel set mass versus the total radiator ORU mass is the same for the ETCS radiator

---

[92] See Section 2.3.3 for details of axial-groove heat pipes.

[93] The mass for this option includes both heat pipe and heat exchanger masses (Nguyen, 1992). An extrusion is assumed to be unnecessary because it could be affixed to the heat pipe during fabrication.

[94] The mass for this option includes the flow tubes, the extrusion used to position the tube within the radiator panel, and the silver epoxy (Oren, 1995).

ORUs and the PV-TCS radiator ORUs, an axial-groove heat pipe PV-TCS radiator ORU will increase by 38.65 kg (85.21 lb$_m$). This is a mass increase of 154.6 kg (340.8 lb$_m$) upon replacing all four PV-TCS radiator ORUs.

Specific Assessments:

Equipment Mass Savings	-309 kg
Power Savings as Mass	negligible
Overall Mass Savings	-309 kg
Composite Qualitative Score	+1

PV-TCS Assessments:

PV-TCS Equipment Mass Savings	-155 kg
PV-TCS Power Savings as Mass	negligible
PV-TCS Mass Savings	-155 kg

3.1.5.8 Arterial Heat Pipe Radiators With Electrohydrodynamic Pumping

As noted in Section 2.3.2, when the heat transport capacity of an arterial heat pipe is exceeded, the working fluid collects in the condenser, leaving the unit unusable. To prevent this, Bryan (1995) proposes applying electrohydrodynamic pumping to each individual unit. This arrangement would guard against the working fluid collecting in the condenser and ensure that each unit would be able to continually reject its applied heat load. In terms of actual hardware, the arterial heat pipes with electrohydrodynamic pumping will replace the 13.11-m arterial heat pipes from Section 3.1.5.6 without electrohydrodynamic pumping. Because the heat pipes with electrohydrodynamic pumping have a lower fin efficiency, the new configuration will be:

	13.11-m Arterial Heat Pipes Without Electrohydrodynamic Pumping [95]	13.11-m Arterial Heat Pipes With Electrohydrodynamic Pumping
Heat Pipe Panel Mass [kg]	40.88	32.29
Fin Efficiency	0.925	0.763
Heat Pipe ORU	138	167
ETCS Heat Exchanger and Interfacial Mechanism	23	28

Thus, this configuration will use 167 heat pipe ORUs and 28 ETCS heat exchangers. They will be deployed in two clusters of ten ETCS heat exchangers plus one cluster of eight ETCS heat exchangers. As above, the radiator beam trusses will require replacement, to be compatible with the arterial heat pipe architecture, and the baseline segment P0 radiator beam truss can be omitted. The power for pumping flow through the

---

[95] From Section 3.1.5.6.

ETCS heat exchangers is again assumed to equal the power required for pumping fluid through the current ISS flow-through radiator ORUs.

Mass Savings Using Arterial Heat Pipes With Electrohydrodynamic Pumping	Item Mass [kg]	Quantity in Year 20	Total Mass [kg]
13.11-m Arterial Heat Pipe ORU	-31.34	(167)	-5233.8
ETCS Heat Exchanger and			
Interfacial Mechanism	-137.40	(28)	-3847.2
Radiator Beam Truss (per ORU panel)	-1.59	(168)	-267.1
Equipment Mass for Arterial Heat Pipe Radiators With Electrohydrodynamic Pumping			-9348.1
Electrohydrodynamic Pumping Power as Mass	-0.95	(167)	-158.7
Total Mass for Arterial Heat Pipe Radiators With Electrohydrodynamic Pumping			-9506.8
ISS Flow-Through Radiator ORU With Fluids (28-Sep-94)	1104.9	(8)	8838.9
Segment P0 Radiator Beam Truss	806.7	(1)	806.7
Total Baseline Configuration Mass			9645.6
Equipment Mass Savings			138.8

The arterial heat pipe radiators with electrohydrodynamic pumping will yield a mass savings of 138.8 kg (306.0 lb$_m$) in hardware compared with the baseline ISS reference mission. However, as outlined in Section 3.1.5.6, arterial heat pipes will save an additional 351.3 kg by not losing ETCS loop ammonia over the final ten years of ISS. Therefore, the total overall mass savings for this option is 490.1 kg (1,080.5 lb$_m$) [96].

Specific Assessments:

Equipment Mass Savings	298 kg
Replacement Mass Savings	351 kg
Power Savings	-0.334 kW
Power Savings as Mass	-159 kg
Overall Mass Savings	490 kg
Composite Qualitative Score [97]	(0)

---

[96] Because electrohydrodynamic pumping is an immature technology, the mass estimates are extremely tentative and may be conservative. In fact, recent measurements by Bryan (1995) indicate that electrohydrodynamic pumping power consumption per arterial heat pipe ORU may be less than the 2.0 W assumed here.

[97] This is a combined technology so no assessment is provided for terrestrial use potential.

3.1.5.9 Lightweight Radiators

A parametric study here examines the potential savings from using lighter materials for various portions of the current radiator ORU assembly. Table 3.1 gives a fairly specific mass breakdown for a radiator ORU as of 29 March 1994. While this design has changed slightly since then, these values reflect the general mass distribution within an ISS radiator ORU. Further, to simplify and structure this study, the major subassemblies can be grouped into four categories.

Category	Mass [kg]	Percentage of ORU Mass
Base Structure, Deployment, and Panel Support:		35.5
Base Structure	200.81	
Scissors Beam and Hinges	92.76	
Torque Panels and Arms	47.26	
Cinching Mechanism	23.26	
Deployment Mechanism	34.40	
Flex Hose and Manifold Set	246.68	22.0
Radiator Panel Set	409.20	36.4
Additional Equipment and Fluids:		6.1
Deployment Motor	11.39	
Electrical	9.71	
Assembly Hardware	8.92	
Fluids	34.86	
Other	3.99	
Total	1123.24	100.0

This study varies the component radiator ORU masses linearly based on the original total mass for that category. Here the radiator panel mass is reduced up to 50% and the flex hose and manifold set masses are reduced up to 25%. This study assumes up to 20% mass savings for the base structure, deployment and panel support. Finally, no mass savings for the fluids and additional equipment is presumed [98].

Lightweight radiators, as presented here, are purely speculative. Two factors which will heavily influence ATCS component mass is the heat-rejection system design and the component materials. Here both the design and the component materials are, out of necessity, vague. The designs are vague because new radiator configurations which are under development may have significantly different mass requirements than current radiator technology. Further, lighter materials will yield additional mass savings which are currently not quantified. Rather, this section attempts to show the overall mass savings that might be realized if certain component radiator masses can be reduced. Some actual lightweight radiator concepts for ISS evolution are mentioned below.

The radiator panel set mass is the largest single component within the radiator ORU. Any technologies or materials which reduce this mass would form the basis for a lightweight radiator design. Assuming the design optimization would target mass

---

[98] See Section 2.4 for additional general background on lightweight radiators plus specific examples of proposed lightweight radiators.

reductions in the radiator panel set, the corresponding flex hoses and manifolds are assumed to decrease in mass at half the rate of the radiator panels. The flex hoses are already probably as light as possible for the appropriate component parts. Thus, any reduction in flex hose mass would require using smaller channel passages. Further, the constraint of using the lightest and strongest materials for the radiator panel set will probably dictate that the flex hose and manifold materials can not be completely optimized in order to maintain compatibility with the radiator panel set materials. (See Howell, *et al.* (1992), for an example of some material interaction problems associated with a radiator design.) The base structure, deployment, and panel support designs are driven more by the overall volume of the radiator ORU than by the mass of the other components. Thus, here it is assumed that the structural component mass can be reduced by only 20% for a reduction in the panel mass of 50%. Finally, the additional equipment and fluids are fixed masses. The additional equipment items are "off the shelf", while the fluid mass is a function of radiator volume and fluid density, both of which are constant. This approach gives an overall radiator ORU mass reduction of 30.8% when the radiator panel set mass is reduced by 50% (Figure 3.10).

Category	Percent Reduction in Radiator Panel Mass		
	10%	30%	50%
Base Structure, Deployment, and Panel Support [kg]	382.55	350.67	318.80
Flex Hose and Manifold Set [kg]	234.35	209.68	185.01
Radiator Panel Set [kg]	368.28	286.44	204.60
Additional Equipment [kg]	68.87	68.87	68.87
Overall Mass per Radiator ORU [kg]	1054.05	915.66	777.27
Overall Mass Reduction per Radiator ORU [kg]	69.19	207.58	345.97
Mass Reduction as a Percentage of the Original Radiator ORU Mass [%]	6.2	18.5	30.8
Radiator Mass Per Surface Area [kg/m^2] [99]	8.12	7.05	5.99

Considering the available lightweight radiators presented in Section 2.4, an overall mass reduction of 18.5% was selected as a representative value. Thus, the mass savings for eight radiator ORUs is 1,660.64 kg (3,661.10 lb$_m$). Because the flow geometry should be the same, the required pumping power is unchanged.

Two lightweight radiator concepts are appropriate for ISS evolution. The first would be to substitute composite flow-through radiator panels for the baseline architecture. This is the case most accurately represented by the analysis above. The second concept would be to use composite heat pipe radiators.

A similar mass savings may be achieved for the PV-TCS radiator ORUs. Assuming the ratio of the components within the PV-TCS radiator ORUs is similar to those in the ETCS radiator ORU, a lightweight PV-TCS radiator ORU will have a mass of 503.7 kg (1,110.4 lb$_m$). This is a savings of 114.3 kg (252.0 lb$_m$) per PV-TCS radiator ORU or 457.2 kg (1,008.0 lb$_m$) upon replacing all four PV-TCS radiator ORUs.

---

[99]   These values are based on a radiating area of 129.8 m^2 per radiator ORU.

Specific Assessments:

Equipment Mass Savings	1,661 kg
Power Savings as Mass	none
Overall Mass Savings	1,661 kg

PV-TCS Assessments:

PV-TCS Equipment Mass Savings	457 kg
PV-TCS Power Savings as Mass	none
PV-TCS Mass Savings	457 kg
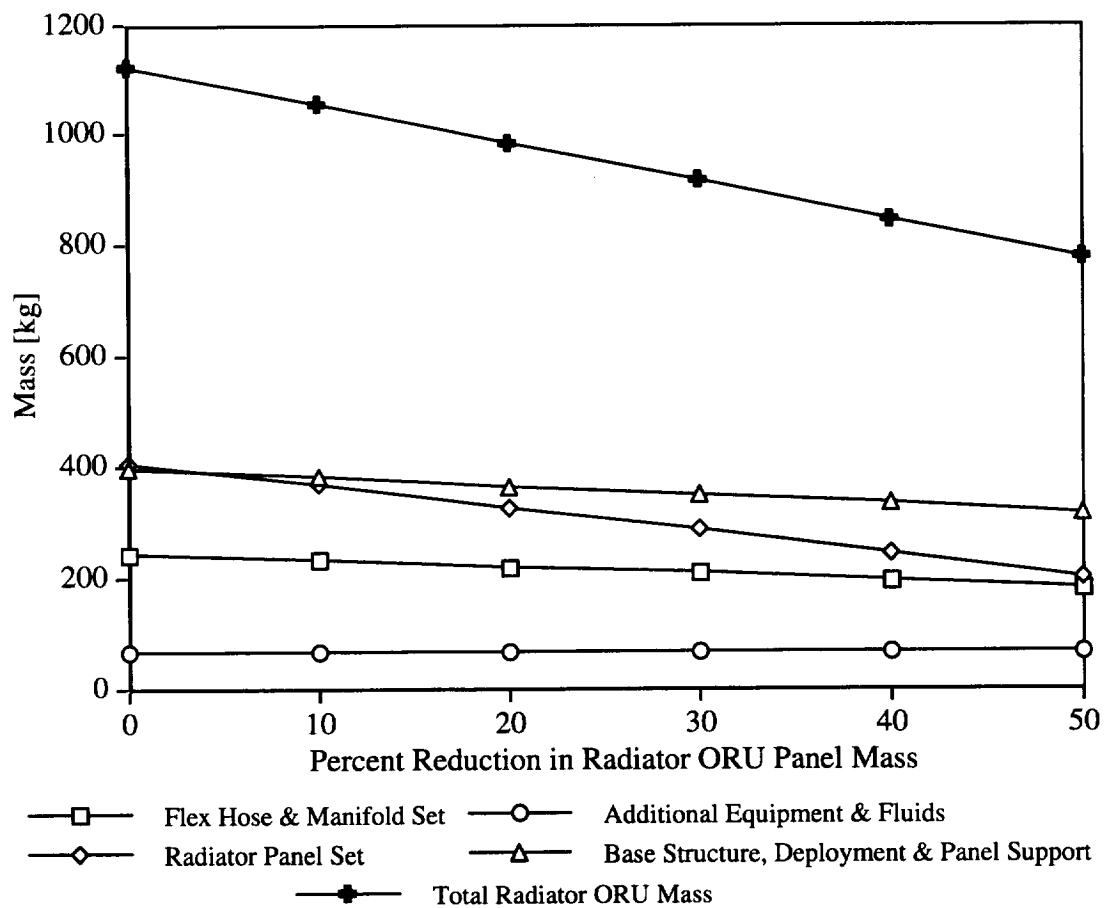
Figure 3.10 Radiator ORU mass as a function of mass reduction within the radiator panel set. Study Assumption: For each 10% mass reduction in the radiator panel set, the mass for the flex hoses and manifolds decreases by 5% and the mass of the base structure, deployment, and panel support decreases by 4%.

3.1.5.10 Rotary Fluid Coupler

The current ISS TCS uses a flex hose coupler with a mass of 159 kg (350 lb$_m$) and an approximate volume of 0.634 m^3 (22.4 ft^3) (Harwell, 1992). Flexible hoses within the flex hose coupler allow ATCS fluid streams to transfer to and from the radiator ORUs irrespective of the TRRJ's orientation. Because the flexible hoses wrap around a central hub as the TRRJ traverses, the entire radiator structure may rotate no more than ±105 degrees before a counter-rotation is required to unwind the flexible hoses. Additionally, the hoses themselves are subject to fatigue. Because ISS can usually perform the required counter-rotation while it is in Earth's shadow, the flex hose coupler has only a small performance penalty. (At some beta angles the rotation limit is reached while ISS is still in sunlight.)

A rotary fluid coupler [100] is a fully rotating device which uses liquid seals to contain and separate the internal fluid flow channels (Harwell, 1992). A fully rotating device allows the radiators to always be aligned with the panel faces parallel to the solar vector. Because the flexible hoses of the flex hose coupler restrict rotation of the radiators, there are some orbital positions in which the best allowable radiator ORU alignment is not optimal. The projected rotary fluid coupler mass is 10.9 kg (24 lb$_m$) with an approximate volume of 0.0127 m^3 (0.45 ft^3). Therefore, the rotary fluid coupler would save 444 kg (978 lb$_m$) and 1.86 m^3 (65.9 ft^3) in three TRRJs when new couplers are necessary.

Specific Assessments:

Equipment Mass Savings	444 kg
Power Savings as Mass	negligible
Overall Mass Savings	444 kg
Composite Qualitative Score	+3

3.1.5.11 Carbon Brush Heat Exchanger

In order to save mass and improve DDCU cooling efficiency for ISS evolution, the current radiant fin interfaces could be replaced by carbon brush interfaces. As Section 2.6.3 implies, a quick one-dimensional heat transfer analysis reveals that this change will increase the interfacial conductivity by almost two orders of magnitude. This, in turn, yields more efficient cooling of the DDCUs. What further advantage or savings this imparts is dependent on the cooling needs of other units on the ETCS loop [101]. The equipment mass savings is summarized below [102]:

---

[100] See Section 2.6.1 for details.

[101] Assuming the DDCU baseplate will remain at its original temperature, then a more efficient, lower resistance interface will allow a lower ETCS flowrate past the DDCUs.

[102] Values followed by a question mark, ?, are assumed values; the actual masses were not identified. The values for the DDCUs on S1 and P1, which are known, were assumed here.

Location (Type of DDCU Coldplate)	Quantity	Coldplate Mass (each coldplate)	Fin Mass (each coldplate)	Total Equipment Mass Savings
S0 (DDCU)	4	62.4 kg	9.86 kg?	78.9 kg?
		137.6 lb$_m$	21.73 lb$_m$?	173.9 lb$_m$?
S1, P1 (DDCU)	2	51.1 kg	9.86 kg	39.4 kg
		112.6 lb$_m$	21.73 lb$_m$	86.9 lb$_m$
S4, S6, P4, P6	8	63.5 kg	4.29 kg	68.6 kg
for PV-TCS (DDCU-E)		139.9 lb$_m$	9.46 lb$_m$	151.3 lb$_m$

The total mass savings is twice the fin mass to account for the corresponding fin set on the coldplate socket on which the DDCU sits. Aluminum 6061-T6 is the assumed coldplate material with a density of 2,713 kg/m^3 (0.098 lb$_m$/in^3). Further, while it is assumed that the carbon brush heat exchangers will have negligible mass, the rest of the baseplate and coldplate mass will remain unchanged.

Specific Assessments:

Equipment Mass Savings	118 kg
Power Savings as Mass	none directly
Overall Mass Savings	118 kg
Composite Qualitative Score	+3

PV-TCS Assessments:

PV-TCS Equipment Mass Savings	69 kg
PV-TCS Power Savings as Mass	none directly
PV-TCS Mass Savings	69 kg

3.1.6   Summary

The various advanced technologies and their estimated benefits are summarized in the table below for the evolution of ISS. From Section 3.1.3, the mass of the baseline ETCS, excluding structural components, is 15,567.8 kg. Assuming the mass determinations throughout this study have associated uncertainties on the order of 10%, an overall TCS with an advanced technology would need to show a savings of at least 1,557 kg to ensure a mass savings. Further, because design and development costs are not trivial, a mass savings of at least 25%, or 3,892 kg, is desirable. Using these criteria, the TCSs with advanced technologies proposed for ISS evolution may be divided into five categories:

- TCSs using advanced technologies requiring a mass penalty greater than 10% of the overall baseline ETCS mass: none.

- TCSs using advanced technologies requiring a mass penalty less than 10% of the overall baseline ETCS mass: vapor compression heat pump (continuously operated), arterial heat pipe radiators, and axial-groove heat pipe radiators.

- TCSs using advanced technologies with a mass savings less than 10% of the overall baseline ETCS mass: two-phase TCS with MP/S, LP two-phase TCS, arterial heat pipe radiators with electrohydrodynamic pumping, and capillary pumped loops.

- TCSs using advanced technologies with a mass savings between 10 and 25% of the overall baseline ETCS mass: lightweight radiators.

- TCSs using advanced technologies with a mass savings greater than 25% of the overall baseline ETCS mass: solar vapor compression heat pump.

The second and third categories include those technologies which show a mass savings or deficit less than 10% of the baseline ETCS mass. These technologies will produce an ETCS which is comparable to the baseline system. The technology in the fourth category is promising but not outstanding for this mission. The technology in the fifth category shows significant promise for this mission.

For ISS evolution, another significant consideration is the time necessary to install any new TCS equipment on orbit. One criterion for grouping options is whether they require installation of an additional truss segment. Of the technologies discussed above, the continuously operated vapor compression heat pump and the solar vapor compression heat pump do not require any additional truss segments. While additional power systems, and their associated supporting trusses, are required for both of these options, it is presumed that these power systems can be readily mounted on either or both ends of the U.S. truss outboard of the alpha joints while the heat pumps are located inboard near the current ATCS heat-rejection equipment.

Several technologies addressed in this section are more correctly identified as enhancing technologies. Enhancing technologies are advanced technologies which will uniformly deliver a mass savings or penalty for a specified reference mission regardless of the type of TCS selected. These technologies include the rotary fluid coupler and the carbon brush heat exchanger. Thus:

- Enhancing technologies which require a mass penalty: none.

- Enhancing technologies which yield a mass savings: rotary fluid coupler and carbon brush heat exchanger.

Table 3.13 Advanced Active Thermal Control System Architecture
for International Space Station Evolution

Summary of Advanced Active Thermal Control System Architecture for International Space Station Evolution	ETCS Overall Mass Savings [kg]	Qual. Score	PV-TCS Overall Mass Savings [kg]	Qual. Score
3.1.5.1 Two-Phase Thermal Control System With Mechanical Pump/Separator	1,203	0	--	--
3.1.5.2 Low-Power Two-Phase Thermal Control System	1,366	-1	--	--
3.1.5.3 Capillary Pumped Loops	1,535	-2	--	--
3.1.5.4 Vapor Compression Heat Pump	-250	0	--	--
3.1.5.5 Solar Vapor Compression Heat Pump	5,021	+1	--	--
3.1.5.6 Arterial Heat Pipe Radiators [103]	-154	+1	--	--
3.1.5.7 Axial-Groove Heat Pipe Radiators	-309	+1	-155	+1
3.1.5.8 Arterial Heat Pipe Radiators With Electrohydrodynamic Pumping	490	(0)	--	--
3.1.5.9 Lightweight Radiators	1,661	--	457	--
3.1.5.10 Rotary Fluid Coupler	444	+3	--	--
3.1.5.11 Carbon Brush Heat Exchanger	118	+3	69	+2

---

[103] This value assumes 6.71-m heat pipe units. Assuming 13.11-m heat pipe units instead gives an overall mass savings of 625 kg and an overall qualitative score of -1.

3.2   SPACE TRANSPORTATION SYSTEM UPGRADE

3.2.1   Reference Mission

This study assumes that the current Space Transportation System (STS), or Shuttle, may be upgraded or refit with new TCS components as part of a program to extend the life of the fleet. Though less likely, this study could also apply to a new replacement vehicle with similar capabilities. The assumed power mass penalty is 100 kg/kW. This value assumes 56 kg/kW for power generation [104] plus 44 kg/kW for power management and distribution. A vehicle (or program) life of 140 missions (seven flights per year for 20 years) following upgrades is assumed. The mass savings are considered cumulative for the life of the vehicle or fleet of vehicles.

3.2.2   Baseline Case

Shuttle uses several devices in its ATCS to cover its wide range of operating environments. Listed here are the major components of the Shuttle ATCS which reject heat from the vehicle (Figure 3.11):

- Ammonia boiler subsystem (ABS): This device was designed for use on descent below 36,600 m (120,000 ft). In practice, except during a launch abort, the ABS provides cooling after Shuttle lands until the ground support personnel complete hookup of the ground support equipment heat exchanger. Simon (1994) lists the ABS heat-rejection ability as 33.2 kW (113,200 Btu/hr). The maximum energy capacity, using available ammonia, is 63,300 kW*s (60,000 Btu).

- Flash evaporator subsystem (FES): This device provides primary cooling during ascent while Shuttle is above 42,700 m (140,000 ft), and during descent while Shuttle is above 30,500 m (100,000 ft). In this high load mode, the FES provides heat rejection up to 43.4 kW (148,000 Btu/hr) (Simon, 1994). On orbit, while the payload bay doors are open, the FES provides supplementary cooling of up to 11.4 kW (39,000 Btu/hr) in its topping mode. When the payload doors are closed on orbit, the FES provides primary cooling for Shuttle in its high load mode. The FES exhaust lines, nozzles, and feedwater lines use up to 1435.5 W for internal heaters to prevent in-line ice blockage.

- Ground support equipment heat exchanger (GSE HX): This device provides cooling while Shuttle is on the ground, both before launch and after ground personnel hook up a portable cooling cart after landing. Simon (1994) lists the maximum heat-rejection capability for the GSE HX as 31.4 kW (107,000 Btu/hr). Jaax (1978) specifies the GSE HX volume as 7.04×10^{-3} m^3 (0.249 ft^3) with a dry mass of 6.1 kg (13.4 lb_m).

---

[104]   The power generation value corresponds to using three sets of hydrogen and oxygen tanks during six days on orbit. This translates to a power output of 15 kW.

- Radiator panels: Shuttle uses six or eight radiator panels mounted inside the payload bay on orbit to reject heat. While the payload doors are open, this is the primary heat-rejection system. To increase the effective radiator heat transfer area, the forward two panels on each side may be deployed away from the payload doors while the aft radiators, plus the kit radiators if they are installed, are fixed to the payload bay doors. These same panels are used, after cold-soaking, as a vehicle heat sink while Shuttle is transiting between altitudes serviced by the other heat-rejection equipment on descent. Rotter (1987) notes that the radiator heat-rejection capability is a function of the orbit altitude and attitude. According to Jaax (1978), the six-panel configuration has a maximum heat rejection of 22.0 kW (75,000 Btu/hr). Physically, this configuration has a total mass of 573.2 kg (1,263.8 lb_m), including the necessary Freon 21 fluid. When fully deployed, the panels display an effective surface area of 114.3 m^2 (1,229.8 ft^2). The mass per surface area is 5.01 kg/m^2. In the eight-panel configuration, the maximum heat rejection is 28.1 kW (96,000 Btu/hr). Physically, the total panel mass is 744.7 kg (1,641.8 lb_m) with an effective radiator surface area of 140.4 m^2 (1,511.6 ft^2). The mass per surface area is 5.30 kg/m^2. Because all working Shuttle flights utilize the eight panel configuration (Rotter, 1996), this will be assumed standard for this analysis. The specifications for the radiator panels are (Jaax, 1978):

Overall Panel Measurements:

Length	(All):	4.60 m (15.1 ft)
Width	(All):	3.20 m (10.5 ft)
Thickness	(Forward or Mid-Forward Panels):	0.0229 m (0.900 in.)
	(Mid-Aft or Aft Panels):	0.0127 m (0.500 in.)

Facesheet (Aluminum 2024):

Thickness:	279×10^{-6} m (0.011 in.)

Panel Honeycomb Core (Aluminum 5056-H39):

Density:	49.7 kg/m^3 (3.1 lb_m/ft^3)

Panel Manifold Lines (Aluminum 5083):

Outer Diameter:	0.0222 m (0.875 in.)
Wall Thickness:	889×10^{-6} m (0.035 in.)

Panel Flow-Through Tubes (Aluminum 6061-T6):

Forward and Mid-Forward Panels:

Number of Tubes per Panel:	68
Outside Diameter:	0.00475 m (0.187 in.)
Wall Thickness:	508×10^{-6} m (0.020 in.)

Mid-Aft and Aft Panels:

Number of Tubes per Panel:	26
Outside Diameter:	0.00599 m (0.236 in.)
Wall Thickness:	508×10^{-6} m (0.020 in.)
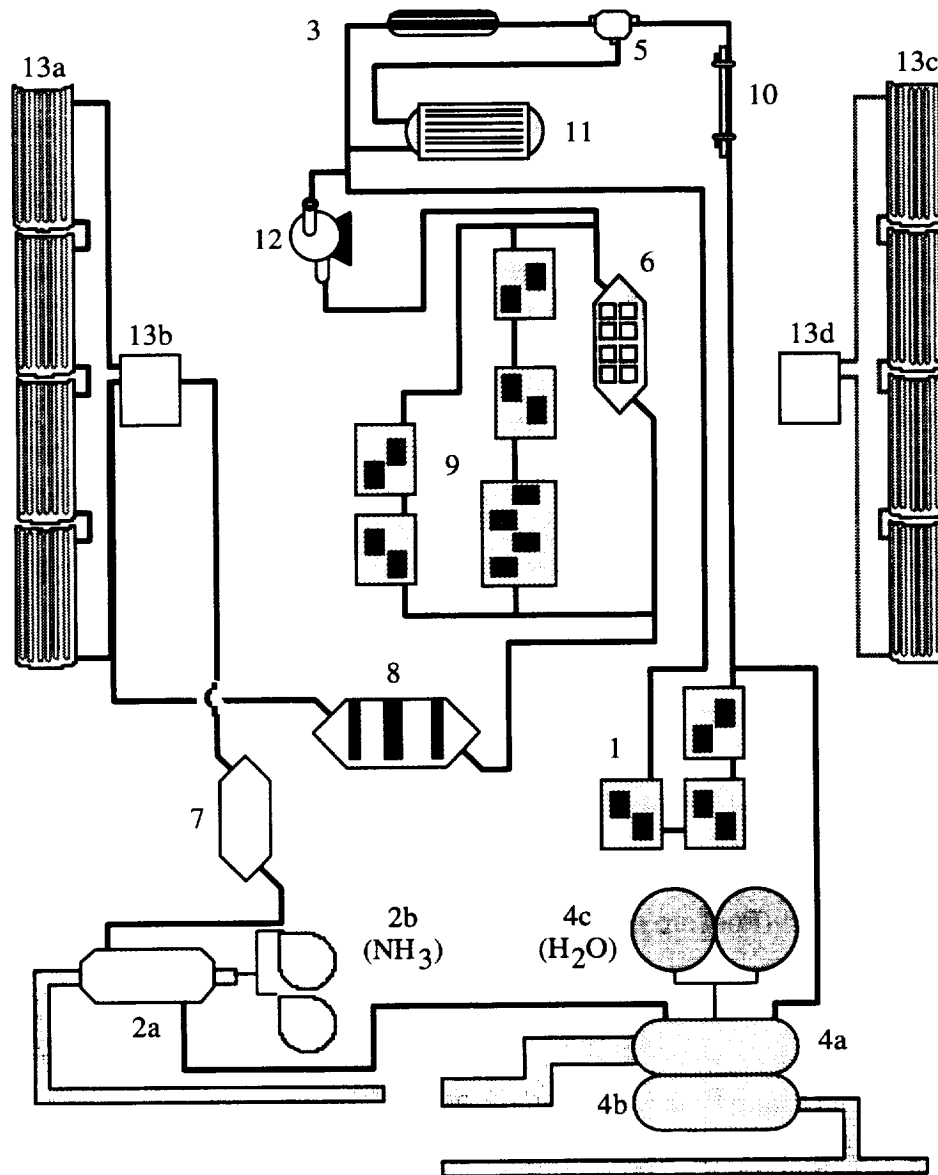
Figure 3.11 An overall schematic of the Space Transportation System active thermal control system. The labels refer to: (1) aft coldplates; (2) ammonia boiler subsystem, (a) boiler, (b) ammonia storage; (3) cabin interchanger; (4) flash evaporator subsystem, (a) high load unit, (b) topping unit, (c) water storage; (5) flow proportioning module; (6) fuel cell heat exchanger; (7) ground support equipment heat exchanger; (8) hydraulics heat exchanger; (9) midbody coldplates; (10) oxygen restrictor; (11) payload heat exchanger; (12) pump package (Freon 21); (13) flow-through radiators, (a) port radiator panels, (b) port flow control assembly, (c) starboard radiator panels, (d) starboard flow control assembly. Only one Freon 21 fluid loop, Loop 1, is shown. The second loop is like the first except that it serves the starboard radiators and not the port radiators.

The breakdown of area and mass within the radiator panels is (Jaax, 1978):

Table 3.14 Effective Area Breakdown of Shuttle Radiator Panels

Shuttle Side (Servicing Freon Loop)	Forward Panels [m^2]	Mid-Forward Panels [m^2]	Mid-Aft Panels [m^2]	Aft Panels [m^2]
Left (Loop 1)	21.93	22.58	12.89	13.15
Right (Loop 2)	21.73	22.32	12.79	13.03
Average Effective Area [105]	21.83	22.45	12.84	13.09

Table 3.15 Mass Breakdown of Shuttle Radiator Panels

Item	Forward Panel [kg]	Mid-Forward Panel [kg]	Mid-Aft Panel [kg]	Aft Panel [kg]
Facesheets	22.8	22.8	22.8	22.8
Honeycomb	15.5	15.5	8.3	8.3
Manifolds	2.0	2.0	2.0	2.0
Flow Tubes	11.4	11.4	5.6	5.6
Other Items	40.2	43.6	38.8	40.2
Fluids (Freon 21)	8.5	7.7	5.7	6.8
Total Mass per Panel	100.4	103.0	83.2	85.7

Aluminum Densities:

2024:	2770 kg/m^3 (0.100 lb$_m$/in^3)
5083 (Assumed):	2660 kg/m^3 (0.096 lb$_m$/in^3)
6061-T6:	2710 kg/m^3 (0.098 lb$_m$/in^3)

- Freon 21 pump package: Shuttle has four pumps housed in two pump modules to circulate Freon 21 within the vehicle. The second pump in each module is a spare and is normally not used. Each package has a mass of 20.3 kg (44.7 lb$_m$) and a volume of 0.180 m^3 (6.34 ft^3). The Freon 21 loops, excluding the accumulator, have a total volume of 0.159 m^3 (5.60 ft^3). The loop volumes are not identical with Loop 2 accounting for 51.8% of the total system volume. From the pump curves in Mistrot (1994), the current pumps have the following characteristics:

Output Mass Flowrate [106] [kg/s]	Pressure Rise Across Pump [kN/m^2]	Required Input Power [kW]
0.283	501	0.340
0.321	469	0.360
0.340	455	0.370
0.378	416	0.389

---

[105] The total effective area, or sum, for all radiator panels is 140.42 m^2. The effective area here accounts for the surface available to exchange heat with the environment (space). This does not include a fin efficiency, which is currently unknown, so a value of 1.0 is assumed.

[106] These flowrates include the minimum and maximum loop flowrates.

The Shuttle ATCS component breakdowns are presented in Table 3.16 and Table 3.17.

Table 3.16 Heat-Rejection ETCS Hardware for Shuttle

STS ETCS Hardware	Qty per STS	Total Item Mass kg	lb$_m$	Maximum Heat-Rejection Capability kW	kBtu/hr
Ammonia Boiler:	(1)			33.2	113.2
Equipment		27.6	60.8		
Ammonia (NH₃)		44.3	97.6		
Vent Line [107]		-- --	-- --		
Flash Evaporator:	(1)				
FES		28.6	63.0		
Ducting & Nozzles		45.8	100.9		
H₂O Accumulators		4.5	10.0		
Feedwater Supply:					
Max. Capacity		299.4	660		
Min. Requirement		90.7	200		
High Load Mode				43.4	148.0
Topping Only Mode				11.4	39.0
Flow Cont. Assembly	(2)				
Dry FCA		22.1	48.8		
FCA Fluid		1.4	3.0		
Ground Support Equipment					
Heat Exchanger	(1)	6.1	13.4	31.4	107.0
Radiator Panels [108]:					
Plumbing		8.3	18.2		
Fluid in Plumbing		2.0	4.5		
Dry Panels	(6)	529.5	1167.4	22.0	75.0
Panel Fluid		43.7	96.4		
Dry Panels + Kit	(8)	687.3	1515.2	28.1	96.0
Panel + Kit Fluid		57.4	126.6		
Total for ETCS Heat Rejection Hardware:					
Using 6 Rad Panels		672.5	1482.5		
Using 8 Rad Panels		830.3	1830.3		
Other Fluids [109]		44.3 + 90.7	97.6 + 200.0		
Max Heat Rejection:					
Ascent or Descent				43.4	148.0
On Orbit (8 Panels)				39.5	135.0
On Ground - ABS				33.2	113.2
On Ground - GSE				31.4	107.0

---

[107] The references consulted did not give a value for the vent line, although this mass is not insignificant.

[108] The heat rejection values here assume the best spacecraft attitude for radiant heat rejection (Jaax, 1978).

[109] This total is expressed as ABS ammonia plus, "+", FES feedwater. The total system Freon 21 is included in Table 3.17 below.

Table 3.17 Other ETCS Hardware for Shuttle

STS ETCS Hardware	Qty per STS	Total Item Mass kg	Total Item Mass lb$_m$	Maximum Heat-Rejection Capability [110] kW	Maximum Heat-Rejection Capability [110] kBtu/hr
Aft Coldplates	(7)	44.0	96.9		
Max. Heat Load				- 2.9	- 10.0
On-Orbit Heat Load				- 1.8	- 6.3
O$_2$ Restrictors	(2)	1.4	3.0		
Interchanger	(1)	14.5	32.0	-14.2	- 48.3
Payload Bay Heat Exchanger:	(1)	14.9	32.8		
Max. Heat Load					
Bay Doors Closed				- 1.5	- 5.2
Bay Doors Open:					
w/ 6 Rad Panels				- 6.3	- 21.5
w/ 8 Rad Panels				- 8.5	- 29.0
Fuel Cell Heat Exchangers	(2)	14.6	32.2	- 13.2	- 44.9
Midbody Coldplates	(2)	28.8	63.6	- 1.4	- 4.7
Hydraulics Heat Exchanger	(1)	10.6	23.4	4.4	15.0
Flow Distribution:					
Flow Proportioning Module	(1)	1.7	3.7		
Pump Package	(2)	40.6	89.5		
Plumbing [111]		-- --	-- --		
Total Fluids (Freon 21 only) [112]		229.5	505.9		
Total for Other ETCS Hardware:					
Equipment (Dry)		171.1	377.1		
Fluids		229.5	505.9		

To be consistent with the definitions used for ISS, all of the equipment listed in these tables are ETCS while the label ITCS is reserved to describe the water loop in the cabin ATCS.

Based on Table 3.16 and Table 3.17 the baseline ETCS mass for STS upgrade includes 1365.9 kg for equipment and 364.5 kg for fluids. An additonal 72.0 kg represents the mass of the ETCS power systems assuming the nominal pumping power consumption is 0.720 kW. Thus, the overall baseline ETCS mass is 1437.9 kg per vehicle, or 201,306 kg for 140 flights.

---

[110] A negative heat transfer capability denotes hardware which contributes heat to the TCS instead of rejecting heat.

[111] The plumbing mass is significant for a vehicle the size of STS, but a value of the plumbing mass is not given in the references consulted.

[112] Based on a total fluid volume for Freon 21 of 0.167 m^3 (5.9 ft^3) at 294.3 K (70°F) and an orbiter configuration using 8 radiator panels. This is the total Freon 21 circulating within the Freon loops.

3.2.3 Parametric Study Using the Baseline Case

Like the study presented in Section 3.1.4 for ISS, a simple model for Shuttle radiator heat rejection can be constructed based on an overall energy balance for the radiators. Actual STS flight data is used for an assumed baseline case. For this study, the chosen mission is STS-41 (1990). To get an accurate estimate of the heat rejected from the radiators, a time index was selected on orbit when the radiator panel exit temperatures were above the Freon loop set-point of 276.5±1.1 K (38±2 °F). This condition implies that the entire Freon loop flow passes through the radiator panels and none uses the radiator bypass line. Such a situation is recorded in the STS-41 data at 14 hours after liftoff.

Assumptions and Restrictions:

- All of the Freon in both loops passes through its corresponding radiator panel set.
- The effective radiator surface area for either loop is half of the total radiator surface area, 70.2 m². This assumes the forward two panels on either side are in the deployed position.
- The difference between the simple average Freon 21 loop temperature within the panels and the average radiator surface temperature is 1.5 K.
- The average specific heat, computed from the known properties for Freon 21 (Mistrot, 1994), may be used for the fluid side heat transfer. Here:

$$\bar{c}_p(\bar{T}) = \left[0.9335 + 0.001231 \exp\left(0.01555 \frac{1}{K} \bar{T} \right) \right] \frac{kW * s}{kg * K}$$

This parametric study computes the heat rejection for both sets of Shuttle radiators. The data for the STS-41 Case (Case A) come directly from that flight. At 14 hours after lift off, Discovery's radiators were rejecting 15.84 kW.

Input study constants:

Stefan-Boltzmann Constant	5.670×10^{-11} kW/(m²*K⁴)
Radiator Area per Freon Loop	70.2 m²
Infrared Emissivity [113]	0.76
Calculation Tolerance	0.00001

The initial case examines the STS-41 Case (Case A). The following series of cases present combinations of the minimum and maximum allowable Freon 21 mass flowrates and inlet temperatures. These cases provide bounds on the current abilities of the Shuttle radiator design.

---

[113] Jaax (1978).

	Case A Loop 1/Loop 2
Mass Flowrate of Freon 21 [kg/s]	0.3340/0.3513
Freon 21 Inlet Temperature [K]	301.1 / 300.4
Sink Temperature [K]	258.9 / 252.5
Average Freon 21 Temperature [K]	290.4 / 289.0
Average Panel Temperature [K]	288.9 / 287.5
Average Freon 21 Specific Heat [kW*s/kg*K]	1.05 / 1.04
Outlet Temperature of Freon 21 [K]	279.7 / 277.6
Loop Heat Rejection [kW]	7.48 / 8.37
Total Heat Rejection per Radiator Panel Set [kW]	15.85
Heat Rejection per Area [kW/m^2]	0.113

	Case B1A Loop 1/Loop 2	Case B1B Loop 1/Loop 2	Case B1C Loop 1/Loop 2
Mass Flowrate of Freon 21 [kg/s]	0.2835/0.2835	0.2835/0.3780	0.3780/0.3780
Freon 21 Inlet Temperature [K]	283.2 / 283.2	283.2 / 283.2	283.2 / 283.2
Sink Temperature [K]	199.8 / 199.8	199.8 / 199.8	199.8 / 199.8
Average Freon 21 Temperature [K]	265.8 / 265.8	265.8 / 269.2	269.2 / 269.2
Average Panel Temperature [K]	264.3 / 264.3	264.3 / 267.7	267.7 / 267.7
Average Freon 21 Specific Heat [kW*s/kg*K]	1.01 / 1.01	1.01 / 1.01	1.01 / 1.01
Outlet Temperature of Freon 21 [K]	248.5 / 248.5	248.5 / 255.3	255.3 / 255.3
Loop Heat Rejection [kW]	9.95 / 9.95	9.95 / 10.72	10.72 / 10.72
Total Heat Rejection per Radiator Panel Set [kW]	19.90	20.67	21.44
Heat Rejection per Area [kW/m^2]	0.142	0.147	0.153

	Case C1A Loop 1/Loop 2	Case C1B Loop 1/Loop 2	Case C1C Loop 1/Loop 2
Mass Flowrate of Freon 21 [kg/s]	0.2835/0.2835	0.2835/0.3780	0.3780/0.3780
Freon 21 Inlet Temperature [K]	322.0 / 322.0	322.0 / 322.0	322.0 / 322.0
Sink Temperature [K]	199.8 / 199.8	199.8 / 199.8	199.8 / 199.8
Average Freon 21 Temperature [K]	293.0 / 293.0	293.0 / 298.6	298.6 / 298.6
Average Panel Temperature [K]	291.8 / 291.8	291.8 / 297.1	297.1 / 297.1
Average Freon 21 Specific Heat [kW*s/kg*K]	1.05 / 1.05	1.05 / 1.06	1.06 / 1.06
Outlet Temperature of Freon 21 [K]	264.6 / 264.6	264.6 / 275.3	275.3 / 275.3
Loop Heat Rejection [kW]	17.11 / 17.11	17.11 / 18.76	18.76 / 18.76
Total Heat Rejection per Radiator Panel Set [kW]	34.22	35.87	37.51
Heat Rejection per Area [kW/m^2]	0.244	0.255	0.267

	Case B2A	Case B2B	Case B2C
	Loop 1/Loop 2	Loop 1/Loop 2	Loop 1/Loop 2
Mass Flowrate of Freon 21 [kg/s]	0.2835/0.2835	0.2835/0.3780	0.3780/0.3780
Freon 21 Inlet Temperature [K]	283.2 / 283.2	283.2 / 283.2	283.2 / 283.2
Sink Temperature [K]	227.6 / 227.6	227.6 / 227.6	227.6 / 227.6
Average Freon 21 Temperature [K]	270.0 / 270.0	270.0 / 272.5	272.5 / 272.5
Average Panel Temperature [K]	268.5 / 268.5	268.5 / 271.0	271.0 / 271.0
Average Freon 21 Specific Heat [kW*s/kg*K]	1.02 / 1.02	1.02 / 1.02	1.02 / 1.02
Outlet Temperature of Freon 21 [K]	256.8 / 256.8	256.8 / 261.9	261.9 / 261.9
Loop Heat Rejection [kW]	7.60 / 7.60	7.60 / 8.21	8.21 / 8.21
Total Heat Rejection per Radiator Panel Set [kW]	15.21	15.81	16.42
Heat Rejection per Area [kW/m^2]	0.108	0.113	0.117

	Case C2A	Case C2B	Case C2C
	Loop 1/Loop 2	Loop 1/Loop 2	Loop 1/Loop 2
Mass Flowrate of Freon 21 [kg/s]	0.2835/0.2835	0.2835/0.3780	0.3780/0.3780
Freon 21 Inlet Temperature [K]	322.0 / 322.0	322.0 / 322.0	322.0 / 322.0
Sink Temperature [K]	227.6 / 227.6	227.6 / 227.6	227.6 / 227.6
Average Freon 21 Temperature [K]	297.1 / 297.1	297.1 / 301.6	301.6 / 301.6
Average Panel Temperature [K]	295.6 / 295.6	295.6 / 300.1	300.1 / 300.1
Average Freon 21 Specific Heat [kW*s/kg*K]	1.06 / 1.06	1.06 / 1.07	1.07 / 1.07
Outlet Temperature of Freon 21 [K]	272.1 / 272.1	272.1 / 281.3	281.3 / 281.3
Loop Heat Rejection [kW]	14.97 / 14.97	14.97 / 16.43	16.43 / 16.43
Total Heat Rejection per Radiator Panel Set [kW]	29.93	31.40	32.86
Heat Rejection per Area [kW/m^2]	0.213	0.224	0.234

	Case B3A	Case B3B	Case B3C
	Loop 1/Loop 2	Loop 1/Loop 2	Loop 1/Loop 2
Mass Flowrate of Freon 21 [kg/s]	0.2835/0.2835	0.2835/0.3780	0.3780/0.3780
Freon 21 Inlet Temperature [K]	283.2 / 283.2	283.2 / 283.2	283.2 / 283.2
Sink Temperature [K]	249.8 / 249.8	249.8 / 249.8	249.8 / 249.8
Average Freon 21 Temperature [K]	274.5 / 274.5	274.5 / 276.2	276.2 / 276.2
Average Panel Temperature [K]	273.0 / 273.0	273.0 / 274.7	274.7 / 274.7
Average Freon 21 Specific Heat [kW*s/kg*K]	1.02 / 1.02	1.02 / 1.02	1.02 / 1.02
Outlet Temperature of Freon 21 [K]	265.8 / 265.8	265.8 / 269.1	269.1 / 269.1
Loop Heat Rejection [kW]	5.03 / 5.03	5.03 / 5.44	5.44 / 5.44
Total Heat Rejection per Radiator Panel Set [kW]	10.06	10.47	10.88
Heat Rejection per Area [kW/m^2]	0.0716	0.0746	0.0775

	Case C3A Loop 1/Loop 2	Case C3B Loop 1/Loop 2	Case C3C Loop 1/Loop 2
Mass Flowrate of Freon 21 [kg/s]	0.2835/0.2835	0.2835/0.3780	0.3780/0.3780
Freon 21 Inlet Temperature [K]	322.0 / 322.0	322.0 / 322.0	322.0 / 322.0
Sink Temperature [K]	249.8 / 249.8	249.8 / 249.8	249.8 / 249.8
Average Freon 21 Temperature [K]	301.2 / 301.2	301.2 / 304.9	304.9 / 304.9
Average Panel Temperature [K]	299.7 / 299.7	299.7 / 303.4	303.4 / 303.4
Average Freon 21 Specific Heat [kW*s/kg*K]	1.07 / 1.07	1.07 / 1.07	1.07 / 1.07
Outlet Temperature of Freon 21 [K]	280.3 / 280.3	280.3 / 287.9	287.9 / 287.9
Loop Heat Rejection [kW]	12.61 / 12.61	12.61 / 13.87	13.87 / 13.87
Total Heat Rejection per Radiator Panel Set [kW]	25.22	26.47	27.73
Heat Rejection per Area [kW/m²]	0.180	0.189	0.198

3.2.4   Advanced ATCS Architecture for Space Transportation System Upgrade

The upgraded STS vehicles are projected to serve for 20 additional years with an average of seven flights per year, or 140 missions overall. It is expected that the advanced architectures outlined below will, once installed, last for the life of the upgraded vehicle. However, regular vehicle ground maintenance should allow any failing components to be identified and replaced while the vehicle is not in use. As with the section on ISS above, each advanced architecture for Shuttle is assessed numerically for overall mass savings (for 140 missions). Qualitative assessments for these advanced technologies are presented in Section 2.0.

3.2.4.1   Low-Power Two-Phase Thermal Control System

To estimate the mass of a LP two-phase TCS [114] for STS upgrade this study extrapolates predictions from Ungar (1995) which gives estimates for space stations. Ungar (1995) includes estimates for three different vehicles using four different TCS architectures. Of the options presented, Shuttle most closely resembles a small system with a single-phase cascade TCS. Ungar also presents a LP two-phase TCS. The LP two-phase TCS requires less pumping power and smaller diameter flow lines than the single-phase cascade TCS. The required radiator area is roughly the same for the two systems. Thus, neglecting the flow line differences, the systems may be summarized by:

	Baseline Shuttle Thermal Control System		Small System (Ungar, 1995)			
			Single-Phase Cascade Thermal Control System		Low-Power Two-Phase Thermal Control System	
	Loop 1	Loop 2	LTL	LTL	LTL	MTL
Pump Power [kW]	0.360	0.360	0.320	0.320	0.068	0.080
Radiator Area [m²]	70.2	70.2	197	197	195	195
Loop Set-Point [K]	276.5	276.5	275.2	275.2	275.2	287.2

LTL refers to the low temperature loop while MTL refers to the moderate temperature loop. Shuttle uses a single-phase TCS which is similar to the single-phase cascade TCS

---

[114]   See Section 2.1.2 for details.

given by Ungar. Comparing the Shuttle TCS with the simple single-phase TCS for a small system reveals that the pumping power per loop is almost the same and the Shuttle TCS loop set-points are approximately that of the LTL for the single-phase cascade TCS. A comparable LP two-phase TCS for Shuttle then would use two LTL loops. The pumping power requirement for the revised Shuttle LP two-phase TCS then is 136 W. Thus:

	Current Shuttle Thermal Control System	Low-Power Two-Phase Shuttle Thermal Control System	Change (for 1 Mission)	Total Change (140 Missions)
Pump Power [kW]	0.720	0.136	-0.584	
Mass Due to Pump Power [kg]	72.0	13.6	-58.4	-8176.0

Because the overall vehicle mass decreases only slightly and approximations for these computations contain significant uncertainty, the two systems effectively have equivalent masses.

Specific Assessments (for 140 missions):

Equipment Mass Savings	negligible
Power Savings	81.76 kW
Power Savings as Mass	8,176 kg
Overall Mass Savings	8,176 kg
Composite Qualitative Score	-1

3.2.4.2　Lightweight Radiators

A parametric study here examines the potential savings from using lighter materials for various portions of the current Shuttle radiator assembly. Table 3.15 gives a fairly specific mass breakdown for the Shuttle radiators. To simplify this analysis, the major subassemblies within the Shuttle radiators can be grouped into four categories.

Category	Mass per Side of an STS [kg]	Percentage of Radiator Mass
Facesheet and Honeycomb:		37.3
Facesheet	91.2	
Honeycomb	47.6	
Flow Tubes and Manifolds:		11.3
Flow Tubes	34.0	
Manifolds	8.0	
Other Items	162.8	43.7
Fluids	28.7	7.7
Total	372.3	100.0

This study varies the component Shuttle radiator masses linearly based on the original total mass for that category. Here the facesheet and honeycomb masses are reduced up to 60% and the flow tube and manifold set masses are reduced up to 24%.

This study assumes up to 18% mass savings for other items, including the panel support and deployment mechanisms. Finally, no mass savings for the fluids is expected [115].

Lightweight radiators, as presented in this report, are purely speculative. Two factors which will heavily influence ATCS component mass are the heat-rejection system design and the component materials. Here both the design and the component materials are, out of necessity, vague. The designs are vague because new radiator configurations currently under development may have significantly different mass requirements than current radiator technology. Further, lighter materials will yield additional mass savings which are currently not quantified. Rather, this section attempts to show the overall mass savings that might be realized if certain component radiator masses can be reduced.

As with the radiator ORUs for ISS, advanced materials are most likely to significantly reduce the mass of the panel facesheets and honeycomb. Some mass reduction can also be expected for the flow tubes and manifolds, but the dimensions, and therefore mass, of these components are primarily determined by their function of containing the fluid within a specified volume. The category "Other Items" includes the deployment and support structures which are sized based upon the overall volume of the radiators and less on their absolute mass. Still, lighter radiators should allow some mass reductions in these supporting structures. Finally, the fluid mass is a function of radiator volume and fluid density, both of which are constant here. Overall, this study gives a radiator mass reduction of 33.0% when the facesheet and honeycomb masses are reduced by 60% (Figure 3.12).

Category	Percent Reduction in Facesheet and Honeycomb Mass		
	20%	40%	60%
Facesheet and Honeycomb [kg]	111.0	83.3	55.5
Flow Tubes and Manifolds [kg]	38.6	35.3	31.9
Other Items [kg]	153.0	143.3	133.5
Fluids [kg]	28.7	28.7	28.7
Overall STS Radiator Mass per Vehicle Side [kg]	331.4	290.5	249.6
Overall Mass Reduction per Vehicle Side [kg]	40.9	81.8	122.7
Mass Reduction as a Percentage of the Original Shuttle Radiator Mass [%]	11.0	22.0	33.0
Radiator Mass Per Surface Area [kg/m^2] [116]	4.72	4.14	3.56

Considering the available lightweight radiators presented in Section 2.4, an overall mass reduction of 22.0% was selected as a representative value. Thus, the mass savings for a complete Shuttle vehicle is 163.6 kg. For the life of the vehicle, which is 140 missions, this is a savings of 22,904.0 kg. Because the flow geometry should be the same, the required pumping power is unchanged. For actual equipment, the composite flow-through radiators are the only concept in the current study which are appropriate for STS upgrade.

---

[115] See Section 2.4 for additional general background on lightweight radiators plus specific examples of proposed lightweight radiators.

[116] These values assume a radiating area of 70.2 m^2 as found in the deployed 8 panel configuration.

Specific Assessments (for 140 missions):

Equipment Mass Savings	22,904 kg
Power Savings as Mass	none
Overall Mass Savings	22,904 kg
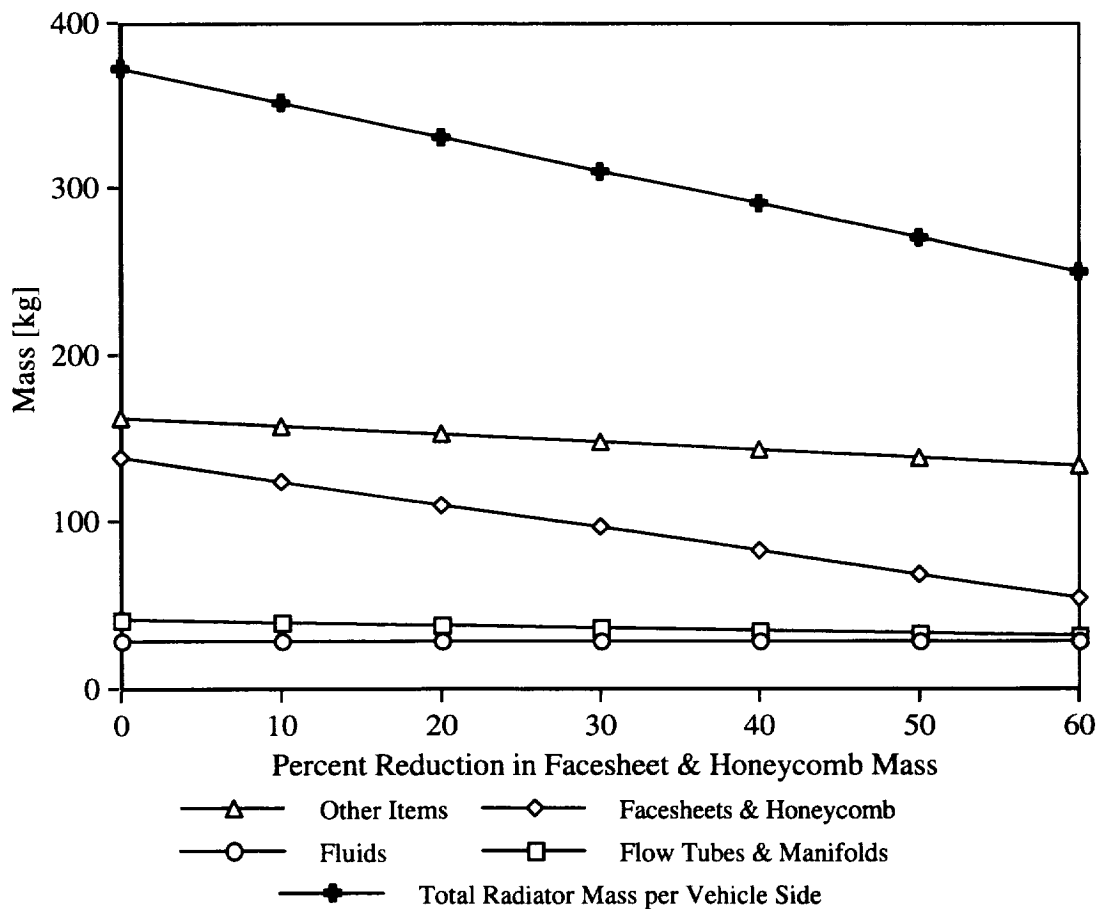
Figure 3.12 Shuttle radiator mass as a function of mass reduction within the radiator facing and honeycomb. The masses here are for one of two equivalent sets of radiator panels on a Shuttle vehicle. Study Assumption: For each 10% mass reduction in the facesheets and honeycomb the mass for the flow tubes and manifolds decreases by 4% and the mass of the other items decreases by 3%.

3.2.4.3   Phase-Change Thermal Storage

At least two scenarios are possible to size a phase-change thermal storage device for Shuttle. One case would presume to replace the ABS with phase-change thermal storage. This would require a system sized for 63,300 kW*s which is the current design capacity for the ABS. Preliminary calculations indicate that a corresponding phase-change

thermal storage system sized to replace the ABS would require 175.8 kg of PCM alone [117]. The mass of a fully charged ABS, however, is only 71.9 kg. Thus, to replace the ABS with phase-change thermal storage would lead to a substantial increase in vehicle launch mass.

A second case assumes that phase-change thermal storage is used to provide auxiliary cooling in conjunction with the radiators and FES. In particular, phase-change thermal storage could be used to reduce FES usage, thereby reducing the mass of cooling water rejected by the vehicle [118]. The PCM packages are solidified while the radiator rejects heat above the average orbital value and the PCM is allowed to melt to provide additional cooling while the radiator is rejecting heat below the average orbital value. Because the radiator heat load varies around an orbit, even when Shuttle is entirely in full sun at high beta angles, this approach is generally applicable. Figure 2.8 schematically illustrates an implementation of phase-change thermal storage for Shuttle [119].

Shuttle is an extremely versatile craft with a correspondingly complex heat-rejection profile. However, any mission will fly somewhere around planet Earth. The most advantageous heat-rejection environment would be at a beta angle of 50 degrees, while the most disadvantageous would be an orbit which is continually in full sun. For this second extreme an orbit at a beta angle of 75 degrees was selected. A constant altitude of 407,400 m (220 nautical miles) and an attitude of payload-bay-to-Earth complete the description of the vehicle thermal environment for this analysis. The radiator inlet temperature was held constant at 308.2 K (95.0 °F) and the working fluid mass flowrate was maintained at a value of 0.352 kg/s (2795 lb_m/hr) per loop. For these parameters, numerical analysis [120] yields:

	Vehicle Orbital Beta Angle [degrees]		
	0	50	75
Average Orbital Radiator Heat Rejection Rate [kW]	20.52	18.91	16.22
Energy Rejected Above the Average Rate / Orbit [kW*s]	3117.9	3859.3	1204.1
Equivalent Mass of FES Water / Orbit [kg] [121]	1.3963	1.7283	0.5392

---

[117] The assumed PCM is water with a thermal density of 10.0 kg/kW*h.

[118] As designed, Shuttle uses water, generated by producing electricity in its fuel cells, as feedwater for the FES. Early in the next century, however, water generated by Shuttle's fuel cells may be tapped as a source of potable water to be delivered to Space Station or for the crew on extended duration Shuttle missions. Use of phase-change thermal storage would save some water which currently is consumed by the FES.

[119] See Section 2.5.1 for more information on phase-change thermal storage.

[120] The analysis here used TSS with SINDA/FLUINT to compute radiator heat rejection profiles for the 310 node LTV model of Shuttle. After determining the average orbital radiator heat rejection, the energy above and below the average heat rejection were determined. The approach includes thermal capacitance for the radiator components.

[121] Based on assuming a heat of vaporization for water within the FES of 2,233 kW*s/kg (960 Btu/lb_m) (Lucas, 1996).

For this study, two materials were considered. Water has a thermal density [122] of 18.0 kg/kW*h including packaging. A long-chain alkane, or wax, such as n-dodecane has a thermal density of 30.2 kg/kW*h including packaging.

Phase-Change Thermal Storage Devices Time Basis: 1 orbit	Phase-Change Materials	
	Water	n-Dodecane
Thermal Density [kg/kW*h]	10.0	16.8
Thermal Density + Packaging [kg/kW*s] [123]	0.00500	0.00840

Beta Angle = 0 degrees:
  Design PCM Load [kW*s]
  Mass of PCM Device [kg]
	3117.9
	15.59
		3117.9
		26.19

Beta Angle = 50 degrees:
  Design PCM Load [kW*s]
  Mass of PCM Device [kg]
	3859.3
	19.30
		3859.3
		32.42

Beta Angle = 75 degrees:
  Design PCM Load [kW*s]
  Mass of PCM Device [kg]
	1204.1
	6.02
		1204.1
		10.11

From the definition of the reference mission, the assumed mission length is 6 days. Assuming an average orbital period of 90 minutes, the standard mission is 96 orbits. The mass savings using n-dodecane as the PCM is:

Mass Savings Using Water for PCM Device per Mission	Vehicle Orbital Beta Angle [degrees]		
	0	50	75
Mass of PCM Device [kg] Mass of FES Water Saved [kg]	26.19 134.04	32.42 165.92	10.11 51.77
Overall Mass Savings [kg]	107.85	133.50	41.66

The worst-case scenario for this technology would be to fly a mission in full sun at a beta angle of 75 degrees using a vehicle with a PCM device sized for a beta angle of 50 degrees. For this case the FES water savings would be only 51.77 kg while the PCM device penalty would be 26.19 kg, yielding a mass savings per mission of 25.58 kg, or 3,581.2 kg for the life of the vehicle. In general, Shuttle will fly at a variety of beta angles from 0 up to 75 degrees or even higher in some cases. Assuming this reflects the spectrum of Shuttle operating conditions, then the average amount of FES water saved per mission would be 117.24 kg. Further, assuming the PCM device is sized for a beta angle of 50 degrees, the average mass savings per mission is 84.82 kg, or 11,875.3 kg for the life of the vehicle.

Specific Assessments (for 140 missions):

Equipment Mass Savings	11,875 kg
Power Savings as Mass	negligible
Overall Mass Savings	11,875 kg
Composite Qualitative Score	+2

---

[122] Thermal density is defined here as 1/(heat of fusion).

[123] Including mass for packaging which is assumed as an additional 80% of the PCM mass.

3.2.5 Summary

The various advanced technologies and their estimated benefits are summarized in the table below for STS upgrade. From Section 3.2.2, the mass of the baseline ETCS is 201,306 kg for 140 missions. Again, assuming the mass determinations throughout this study have associated uncertainties on the order of 10%, a complete TCS with an advanced technology would need to show a savings of at least 20,131 kg to ensure a mass savings. Further, because design and development costs are not trivial, a mass savings of 25%, or 50,327 kg, is desirable. Using these criteria, the TCSs with advanced technologies proposed for STS upgrade may be divided among five categories:

- TCSs using advanced technologies requiring a mass penalty greater than 10% of the overall baseline ETCS mass: none.

- TCSs using advanced technologies requiring a mass penalty less than 10% of the overall baseline ETCS mass: none.

- TCSs using advanced technologies with a mass savings less than 10% of the overall baseline ETCS mass: LP two-phase TCS.

- TCSs using advanced technologies with a mass savings between 10 and 25% of the overall baseline ETCS mass: lightweight radiators.

- TCSs using advanced technologies with a mass savings greater than 25% of the overall baseline ETCS mass: none.

The technology in the third category will produce an ETCS which is comparable to the baseline system. The technology in the fourth category is promising for this mission.

One technology presented above is really an enhancing technology. In other words, this technology will deliver a mass savings or penalty regardless of the TCS selected. Thus:

- Enhancing technologies which require a mass penalty: none.

- Enhancing technologies which yield a mass savings: phase-change thermal storage.

**Table 3.18 Advanced Active Thermal Control System Architecture
for Space Transportation System Upgrade**

Summary of Advanced Active Thermal Control System Architecture for Space Transportation System Upgrade	Overall Mass Savings [kg]	Qualitative Score
3.2.4.1 Low-Power Two-Phase Thermal Control System	8,176	-1
3.2.4.2 Lightweight Radiators	22,904	--
3.2.4.3 Phase-Change Thermal Storage	11,875	+2

4.0   PLANETARY MISSIONS

Several aspects of surface operations distinguish planetary missions from other missions. Most obvious is the presence of a nontrivial gravity field. Further, the time constant associated with the sunlight/shade cycle on a planetary surface is on the order of tens to hundreds of hours. The planet itself provides an additional support surface for equipment including TCSs. Finally, some planets also have an atmosphere which can deposit material on TCS surfaces and buffet fragile structures which are best suited to a vacuum.

4.1   FIRST LUNAR OUTPOST LANDER

4.1.1   Reference Mission

One possible approach to re-establish a human presence on Luna is to send a series of expendable vehicles similar to those used by the Apollo program. One proposal, known as First Lunar Outpost (FLO), would utilize two vehicles to place a crew of up to four on the lunar surface for up to 45 days (including one lunar day and one lunar night.) (Woodcock, 1993) The first transfer vehicle would carry the crew from Earth to the lunar surface and then back to Earth. The second vehicle, which would actually arrive on the lunar surface before the crew, would be a pilotless lander which would serve as a habitat while the crew is on the lunar surface. This second lander is to be built around a Space Station habitation module with appropriate modifications to make it an independent vehicle. This will be FLO Lander. In addition to the habitation module, FLO Lander will include a base containing landing gear and a descent motor, external tankage and ladders, an airlock, and a complete ATCS designed for both lunar day and lunar night. For this study, the continuous power mass penalty is 616 kg/kW while the daytime penalty, which presumes solar power generation, is 42.2 kg/kW (Woodcock, 1993). Here, two FLO Landers (one for each of two human missions) are assumed, and mass savings are considered cumulative for both missions. The crew transfer vehicle and the Earth to Luna transfer of FLO Lander are not considered in this study.

4.1.2   Baseline Case

The baseline FLO Lander ETCS will use a low solar absorptivity, horizontal radiator [124] with single-phase ammonia as the ETCS fluid. The ITCS loop is assumed to use water. No additional cooling devices are presumed, although some may be required for mission phases other than surface operations. The radiator upper surface coating is silver Teflon with an assumed surface emissivity of 0.80 and a solar absorptivity of 0.10. The lower radiator surface is insulated to reduce heating from solar irradiation reflected by the lunar surface. The radiator fin efficiency and mass per surface area are 0.85 and

---

[124]   A study by Cross (1995) indicates that radiators are significantly less massive than evaporative systems for spacecraft in near-Earth space on missions lasting more than a week.

6.00 kg/m^2 [125], respectively. Woodcock (1993), assuming an ETCS with a heat pump, sized the FLO Lander radiator at 63 m^2 and placed it directly above the habitation module. Here it is assumed that any radiator area in excess of 63 m^2 will initially be folded on top of a base radiator of 63 m^2. The additional radiating area will be deployed once FLO Lander is in place on the lunar surface (Figure 4.1). The deployable radiator panels have an assumed mass per surface area of 9.00 kg/m^2. This higher penalty accounts for the additional deployment mechanism and structure associated with the deployable panel segments. The heat-rejection requirement of the ETCS is 16.0 kW and the total pumping power is 0.30 kW (Woodcock, 1993). In this study a heat pump is not included in the baseline ETCS because heat pumps are considered an advanced technology. Thus, the baseline FLO Lander ETCS design is:

- Overall ETCS Performance:

Heat Rejected	16.0 kW
ETCS Mass Flowrate	0.1453 kg/s
ETCS Working Fluid	single-phase ammonia

- Low Solar Absorptivity, Horizontal Radiators:

Surface Emissivity	0.80
Solar Absorptivity	0.10
Fin Efficiency	0.85
Average Radiator Surface Temperature	285.0 K
Average ETCS Fluid Temperature	286.5 K
Radiator Outlet Temperature	274.82 K
Radiator Inlet Temperature	298.18 K
Radiator Pressure Drop (as per ISS)	48.26 kN/m^2
Pump Efficiency	0.45
Pumping Power for Radiators	0.0248 kW

---

[125] This penalty includes 5.20 kg/m^2 for radiator panel mass and 0.80 kg/m^2 for base structure and support (Woodcock, 1993).
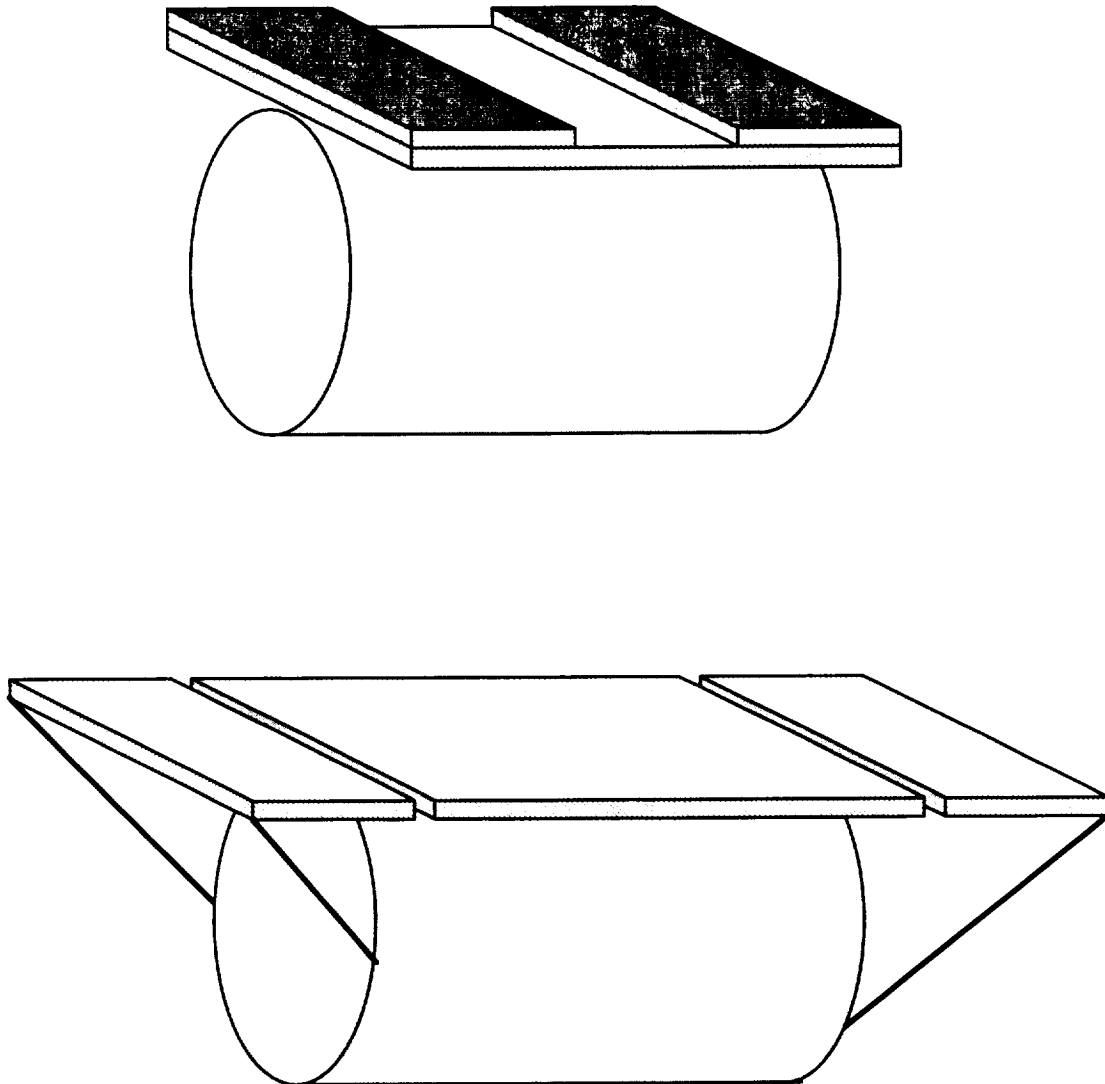
Figure 4.1   A sketch of a typical deployable radiator, as proposed for the baseline, mounted on top of the modified Space Station habitation module of First Lunar Outpost Lander.   The top figure illustrates the radiators stowed for flight and to protect the radiating surface while the vehicle external thermal control system is not in use.   The lower figure illustrates how the radiators might look when deployed.   The large radiator directly affixed to the habitation module has a radiating area of 63 m^2 while the two panels deployed on either end provide any additional radiating area.

- Summary of ETCS Masses for a Single FLO Lander Vehicle:

Radiator Surface Area [126]	116.08 m^2
Base Radiator Support and Structure	50.40 kg
Radiator Panel Mass	603.62 kg
Support and Deployment for Added Panels	201.70 kg
Total Radiator Mass	855.72 kg
Deployment Motor (assumed)	10 kg
Overall Pumping Power	0.300 kW
Pumping Power as Mass	184.80 kg
Total ETCS Heat-Rejection System Mass [127]	1050.5 kg

The average radiator mass per surface area is 7.37 kg/m^2 for the baseline configuration. Figure 4.2 presents an overall sketch of the FLO Lander ETCS reference or baseline.

4.1.3 Parametric Study Using the Baseline Case

Because FLO Lander is still in the design stage, the baseline ETCS for this study was determined through a parametric analysis. Density and specific heat for single-phase ammonia were determined based on the average ETCS loop temperature using curve fits to existing thermodynamic data.

$$\bar{\rho}(\bar{T}) = \left[-0.002 \frac{1}{K^2} \bar{T}^2 - 0.233 \frac{1}{K} \bar{T} + 858.966 \right] \frac{kg}{m^3}$$

$$\bar{c}_p(\bar{T}) = \left[0.006 \frac{1}{K} \bar{T} + 2.995 \right] \frac{kW * s}{kg * K}$$

In addition to the constants above, other assumed study constants are:

Stefan-Boltzmann Constant	5.670 × 10^{-11} kW/(m^2*K^4)
Solar Irradiation at Lunar Noon	1.371 kW/m^2
Environmental Temperature (space)	3 K
Maximum Radiator Outlet Temperature (ETCS set-point temperature)	274.82 K
ETCS Loop Temp. - Radiator Surface Temp.	1.5 K

---

[126] The radiator was sized using the study presented in Section 4.1.3 below by assuming an average radiator surface temperature of 285.0 K.

[127] This total excludes the mass of the ETCS working fluid, pump package, and piping and fittings. While these masses are significant, their total is not expected to change significantly between the baseline and the advanced technology options discussed below. For comparison, if an Apollo era sublimator were used to reject a heat load of 16 kW for 45 days it would consume 25,500 kg of water, not including tankage and other equipment masses.
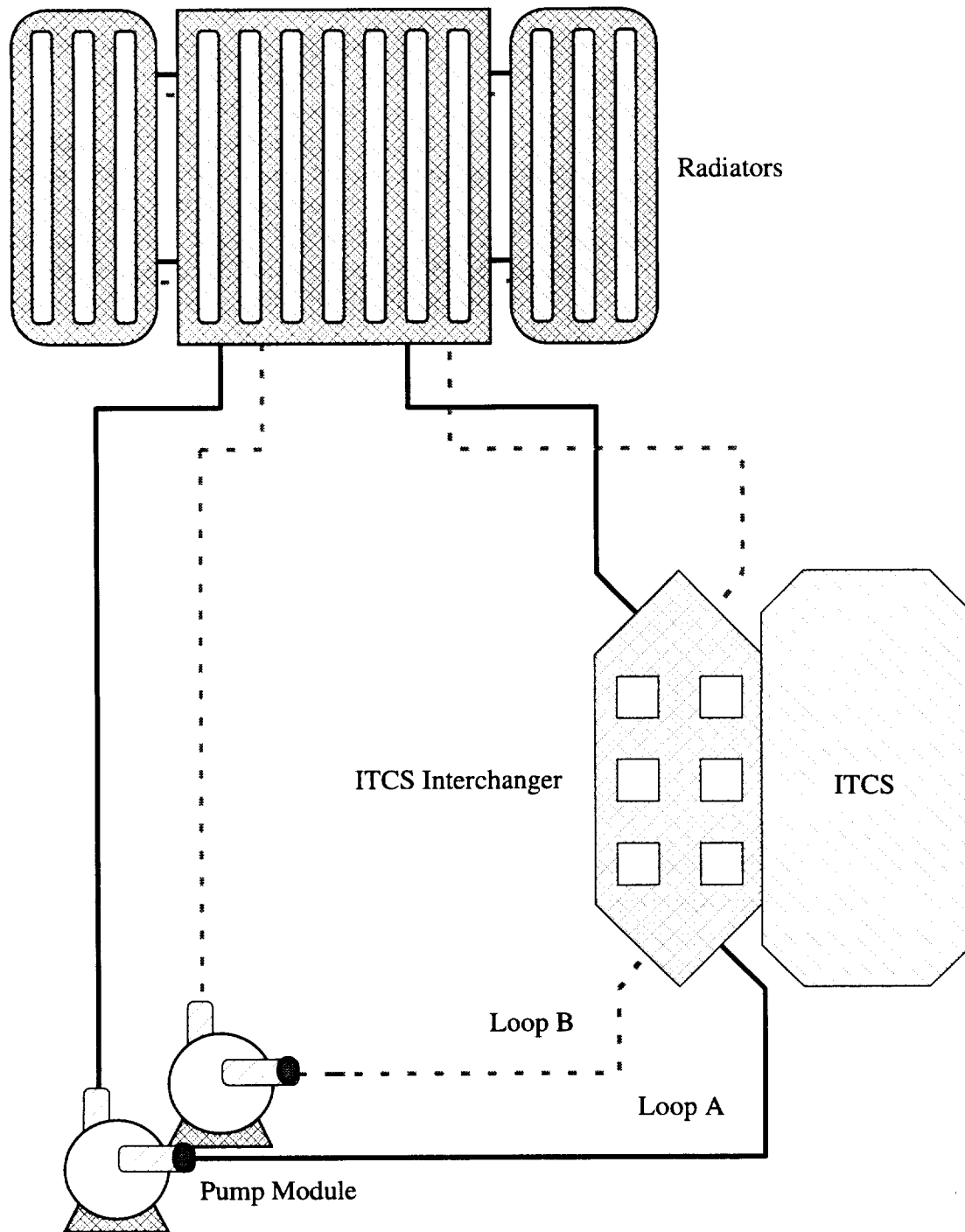
Figure 4.2 An overall sketch of the baseline external thermal control system for First Lunar Outpost Lander. Two flow loops are shown because the actual vehicle will probably use two loops as a safety precaution. However, to simplify calculations and analysis, the heat load and pumping power for both loops has been lumped into single values for the First Lunar Outpost Lander vehicle as a whole.

Because the FLO Lander radiator was not sized when this study was initiated, both the surface solar absorptivity and the average radiator temperature were initially restricted to a range of values. Both of these parameters were varied to determine their effect on the required radiating area. While silver Teflon has a solar absorptivity when new of 0.08 to 0.09 (Peck, 1990), the landing of the vehicle with the crew and actual radiator usage over 45 days will degrade this coating slightly, so a value of 0.10 was assumed. The radiator area was expected to be about twice that quoted by Woodcock (1993) because the baseline would not include a heat pump. Further, a higher ETCS loop temperature than used by either ISS or Shuttle would be permitted. An analysis of the required radiating area is presented in Table 4.1 and Table 4.2, and graphically in Figure 4.3 and Figure 4.4.

Table 4.1 Various ETCS Flow Loop Values for First Lunar Outpost Lander as a Function of Radiator Panel Temperature

	Average Radiator Panel Temperature					
	275.0 K	280.0 K	285.0 K	290.0 K	295.0 K	300.0 K
Average ETCS Loop Temperature [K]	276.5	281.5	286.5	291.5	296.5	301.5
Average NH_3 Specific Heat [kW*s/(kg*K)]	4.65	4.68	4.71	4.74	4.77	4.80
Average NH_3 Density [kg/m^3]	641.6	634.9	628.1	621.1	614.1	606.9
NH_3 Flowrate [kg/s]	1.0239	0.2557	0.1453	0.1011	0.0773	0.0624
Required Radiator Pumping Power [kW]	0.1711	0.0432	0.0248	0.0175	0.0135	0.0110
Required Radiator Area at Night [m^2]	72.56	67.52	62.90	58.67	54.80	51.23

Table 4.2 Daytime First Lunar Outpost Lander Radiator Area [m^2] as a Function of Both Solar Absorptivity and Radiator Panel Temperature

Solar Absorptivity	Average Radiator Panel Temperature					
	275.0 K	280.0 K	285.0 K	290.0 K	295.0 K	300.0 K
0.080	125.71	111.30	99.29	89.15	80.50	73.04
0.085	131.74	116.00	103.02	92.14	82.93	75.03
0.090	138.38	121.12	107.03	95.34	85.51	77.14
0.095	145.73	126.71	111.37	98.77	88.26	79.37
0.10	153.89	132.84	116.08	102.46	91.19	81.73
0.11	173.32	147.07	126.80	110.72	97.68	86.90
0.12	198.36	164.71	139.70	120.43	105.16	92.78
0.13	231.86	187.16	155.53	132.01	113.88	99.50
0.14	278.97	216.70	175.40	146.06	124.18	107.27
0.15	350.10	257.32	201.09	163.44	136.53	116.37
0.16	469.93	316.66	235.59	185.53	151.60	127.14
0.17	714.47	411.59	284.40	214.52	170.42	140.12
0.18	1489.67	587.80	358.69	254.24	194.57	156.04
0.19	--	1027.85	485.54	312.02	226.70	176.05
0.20	--	4088.93	751.20	403.78	271.54	201.95
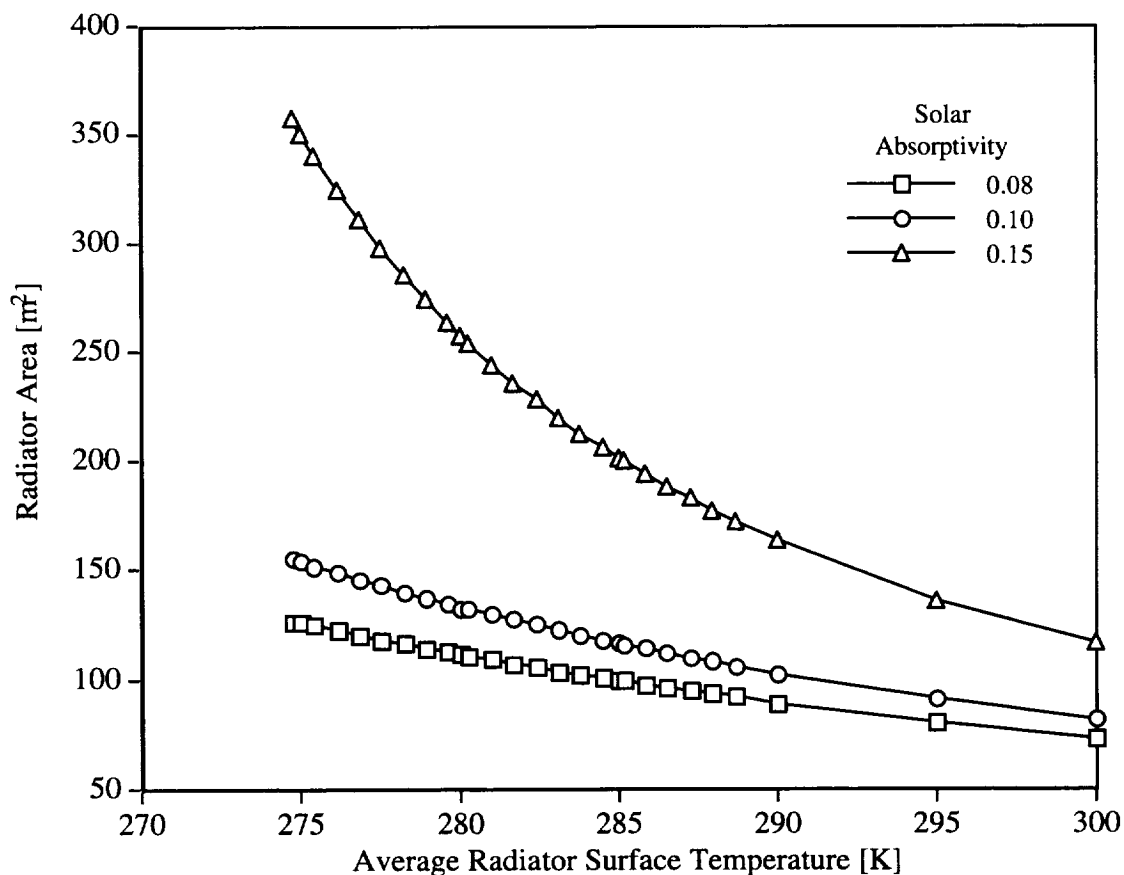
Figure 4.3 Required radiator surface area to reject a 16.0 kW heat load during lunar noon at the lunar equator as a function of the average radiator surface temperature for a horizontal, low solar absorptivity radiator on First Lunar Outpost Lander. A surface emissivity of 0.8 and a fin efficiency of 0.85 are assumed. Silver Teflon coating, the assumed surface coating, has a solar absorptivity of 0.08 when new and a value of 0.15 at end-of-life.

4.1.4   Advanced ATCS Architecture for First Lunar Outpost Lander

FLO Lander vehicles are assumed here to be expendable. They will be placed on the lunar surface and left behind once the objectives at their landing site have been accomplished. This is not to say that the vehicle may not be used by more than one crew. In fact, FLO Lander may be used multiple times by crews to carry out studies at a single lunar site, especially if the perishable items are replenished between visits. However, to bound this study, it is assumed that the vehicle usage does not permit significant degradation of the ETCS components either by solar irradiation, debris impact, or

abrasion due to lunar soil propelled by the thrust of other vehicles landing nearby [128]. As noted earlier, only two FLO Lander vehicles are presumed. Each advanced architecture is, where applicable, assessed numerically for the overall mass savings when compared with the FLO Lander baseline. Qualitative assessments for these advanced technologies are presented in Section 2.0.
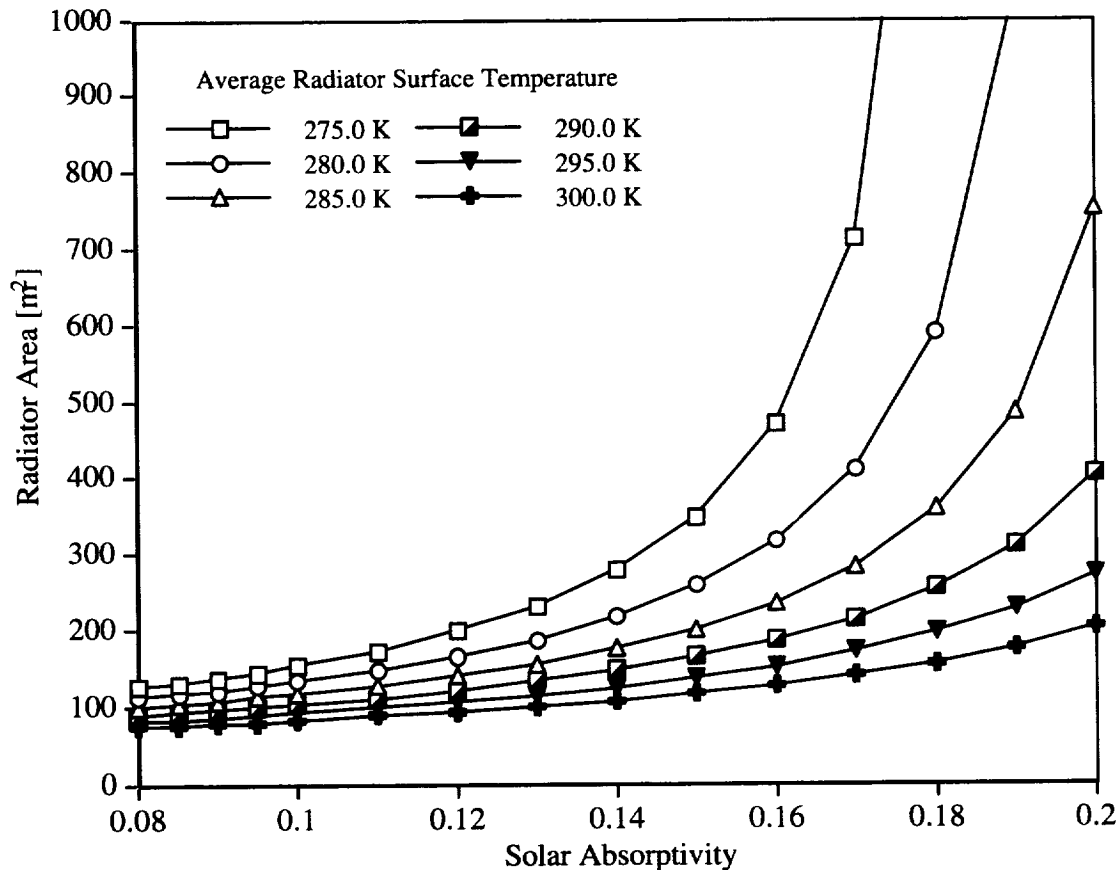
Figure 4.4 Required radiator surface area to reject a 16.0 kW heat load during lunar noon at the lunar equator as a function of the solar absorptivity for a horizontal, low solar absorptivity radiator on First Lunar Outpost Lander. A surface emissivity of 0.8 and a fin efficiency of 0.85 are assumed. The curves represent performance for various average radiator surface temperatures. For comparison, the STS-41 case for Shuttle has an average radiator surface temperature of 288.3 K and the LVS Base Case for International Space Station has an average radiator surface temperature of 273.9 K.

---

[128] By assuming that the radiators will be stowed while other vehicles are landing or taking off, there should be little erosion of the surface coatings due to lunar soil propelled at the radiators by the thrust of other vehicles nearby.

4.1.4.1   Low-Power Two-Phase Thermal Control System

To estimate the mass of a LP two-phase TCS [129] for FLO Lander, this study extrapolates predictions from Ungar (1995) which gives estimates for space stations. Ungar (1995) includes estimates for three different vehicles using four different TCS architectures. Of the options presented, FLO Lander most closely resembles a small system with a single-phase cascade TCS. Ungar also presents a LP two-phase TCS. The LP two-phase TCS requires less pumping power and smaller diameter flow lines than the single-phase cascade TCS. The required radiator area is roughly the same for both the single-phase cascade TCS and the LP two-phase TCS. Thus, neglecting the differences in the flow line mass, the systems may be summarized by:

	First Lunar Outpost Lander Baseline Thermal Control System	Small System (Ungar, 1995)			
		Single-Phase Cascade Thermal Control System		Low-Power Two-Phase Thermal Control System	
		LTL	LTL	LTL	MTL
Pump Power [kW]	0.300	0.320	0.320	0.068	0.080
Radiator Area [m^2]	116.1	197	197	195	195
Loop Set-Point [K]	274.8	275.2	275.2	275.2	287.2

LTL refers to the low temperature loop while MTL refers to the moderate temperature loop. Actually, the baseline TCS for FLO Lander uses a pair of single-phase cascade, low temperature loops. The listed values in the table above, however, are for the entire baseline TCS for FLO Lander. Thus, comparing the FLO Lander TCS with the single-phase cascade TCS for a small system reveals that the pumping power per loop is about half, the FLO Lander TCS loop set-points are approximately that of the LTL for the single-phase cascade TCS, and FLO Lander uses 37% of the effective radiator area of the single-phase cascade TCS. A comparable LP two-phase TCS for FLO Lander, then, would use two LTL loops. The total pumping power requirement for the revised FLO Lander LP two-phase TCS is 68 W, which is half of the total pumping power for two LTL loops on Ungar's LP two-phase TCS for a small station. Thus:

Mass Gained Using a Low-Power Two-Phase Thermal Control System	Baseline First Lunar Outpost Lander TCS	Low-Power Two-Phase First Lunar Outpost Lander TCS	Change (for 1 Vehicle)	Total Change (2 Vehicles)
Pump Power [kW]	0.300	0.068	-0.232	
Mass due to Pump Power [kg]	184.8	41.9	-142.9	-285.8

Overall, the LP two-phase TCS is lighter than the baseline single-phase cascade TCS. However, because FLO Lander is a very small vehicle, like Shuttle, a two-phase TCS does not provide a large savings.

---

[129]   See Section 2.1.2 for details.

Specific Assessments (for 2 missions):

Equipment Mass Savings	negligible
Power Savings	0.464 kW
Power Savings as Mass	+286 kg
Overall Mass Savings	286 kg
Composite Qualitative Score	-1

4.1.4.2 Two-Phase Thermal Control System With Electrohydrodynamic Pumping

Based on the discussion in Section 2.1.3, FLO Lander could utilize a two-phase TCS with electrohydrodynamic pumping. A two-phase TCS with electrohydrodynamic pumping may yield a slight mass savings over a LP two-phase TCS. A significant mass savings over the baseline TCS would also be expected. However, without more data on this technology, no mass savings estimates may be determined.

Specific Assessments (for 2 missions):

Equipment Mass Savings	unknown
Power Savings as Mass	unknown
Overall Mass Savings	unknown
Composite Qualitative Score	+2

4.1.4.3 Capillary Pumped Loops

Based on the baseline architecture given in Section 4.1.2, a capillary pumped loop [130] could save 0.30 kW, which is the estimated ETCS pumping power for a FLO Lander. A single capillary pumped loop might be used for the heat load rejected by this vehicle. However, such considerations do not affect the mass estimates for this study because the capillary pumped loop equipment mass is assumed to be comparable to the equipment mass for the baseline single-phase TCS architecture. The overall savings for this option is 369.6 kg for two FLO Landers based on saving power for pumping and a power mass penalty of 616 kg/kW.

Specific Assessments (for 2 missions):

Equipment Mass Savings	none
Power Savings	0.30 kW
Power Savings as Mass	370 kg
Overall Mass Savings	370 kg
Composite Qualitative Score	0

---

[130] See Section 2.1.4 for background on capillary pumped loops.

4.1.4.4 Solar Vapor Compression Heat Pump

A vapor compression heat pump could be used to reject heat at higher temperatures so as to reduce the required radiator area. In fact, Woodcock (1993) decided against using just a radiator, as in the baseline for FLO Lander here, and sized the ETCS assuming a vapor compression heat pump. As will be shown below, a continuous heat pump is not necessary on Luna and, therefore, is inefficient because it consumes power during the night. Further, insufficient detail is present in this study to consider a non-solar heat pump separately from a solar heat pump. The analysis here follows that in Section 3.1.5.4 using the baseline from Section 4.1.2 to size the heat pump for FLO Lander. Some assumptions are:

- Because this is a solar heat pump, the appropriate power mass penalty for the heat pump power is 42.2 kg/kW.
- Because FLO Lander is compact and even smaller than Shuttle, the heat pump evaporator will take heat directly from the ITCS through a heat exchanger (Figure 4.5).
- The ITCS pumping power is assumed to be unchanged.
- The baseline ETCS pumping power is retained and added to the ITCS pumping power [131].

A two-parameter parametric study (Figure 4.6) indicates that the ETCS mass is minimized for FLO Lander when the heat pump temperature lift is 27.5 K and the ETCS fluid mass flowrate is increased to 0.368 kg/s. Specifically then:

Cold Source Temperature, T_C (evaporator temperature)	286.5 K
Temperature Lift, $T_H - T_C$	27.5 K
Hot Source Temperature, T_H (condenser temperature)	314.0 K
Radiator Inlet Temperature, T_{in}	310.0 K
Lunar Surface Solar Irradiation	1.371 kW/m^2
Environmental Temperature, T_{space}	3.0 K
Total Cooling Load, Q_C	16.00 kW
Ideal Coefficient of Performance, COP_{Carnot}	10.05
Heat Pump Efficiency, η [132] (Ewert, 1991)	0.50
Necessary Input Power, W_{real}	3.18 kW

The ETCS radiators are represented by the model developed for the parametric study in Section 4.1.3.

Emissivity	0.80
Solar Absorptivity	0.10
Fin Efficiency	0.85
Radiator Mass Flowrate of Ammonia	0.368 kg/s

---

[131] This accounts for the longer ITCS lines and increased ITCS pumping loads.

[132] Percentage of Carnot coefficient of performance (COP).
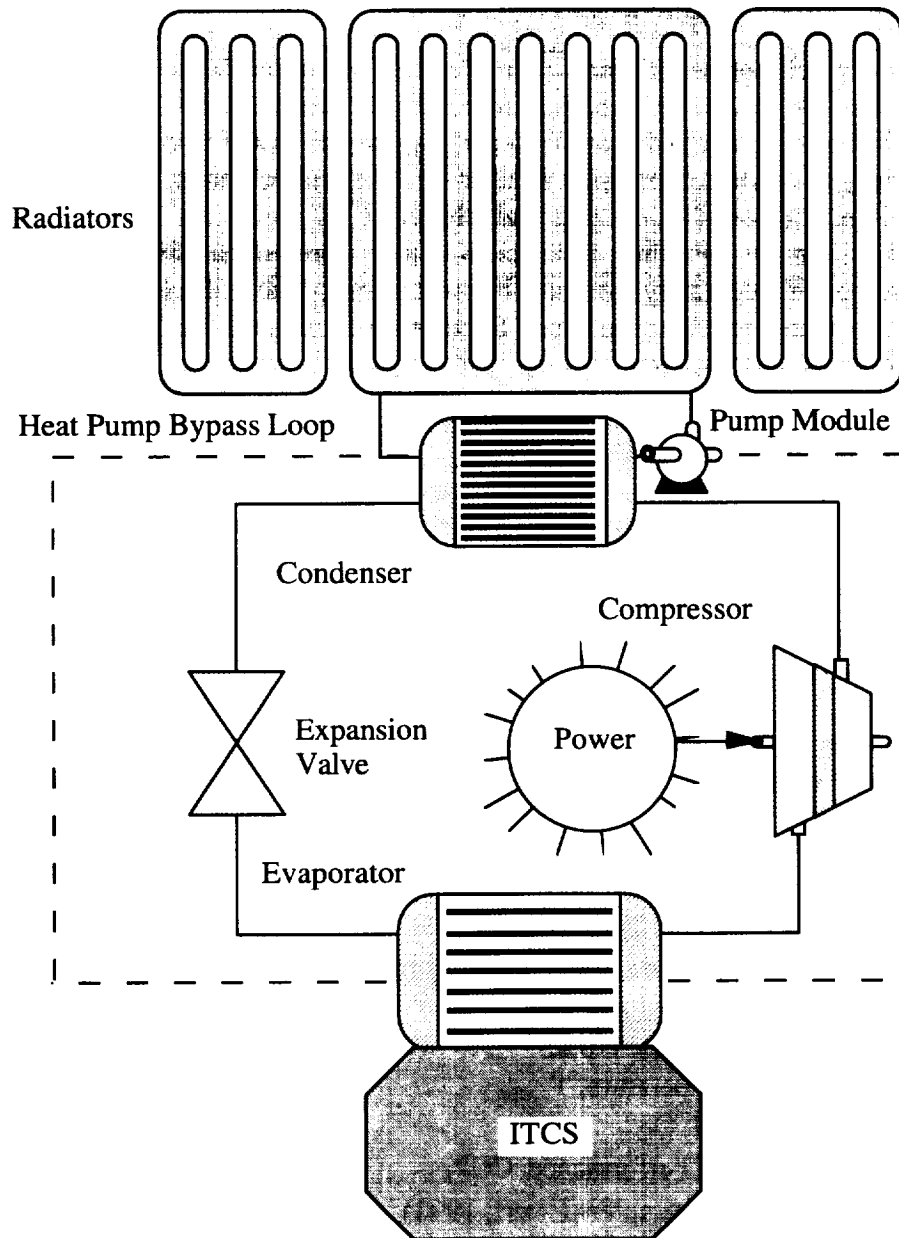
Figure 4.5 An overall sketch of the First Lunar Outpost Lander external thermal control system using a solar vapor compression heat pump. Because the heat pump evaporator receives heat directly from the internal thermal control system loop, the external thermal control system flow loop exists only to carry heat from the heat pump condenser to the radiators and to bypass the heat pump during the lunar night.

Average Ammonia Temperature   300.0 K
Average Panel Surface Temperature   298.5 K
Heat Rejection per Unit Area   0.304 kW/m^2
Total Heat Rejected by the Radiators, $Q_{H,real}$ 19.18 kW
Radiator Mass Per Unit Area (< 63 m^2)   6.00 kg/m^2
Radiator Mass Per Unit Area (> 63 m^2)   9.00 kg/m^2
Necessary Radiator Surface Area During the Day   62.82 m^2

Mass Gained by Using a Solar Vapor Compression Heat Pump	Baseline FLO Lander TCS	Solar Heat Pump FLO Lander TCS	Change (for 1 Vehicle)	Total Change (2 Vehicles)
Radiator and Support Mass [kg]	855.7	376.9	-478.8	-957.6
Heat Pump Mass [133] [kg]	--	149.7	+149.7	+299.4
Radiator Plus Heat Pump Mass [kg]	855.7	526.6	-329.1	-658.2
Heat Pump Power [kW]	--	3.07	+3.07	
Additional Pumping Power [kW]	--	0.11	+0.11	
Power as Mass[kg]	--	199.5	+199.5	+399.0
Total Mass [kg]	855.7	726.1	-129.6	-259.2

As Woodcock (1993) and the tabulation suggest, a solar vapor compression heat pump offers a mass savings for FLO Lander. While the radiator area decreases, the added solar array will offset this savings. The deployment should be easier because the deployable radiator wings have been omitted. The deployment motor is retained for the solar heat pump configuration to deploy and retract a thin protective covering over the radiator surface while other vehicles are taking off or landing near FLO Lander. Though the motor can be lighter, it is assumed that the covering mass will offset any savings.

Specific Assessments (for 2 missions):

Equipment Mass Savings   658 kg
Power Savings   -6.36 kW
Power Savings as Mass   -399 kg

Overall Mass Savings   259 kg

Composite Qualitative Score [134]   +1

---

[133]   See the footnotes for Section 3.1.5.4 for the heat pump sizing correlation.
[134]   Volume is rated as "average" for this mission because this attribute is expected to be comparable to the baseline architecture for the solar vapor compression heat pump.
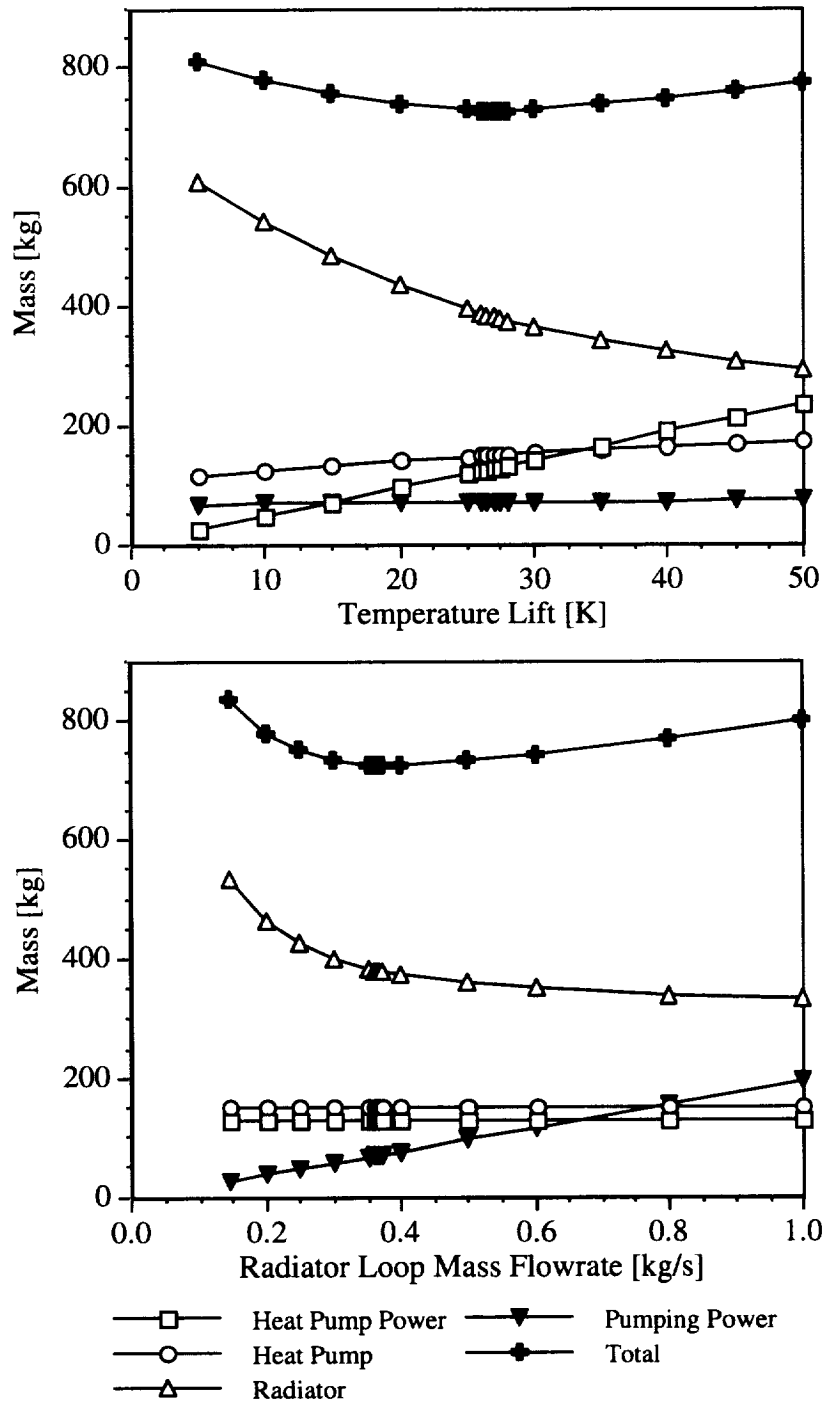
Figure 4.6 Variation of First Lunar Outpost Lander external thermal control system mass as a function of the vapor compression heat pump temperature lift and the radiator loop mass flowrate. The baseline from Section 4.1.2 forms the basis for this study. This study optimized external thermal control system mass with respect to both of the variables mentioned.

4.1.4.5 Lightweight Radiators

A parametric study here is employed to identify potential mass savings through using lighter materials for portions of the FLO Lander ETCS. Unlike ISS and Shuttle, the FLO Lander ETCS is not well defined, so the components and categories listed here are, out of necessity, vague.

Category Within External Thermal Control System	Mass per First Lunar Outpost Lander Vehicle [kg]	Mass Percentage of External Thermal Control System
Structure and Deployment:		24.0
Base Radiator Support and Structure	50.4	
Support and Deployment for Added Panels	201.7	
Radiator Panels	603.6	57.5
Other Items:		18.5
Deployment Motor	10.0	
Pumping Power Mass	184.8	
Total	1050.5	100.0

This study varies the component FLO Lander ETCS masses linearly based on the original mass in each category. The structure and deployment masses are reduced by up to 20% when the radiator panel mass is reduced by up to 40%. The ETCS working fluid is not listed, but it is not expected to change as a result of lighter material components throughout the rest of the ETCS [135].

The underlying assumption is that composites and other advanced materials are most likely to offer a mass reduction for some components of the radiator panels such as the honeycomb and the facesheets. Because the radiator panels are the single most massive item of the FLO Lander ETCS, such savings would constrain the remainder of the design. A less significant mass reduction is assumed for the structures and deployment because the sizes of these components are primarily dictated by the dimensions of the radiator array. However, composites should allow comparable components to replace some of the structure and deployment with lighter parts. In summary, this approach yields an overall ETCS mass reduction of 27.8% for a 40% reduction in the radiator panel mass (Figure 4.7).

---

[135] See Section 2.4 for additional general background on lightweight radiators plus specific examples of proposed lightweight radiators.
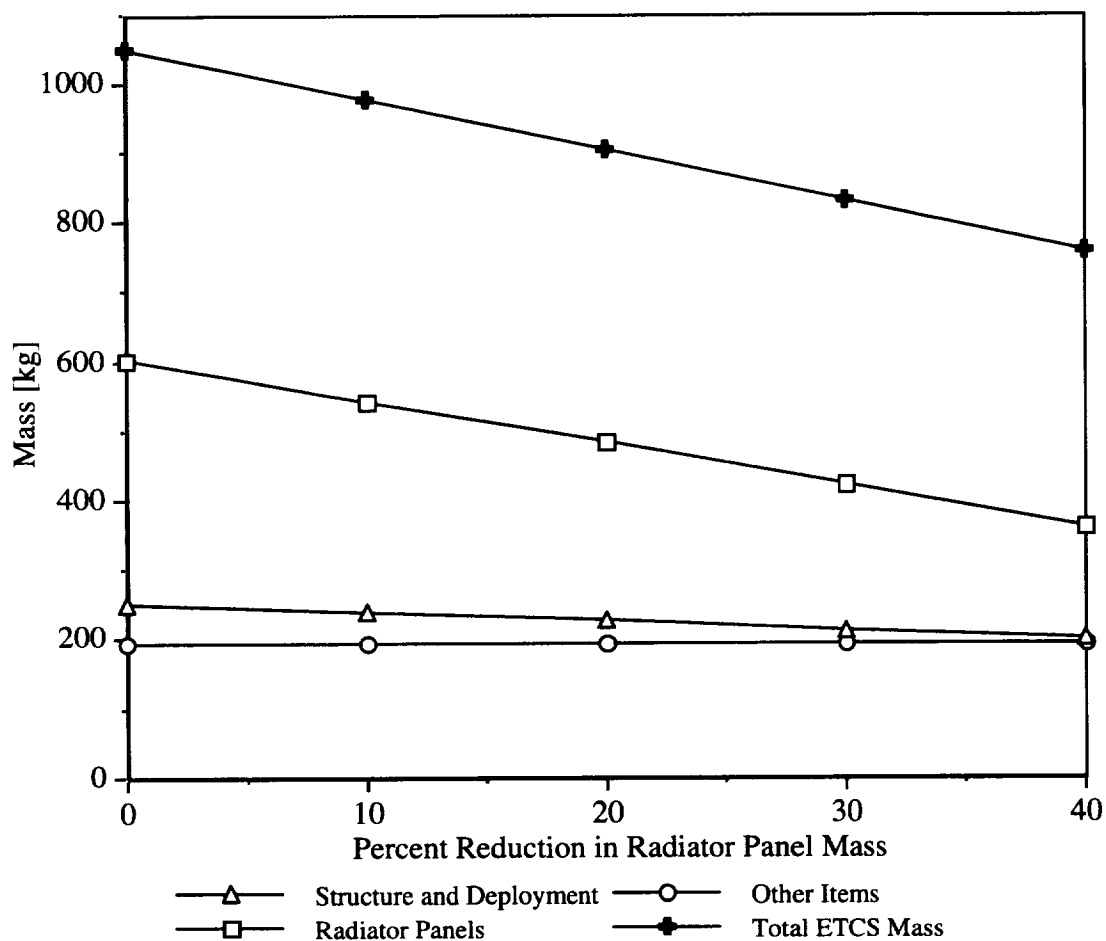
Figure 4.7 First Lunar Outpost Lander radiator mass as a function of mass reduction within the radiator panel set. Study Assumption: For each 10% mass reduction in the radiators the mass for the structure and deployment decreases by 5%.

Category Within External Thermal Control System	Percent Reduction in Radiator Panel Mass	
	20%	40%
Structure and Deployment [kg]	226.9	201.7
Radiator Panels [kg]	482.9	362.2
Other Items [kg]	194.8	194.8
Total ETCS Mass per Vehicle [kg]	904.6	758.7
Overall Mass Reduction per Vehicle [kg]	145.9	291.9
Mass Reduction as a Percentage of the Original FLO Lander ETCS	13.9	27.8
Radiator Mass Per Surface Area [kg/m^2] [136]	6.11	4.86

Considering the available lightweight radiators presented in Section 2.4, an overall mass reduction of 27.8% was selected as a representative value. Thus, the mass savings for one FLO Lander vehicle is 291.9 kg, or 583.8 kg for the reference mission of two vehicles. The power requirements will be unchanged because the internal fluid dynamics and, therefore, the pumping power are functions of the working fluid material properties.

Because FLO Lander is a planetary mission, any of the lightweight radiator concepts may be used. All of the radiators presented in Section 2.4 can be deployed vertically. However, vertical radiators away from polar regions require integration with either a radiator shade or a heat pump to reject life support heat loads at lunar noon. Additionally, the composite flow-through radiators could also be oriented horizontally like the radiator in the baseline architecture.

Specific Assessments (for 2 missions):

Equipment Mass Savings	584 kg
Power Savings as Mass	none
Overall Mass Savings	584 kg

4.1.4.6   Parabolic Radiator Shade

Parabolic radiator shades provide a means of lowering the effective sink temperature around a radiator to allow rejection at temperatures associated with waste heat from environmental control and life support systems for human beings [137].

Two possible deployments using a parabolic radiator shade for FLO Lander at an equatorial landing site are presented in Figure 4.8. The first would place the shade on top of the modified Space Station habitation module with a vertical radiator. This option is difficult to employ for at least two reasons. Preliminary calculations indicate that the top of the FLO Lander vehicle has insufficient room for a radiator shade. Further, because FLO Lander is pilotless, computer guidance would need to flawlessly position the vehicle on touchdown to align the radiator's main axis with the local incident solar vector.

---

[136]   These values are based on a radiating area of 116.08 m^2 as per the baseline architecture for FLO Lander. Further, these values include only the radiator mass and not the Other Items in the ETCS.

[137]   See Section 2.5.2 for more information on parabolic radiator shades.

Without allowing for additional equipment to adjust the radiator's alignment on top of the vehicle, this approach is unworkable.
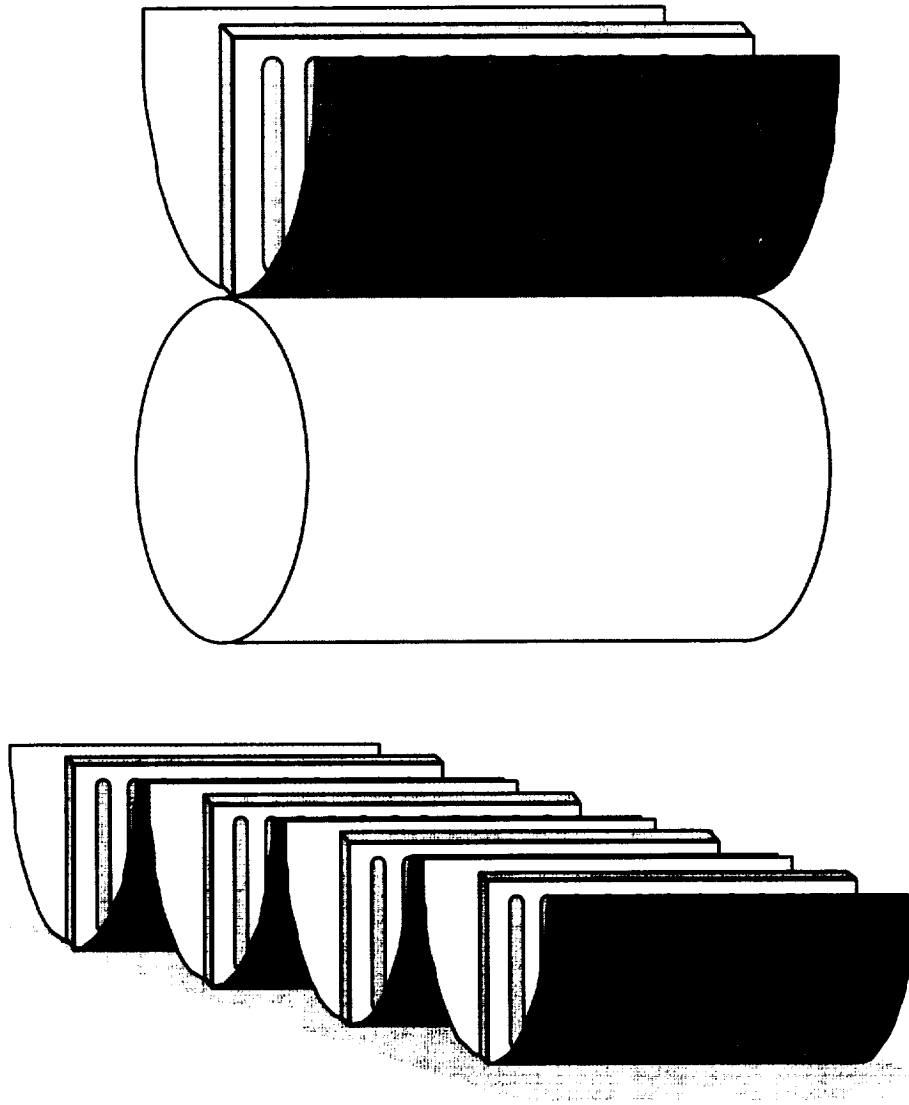
Figure 4.8 Two deployments for a parabolic radiator shade. The first deploys the shade on top of First Lunar Outpost Lander. This option could be deployed remotely but would rely on the First Lunar Outpost Lander vehicle positioning itself in the proper position relative to the solar vector. The second deploys the radiator with parabolic shade on the lunar surface. This option would be carried in a box and deployed by the crew after arrival. The positioning of the First Lunar Outpost Lander vehicle itself would not be critical because the crew themselves could adjust the parabolic shade and radiator assembly to align with the solar vector.

A second approach would use the crew to set up the radiator and shade on the lunar surface after arrival. This approach allows the shade to be aligned properly with respect to the local solar vector. Further, preliminary calculations indicate that this option requires significantly less mass than a vehicle-mounted installation [138]. This implies that the habitat will not be ready for the crew when they reach the lunar surface. Because the mission profile calls for an extravehicular activity only sufficient for the crew to transfer from the piloted vehicle to the habitat, the habitat should be remotely readied (Woodcock, 1993). However, assuming that this readiness issue can be solved, a surface installation of a vertical radiator with a parabolic shade is the most reasonable approach [139]. The radiator and shade combination could be set up as illustrated in the lower part of Figure 4.8 or as a single continuous unit. In either case, endsheets (not pictured) should be used to further minimize heating from surface irradiation.

For a parabolic radiator shade on the lunar surface (Ewert and Clark, 1991):

Heat Rejected	16.0 kW
Radiator Surface Temperature	285.0 K
Lunar Surface	
Emissivity	0.93
Absorptivity	0.93
Albedo	0.07
Solar Irradiation	1.371 kW/m^2
Incident Angle	90.0°
Orbital Inclination	1.53°
Radiator (with silver Teflon)	
Fin Efficiency	0.85
Infrared Emissivity	0.80
Solar Absorptivity	0.10
Shade	
Specular Upper Surface	
Emissivity	0.03
Absorptivity	0.04
Diffuse Lower Surface	
Emissivity	0.81
Absorptivity	0.371
Sink Temperature [140]	155.0 K

---

[138] The preliminary mass calculations include only a modest estimate for a shade deployment based on a surface installation. A vehicle-mounted installation would probably require more massive pointing mechanisms.

[139] To allow the habitat to be remotely readied, radiators could be vehicle-mounted when the crew arrives. Assuming the crew arrives at lunar sunrise, the unshaded radiators should be sufficient to cool the vehicle until the crew can set up the parabolic shade on a subsequent extravehicular activity. Finally, the vehicle-mounted radiators might be transferred to the lunar surface for use with the parabolic shade.

[140] Keller (1995 a) computed a sink temperature of 153.58 K for a parabolic shade and radiator assembly mounted on a lander vehicle 10 m off of the lunar surface. For a shade on the lunar

Radiator
　Area　　　　　　　　　　　　　　　　　　　　68.9 m^2
　Mass Penalty (Keller, 1994)　　　　　　　　4.5 kg/m^2
　Mass　　　　　　　　　　　　　　　　　　　310.2 kg
　Dimensions
　　Height　　　　　　　　　　　　　　　　　1.00 m
　　Length　　　　　　　　　　　　　　　　　34.47 m

Shade
　Parabolic Arc Length [141]　　　　　　　　　4.59 m
　Length　　　　　　　　　　　　　　　　　　34.47 m
　Area　　　　　　　　　　　　　　　　　　　158.2 m^2
　Mass Penalty [142]　　　　　　　　　　　　1.1 kg/m^2
　Mass　　　　　　　　　　　　　　　　　　　174.0 kg

Total System Mass [143]　　　　　　　　　　484.2 kg

Comparing the radiator and flexible parabolic shade with the baseline presented in Section 4.1.2 yields:

Mass Gained by Using a Parabolic Radiator Shade	Baseline First Lunar Outpost Lander Thermal Control System	First Lunar Outpost Lander With Parabolic Radiator Shade	Change (for 1 Vehicle)	Total Change (2 Vehicles)
Radiator Area [m²]	116.1	68.9	-47.2	
Radiator Mass [kg]	603.6	310.2	-293.4	-586.8
Added Panel Support & Deployment [kg]	201.7	--	-201.7	-403.4
Shade Area [m²]	--	158.2	+158.2	
Shade Mass [kg]	--	174.0	+174.0	+348.0
Total Mass [kg]	805.3	484.2	-321.1	-642.2

The deployment motor mass is retained in this configuration to account for the mass of a remotely removable covering over the radiators while they are vehicle-mounted. The overall savings for using a parabolic radiator shade is 642.2 kg.

---

surface the effective sink temperature would be slightly higher. The shade properties assumed here are beginning-of-life values which are appropriate for this mission because dust accumulation will be negligible. This explains the difference between the lower sink temperature here and the higher value listed for the PLB shade which is sized using end-of-life shade properties. Keller used TSS.

[141] A full parabolic shade is assumed. In other words, the shade top is even with the radiator top and the shade focus is at the height of the radiator.

[142] This penalty includes mass for a flexible parabolic shade plus appropriate support structure. This penalty is twice that used by Keller (1994). The additional mass accounts for more extensive deployment structure which will allow for the radiator and shade to be deployed quickly.

[143] This value does not include mass for piping, fittings, and working fluid to and from the radiators.

Specific Assessments (for 2 missions):

Equipment Mass Savings	642 kg
Power Savings as Mass	negligible
Overall Mass Savings	642 kg
Composite Qualitative Score [144]	-2

4.1.5 Summary

The various advanced technologies and their estimated benefits are summarized in the table below for FLO Lander. From Section 4.1.2, the mass of the baseline ETCS is 2,101.0 kg for two missions. Assuming the mass determinations throughout this study have associated uncertainties on the order of 10%, an overall TCS with an advanced technology would need to show a savings of at least 210 kg to ensure a mass savings. Further, because design and development costs are not trivial, a mass savings of 25%, or 525 kg, is desirable. Using these criteria, the TCSs with advanced technologies proposed for FLO Lander may be divided among five categories:

- TCSs using advanced technologies requiring a mass penalty greater than 10% of the overall baseline ETCS mass: none.

- TCSs using advanced technologies requiring a mass penalty less than 10% of the overall baseline ETCS mass: none.

- TCSs using advanced technologies with a mass savings less than 10% of the overall baseline ETCS mass: none.

- TCSs using advanced technologies with a mass savings between 10 and 25% of the overall baseline ETCS mass: LP two-phase TCS, capillary pumped loops, and solar vapor compression heat pump.

- TCSs using advanced technologies with a mass savings greater than 25% of the overall baseline ETCS mass: lightweight radiators and parabolic radiator shade.

The technologies in the fourth category are promising but not outstanding for this mission. The technologies in the final category show significant promise for this mission. However, as discussed above, the parabolic radiator shade needs to be properly deployed on the lunar surface to function properly and this may require an extravehicular activity.

---

[144] The deployment is rated as "difficult" for this mission because the mass assessment assumes a crew extravehicular activity to place the parabolic shade on the lunar surface.

Table 4.3 Advanced Active Thermal Control System Architecture
for First Lunar Outpost Lander

Summary of Advanced Active Thermal Control System Architecture for First Lunar Outpost Lander	Overall Mass Savings [kg]	Qualitative Score
4.1.4.1 Low-Power Two-Phase Thermal Control System	286	-1
4.1.4.2 Two-Phase TCS with Electrohydrodynamic Pumping	unknown	+2
4.1.4.3 Capillary Pumped Loops	370	0
4.1.4.4 Solar Vapor Compression Heat Pump	259	+1
4.1.4.5 Lightweight Radiators	584	--
4.1.4.6 Parabolic Radiator Shade	642	-2

4.2   PERMANENT LUNAR BASE

4.2.1   Reference Mission

In order to intensively investigate and utilize Luna, a Permanent Lunar Base (PLB) is, for expedience, necessary. It is conceivable that PLB could become a reality sometime early in the next century. One proposal, as presented in Figure 4.9, would bury three modified Space Station modules under two meters of lunar regolith and provide living and working space continually for a crew of three or four. The regolith acts as a radiation shield for typical levels of incident irradiation. The base elements would include a habitation module, a laboratory module, and a plant growth module. The plant growth module would be an integral part of the base environmental control and life support system by replenishing atmospheric oxygen and removing carbon dioxide. The plants are also expected to provide food for the crew. Power for the base would be supplied by photovoltaic solar arrays located near the crew's quarters on the lunar surface. Base access would be through Space Station-type nodes connected to airlocks on the surface. Baseline ATCS heat rejection would be accomplished through horizontal radiators with low surface solar absorptivity [145]. These radiators would be insulated from below, using lunar regolith, and deployed on the lunar surface above the living areas. The overall nominal ATCS heat load is projected at 50 kW with peak individual module loads of 25 kW. The ETCS fluid is single-phase liquid ammonia. The continuous power mass penalty is 750 kg/kW which assumes solar photovoltaic power generation with regenerative fuel cell energy storage. The power mass penalty for "daytime only" power usage is 35.3 kg/kW for electricity taken from the main PLB power grid and 20.2 kg/kW for electricity taken from a dedicated photovoltaic array (Hughes, 1995). The project life is 15 years and the total mass savings computed below are for a single base.

4.2.2   Baseline Case

The baseline PLB ETCS uses low solar absorptivity, horizontal radiators with single-phase liquid ammonia as the working fluid. As illustrated in Figure 4.10, each module is serviced by two of the three ETCS loops. The TCS utilizes a single-phase cascade similar to the TCS for ISS. Each module is supplied with both a low-temperature ETCS loop interface (LTL) and a moderate-temperature ETCS loop interface (MTL). Radiator bypass valves provide ETCS loop set-point temperature control. Further, each PLB module has two ITCS loops using liquid water as the working fluid. Additional fittings in each PLB module allow either ITCS loop to service all of the module's coldplates and heat exchangers. This arrangement provides extra flexibility if any one of the ITCS or ETCS loops fail. Each ETCS loop also has a dedicated pump module. The overall base ATCS heat load is 50 kW, but each module may have a peak load up to 25 kW. A value of 7.50 kg/m^2 is assumed for the radiator mass per radiating area for horizontal radiators. Vertical radiators are assumed to use 5.625 kg/m^2 [146]. This base will

---

[145] These are also known as low alpha, horizontal radiators.

[146] The radiators on ISS, which are completely vehicle-mounted and use an extensive deployment mechanism, have a mass of 8.24 kg per m^2 of radiating area. The ISS radiators are two-sided. The

be located at the lunar equator which has the most severe thermal environment on Luna. Here surface temperatures range from 102 K at night to 384 K at lunar noon (Ewert, Petete, and Dzenitis, 1990). The solar irradiation at noon is 1.371 kW/m^2 with a surface albedo on average of 0.07 [147]. The lunar surface has the properties of a diffuse gray surface with an emissivity of 0.93 to 0.94 [148].

- Overall ETCS Performance:

Heat Rejected	50.0 kW
ETCS Working Fluid	single-phase ammonia

- Low Solar Absorptivity, Horizontal Radiators [149]:

Service Life (each set of panels)	7.5 years
Surface Coating	10 mil silver Teflon
Surface Emissivity (end-of-life)	0.86
Solar Absorptivity (end-of-life)	0.14
Fin Efficiency	0.85
Average Radiator Surface Temperature	275.0 K
Radiator Surface Area (day load)	650.81 m^2
Radiator Surface Area (night load)	217.26 m^2
Mass Penalty for Dry Radiators [150]	7.50 kg/m^2
Radiator Panel Mass	4881.08 kg
Number of Radiator Panel Sets per Project Life	2
Total Project Radiator Mass	9765.16 kg
Radiator Working Fluid Mass Penalty (ISS)	0.358 kg/m^2
Radiator Working Fluid Mass [151]	232.99 kg

---

radiator on FLO Lander is also vehicle-mounted, but single-sided (it is insulated on its underside), and has a base mass of 6.00 kg per m^2 of radiating area when not considering the heavier deployable panel sections. For PLB, the radiators will probably be packaged in some manner such that they can be deployed with minimal extravehicular activity time while using the lunar surface for support. Thus, some integral mass for a deployment mechanism is appropriate. However, the overall package is expected to be less complicated and lighter than the ISS radiators, yet heavier and possibly more complex than the FLO Lander radiators.

[147] This value is characteristic of a lunar mare. Surface albedo may vary between 0.07 and 0.24 according to Binder (1990).

[148] Keller (1995 a) indicates that surface solar absorptivity can vary between 0.7 and 1.0. Thus, a diffuse gray surface is an approximation for the lunar surface.

[149] The radiators were sized based on the parametric study given in Section 4.2.3 below.

[150] This mass penalty includes structure and deployment mass as well as actual radiator panel mass.

[151] The ETCS working fluid is assumed to not require replacement during the project life except if the original fluid is somehow lost (such as through a puncture in the radiators). This mass estimate is based on data for the working fluid mass used in the ISS radiator ORUs as a function of radiating area.
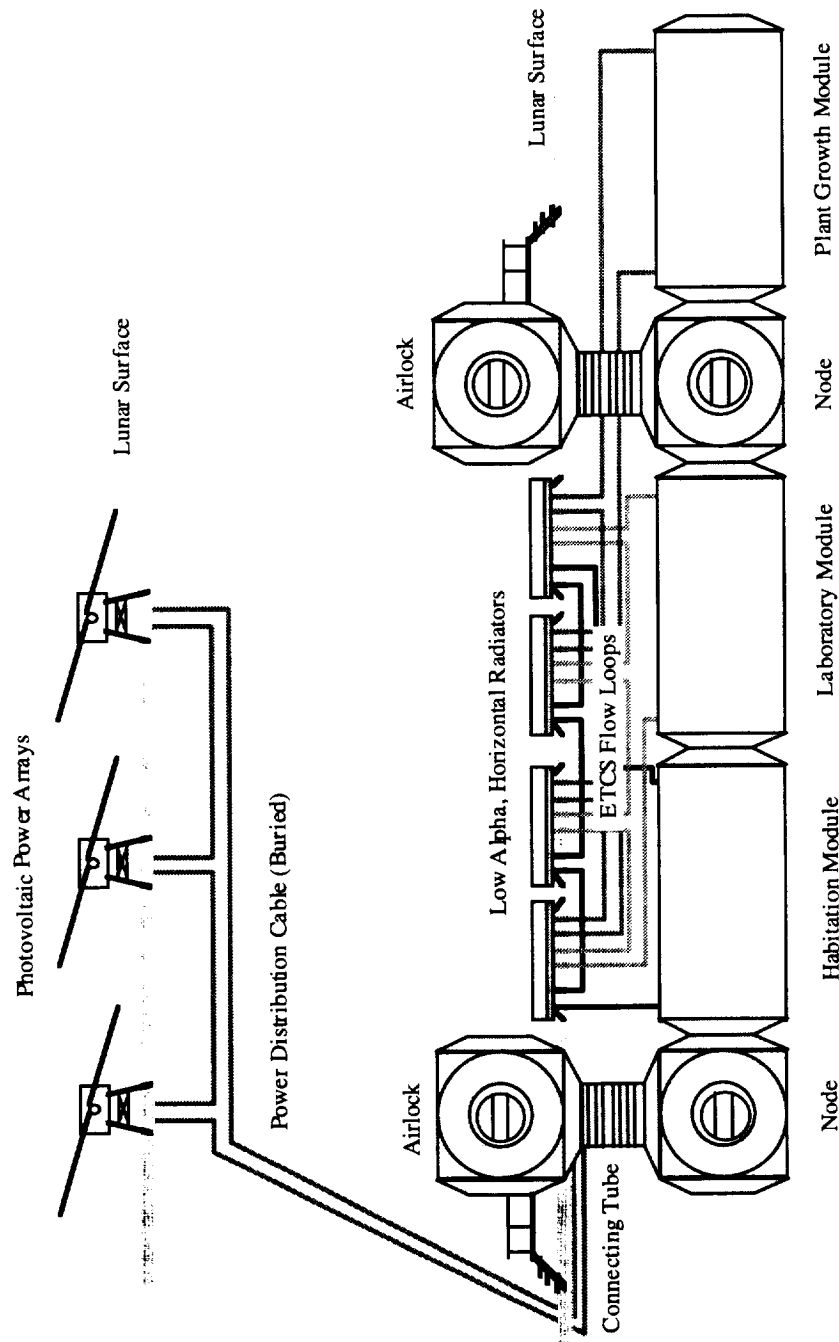
Figure 4.9 A side view of the Permanent Lunar Base baseline case. Shown are the three Space Station modules buried under 2 m of regolith. The external thermal control system uses three flow loops (two-fault tolerant) and low solar absorptivity, horizontal radiators with 10 mil silver Teflon surface coating. The power grid is also two-fault tolerant. The flow loops and the power distribution lines are for illustrative purposes only. (See Figure 4.10 for details of the external thermal control system plumbing.)

Low Solar Absorptivity, Horizontal Radiators (2 Flow Loops Within Each)
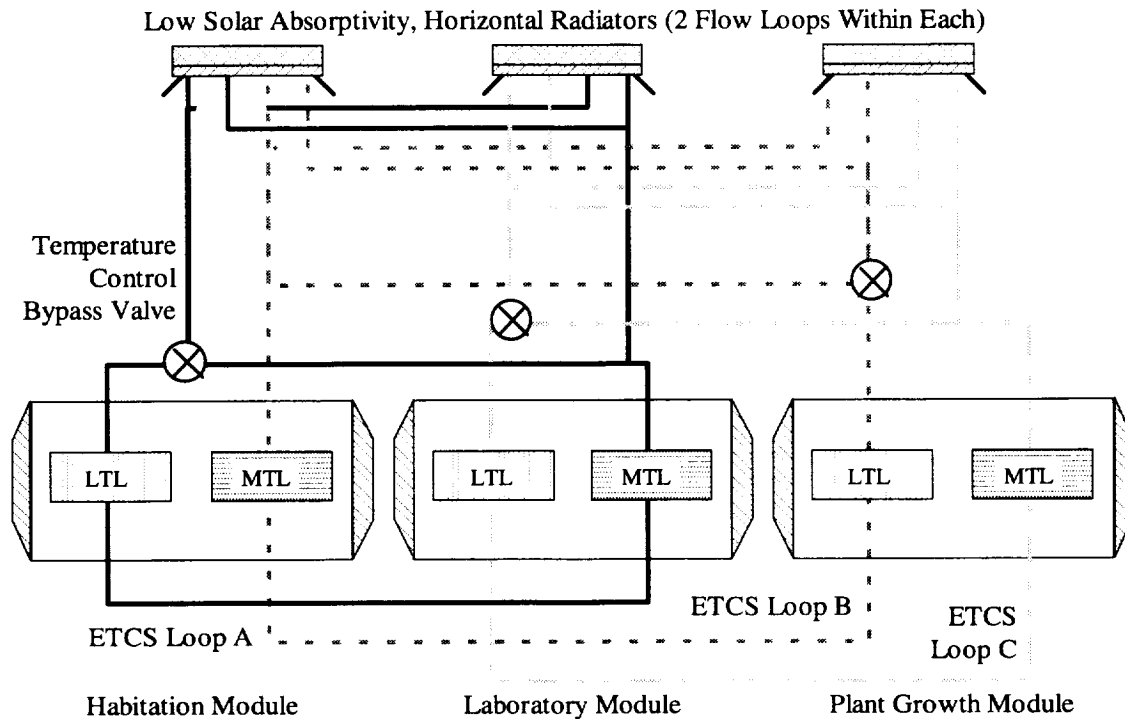
Figure 4.10 Plumbing for the baseline PLB ETCS. LTL is low-temperature ETCS loop and MTL is moderate-temperature ETCS loop. The system uses three ETCS loops to give two-fault tolerance with single-phase liquid ammonia as the working fluid. The bypass valves allow for temperature control. Each module has two ITCS water loops which can be interconnected to allow all of a module's heat load to be removed by either the LTL heat exchanger or MTL heat exchanger. A pump module (not pictured) is assumed for each of the three ETCS loops.

• ETCS Working Fluid Loop Mass Flowrates:

Average ETCS Fluid Temperature	278.0 K
Radiator Outlet Temperature	274.82 K
Radiator Inlet Temperature	281.18 K
Average Ammonia Specific Heat	4.62 (kW*s)/(kg*K)
Total Mass Flowrate (full load/equal distribution)	1.702 kg/s
Average Flowrate per Loop (full load/equal distribution)	0.5672 kg/s
Maximum Flowrate per Loop [152]	0.6807 kg/s

---

[152] This assumes a module loading of: habitation module: 10 kW, laboratory module: 25 kW, and plant growth module: 15 kW. This arrangement includes the maximum loading for any one module plus

- ETCS Pump Module: Two cases were considered for pumping power calculations. They may be summarized as:

Case	Heat Load [kW]	Flowrate [kg/s]	Pump Efficiency
Nominal Load:			
Loop A	16.67	0.5672	0.40
Loop B	16.67	0.5672	0.40
Loop C	16.67	0.5672	0.40
Maximum Load:			
Loop A	12.50	0.4254	0.35
Loop B	20.00	0.6807	0.45
Loop C	17.50	0.5956	0.40

Average Ammonia Density	631.96 kg/m^3
Radiator Pressure Drop per Radiating Area [153]	0.3718 kN/m^4
Radiator Pressure Drop	242.0 kN/m^2
Pumping Power for Radiators (day load) [154]	1.629 kW
Pumping Power for Radiators (night load) [155]	0.544 kW
Estimated Effective Line Lengths [156]:	
Loop A	25.65 m
Loop B	71.10 m
Loop C	57.90 m
Line Diameter [157]	0.0236 m
Maximum Line Pumping Power [158]	0.628 kW
Overall Pumping Power [159]	2.26 kW
Continuous Power Mass Penalty	750 kg/kW
Daytime Only Power Mass Penalty	35.3 kg/kW
Pumping Power as Mass [160]	917.3 kg
Mass of Ammonia in Lines	32.76 kg

---

reserves 15 kW, as specified, for the plant growth module. The maximum per loop load is 20 kW assuming each loop picks up half of a module's heat load.

[153] This penalty is based on the values for ISS which specify a maximum radiator pressure drop of 48.26 kN/m^2 for 129.8 m^2 of radiating area.

[154] The nominal load yielded the greatest pumping power requirement for the radiators.

[155] The night load pumping power is the day load pumping power multiplied by the ratio of the night load and day load radiator areas.

[156] These values are the sum of the estimated line lengths based on Figures 28 and 29 plus an additional 50% to account for fittings and valves.

[157] This is the inside diameter of the ETCS lines within ISS modules. Specifically, this value is 0.93 in.

[158] The maximum load yielded the greatest pumping power requirement for the ETCS lines.

[159] This value includes 0.63 kW to pump ammonia through the ETCS loops and 1.63 kW to pump ammonia through the radiators.

[160] Assumption: The ETCS flowrate is constant with portions of the radiator either freezing and/or being closed off at night when the heat rejection requirement is less. In pratical terms, this implies that the pumping power is less at night than during daylight. Thus, the continuous power mass penalty is applied only to the power associated with running the pumps continuously. The daytime

- Summary of Permanent Lunar Base Active Thermal Control System:

Heat Load Rejected	50.0 kW
Total Dry Radiator Mass (for 15 years)	9765.2 kg
Working Fluid Mass	265.8 kg
Pumping Power	2.26 kW
Pumping Power as Mass	917.3 kg
Total ETCS Heat-Rejection System Mass [161]	10,948.3 kg

The baseline radiator mass per area, based on a single set of radiator panels, is 7.86 kg/m^2. Upon considering both sets of radiator panels, this value increases to 15.36 kg/m^2.

4.2.3 Parametric Study Using the Baseline Case

PLB is still undergoing preliminary design work, so the baseline for the ETCS assumes only the values mentioned above. The actual baseline hardware includes low solar absorptivity, horizontal radiators fabricated from materials like those specified for ISS. Several radiator surface coatings are available, including silver Teflon and Z-93. Additionally, the radiators could be designed for the entire project life of 15 years, or they could be designed for a shorter time and then replaced as appropriate during scheduled maintenance. The possible benefit of using radiators with a design life less than 15 years is that the end-of-life surface coating properties would not be as severely degraded due to environmental effects so that the overall radiator size could be smaller. For this study, the masses of the surface coatings themselves were assumed negligible compared with the masses for the other radiator components. A comparison of radiator designs for a 50.0 kW heat load using three surface coatings and two radiator panel surface temperatures is presented below and in Figure 4.11 and Figure 4.12. The radiators are deployed horizontally on the lunar surface.

Table 4.4 Total Masses for the Lunar Base Radiator [kg]
Using Various Surface Coatings and Various Total Design Lives

Design Radiator Panel Set Life [years]	Average Radiator Panel Surface Temperature (Horizontal Units)					
	275.0 K			280.0 K		
	5.5 mil Silver Teflon	10 mil Silver Teflon	Z-93	5.5 mil Silver Teflon	10 mil Silver Teflon	Z-93
15.0		12,258.9		52,765.9	7,846.8	
7.5	16,025.6	9,762.1		12,080.7	7,935.0	52,662.3
5.0	16,189.6	11,706.6	89,466.0	13,231.5	9,869.6	36,157.2
2.5	23,815.1	19,181.4	73,383.3	20,403.5	16,617.0	45,731.3
1.0	50,870.4	42,955.8	133,625.2	44,454.6	37,704.3	92,768.4

only power mass penalty is applied to the additional power used to run the pumps during the day when the entire radiator is in use.

[161] This value does not include masses for the pumps, lines, and fittings, but these are expected to be roughly the same for all PLB ATCS configurations.
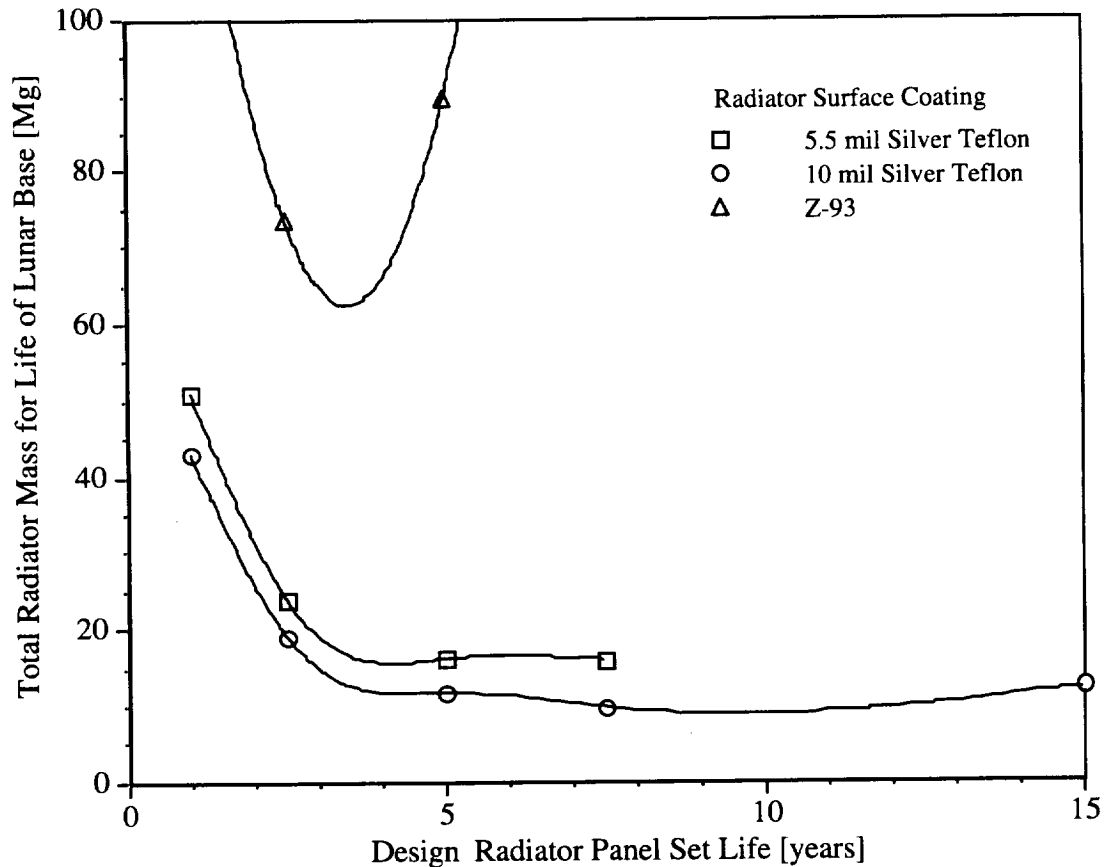
Figure 4.11 Total mass of horizontal radiator panels for the life of Permanent Lunar Base (15 years) as a function of the expected design life for the panel sets. The study assumptions are: Rejected heat load is 50 kW, the radiator mass per rejection area for a dry panel is 7.50 kg/m^2, the fin efficiency is 0.85, and the radiator surface temperature is 275.0 K. The units on the vertical axis are Megagrams [Mg].

Table 4.5 Surface Coatings as a Function of Time (Peck, 1990)

Time [years]	5.5 mil Silver Teflon		10 mil Silver Teflon		Z-93	
	ε	α	ε	α	ε	α
0	0.78	0.08	0.89	0.09	0.90	0.17
10	0.73	0.15	0.85	0.15	0.90	0.23
30	0.65	0.20	0.81	0.20	0.90	0.30

Surface properties were estimated with second order polynomials using data from Peck (1990) to set the function constants.

In all cases the 10 mil silver Teflon yields design estimates which are significantly less massive than those for the other two coatings. Thus, barring excessive cost or mass contingencies, this is the recommended coating for this application.
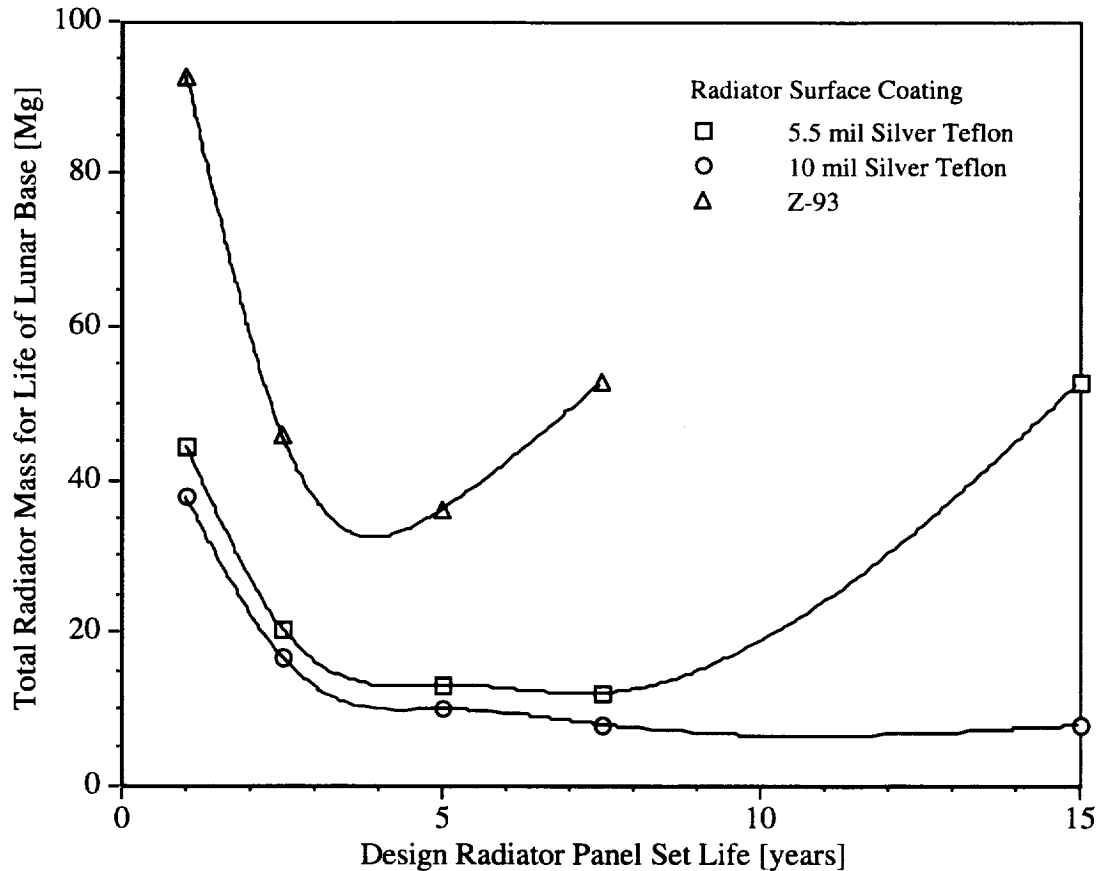
Figure 4.12 Total mass of horizontal radiator panels for the life of Permanent Lunar Base (15 years) as a function of the expected design life for the panel sets. The study assumptions are: Rejected heat load is 50 kW, the radiator mass per rejection area for a dry panel is 7.50 kg/m^2, the fin efficiency is 0.85, and the radiator surface temperature is 280.0 K. The units on the vertical axis are Megagrams [Mg].

For the baseline, which uses a panel temperature of 275.0 K, the least massive radiators have a design life of 7.5 years. Thus, the radiators will be replaced once as scheduled maintenance. In addition to surface properties, the radiator design for PLB is sensitive to the radiator surface temperature. Increasing the surface temperature by five degrees to 280.0 K leads to a different optimal design. For this hotter case, a single radiator with a design life of 15 years is the least massive option.

4.2.4 Advanced ATCS Architecture for Permanent Lunar Base

The PLB will be a single base with a projected life of 15 years. As stated above, the radiators will be replaced once after 7.5 years. Unless otherwise noted, all advanced technologies are expected to last at least for the entire project life of 15 years. Each advanced architecture is, where applicable, assessed numerically for the overall mass

savings when compared with the baseline. Qualitative assessments for these advanced technologies are presented in Section 2.0.

4.2.4.1   Two-Phase Thermal Control System With Mechanical Pump/Separator

To convert PLB to use a two-phase TCS this study extrapolates predictions from Ungar (1995) which provides estimates for space stations. Ungar (1995) includes a medium space station which is similar to PLB. Ungar's medium station with a single-phase cascade TCS is like the baseline PLB TCS. Ungar (1995) also presents a comparable two-phase TCS with MP/S [162].

	PLB Baseline TCS (1 loop)	Total PLB Baseline TCS	Medium Space Station (Ungar, 1995)			
			Single-Phase Cascade TCS		Two-Phase TCS With MP/S	
			LTL	LTL	LTL	MTL
Pump Power [kW]	0.753	2.260	0.615	0.615	0.299	0.330
Radiator Area [m^2]	216.9	650.8	395	395	390	390
Loop Set-Point [K]	274.8	274.8	275.2	275.2	275.2	287.2

LTL refers to the low temperature loop while MTL refers to the moderate temperature loop. The baseline ETCS for PLB uses three single-phase cascade, low temperature loops. Comparing the PLB TCS with the single-phase cascade TCS for a medium station reveals that the pumping power per loop is about 22% more for PLB and the PLB TCS loop set-points are approximately that of the LTL for the single-phase cascade TCS. A comparable two-phase TCS with MP/S for PLB would use two LTL loops and one MTL loop. The radiator area will remain approximately the same. The pumping power is estimated to be 0.366 kW for each LTL and 0.404 kW for the MTL [163]. Thus, the significant savings for this option compared with the baseline TCS is a reduction in pumping power.

Mass Saved by Using a Two-Phase Thermal Control System With Mechanical Pump/Separator	Baseline PLB TCS	TCS With MP/S for PLB	Total Change for TCS
Pump Power [kW]	2.260	1.136	
Mass Due to Pump Power [kg] [164]	917.3	461.1	456.2

The two-phase TCS with MP/S uses smaller fluid lines than the baseline single-phase cascade TCS which translates into an additional mass savings. However, this savings is not included here.

A more important issue related to this technology is whether PLB will end after its initial project life of 15 years or will it be an initial phase for a much larger installation? From Ungar (1995), the two-phase TCSs offer the greatest advantage for large systems with long ETCS transport lines. If PLB will end after its initial project life, then the mass savings associated with reduction in pumping power is not as great as some of the other

---

[162]   Ungar (1995) refers to this option as a rotary fluid management device (RFMD) type two-phase TCS. See Section 2.1.1 for additional details about the MP/S.

[163]   These values are 22% more than Ungar's values for the two-phase TCS with MP/S.

[164]   See Section 4.2.2 for details.

advanced technologies presented below. However, if PLB will eventually expand into a much larger facility, a two-phase TCS will yield substantial mass savings due to reductions in pumping power, line mass, and radiator mass for that larger facility. As such, a two-phase TCS for PLB would be a sound investment on which to build a larger TCS at a later date.

Specific Assessments:

Equipment Mass Savings	negligible
Power Savings	1.124 kW
Power Savings as Mass	456 kg
Overall Mass Savings	456 kg
Composite Qualitative Score	0

4.2.4.2 Low-Power Two-Phase Thermal Control System

To convert PLB to use a two-phase TCS this study extrapolates predictions from Ungar (1995) which gives estimates for space stations. Ungar (1995) includes a medium space station which is similar to PLB. Ungar's medium station with a single-phase cascade TCS is comparable to the baseline PLB TCS. A comparable LP two-phase TCS [165] is also presented.

	PLB Baseline TCS (1 loop)	Total PLB Baseline TCS	Medium Space Station (Ungar, 1995)			
			Single-Phase Cascade TCS		LP Two-Phase TCS	
			LTL	LTL	LTL	MTL
Pump Power [kW]	0.753	2.260	0.615	0.615	0.094	0.147
Radiator Area [m²]	216.9	650.8	395	395	390	390
Loop Set-Point [K]	274.8	274.8	275.2	275.2	275.2	287.2

LTL and MTL refer to low and moderate temperature loops, respectively. The Baseline ETCS for PLB uses three single-phase cascade, low temperature loops. Comparing the TCS for PLB with the single-phase cascade TCS for a medium station reveals that the pumping power per loop is about 22% more for PLB and the PLB TCS loop set-points are approximately that of the LTL for the single-phase cascade TCS. A comparable LP two-phase TCS for PLB would use two LTL loops and one MTL loop. The radiator area will remain approximately the same. The pumping power is estimated to be 0.115 kW for each LTL and 0.180 kW for the MTL [166]. Thus, the significant savings for this option compared with the baseline TCS is a reduction in pumping power.

---

[165] See Section 2.1.2 for additional details on LP two-phase TCSs.

[166] These values are 22% more than Ungar's values for a LP two-phase TCS.

Mass Saved by Using a Low-Power Two-Phase Thermal Control System	Baseline PLB TCS	LP Two-Phase TCS for PLB	Total Change for TCS
Pump Power [kW]	2.260	0.410	
Mass Due to Pump Power [kg] [167]	917.3	166.4	750.9

The LP two-phase TCS uses smaller fluid lines than the baseline single-phase cascade TCS which translates into an additional mass savings. However, this savings is not included here.

As in the previous section, a more important issue related to this technology is whether PLB will end after its initial project life of 15 years or will it be an initial phase for a much larger installation? From Ungar (1995), the two-phase TCSs offer the greatest advantage for large systems with long ETCS transport lines. If PLB will end after its initial project life, then the mass savings associated with reduction in pumping power is not as great as some of the other advanced technologies presented below. However, if PLB will eventually expand into a larger facility, a two-phase TCS will yield substantial mass savings due to reductions in pumping power, line mass, and radiator mass for that larger facility. As such, a two-phase TCS for PLB would be a sound investment on which to build a larger TCS at a later date.

Specific Assessments:

Equipment Mass Savings	negligible
Power Savings	1.850 kW
Power Savings as Mass	751 kg
Overall Mass Savings	751 kg
Composite Qualitative Score	-1

4.2.4.3   Two-Phase Thermal Control System With Electrohydrodynamic Pumping

Based on the discussion in Section 2.1.3, PLB could utilize a two-phase TCS with electrohydrodynamic pumping. A two-phase TCS with electrohydrodynamic pumping may yield a mass savings over a LP two-phase TCS. A significant mass savings over the baseline TCS would also be expected. However, without more data on this technology, no mass savings estimates may be determined.

Specific Assessments:

Equipment Mass Savings	unknown
Power Savings as Mass	unknown
Overall Mass Savings	unknown
Composite Qualitative Score	+2

---

[167]   See Section 4.2.2 for details.

4.2.4.4 Capillary Pumped Loops

Based on Section 4.2.2, capillary pumped loops [168] will save 2.26 kW, which is the estimated ETCS pumping power for PLB. As above, the capillary pumped loop equipment mass is assumed to be comparable to the equipment mass for the baseline single-phase TCS architecture. Thus, the overall savings for this option is 917.3 kg based on saving power for pumping [169].

Specific Assessments:

Equipment Mass Savings	none
Power Savings	2.26 kW
Power Savings as Mass	917 kg
Overall Mass Savings	917 kg
Composite Qualitative Score	0

4.2.4.5 Vapor Compression Heat Pump

A vapor compression heat pump [170] could be used to reject heat at higher temperatures so as to reduce the required radiator area. In general, as the effective environmental temperature and, correspondingly, the ETCS mass increases, heat pumps are more likely to offer a mass savings compared with an ETCS using only radiators. While PLB can operate without a heat pump, an ETCS incorporating a heat pump is expected to yield a mass savings compared with the PLB baseline. Because the PLB ETCS is expected to be two-fault tolerant, this study assumes a heat pump rejecting a nominal load of 16.67 kW for each ETCS loop. Further, to reject a full load of 50 kW even after a single failure, the actual heat pumps must each have a 25 kW capacity. The analysis is for a single ETCS loop. Here the heat pumps will operate only while PLB is in sunlight drawing power from the main PLB power grid. The appropriate power mass penalty for "daytime only" usage for this scenario is 35.3 kg/kW (Hughes, 1995). The continuous power mass penalty of 750 kg/kW applies for any continuous use.

The radiators may be oriented in numerous ways. The configurations of greatest interest are the horizontal radiator, as included in the baseline TCS, and a vertical radiator. Because PLB will have an equatorial site, the vertical radiator is positioned so its radiating areas face north and south with its length parallel to the lunar equator. Further, because the radiator rejection temperature with a heat pump will be above 280 K, as Section 4.2.3 indicates, a single set of radiator panels designed for 15 years will be less massive than two sets of radiator panels designed for 7.5 years each. Thus, the assumed surface properties are those for 10 mil silver Teflon after 15 years of service.

---

[168] See Section 2.1.4 for background on capillary pumped loops.
[169] See Section 4.2.2 for details.
[170] See Section 2.2.1 for background on vapor compression heat pumps.

Horizontal Radiators

A two parameter parametric study (Figure 4.13) indicates that the ETCS mass is minimized for PLB using horizontal radiators when the heat pump temperature lift is 52.3 K and the radiator fluid mass flowrate is increased to 1.27 kg/s per ETCS loop. Actually, as Figure 4.14 shows, this heat pump design is constrained by the minimum radiating area for rejecting a full heat load at night without a heat pump at an average panel temperature of 275.0 K. Specifically then (for one of three ETCS loops):

Cold Source Temperature, T_C (evaporator temperature)	274.0 K
Temperature Lift, $T_H - T_C$	52.3 K
Hot Source Temperature, T_H (condenser temperature)	326.3 K
Radiator Inlet Temperature, T_{in}	322.3 K
Lunar Surface Solar Irradiation	1.371 kW/m^2
Environmental Temperature, T_{space}	3.0 K
Effective Sink Temperature, T_{sink} [171]	265.3 K
Total Nominal Cooling Load per Loop, Q_C	16.67 kW
Ideal Coefficient of Performance, COP_{Carnot}	5.24
Heat Pump Efficiency, η [172] (Ewert, 1991)	0.50
Necessary Input Power, W_{real}	6.36 kW

The low solar absorptivity, horizontal radiators are simulated by the model developed for the parametric study.

Emissivity (end-of-life)	0.83
Solar Absorptivity (end-of-life)	0.17
Fin Efficiency	0.85
Radiator Mass Flowrate of Ammonia (per ETCS loop)	1.17 kg/s
Average Ammonia Temperature	316.3 K
Average Panel Surface Temperature	314.8 K
Heat Rejection per Unit Area	0.318 kW/m^2
Total Heat Rejected per Loop by the Radiators, $Q_{H,real}$	23.03 kW
Radiator Mass Per Unit Area	7.50 kg/m^2
Number of Radiator Panel Sets per Project Life	1
Radiator Working Fluid Mass Per Unit Area	0.36 kg/m^2
Necessary Radiator Surface Area During the Day	72.44 m^2
Necessary Radiator Surface Area at Night	72.42 m^2

Here the radiator design is constrained by the radiating area necessary to reject the nominal load at night (Figure 4.14). The power may be grouped according to its applicable power mass penalty.

---

[171] The effective environmental sink temperature is provided here for comparison. These computations used the solar irradiation and the temperature of space, not the effective sink temperature.

[172] Percentage of Carnot coefficient of performance (COP).
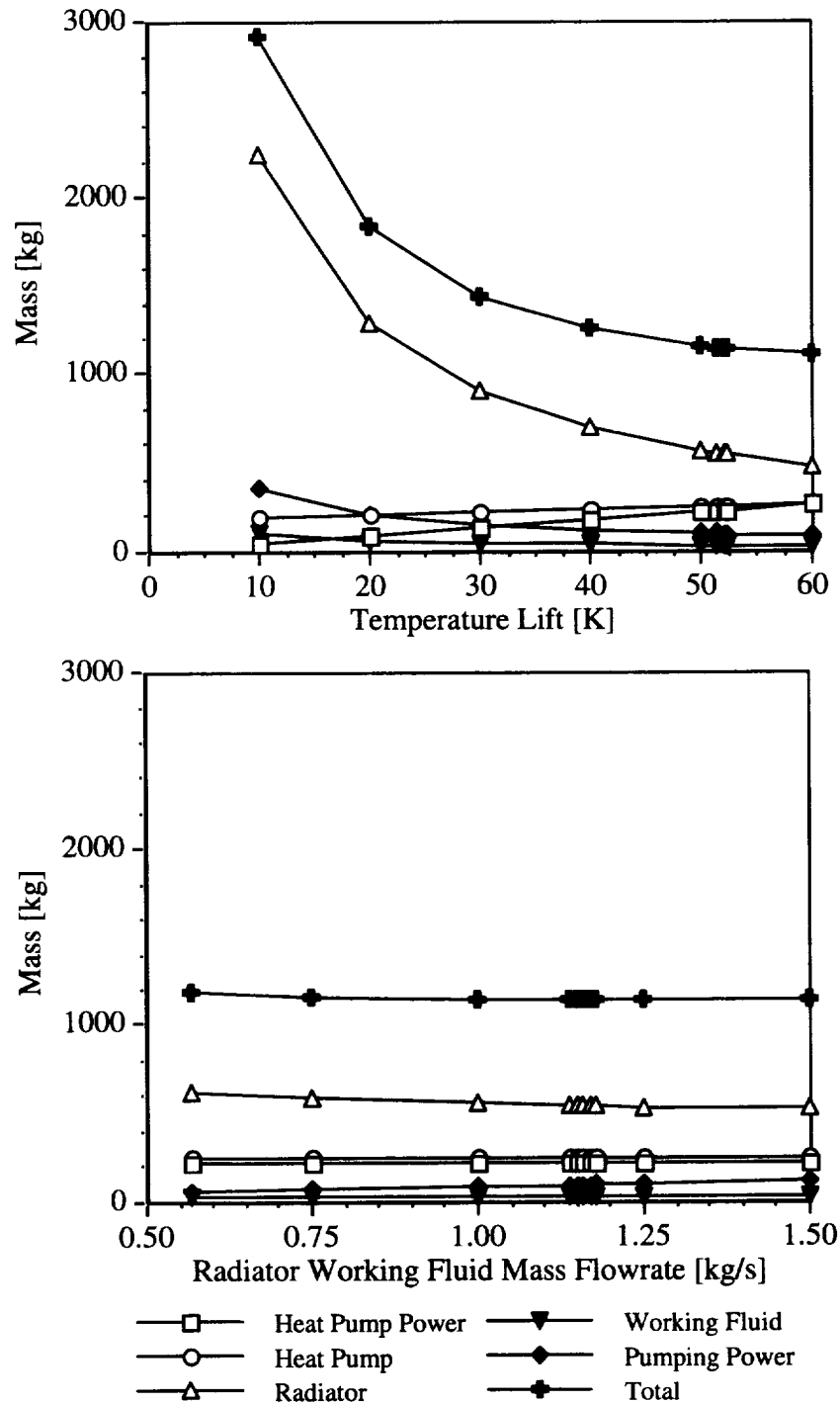
Figure 4.13 Variation of Permanent Lunar Base external thermal control system mass per loop as a function of the vapor compression heat pump temperature lift and the radiator loop mass flowrate. This study used horizontal radiators. The baseline mission from Section 4.2.2 forms the basis for this study. The external thermal control system mass was optimized with respect to both variables mentioned above.

Power Mass Penalties:

Heat Pump Power	Daytime Only
Evaporator Pumping Power	Daytime Only
Condenser Pumping Power	Daytime Only
Radiator Pumping Power	Continuous

Mass Gained by Using a Vapor Compression Heat Pump	PLB ETCS Loop With Heat Pump	Total PLB ETCS With Heat Pumps	Baseline PLB TCS	Change for PLB ETCS
Radiator Mass [kg]	543.3	1629.9	9765.2	-8135.3
Working Fluid [kg]	25.9	77.7	233.0	-155.3
Heat Pump Mass [173] [kg]	255.1	765.3	--	+765.3
Radiator, Fluid, and Heat Pump Mass [kg]	824.3	2472.9	9998.2	-7525.3
Power:				
Heat Pump [kW]	6.36	19.08	--	
Evaporator Pumping Power [kW]	0.27	0.81	--	
Condenser Pumping Power [kW]	0.06	0.18	--	
Radiator Pumping Power [kW]	0.12	0.36	1.63	
Total Power [kW]	6.81	20.43	1.63	
Mass due to Power [kg]	326.2	978.6	471.0	+507.6
Total Mass [kg]	1150.5	3451.5	10469.2	-7017.7

The ETCS line pumping power is unchanged. The power values include penalties for the pressure drops associated with the condenser and the evaporator. The condenser power penalty is 50% of the power to pump fluid through the radiators designed for use with the heat pump (or 0.5×0.12 kW). The evaporator power penalty is 50% of the power to pump fluid through the baseline radiator configuration (or 0.5×1.63 kW/3). The radiator pumping power is proportional to the radiator size, in terms of radiating area, and is based on values from ISS.

Vertical Radiators

A two-parameter parametric study (Figure 4.15) indicates that the ETCS mass is minimized for PLB using vertical radiators when the heat pump temperature lift is 122.3 K and the radiator fluid mass flowrate is increased to 0.88 kg/s per ETCS loop. Again, as Figure 4.16 shows, this heat pump design is constrained by the minimum radiating area for rejecting a full heat load at night without a heat pump at an average panel temperature of 275.0 K. Specifically then (for one of three ETCS loops):

Cold Source Temperature, T_C (evaporator temperature)	274.0 K
Temperature Lift, $T_H - T_C$	121.6 K
Hot Source Temperature, T_H (condenser temperature)	395.6 K

---

[173] See the footnotes in Section 3.1.5.4 for the heat pump sizing correlation.
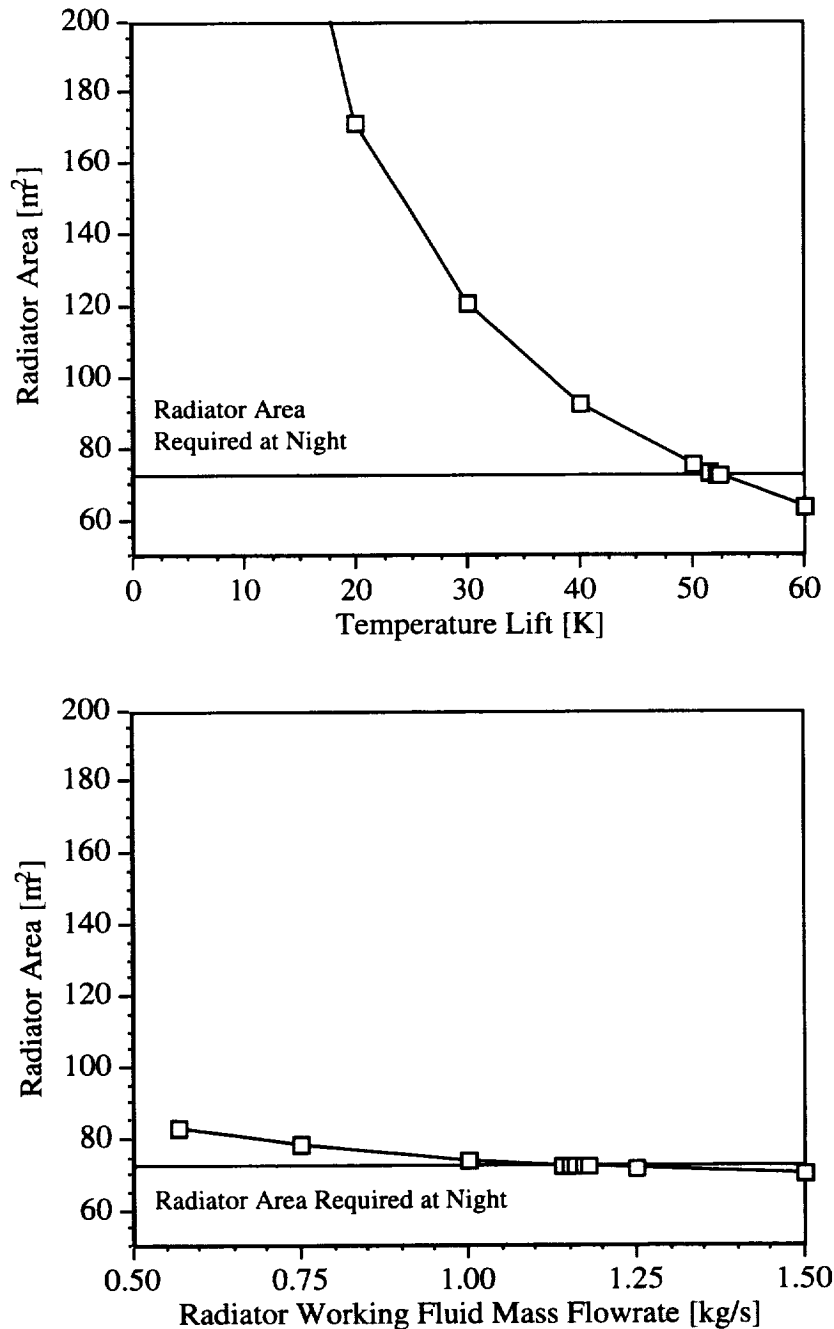
Figure 4.14 Variation of radiator area for Permanent Lunar Base per external thermal control system loop using horizontal radiators as a function of the vapor compression heat pump temperature lift and the radiator loop mass flowrate. This heat pump option is constrained by the radiator area required for rejection of the active thermal control system heat load at night without the heat pump operating.

Radiator Inlet Temperature, T_{in}	391.6 K
Effective Sink Temperature, T_{sink}	317.1 K
Total Nominal Cooling Load per Loop, Q_C	16.67 kW
Ideal Coefficient of Performance, COP_{Carnot}	2.25
Heat Pump Efficiency, η [174] (Ewert, 1991)	0.50
Necessary Input Power, W_{real}	14.80 kW

The low solar absorptivity, vertical radiators are simulated by the model developed for the parametric study using the appropriate higher effective sink temperature.

Emissivity (end-of-life)	0.83
Solar Absorptivity (end-of-life)	0.17
Fin Efficiency	0.85
Radiator Mass Flowrate of Ammonia (per ETCS loop)	0.88 kg/s
Average Ammonia Temperature	381.6 K
Average Panel Surface Temperature	380.1 K
Heat Rejection per Unit Area	0.430 kW/m^2
Total Heat Rejected per Loop by the Radiators, $Q_{H,real}$	31.46 kW
Radiator Mass Per Unit Area	5.625 kg/m^2
Number of Radiator Panel Sets per Project Life	1
Radiator Working Fluid Mass Per Unit Area	0.27 kg/m^2
Necessary Radiator Surface Area During the Day	73.11 m^2
Necessary Radiator Surface Area at Night	73.07 m^2

| Mass Gained by Using a Vapor Compression Heat Pump	PLB ETCS Loop With Heat Pump	Total PLB ETCS With Heat Pump	Baseline PLB TCS	Change for PLB ETCS
Radiator Mass [kg]	411.2	1233.6	9765.2	-8531.6
Working Fluid [kg]	19.7	59.1	233.0	-173.9
Heat Pump Mass [175] [kg]	335.6	1006.8	--	+1006.8
Radiator, Fluid, and Heat Pump Mass [kg]	766.5	2299.5	9998.2	-7698.7
Power: Heat Pump [kW]	14.80	44.40	--	
Evaporator Pumping Power [kW]	0.27	0.81	--	
Condenser Pumping Power [kW]	0.06	0.18	--	
Radiator Pumping Power [kW]	0.12	0.36	1.63	
Total Power [kW]	15.25	45.75	1.63	
Mass due to Power [kg]	624.1	1872.3	471.0	+1401.3
Total Mass [kg]	1390.6	4171.8	10469.2	-6297.4

The ETCS line pumping power is unchanged. As above, the power values include penalties for the pressure drops associated with the condenser and the evaporator.

---

[174] Percentage of Carnot coefficient of performance (COP).

[175] See the footnotes in Section 3.1.5.4 for the heat pump sizing correlation.
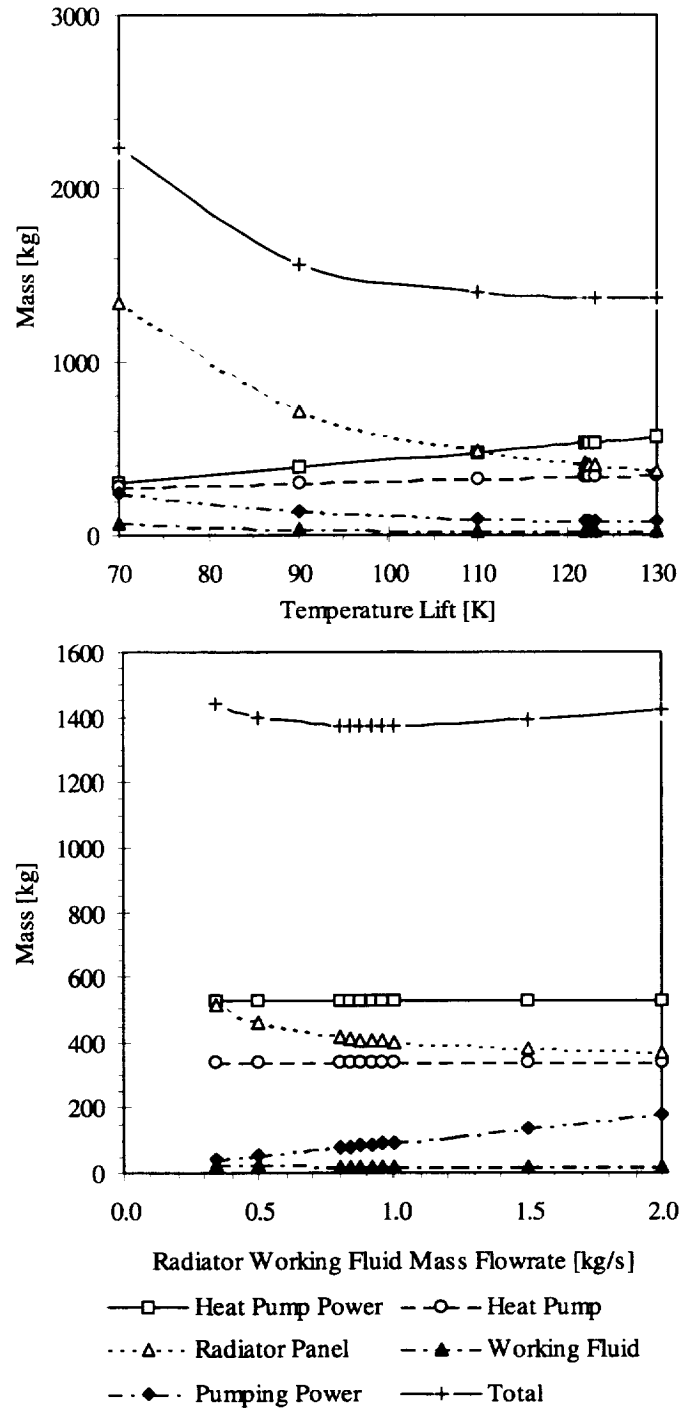
Figure 4.15 Variation of Permanent Lunar Base external thermal control system mass per loop as a function of the vapor compression heat pump temperature lift and the radiator loop mass flowrate. This study uses vertical radiators. The external thermal control system mass was optimized with respect to both variables mentioned above.
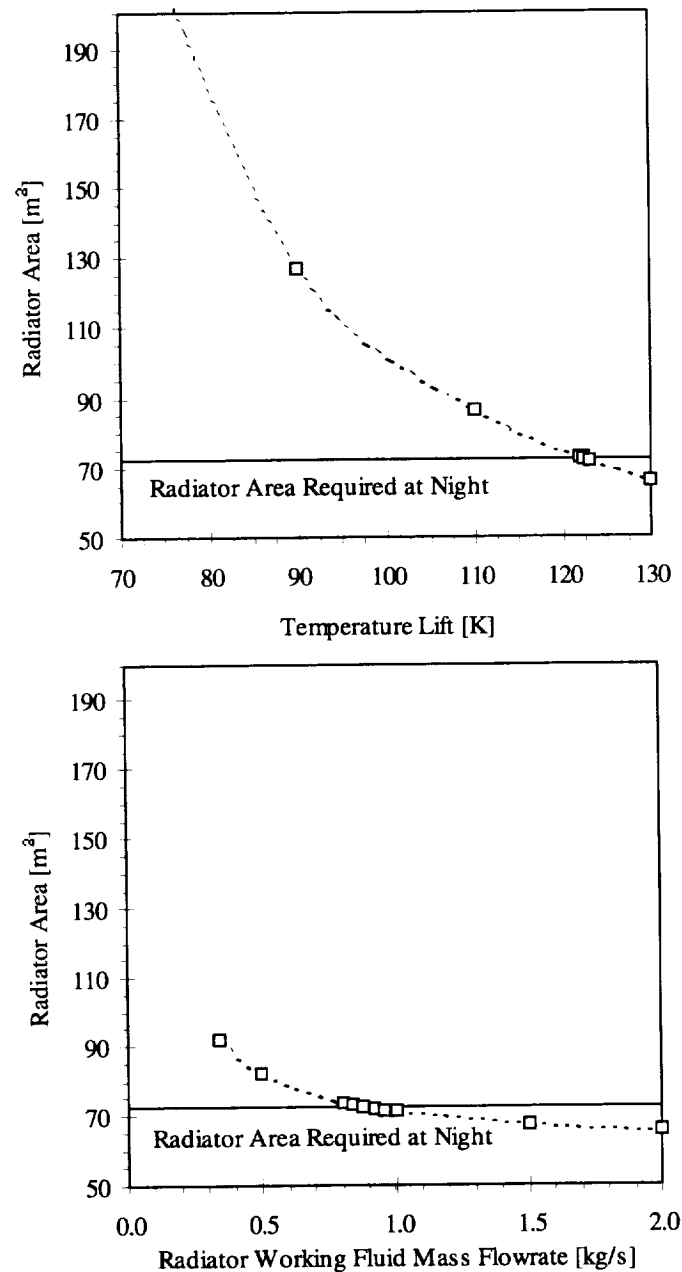
Figure 4.16 Variation of radiator area for PLB per external thermal control system loop using vertical radiators as a function of the vapor compression heat pump temperature lift and the radiator loop mass flowrate. This heat pump option is constrained by the radiator area required for rejection of the active thermal control system heat load at night without the heat pump operating (solid line).

Both designs using vapor compression heat pumps are less massive than the baseline ETCS configuration. However, the horizontal radiators provided a less massive system than using vertical radiators. The vertical radiator units are less massive simply because they have a lower mass per radiating area than the horizontal radiator units.

However, the vertical radiators partially view the lunar surface while horizontal radiators view only the Sun and space. The lunar surface radiates its energy in the same frequency band that the radiator uses to reject heat. This rejection frequency band is associated with the radiating surface's infrared emissivity. The Sun irradiates at frequencies which are much greater than the heat-rejection frequency band. The solar irradiation frequency band is associated with the radiating surface's solar absorptivity. Because the emissivity is large compared with the solar absorptivity, the overall effective sink temperature for the vertical radiators is significantly greater than for the horizontal radiators. Therefore, the heat pumps using vertical radiators use a greater temperature lift which requires more power input and a larger capacity heat pump. In summary, the configuration using vertical radiators has lighter radiators while the configuration using horizontal radiators sees a lower effective sink temperature at lunar noon and uses less power and lower capacity heat pumps. Thus, assuming the loss of either power generation capacity or heat pump units, the configuration with horizontal radiators would be the more suitable system because it uses less power to operate and it experiences the lower effective sink temperature at lunar noon which allows this system to reject more heat without heat pumping than the corresponding system using vertical radiators [176].

Specific Assessments:

	Using Horizontal Radiators:	Using Vertical Radiators:
Equipment Mass Savings	7,525 kg	7,708 kg
Power Savings	-18.80 kW	-44.36 kW
Power Savings as Mass	-508 kg	-1401 kg
Overall Mass Savings	7,017 kg	6,297 kg
Composite Qualitative Score [177]	+2	

4.2.4.6   Solar Vapor Compression Heat Pump

As with ISS, the single greatest drawback of a TCS using a vapor compression heat pump is the power requirement. The configuration in the previous section using horizontal radiators consumed power equivalent to 41% of the nominal load for PLB. The configuration using vertical radiators consumed power equivalent to 92% of the nominal load for PLB. To minimize the mass of this commodity, dedicated photovoltaic solar arrays can be installed with the heat pumps. This option is called the solar vapor compression heat pump [178]. The appropriate mass penalty for equipment which will

---

[176]   At an effective sink temperature of 265.3 K, which applies for horizontal radiators, heat can be rejected without a heat pump at a panel surface temperature of 275 K. This is the basis for the baseline TCS design. However, at an effective sink temperature of 317.1 K, the corresponding value for vertical radiators, no heat can be rejected without a heat pump. Therefore, on Luna horizontal radiators display an added factor of safety compared with vertical radiators.

[177]   For this application the volume is "compact" compared with the baseline architecture.

[178]   Technically, both heat pumps presented for PLB are "solar heat pumps" because they only operate while PLB is in sunlight and their assumed power mass does not include any mass for power storage.

require power only during the day is 20.2 kg/kW (Hughes, 1995). The continuous power mass penalty is still 750 kg/kW.

From an analysis standpoint, this option differs from the previous section only in the value of the "daytime only" power mass penalty assigned. As such, the equipment masses, capacities, and set-points are the same for these two options. The masses for the power, however, will differ. Thus, assuming the configuration from the previous section using horizontal radiators:

Mass Gained by Using a Solar Vapor Compression Heat Pump [179]	PLB ETCS Loop With Solar Heat Pump	Total PLB ETCS With Solar Heat Pump	Baseline PLB TCS	Change for PLB ETCS
Radiator, Fluid, and Heat Pump Mass [kg]	824.3	2472.9	9998.2	-7525.3
Power: Heat Pump [kW]	6.36	19.08	--	
Evaporator Pumping Power [kW]	0.27	0.81	--	
Condenser Pumping Power [kW]	0.06	0.18	--	
Radiator Pumping Power [kW]	0.12	0.36	1.63	
Total Power [kW]	6.81	20.43	1.63	
Mass Due to Power [kg]	225.1	675.3	471.0	+204.3
Total Mass [kg]	1049.4	3148.2	10469.2	-7321.0

The ETCS line pumping power is unchanged. As in the previous section, the power values include penalties for the pressure drops associated with the condenser and the evaporator. It is assumed that the pumping power for flow through the heat pump condensers and evaporators is supplied by the arrays dedicated to the heat pumps.

Specific Assessments:

Equipment Mass Savings	7,525 kg
Power Savings	-18.80 kW
Power Savings as Mass	-204 kg
Overall Mass Savings	7,321 kg
Composite Qualitative Score	+2

4.2.4.7   Complex Compound Heat Pump

A complex compound heat pump [180] requires a source of high temperature heat to drive its operating cycle. The assumed method within this study uses a collector to focus

---

However, Section 4.2.4.5 assumes power comes from the main PLB power grid while Section 4.2.4.6 assumes power comes from a dedicated solar photovoltaic power array. See also Section 2.2.2.

[179]   Please see Section 4.2.4.5 (Horizontal Radiators) for details supporting these results.

solar radiation on a tube containing a working fluid. This is the method assumed while updating the work of Ewert (1993) for the complex compound heat pump. Ewert also includes systems using the vapor compression heat pump with vertical and horizontal radiators. Because Ewert's work differs from the other heat pump studies presented in this report, his systems are all presented below.

Overall Values:
Radiator Surface Properties:
Emissivity (end-of-life)	0.83
Solar Absorptivity (end-of-life)	0.17
Fin Efficiency	0.85

Radiator Effective Sink Temperature, T_{sink}:
Horizontal Radiator	265 K
Vertical Radiator	317 K

Radiator Mass (dry) per Radiating Area:
Horizontal	7.50 kg/m^2
Vertical	5.63 kg/m^2
Heat Source Mass (dry) per Heat Energy Required [181]	2.4 kg/kW
Total Nominal Cooling Load, Q_C	50 kW
Power Mass Penalty	35.3 kg/kW

	Complex Compound Heat Pump	Vapor Compression Heat Pumps	
Cold Source (minimum ITCS) Temperature [K]	282	275	275
Temperature Lift [K]	78	85	85
Hot Source (radiator) Temperature [K]	360	360	360
Heat Input per Cooling Load [kW$_{heat\ input}$/kW$_{cooling}$]	3.34	--	--
Heat Source Temperature [K]	500	--	--
Peak Power Input per Cooling Load [kW$_{power}$/kW$_{cooling}$]	--	0.667	0.667
Radiator Orientation	vertical	vertical	horizontal
Heat Rejection per Cooling Load by Primary Radiator [kW$_{rejected}$/kW$_{cooling}$]	4.34	1.67	1.67
Heat Pump Mass per Cooling Load [kg/kW$_{cooling}$]	4.7	11.0	11.0

---

[180]   See Section 2.2.3 for additional background material.

[181]   This mass penalty is for a solar collector which will direct solar energy into a working fluid passing through an enclosed channel. This value is "optimistic" and does not include mass for the piping, pumps, pumping power, or working fluid needed to transfer the collected energy to a heat-driven heat pump.

	Complex Compound Heat Pump	Vapor Compression Heat Pumps	
Radiator Orientation	vertical	vertical	horizontal
Heat Rejection per Unit Area [kW/m^2]	0.268	0.268	0.475
Required Radiator Area During the Day [m^2]	810	312	176
Radiator Mass (dry) [kg]	4556	1750	1317
Power as Mass [kg]	--	1177	1177
Heat Pump Mass [kg]	235	550	550
Mass of Solar Collector for Heat Source [kg]	401	--	--
Total Heat Pump System Mass [kg]	5192	3477	3044
For Comparison (from Section 4.2.4.5):			
Total System Mass [kg]		4171	3452
Mass Savings Compared to PLB Baseline [kg]		6297	7017

Based on the system masses given above, a complex compound heat pump using the analytical process from Section 4.2.4.5 would have a total mass of (4171 kg/3477 kg) × 5192 kg, or 6,228 kg. Thus, compared with the mass of the baseline ETCS for PLB of 10,469 kg, the complex compound heat pump will save 4,241 kg.

Specific Assessments:

Overall Mass Savings [182]   4,241 kg

Composite Qualitative Score   +1

4.2.4.8 Zeolite Heat Pump

Zeolite heat pumps also use a heat-driven cycle and require a high-temperature heat source [183]. Ewert (1993) also examined this system. From the perspective of this report, zeolite heat pumps have many of the same attributes as complex compound heat pumps. Therefore, the same overall approach as in the preceding section is employed here. The previous work of Ewert (1993) may be revised for use here for the zeolite heat pump by assuming the high-temperature heat source is supplied using a solar energy focusing collector instead of waste heat from a nuclear power plant. Again, Ewert also includes systems using the vapor compression heat pump with vertical and horizontal radiators. Because Ewert's work differs from the other heat pump studies presented in this report, his systems are all presented below.

Overall Values:

Radiator Surface Properties:
Emissivity (end-of-life)   0.83
Solar Absorptivity (end-of-life)   0.17
Fin Efficiency   0.85

---

[182] Only an overall mass savings is given because this estimate is lacking in detail.

[183] See Section 2.2.4 for additional background details.

Radiator Effective Sink Temperature, T_{sink}:

Horizontal Radiator	265 K
Vertical Radiator	317 K

Radiator Mass (dry) per Radiating Area:

Horizontal	7.50 kg/m^2
Vertical	5.63 kg/m^2
Heat Source Mass (dry) per Heat Energy Required [184]	2.4 kg/kW
Total Nominal Cooling Load, Q_C	50 kW
Power Mass Penalty	35.3 kg/kW

	Zeolite Heat Pump	Vapor Compression Heat Pumps	
Cold Source (minimum ITCS) Temperature [K]	275	275	275
Temperature Lift [K]	85	85	85
Hot Source (radiator) Temperature [K]	360	360	360
Heat Input per Cooling Load [kW$_{heat input}$/kW$_{cooling}$]	2.5	--	--
Heat Source Temperature [K]	700	--	--
Peak Power Input per Cooling Load [kW$_{power}$/kW$_{cooling}$]	--	0.667	0.667
Radiator Orientation	vertical	vertical	horizontal
Heat Rejection per Cooling Load by Primary Radiator [kW$_{rejected}$/kW$_{cooling}$]	3.5	1.67	1.67
Heat Pump Mass per Cooling Load [kg/kW$_{cooling}$]	31.4	11.0	11.0

	Zeolite Heat Pump	Vapor Compression Heat Pumps	
Radiator Orientation	vertical	vertical	horizontal
Heat Rejection per Unit Area [kW/m^2]	0.268	0.268	0.475
Required Radiator Area during the Day [m^2]	652	312	176
Radiator Mass (dry) [kg]	3674	1750	1317
Power as Mass [kg]	--	1177	1177
Heat Pump Mass [kg]	1570	550	550
Mass of Solar Collector for Heat Source [kg]	300	--	--
Total Heat Pump System Mass [kg]	5544	3477	3044
For Comparison (from Section 4.2.4.5):			
Total System Mass [kg]		4171	3452
Mass Savings Compared to PLB Baseline [kg]		6297	7017

Based on the system masses given above, a zeolite heat pump using the analytical process from Section 4.2.4.5 would have a total mass of (4171 kg/3477 kg) × 5544 kg, or 6,651 kg. Compared with the mass of the baseline ETCS for PLB of 10,469 kg, the zeolite heat pump will save 3,818 kg.

---

[184]   This mass penalty is for a solar collector which will direct solar energy into a working fluid passing through an enclosed channel. This value is "optimistic" and does not include mass for the piping, pumps, pumping power, or working fluid needed to transfer the collected energy to a heat-driven heat pump.

Specific Assessments:

Overall Mass Savings [185]   3,818 kg

Composite Qualitative Score   +1

4.2.4.9 Lightweight Radiators

A parametric study may be used to identify potential mass savings by using lighter materials for portions of the PLB radiator assembly. As with FLO Lander, the PLB ETCS is not well defined, so again the components and categories listed here are out of necessity vague.

Category Within Permanent Lunar Base Radiator Assembly [186]	Mass [kg]	Mass Percentage
Structure and Deployment: Base Radiator Support Structure Deployment Mechanism	1041.3 1952.4	30.0
Radiator Panels	6768.4	67.7
Radiator Panel Working Fluid (ammonia)	233.0	2.3
Total	9995.1	100.0

This study varies the component PLB radiator assembly masses linearly based on the original total mass in each category. The structure and deployment masses are reduced by up to 20% when the radiator panel mass is reduced by up to 40%. The radiator panel working fluid volume will be unchanged, so the working fluid mass will be unchanged [187].

The most important underlying assumption is that composites and other advanced materials are most likely to offer significant mass reduction for only some components of the radiator panels such as the honeycomb and the facesheets. Because the radiator panels are the single most massive item of the PLB radiator assembly, such savings would constrain the remainder of the design. A less significant mass reduction is assumed for the structures and deployment because the sizes of these components are primarily dictated by the dimensions of the radiator array and the deployment scheme. However, composites should allow comparable components to replace some of the structure and deployment with lighter parts. In summary, this approach yields an overall ETCS mass reduction of

---

[185] Again, only an overall mass savings is given because this estimate is lacking in detail.

[186] The radiators here will be changed after 7.5 years as in the baseline case. Further, as a worst case, the structure and deployment will be replaced at the same time. Thus, the masses include two sets of radiator panels, two support structures, and two deployment mechanisms. As in the baseline mission, the radiator working fluid will not require replacement. Here the overall mass per radiating area is 7.5 kg/m^2 for the dry radiator panel assembly. The assumed component composition is: 5.2 kg/m^2 for radiator panels, 0.8 kg/m^2 for the base support structure, and 1.5 kg/m^2 for deployment. As presented above, the radiator panel working fluid mass is 0.358 kg/m^2 of radiating area.

[187] See Section 2.4 for additional general background on lightweight radiators plus specific examples of proposed lightweight radiators.

33% for a 40% reduction in the radiator panel mass (Figure 4.17). It is further assumed that, as in the baseline case, PLB will use two sets of radiator panels during the 15 years of the initial project. As a worst case, the radiator support structure and deployment mechanisms will be replaced when the radiator panels are replaced after 7.5 years.

Category Within Permanent Lunar Base Radiator Assembly	Percent Reduction in Radiator Panel Mass	
	20%	40%
Structure and Deployment [kg]	2694.4	2395.0
Radiator Panels [kg]	5414.7	4061.1
Radiator Working Fluid [kg]	233.0	233.0
Overall Radiator Mass [kg]	8342.1	6689.1
Overall Mass Reduction in Radiators [kg]	1653.0	3306.0
Overall Mass Reduction as a Percentage of the Baseline Permanent Lunar Base Radiator Assembly	16.5	33.1
Radiator Mass Per Surface Area [kg/m^2]	12.82	10.28

Considering the available lightweight radiators presented in Section 2.4, an overall mass reduction of 33.1% was selected as a representative value. Thus, the mass savings for PLB is 3306.0 kg for the reference mission. The power requirements will be unchanged because the internal fluid dynamics and, therefore, the pumping power are functions of the working fluid material properties.

Any of the lightweight radiator concepts may be used for a base on the lunar surface. All of the radiators presented in Section 2.4 can be deployed vertically. The vertical radiators will require integration with either a radiator shade or a heat pump to reject life support heat loads at lunar noon away from the polar regions. However, the composite flow-through radiators could also be oriented horizontally like the radiators in the baseline architecture.

Specific Assessments:

Equipment Mass Savings	1,999 kg
Power Savings as Mass	none
Overall Mass Savings	1,999 kg
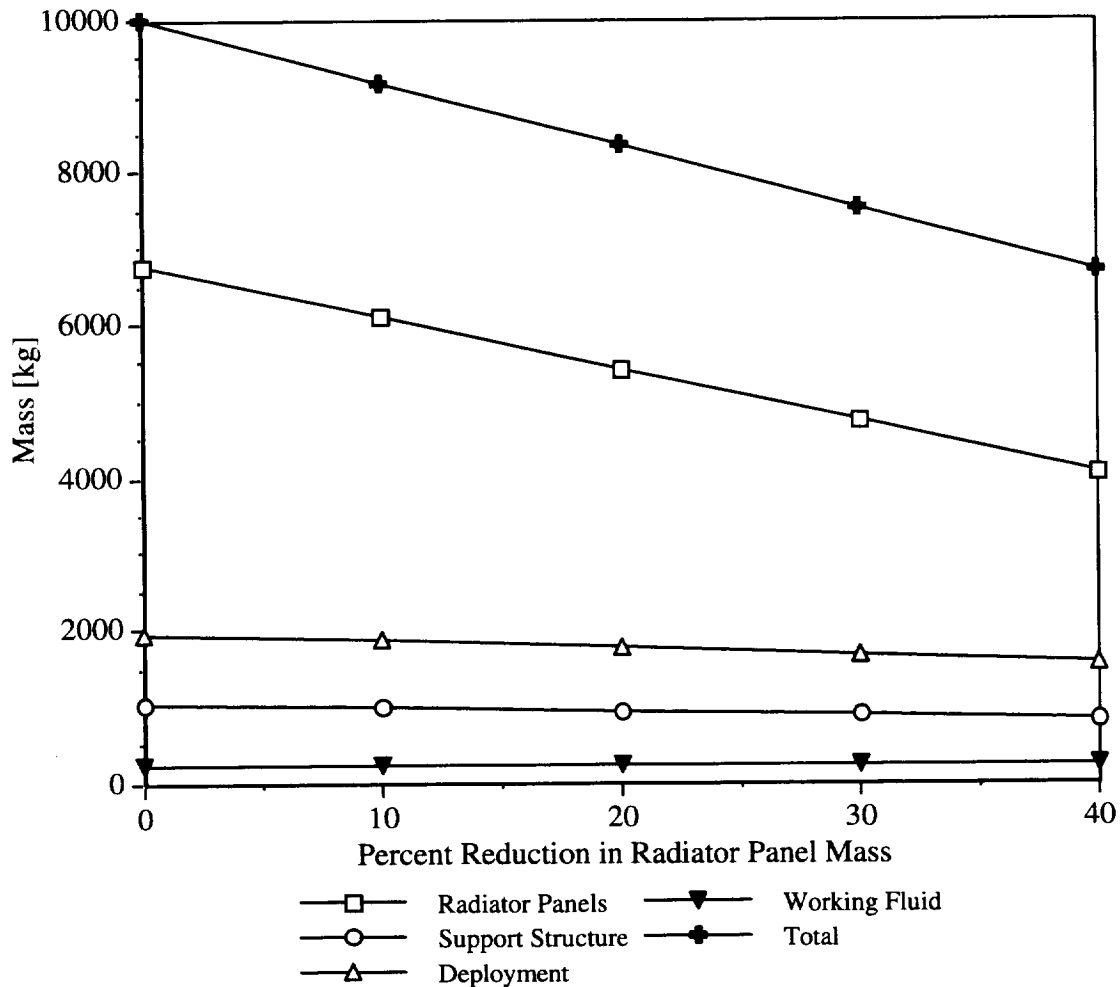
Figure 4.17 Permanent Lunar Base radiator mass as a function of mass reduction within the radiator panel set. Study Assumptions: 1) For each 10% mass reduction in the radiators the masses for the support structure and the deployment decrease by 5%, and 2) Permanent Lunar Base will use two panel sets during the initial 15-year project life.

4.2.4.10 Parabolic Radiator Shade

The parabolic radiator shade [188] is an excellent option for lowering the effective sink temperature that a vertical radiator experiences during lunar noon at an equatorial site [189]. For PLB, the radiator and shade would be deployed on the lunar surface near the buried habitation and laboratory modules. Alignment of the shade and radiator is not difficult because the entire system can be deployed under human supervision. The final system might look something like the lower portion of Figure 4.8 or it might be deployed

---

[188] See Section 2.5.2 for additional background information.

[189] For a vertical radiator with the end-of-life surface properties assumed above for the baseline mission (emissivity of 0.86 and solar absorptivity of 0.14) the effective sink temperature is 319.6 K.

with the radiator panels in a single line. In either case endsheets (not pictured) should be included to prevent infrared surface emissions from impinging on the radiator and to inhibit contamination of the shade by lunar dust.

For the mission using a parabolic radiator shade, a single set of vertical radiators coated with silver Teflon is assumed. However, the shade and its deployment mechanism will be replaced once every five years [190]. Thus, for a parabolic radiator shade at PLB:

Heat Rejected	50.0 kW
Radiator Surface Temperature	275.0 K
Lunar Surface	
Emissivity	0.93
Absorptivity	0.93
Albedo	0.07
Solar Irradiation	1.371 kW/m^2
Incident Angle	90.0°
Orbital Inclination	1.53°
Radiator [191]	
Fin Efficiency	0.85
Infrared Emissivity	0.83
Solar Absorptivity	0.17
Shade (End-of-Life) [192]	
Specular Upper Surface	
Emissivity	0.06
Absorptivity	0.14
Diffuse Lower Surface	
Emissivity	0.90
Absorptivity	0.90
Sink Temperature [193]	195 K

---

[190] The thermal protection value of the shade is highly sensitive to its surface properties. While the actual material and its surface coatings are expected to withstand continuous use for the life of PLB, dust accumulation is a significant concern. It is expected that possible dust accumulation due to human activities near PLB can be anticipated and controlled. However, dust accumulation due to other aspects of the lunar environment are currently unknown. Thus, a relatively high rate of replacement is assumed here for the parabolic shade to ensure its reliability.

[191] The radiator is assumed to have a 15-year service life.

[192] Keller (1995 a). The shade is assumed to have a 5-year service life.

[193] Keller (1995 a) computed a sink temperature of 188.8 K for a vertical radiator with a surface emissivity of 0.86 and a solar absorptivity of 0.14 using TSS.

Radiator (with silver Teflon)

Area	292.5 m^2
Mass Penalty	5.63 kg/m^2
Total Dry Radiator Panel Mass (one set)	1645.3 kg
Dimensions	
Height	1.0 m
Length	146.3 m
Working Fluid Mass Penalty	0.269 kg/m^2
Working Fluid Mass	78.7 kg

Shade

Parabolic Arc Length [194]	4.59 m
Length	146.3 m
Area	671.5 m^2
Mass Penalty [195]	0.56 kg/m^2
Mass (per parabolic radiator shade)	376.0 kg
Shades per Project Life	3
Total Shade Mass	1128.0 kg
Total System Mass [196]	2852.0 kg

Comparing the radiator and flexible parabolic shade with the baseline mission presented above yields:

Mass Gained by Using a Parabolic Radiator Shade	Baseline PLB TCS	PLB TCS With Shade	Total Change
Radiator Area [m^2]	650.8	292.5	
Radiator Mass per Panel Set [kg]	4881.1	1645.3	
Panel Sets for Life of PLB	2	1	
Total Dry Radiator Mass [kg]	9765.2	1645.3	-8119.9
Radiator Pressure Drop [kN/m^2]	242.0	108.8	
Radiator Pumping Power [kW]	1.629	0.733	
Radiator Pumping Power Mass [kg]	471.0	200.8	-270.2
Radiator Working Fluid [kg]	233.0	78.7	-154.3
Shade Area [m^2]	--	671.5	
Shade Mass per Shade [kg]	--	376.0	
Number of Shades for Life of PLB		3	
Total Shade Mass [kg]	--	1128.0	+1128.0
Total Mass [kg]	10469.2	3052.8	-7416.4

---

[194] A full parabolic shade is assumed. In other words, the shade top is even with the radiator top and the shade focus is at the height of the radiator.

[195] This penalty includes mass for a flexible parabolic shade plus appropriate support structure (Keller, 1994).

[196] This value includes mass for one set of radiator panels and three parabolic radiator shades plus one charge of working fluid. Masses for piping, fittings, and working fluid to and from the radiators are not included. The pumping power mass is also omitted from this value.

The overall savings for using a parabolic radiator shade is 7,416.4 kg. Because PLB is a longer mission, the issue of dust accumulation on the radiator shade, which degrades the shade's effectiveness, is a significant concern. Further research in this area should indicate how to maintain a parabolic shade on the lunar surface for extended missions. Several ideas to either decontaminate or guard the shade are under consideration (Keller, 1995 b).

Specific Assessments:

Equipment Mass Savings	7,146 kg
Power Savings	0.896 kW
Power Savings as Mass	270 kg
Overall Mass Savings	7,416 kg
Composite Qualitative Score	-1

4.2.4.11 Plant Chamber Cooling Improvements

Regenerative life support systems are of great importance as an enabling technology for extended-duration missions with crews. In particular, plant growth chambers promise to provide future space explorers with both food and air revitalization. Therefore, a plant growth module will be included in PLB. The practical aspect of this system then becomes optimizing the biomass (food) produced by a plant growth module as a function of system mass. The baseline plant growth module is in Section 2.6.2 which provides details for a unit based on half of the Johnson Space Center Variable Pressure Growth Chamber.

Several design changes are expected to reduce the mass of the plant module over its baseline configuration. Further, each design change is assumed to be completely independent of any other design change. As such, the savings for all options here are assumed to be cumulative. Figure 2.10 provides a general illustration of a portion of the plant growth chamber.

1) Heaters: With proper management of the air stream dehumidification process, it should be possible to completely eliminate any reheat. The mass of the heaters (36.5 kg total) plus the associated power (3.0 kW which is 2250.0 kg as mass) may be eliminated.

Total Savings: 2,286.5 kg

2) Ducting and Vents: The current ducting and vents, which are fabricated of metal, have a mass of 125.7 kg. Using lighter materials, such as plastic and composites, it is estimated that this mass may be cut in half.

Total Savings: 62.9 kg

3) Lightbox Barriers: The baseline lightbox barriers between the plant growth lamps and the plants are tempered glass (4.76 mm thick) and have a total mass of 63.8 kg. The glass barriers can be replaced with Teflon FEP fluorocarbon film (0.127 mm thick)

which removes approximately all of the mass associated with the lightbox barriers (Ewert, Paul, and Barta, 1995).   Total Savings: 63.8 kg

4)   Coldplate Lamp Cooling: A more efficient method of removing heat generated by plant growth lamps from the plant chamber is to mount the lamps on coldplates. It is assumed that 40% of the lighting heat energy can be removed by the coldplates. Thus, this energy will not reach the plant chamber atmosphere. To maintain the same temperature distribution across the plant chamber, 40% less volumetric flowrate of air is required which corresponds to a 40% savings in blower power. This corresponds to a savings of 570 kg (1.9 kW × 0.4 × 750 kg/kW). The coldplates have a mass of 41.9 kg each or 167.6 kg total (four coldplates are required).

Total Savings: 402.4 kg

5)   Ballasts: The lamp ballasts have a total mass of 103.4 kg. Using lighter materials it is assumed that this mass may be cut in half.

Total Savings: 51.7 kg

The overall savings for all of these options is 2,867.3 kg.

Specific Assessments:	
Equipment Mass Savings	47 kg
Power Savings	3.76 kW
Power Savings as Mass	2,820 kg
Overall Mass Savings	2,867 kg
Composite Qualitative Score	+1

4.2.4.12 Carbon Brush Heat Exchanger

It is assumed that the baseline design for PLB will include DDCUs affixed to coldplates transferring heat to the ETCS working fluid using radiant fin interfaces. As presented above, radiant fin interfaces are the current standard for power converter units aboard ISS. Here the same dimensions and masses are assumed for the coldplates associated with the converter units for PLB. Replacement of the coldplates and the coldplate sockets is again the reference mission for this technology. According to Hughes (1995), a representative power grid for PLB will use twelve DDCUs, three main bus switching units (MBSU), and three dc switching units (DCSU). While these latter two units are functionally different from DDCUs, they are power conditioning devices which depend on the same coldplate/radiant-fin structure used by the DDCUs for proper cooling. Thus, it is assumed here that the MBSUs and DCSUs will use the same coldplate design as

the DDCUs, and that this coldplate design is equivalent to an external DDCU (DDCU-E) coldplate design designated for ISS units [197].

In order to save mass and improve DDCU cooling efficiency, the radiant fin interfaces could be replaced by carbon brush interfaces. The equipment mass savings assuming 18 equivalent DDCU coldplate fin masses are replaced is:

Power Conversion and/or Conditioning Coldplate	Quantity	Coldplate Mass [kg]	Fin Mass (each coldplate) [kg]	Total Mass Savings [kg]
DDCU	12	63.5	4.29	102.96
MBSU	3	63.5	4.29	25.74
DCSU	3	63.5	4.29	25.74

The total mass savings is twice the fin mass to account for the corresponding fin set on the coldplate socket on which the DDCU sits. Aluminum 6061-T6 is the assumed coldplate material with a density of 2,713 kg/m^3. Further, while it is assumed that the carbon brush heat exchangers will have negligible mass, the rest of the baseplate and coldplate mass will remain unchanged.

Specific Assessments:

Equipment Mass Savings	154 kg
Power Savings as Mass	none directly
Overall Mass Savings	154 kg
Composite Qualitative Score	+3

4.2.5 Summary

The various advanced technologies and their estimated benefits are summarized in the table below for PLB. From Section 4.2.2, the mass of the baseline ETCS is 10,948.3 kg. Assuming the mass determinations throughout this study have associated uncertainties on the order of 10%, a complete TCS with an advanced technology would need to show a savings of at least 1,095 kg to ensure a mass savings. Further, because design and development costs are not trivial, a mass savings of 25%, or 2,737 kg, is desirable. Using these criteria, the TCSs with advanced technologies proposed for PLB may be divided into five categories:

- TCSs using advanced technologies requiring a mass penalty greater than 10% of the overall baseline ETCS mass: none.

- TCSs using advanced technologies requiring a mass penalty less than 10% of the overall baseline ETCS mass: none.

---

[197] See Section 2.6.3 for details of the radiant fin design. These assumptions, though simple, should give reasonable estimates of the fin mass for power conversion and conditioning unit coldplates if the units are mounted externally. The DDCU-E from ISS was selected because this unit's intended usage most nearly reflects the mission for which the units here are envisioned. Further, the DDCU-E is the most numerous DDCU on ISS.

- TCSs using advanced technologies with a mass savings less than 10% of the overall baseline ETCS mass: two-phase TCS with MP/S, LP two-phase TCS, and capillary pumped loops.

- TCSs using advanced technologies with a mass savings between 10 and 25% of the overall baseline ETCS mass: none.

- TCSs using advanced technologies with a mass savings greater than 25% of the overall baseline ETCS mass: vapor compression heat pump, solar vapor compression heat pump, complex compound heat pump, zeolite heat pump, lightweight radiators, and parabolic radiator shade.

Overall, the baseline PLB ETCS is massive and unwieldy though it uses familiar and dependable technology. As such, most of the advanced technologies considered provide a significant mass savings compared to the baseline ETCS. The technology in the third category will produce an ETCS which is comparable to the baseline system. This category includes the two-phase TCSs. The technologies in the final category show significant promise. These include the various heat pumps, the parabolic radiator shade, and lightweight radiators. Within this category, the two vapor compression heat pumps and the parabolic radiator shade offer the greatest mass savings at roughly 65%. The two heat pumps using heat-driven cycles fall into a second tier with mass savings around 40%.

Several technologies addressed for PLB are enhancing technologies. As before, enhancing technologies are advanced technologies which will uniformly deliver a mass savings or penalty for a specified reference mission regardless of the type of TCS selected. These technologies include plant chamber cooling improvements and the carbon brush heat exchanger. Thus:

- Enhancing technologies which require a mass penalty: none.

- Enhancing technologies which yield a mass savings: plant chamber cooling improvements and carbon brush heat exchanger.

Table 4.6 Advanced Active Thermal Control System Architecture
for Permanent Lunar Base

Summary of Advanced Active Thermal Control System Architecture for Permanent Lunar Base	Overall Mass Savings [kg]	Qualitative Score
4.2.4.1 Two-Phase Thermal Control System With Mechanical Pump/Separator	456	0
4.2.4.2 Low-Power Two-Phase Thermal Control System	751	-1
4.2.4.3 Two-Phase Thermal Control System With Electrohydrodynamic Pumping	unknown	+2
4.2.4.4 Capillary Pumped Loops	917	0
4.2.4.5 Vapor Compression Heat Pump [198]	7,017	+2
4.2.4.6 Solar Vapor Compression Heat Pump	7,321	+2
4.2.4.7 Complex Compound Heat Pump	4,241	+1
4.2.4.8 Zeolite Heat Pump	3,818	+1
4.2.4.9 Lightweight Radiators	3,306	--
4.2.4.10 Parabolic Radiator Shade	7,416	-1
4.2.4.11 Plant Chamber Cooling Improvements	2,867	+1
4.2.4.12 Carbon Brush Heat Exchanger	154	+3

---

[198] The value here is for a configuration with horizontal radiators. A configuration using vertical radiators saves 6297 kg.

4.3   MARS LANDER (ML)

4.3.1   Reference Mission

Mars is, like Luna, a planetary body of extremes. Surface temperatures vary between 130 K at the height of the martian winter to 300 K during the martian summer (Reich and Scoon, 1993). The planetary inclination is similar to Earth's at 24.8 degrees. Further, the martian days correspond to 24.66 hours. However, unlike Earth, the martian orbit is much more elliptical. At its warmest, during summer in the southern hemisphere, Mars is 1.381 astronomical units [AU] from the Sun. During the much cooler Northern summer, Mars reaches 1.666 AU from the Sun (Dzenitis, 1992). Additionally, Mars has a thin, yet significant, atmosphere comprised of 96% carbon dioxide and 3% nitrogen. Atmospheric pressures vary between 600 and 1000 N/m^2 (Dzenitis, 1992). As such, Mars can support wind velocities up to 30 m/s which permit huge dust storms to spread over the entire planetary surface during the southern summer (Reich and Scoon, 1993).

For an initial human exploration of Mars a current design philosophy is to use an expendable craft which, like Apollo, is comprised of a crew transport vehicle and a landing vehicle. The crew transport vehicle would house the mission personnel while in transit from Earth orbit to an orbit around Mars. An aero-braking maneuver would be used to decelerate from interplanetary speeds into a stable martian orbit. The crew would then descend to an equatorial site on the martian surface in a landing vehicle, Mars Lander (ML). After a 30-day stay, the crew would return to the crew transport vehicle and return to Earth. A capsule with an independent heat shield would allow the crew to return directly to the Earth's surface following an interplanetary voyage from Mars.

This study concentrates on ML while it is situated on the martian surface. The transport of ML to the martian surface is not considered, nor is the crew transit vehicle considered. The ML itself will have both habitation and laboratory space for a crew of four. The overall architecture will probably be similar to FLO Lander except that this vehicle is not necessarily expected to fit entirely within a standard 10-m launch shroud. In fact, the combined Mars expedition vehicle will probably be assembled in Earth orbit. The ML ATCS will be designed to effectively reject a nominal load of 30 kW regardless of environmental conditions at an equatorial landing site. The assumed continuous power mass penalty is 111 kg/kW while the "daytime" only power mass penalty is 25 kg/kW. These power mass penalties are not currently attainable and assume some improvements in power systems [199]. One mission is assumed.

4.3.2   Baseline Case

The baseline ML ETCS uses low solar absorptivity, vertical radiators with single-phase liquid ammonia as the working fluid. For redundancy, three ETCS loops are provided. Each loop will service two module zones in cascade. Physically, each zone may be an individual module or a single module may be subdivided into more than one zone. Each loop will be sized to handle half of the total nominal heat load, 15 kW, so as to

---

[199]   For purposes of comparison, the power mass penalties assumed for PLB are based on current technology or anticipated technology from current research.

provide complete capacity even after one fault. The TCS utilizes a single-phase cascade similar to the TCS for ISS. Each ETCS loop functions as both low temperature and moderate temperature service in series. In short, those areas requiring the lowest temperature cooling are placed upstream of those items with higher temperature needs. Radiator bypass valves provide ETCS loop set-point temperature control. Further, each ML zone has two ITCS loops using liquid water as the working fluid. Additional fittings will allow either ITCS loop to service all of ML's coldplates and heat exchangers. This arrangement provides extra flexibility if any one of the ITCS or ETCS loops fail. Each ETCS loop also has a dedicated pump module (Figure 4.18).

The overall base ATCS heat load is 30 kW. A value of 7.50 kg/m^2 is assumed for the radiator mass per radiating area for horizontal radiators. Vertical radiators are assumed to use 5.625 kg/m^2 [200]. The ML will land at the martian equator which has surface temperatures ranging from 185 K to 190 K at night to 220 K to 260 K during the day (Reich and Scoon, 1993). The solar irradiation at noon varies between 0.493 kW/m^2 at aphelion to 0.718 kW/m^2 at perihelion. The martian surface has the properties of a diffuse gray surface with an emissivity of 0.90 to 0.98 (Dzenitis, 1992).

- Overall ETCS Performance:

Heat Rejected	30.0 kW
ETCS Working Fluid	single-phase ammonia

- Low Solar Absorptivity, Vertical Radiators [201]:

Surface Emissivity	0.8
Solar Absorptivity	0.2
Fin Efficiency	0.85
Average Radiator Surface Temperature	275.0 K
Heat Rejection per Area (worst/design case)	0.10 kW/m^2
Radiator Surface Area	352.94 m^2
Mass Penalty for Dry Radiators [202]	5.625 kg/m^2
Radiator Panel Mass	1985.3 kg
Radiator Working Fluid Mass Penalty [203]	0.269 kg/m^2
Radiator Working Fluid Mass	94.9 kg
Total Radiator Mass (wet) [204]	2080.2 kg

---

[200] These radiator masses are identical to those assumed for PLB. They are not as frugal as the values used for a similar vehicle, FLO Lander, but rather reflect a desire to include more robustness.

[201] The radiators were sized based on the parametric study given in Section 4.3.3 below.

[202] This mass penalty includes structure and deployment mass as well as actual radiator panel mass.

[203] This mass penalty estimate is based on data for the working fluid mass used in the ISS radiator ORUs as a function of radiating area.

[204] A comparable horizontal radiator design, based on heat rejection during a dust storm, has 392.59 m^2 of radiating area, with a mass of 2944.4 kg for the radiator plus 140.6 kg for the working fluid.

Two-Sided, Vertical Radiator
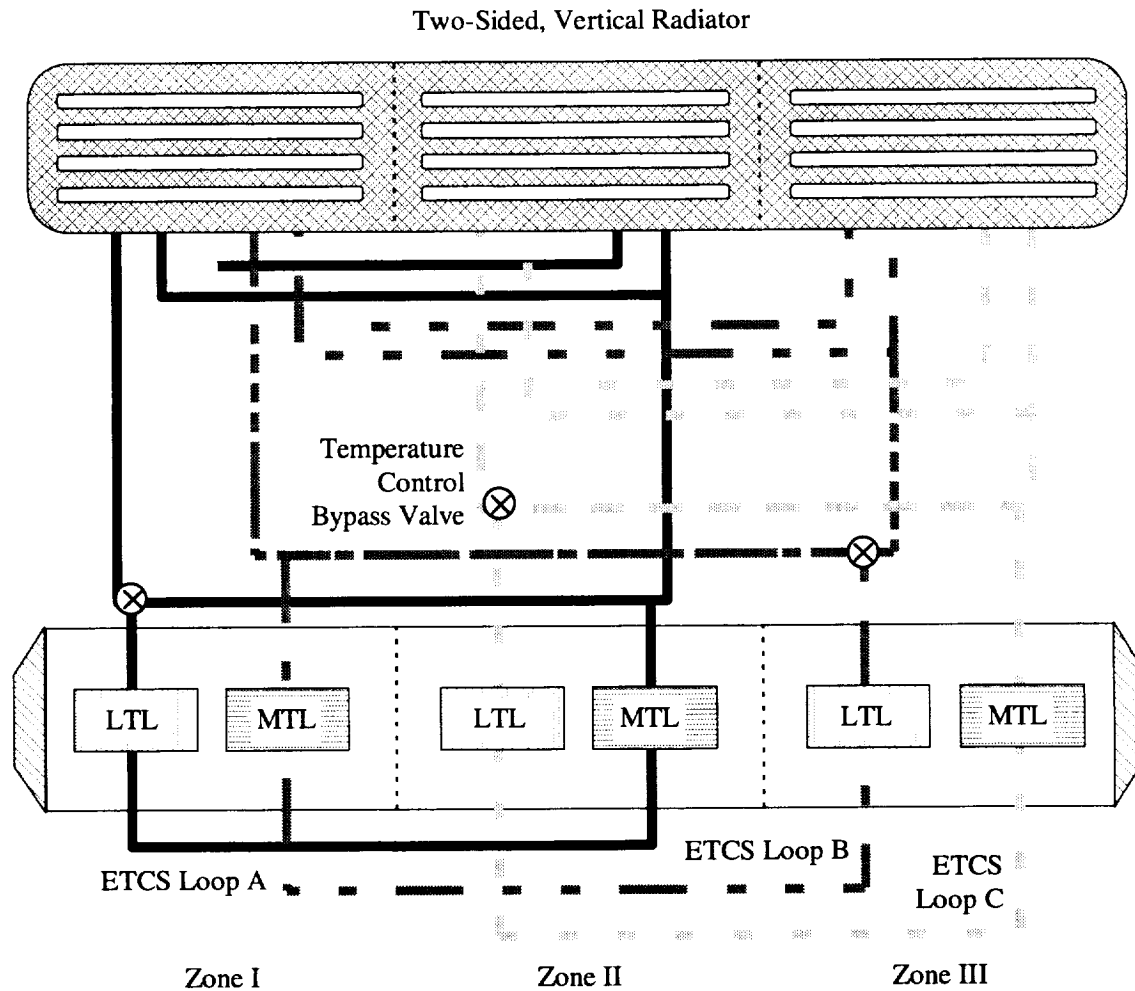
Figure 4.18 Plumbing for the baseline Mars Lander external thermal control system. LTL is low temperature loop and MTL is moderate temperature loop. The system uses three external thermal control system loops to give two-fault tolerance with single-phase liquid ammonia as the working fluid. The bypass valves allow for temperature control. Overall, both the radiator and the volume occupied by the crew are subdivided into three cooling zones. Each zone may correspond to a separate physical device, such as a module, or one larger device may be subdivided. Each cooling zone has two water internal thermal control system loops which are internally interconnected so that any heat load can be serviced by either loop. A pump module is assumed for each loop.

- ETCS Working Fluid Loop Mass Flowrates:

Average ETCS Fluid Temperature	278.0 K
Radiator Outlet Temperature	274.82 K
Radiator Inlet Temperature	281.18 K
Average Ammonia Specific Heat	4.62 (kW*s)/(kg*K)

Total Mass Flowrate
(full load/equal d :ribution)   1.021 kg/s
Nominal Flowrate per Loop
(full load/equal distribution)   0.340 kg/s
Maximum Flowrate per Loop   0.510 kg/s

• ETCS Pump Module:

Pump Efficiency   0.45
Average Ammonia Density   631.96 kg/m^3
Radiator Pressure Drop per Radiating Area [205]   0.3718 kN/m^4
Radiator Pressure Drop   131.2 kN/m^2
Pumping Power for Radiators   0.471 kW
Assumed Effective Line Length per Loop   40 m
Number of ETCS Loops   3
Line Diameter [206]   0.0236 m
Nominal Pressure Drop Line (per loop)   14.58 kN/m^2
Nominal Line Pumping Power (per loop)   0.0174 kW
Overall Pumping Power   0.523 kW
Continuous Power Mass Penalty   111 kg/kW
Pumping Power as Mass   58.1 kg
Mass of Ammonia in Lines   33.2 kg

• Summary of the Mars Lander Active Thermal Control System:

Heat Load Rejected   30.0 kW
Radiator Mass (dry)   1985.3 kg
Working Fluid Mass   128.1 kg
Pumping Power   0.523 kW
Pumping Power as Mass   58.1 kg

Total ETCS Heat-Rejection System Mass [207]   2171.5 kg

The baseline radiator mass per area, including fluids, is 5.89 kg/m^2.

4.3.3   Parametric Study Using the Baseline Case

Dzenitis (1992) presents a package of models for heat transfer with the martian environment. For the study here, the ML radiators were sized considering only radiation. The radiation case is, assuming no wind, a worst-case scenario because any wind will provide some convection cooling which will in turn lower the effective environmental temperature and aid heat rejection by the radiator. Further, as found by Dzenitis (1992),

---

[205]   This penalty is based on the values for ISS which specifies a maximum radiator pressure drop of 48.26 kN/m^2 for 129.8 m^2 of radiating area.

[206]   This the inside diameter of the ETCS lines within ISS modules. Specifically this value is 0.93 in.

[207]   This value does not include masses for the pumps, lines, and fittings, but these are expected to be roughly the same for all ML ATCS configurations.

convection cooling is expected to only account for about 10% of the heat rejected by a radiator in a fairly strong martian surface wind of 10 m/s. Thus, heat rejection from human spacecraft on Mars will primarily be by radiant heat transfer.

Dzenitis (1992) divides the irradiation in a martian environment for any flat surface into solar fluxes and infrared fluxes. This model, from Section 2.0 of Dzenitis (1992), was implemented, with the exception of Equation (2.18) [208], in a spreadsheet program. Heat rejection results for both vertical and horizontal surfaces were obtained for a typical "hot" equatorial site [209]. Data for this study come primarily from Dzenitis (1992) and Reich and Scoon (1993). Specifically:

Surface and Orbital Location:

Orbital Position, L_S [210]	270 degrees
Surface Latitude, λ	0 degrees

Time:

Local Midnight	-6.16 hours
Local Sunrise, t_{sr} (also assumed as t_c)	0.00 hours
Local Noon, t_{noon}	6.16 hours
Time of Local High Temperature, t_h	7.19 hours
Local Sunset, t_{ss}	12.33 hours
Length of Local Day, t_{day}	24.66 hours

Local Environmental Parameters Under Clear Skies (optical depth, τ, of 0.1):

Solar Absorptivity of Martian Surface, α_G	0.7
Infrared Emissivity of Martian Surface, ε_G	0.94
Average Surface Temperature, $\overline{T}_G$	225 K
Diurnal Surface Temperature Variation, ΔT_G	70 K
Infrared Emissivity of Martian Atmosphere, ε_A	0.225
Average Atmospheric Temperature, $\overline{T}_A$	205 K
Diurnal Atmospheric Temperature Variation, ΔT_A	6.05 K

---

[208] Equation (2.18) is a correction for the optical depth of the atmosphere when the surface of interest is not horizontal to the mean horizon. This effect, when included in the model, gives questionable results for vertical surfaces, something Dzenitis noted in his paper. While the effective optical depth for a vertical surface may differ from that of a horizontal surface, this adjustment should probably be omitted until more work in this area can be completed.

[209] Environmentally, the hottest site on Mars is located 40 degrees south of the equator during summer in the southern hemisphere. This corresponds to the time when the most severe dust storms form beginning within the southern hemisphere (Reich and Scoon, 1993).

[210] The variables listed in this section correspond to the nomenclature employed by Dzenitis (1992).

Local Environmental Parameters in a Dust Storm (optical depth, τ, of 2.8 [211]):

Solar Absorptivity of Martian Surface, α_G	0.7
Infrared Emissivity of Martian Surface, ε_G	0.94
Average Surface Temperature, $\overline{T}_G$	220 K
Diurnal Surface Temperature Variation, ΔT_G	30.25 K
Infrared Emissivity of Martian Atmosphere, ε_A	0.83
Average Atmospheric Temperature, $\overline{T}_A$	219 K
Diurnal Atmospheric Temperature Variation, ΔT_A	25.93 K

Radiator Properties:

Surface Infrared Emissivity	0.8
Surface Solar Absorptivity	0.2
Average Surface Temperature	275 K

Here two types of radiators are examined. The first is a single-sided, horizontal unit mounted on top of ML similar to the radiator for FLO Lander. The second is a two-sided, vertical unit which is also assumed to be mounted on top of ML. Table 4.7 and Table 4.8 below present the radiator heat fluxes as a function of time for a typical clear or dusty day at a hot equatorial landing site.

Table 4.7 Daytime Heat Rejection From Mars Lander Radiators
for an Equatorial Site on a Clear Day ($\tau = 0.1$)

Time of Day [hours]	Horizontal Radiator [kW/m^2]	Vertical Radiator Facing North/South [kW/m^2]	Vertical Radiator Facing East/West [kW/m^2]
0.00 (Sunrise)	0.2424	0.2231	0.2231
1.23	0.2074	0.1907	0.1693
2.47	0.1712	0.1710	0.1530
3.70	0.1429	0.1491	0.1423
4.93	0.1246	0.1259	0.1344
(Noon) 6.16	0.1181	0.1082	0.1341
7.40	0.1241	0.1042	0.1127
8.63	0.1419	0.1091	0.1023
9.86	0.1697	0.1189	0.1009
11.10	0.2057	0.1350	0.1136
12.33 (Sunset)	0.2407	0.1719	0.1719
Minimum Rejection	0.1181	0.1042	0.1009

---

[211] Reich and Scoon (1993) note that the most severe dust storm observed at a Viking landing site corresponded to an optical thickness of roughly 3.0. Pollack, Colburn, Flasar, Kahn, Carlston, and Pidek (1979) list the landing sites for both Viking spacecraft. Viking Lander 1 is at 22.3 degrees north latitude and 47.9 degrees west longitude, while Viking Lander 2 is at 47.7 degrees north latitude and 225.7 degrees west longitude.

Table 4.8 Daytime Heat Rejection From Mars Lander Radiators
for an Equatorial Site During a Dust Storm ($\tau = 2.8$)

Time of Day [hours]	Horizontal Radiator [kW/m^2]	Vertical Radiator Facing North/South [kW/m^2]	Vertical Radiator Facing East/West [kW/m^2]
0.00 (Sunrise)	0.1916	0.1879	0.1879
1.23	0.1788	0.1784	0.1784
2.47	0.1568	0.1606	0.1605
3.70	0.1283	0.1373	0.1371
4.93	0.1044	0.1167	0.1170
(Noon) 6.16	0.0899	0.1033	0.1046
7.40	0.0939	0.1042	0.1046
8.63	0.1077	0.1129	0.1127
9.86	0.1278	0.1266	0.1265
11.10	0.1457	0.1398	0.1398
12.33 (Sunset)	0.1598	0.1509	0.1509
Minimum Rejection	0.0899	0.1033	0.1046

The fluxes for the vertical radiator facing north and south are the average of values for a single surface facing north and a second surface facing south. Likewise the fluxes for the vertical radiator facing east and west are the average of values for a single surface facing east and a second surface facing west.

The performance of the horizontal radiator has several noteworthy features. In both environments the horizontal radiator is least effective at rejecting heat at local noon, which corresponds to the greatest direct solar irradiation load. Further, the horizontal radiator rejected less heat when the direct solar load was mostly blocked by a severe dust storm. This reduced performance results from receiving a much higher infrared irradiation from the atmosphere which, while filled with dust, absorbs a greater percentage of the direct solar irradiation and then reradiates the energy as infrared radiation. Because the radiator's surface coatings are designed to most readily transfer heat in the infrared range, the radiator's heat-rejection capability degrades during a dust storm [212].

Vertical radiators displayed a variety of results. Because of ML's position on the equator during summer in the southern hemisphere, a surface facing north never receives any direct solar irradiation while a surface facing south receives direct solar irradiation while the Sun is up. A surface facing east receives direct solar irradiation before local noon, and a surface facing west receives direct solar irradiation after local noon. The local high temperature occurs shortly after local noon. This time is assumed in this study to correspond to 1/24th of a day after local noon. As the results above indicate, a vertical radiator will reject at least 0.1 kW/m^2 regardless of the radiator's orientation. The radiator facing north and south was more effective on a clear day, while the radiator facing east

---

212 Another explanation is that the dust storm blocks a radiator's view of its coldest sink, space. As such, the radiator's performance decreases.

and west was slightly more effective during a dust storm. From the individual surface results (not presented), the heat rejection for a radiator surface not receiving direct solar irradiation degraded during a dust storm because of an increase in atmospheric infrared irradiation. However, this degradation was partially offset by an increase in heat rejection during a dust storm for surfaces normally exposed to higher levels of direct solar irradiation. The dust storm acted as a shield against the Sun, especially for radiators facing east and west which normally view both the early morning and late evening sunlight.

The variation in performance between the vertical and horizontal radiators arises from the difference in the effective view factor for each surface. The horizontal radiator views only sky, so its performance is especially susceptible to variations in the atmospheric infrared irradiation level. However, half of the view of the vertical radiator is the martian surface, which has a more constant infrared irradiation flux. Further, the infrared flux of the ground actually decreases during a dust storm because the maximum surface temperature is not quite as great (Reich and Scoon, 1993).

The radiator performance as a function of surface radiator temperature was also investigated. The results are presented in tabular form in Table 4.9 through Table 4.12, and graphically in Figure 4.19 and Figure 4.20. The first figure presents radiator area as a function of orientation and radiator surface temperature. The second figure presents the dry radiator mass as a function of the radiator orientation and radiator surface temperature. The assumed fin efficiency for this study is 1.00.

Table 4.9 Required Daytime Radiator Area
for an Equatorial Site on a Clear Day ($\tau = 0.1$)

Radiator Surface Temperature [K]	Horizontal Radiator [m²]	Vertical Radiator Facing North/South [m²]	Vertical Radiator Facing East/West [m²]
265.0	364.1	438.4	460.4
267.5	329.8	389.6	406.9
270.0	300.7	349.7	363.5
272.5	275.7	316.3	327.6
275.0	254.0	288.0	297.4
277.5	235.0	263.8	271.6
280.0	218.2	242.8	249.4
282.5	203.3	224.5	230.1
285.0	189.9	208.3	213.2

The required radiator area is a strong function of the radiator surface temperature for the range of temperatures normally associated with the rejection of metabolic heat. For a radiator facing east and west in a dust storm, the required radiator area decreases by 44% if the radiator temperature increases from 265 K to 275 K. Increasing the temperature from 275 K to 285 K decreases the required radiator area by a third for the same radiator orientation. Henson (1995) provides similar results.
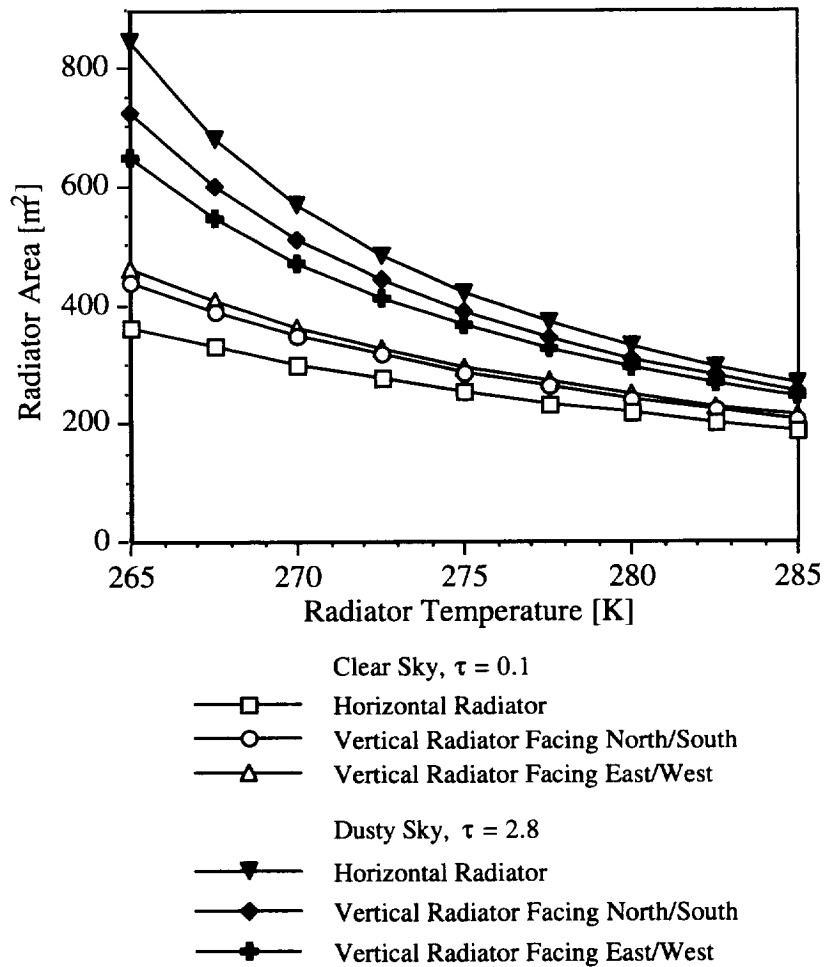
Figure 4.19 Mars Lander radiator area as a function of radiator surface temperature for various radiator orientations and environmental conditions. The assumed fin efficiency is 1.00 for these results.

**Table 4.10 Daytime Dry Radiator Mass
for an Equatorial Site on a Clear Day ($\tau = 0.1$)**

Radiator Surface Temperature [K]	Horizontal Radiator [kg]	Vertical Radiator Facing North/South [kg]	Vertical Radiator Facing East/West [kg]
265.0	2730.8	2465.9	2589.6
267.5	2473.7	2191.7	2288.9
270.0	2255.4	1966.8	2044.7
272.5	2067.8	1779.1	1842.6
275.0	1904.9	1620.1	1672.6
277.5	1762.2	1483.9	1527.8
280.0	1636.3	1365.9	1403.0
282.5	1524.4	1262.8	1294.4
285.0	1424.4	1171.9	1199.1
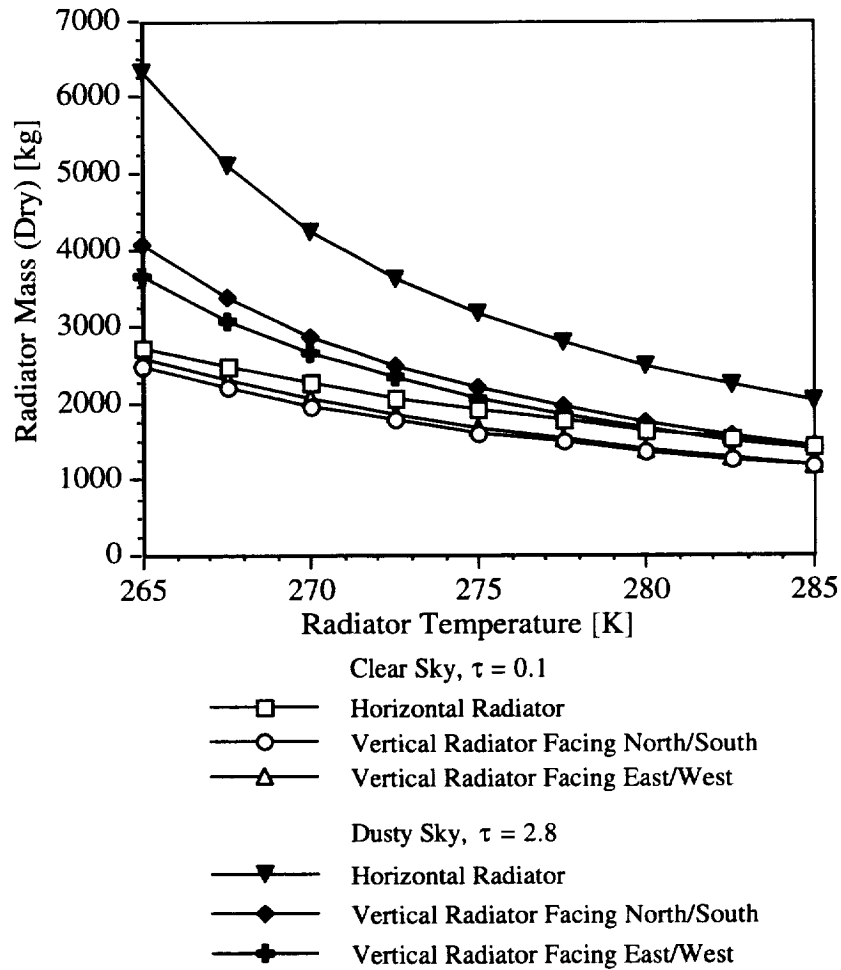
Figure 4.20 Mars Lander dry radiator mass as a function of radiator surface temperature for various radiator orientations and environmental conditions. The assumed fin efficiency is 1.00 for these results. The horizontal radiator uses a mass penalty of 7.50 kg/m^2 while the vertical radiators use a penalty of 5.625 kg/m^2.

Table 4.11 Required Daytime Radiator Area
for an Equatorial Site During a Dust Storm (τ = 2.8)

Radiator Surface Temperature [K]	Horizontal Radiator [m²]	Vertical Radiator Facing North/South [m²]	Vertical Radiator Facing East/West [m²]
265.0	843.4	724.6	647.8
267.5	679.8	600.5	546.7
270.0	566.7	510.5	471.1
272.5	483.9	442.4	412.5
275.0	420.8	389.0	365.7
277.5	371.0	346.1	327.5
280.0	330.8	310.8	295.8
282.5	297.7	281.4	269.0
285.0	269.9	256.5	246.1

Table 4.12 Daytime Dry Radiator Mass
for an Equatorial Site During a Dust Storm (τ = 2.8)

Radiator Surface Temperature [K]	Horizontal Radiator [kg]	Vertical Radiator Facing North/South [kg]	Vertical Radiator Facing East/West [kg]
265.0	6325.1	4076.1	3643.7
267.5	5098.1	3377.6	3075.2
270.0	4250.2	2871.5	2650.0
272.5	3629.5	2488.2	2320.2
275.0	3155.8	2188.0	2057.0
277.5	2782.6	1946.6	1842.2
280.0	2481.1	1748.5	1663.8
282.5	2232.7	1583.0	1513.2
285.0	2024.5	1442.7	1384.6

4.3.4　Advanced ATCS Architecture for Mars Lander

ML is designed for a single 30-day stay on the martian surface at an equatorial site. The baseline mission assumes a vertical, double-sided radiator with single-phase ammonia as the working fluid. Each advanced architecture is, where applicable, assessed numerically for the overall mass savings when compared with the baseline design. Qualitative assessments for these advanced technologies are presented in Section 2.0.

4.3.4.1　Low-Power Two-Phase Thermal Control System

To size a LP two-phase TCS [213] for ML this study extrapolates predictions from Ungar (1995) which is based on work for space stations. Ungar (1995) includes a small space station which, of the cases presented, is closest in size to the TCS for ML. Ungar's small station with a single-phase cascade TCS compares well with the baseline TCS for ML. Ungar (1995) also presents a comparable LP two-phase TCS for the small station.

---

[213]　See Section 2.1.2 for additional material on LP two-phase TCSs.

	ML Baseline TCS (1 loop)	Total ML Baseline TCS	Small Space Station (Ungar, 1995)			
			Single-Phase Cascade Thermal Control System		Low-Power Two-Phase Thermal Control System	
			LTL	LTL	LTL	MTL
Pump Power [kW]	0.174	0.523	0.320	0.320	0.068	0.080
Radiator Area [m²]	117.6	352.9	197	197	195	195
Loop Set-Point [K]	274.8	274.8	275.2	275.2	275.2	287.2

LTL refers to the low temperature loop while MTL refers to the moderate temperature loop. The baseline TCS for ML uses three single-phase cascade, low temperature loops. Upon comparing the ML baseline TCS with the single-phase cascade TCS for the small station several things are apparent. The ML TCS uses about 45% less pumping power than the small station with a single-phase cascade TCS. Further, the ETCS loop set-point temperatures are about the same for the two systems. A comparable LP two-phase TCS for ML then should use only about 55% of the pumping power listed in Ungar (1995) for a small station. Thus, the pumping power for a LTL in a LP two-phase TCS for ML would use 0.037 kW, while a corresponding MTL loop would use 0.044 kW. A complete LP two-phase TCS for ML will use two LTL loops and one MTL loop with a total ETCS pumping power requirement of 0.118 kW. Based on Ungar (1995), the radiator area is more dependent on the heat load rejected than on the TCS employed, so the radiator area for ML with a LP two-phase TCS will be similar to that for the baseline TCS. Thus, LP two-phase TCS will lead to a reduction in pumping power.

Mass Saved by Using a Low-Power Two-Phase Thermal Control System	Baseline Mars Lander TCS	LP Two-Phase TCS for ML	Total Change for TCS
Pump Power [kW] Mass due to	0.523	0.118	
Pump Power [kg]	58.1	13.1	45.0

Finally, the LP two-phase TCS uses smaller fluid lines than the baseline single-phase cascade TCS which translates into an additional mass savings. However, these savings are not included here.

Specific Assessments:

Equipment Mass Savings	negligible
Power Savings	0.405 kW
Power Savings as Mass	45 kg
Overall Mass Savings	45 kg
Composite Qualitative Score	-1

4.3.4.2   Two-Phase Thermal Control System With Electrohydrodynamic Pumping

Based on the discussion in Section 2.1.3, ML could utilize a two-phase TCS with electrohydrodynamic pumping. A two-phase TCS with electrohydrodynamic pumping may yield a slight mass savings over a LP two-phase TCS. A significant mass savings

over the baseline TCS would also be expected. However, without more data on this technology, no mass savings estimates may be determined.

Specific Assessments:

Equipment Mass Savings	unknown
Power Savings as Mass	unknown
Overall Mass Savings	unknown
Composite Qualitative Score	+2

4.3.4.3   Capillary Pumped Loops

Based on the baseline architecture given in Section 4.3.2, a capillary pumped loop [214] could save 0.523 kW, which is the estimated ETCS pumping power for ML. While it is possible that a single capillary pumped loop might be employed, that does not affect the mass estimates for this study because the capillary pumped loop equipment mass is assumed to be comparable to the equipment mass for the baseline single-phase TCS architecture. Thus, the overall savings for this option is 58.1 kg based on saving power for pumping.

Specific Assessments:

Equipment Mass Savings	none
Power Savings	0.523 kW
Power Savings as Mass	58 kg
Overall Mass Savings	58 kg
Composite Qualitative Score	0

4.3.4.4   Vapor Compression Heat Pump

In contrast to Luna, Mars offers a somewhat less extreme thermal environment. The days are only slightly longer than terrestrial days and the diurnal temperature variations are less extreme than on Luna. However, using a heat pump to increase the radiator temperature is still a reasonable idea. This section examines using a vapor compression heat pump [215] continuously throughout the martian day and night.

As in the baseline mission, the ML ETCS here is two-fault tolerant and each ETCS loop has its own heat pump. During nominal operation, each heat pump handles one third of the nominal load, or 10 kW. However, each heat pump is sized to handle a load 50% greater than the nominal load, or 15 kW, to allow ML to still reject its full heat load after losing one heat pump. The analysis uses a single ETCS loop for a basis.

A two parameter parametric study assuming a vertical radiator (Figure 4.21) indicates that the ETCS mass is minimized for ML when the heat pump temperature lift is

---

[214]   See Section 2.1.4 for background on capillary pumped loops.

[215]   Section 2.2.1 provides additional background on vapor compression heat pumps.

26.0 K and the radiator fluid mass flowrate is increased to 1.13 kg/s per ETCS loop. Specifically then (for one of three ETCS loops):

|	
Cold Source Temperature, T_C (evaporator temperature)	274.0 K
Temperature Lift, $T_H - T_C$	26.0 K
Hot Source Temperature, T_H (condenser temperature)	300.0 K
Radiator Inlet Temperature, T_{in}	296.0 K
Environmental Temperature, T_{sink} [216]	243.14 K
Total Cooling Load per Loop, Q_C	10.0 kW
Ideal Coefficient of Performance, COP_{Carnot}	10.54
Heat Pump Efficiency, η [217] (Ewert, 1991)	0.50
Necessary Input Power, W_{real}	1.90 kW

The vertical radiators are simulated by the model developed for the parametric study. Vertical radiators, compared to comparable horizontal units, have better heat rejection under their worst-case conditions [218].

Emissivity	0.80
Solar Absorptivity	0.20
Fin Efficiency	0.85
Radiator Mass Flowrate of Ammonia (per ETCS loop)	1.13 kg/s
Average Ammonia Temperature	294.4 K
Average Panel Surface Temperature	292.9 K
Heat Rejection per Unit Area	0.149 kW/m²
Total Heat Rejected per Loop by the Radiators, $Q_{H,real}$	11.90 kW
Radiator Mass Per Unit Area	5.625 kg/m²
Radiator Working Fluid Mass Per Unit Area	0.269 kg/m²
Necessary Radiator Surface Area during the Day	79.90 m²

---

[216] The sink temperature is computed for the poorest heat rejection by a vertical radiator facing east and west on a completely clear day. Using the poorest heat rejection for a horizontal radiator, which occurs during a dust storm, the corresponding effective sink temperature is 247.23 K.

[217] Percentage of Carnot coefficient of performance (COP).

[218] This occurs for a vertical radiator facing east and west on a clear day during the late afternoon.
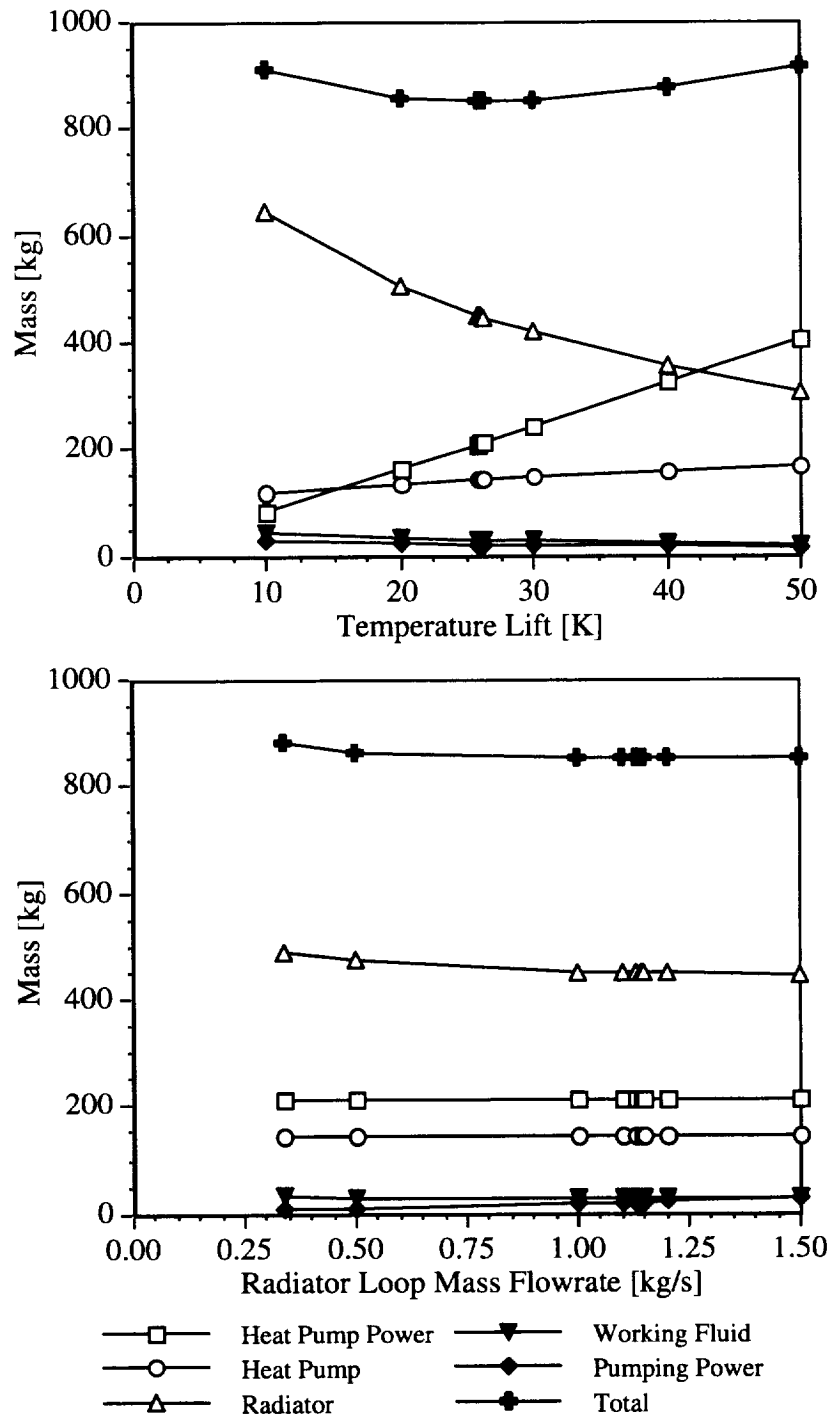
Figure 4.21 Variation of the Mars Lander ETCS mass per ETCS loop as a function of the vapor compression heat pump temperature lift and the radiator loop mass flowrate. The baseline mission from Section 4.3.2 forms the basis for this study. The ETCS mass was optimized with respect to both variables mentioned above.

Mass Gained by Using a Vapor Compression Heat Pump	Mars Lander ETCS Loop With Heat Pump	Total Mars Lander ETCS With Heat Pumps	Total Baseline Mars Lander TCS	Change for Mars Lander ETCS
Radiator Mass [kg]	449.4	1348.2	1985.3	-637.1
Working Fluid [kg]	21.5	64.5	94.9	-30.4
Heat Pump Mass [219] [kg]	141.7	425.1	--	+425.1
Radiator, Fluid, and Heat Pump Mass [kg]	612.6	1837.8	2080.2	-242.4
Power: Heat Pump [kW]	1.90	5.70	--	
Evaporator Pumping Power [kW]	0.08	0.24	--	
Condenser Pumping Power [kW]	0.06	0.18	--	
Radiator Pumping Power [kW]	0.12	0.36	0.47	
Total Power [kW]	2.16	6.48	0.47	
Mass due to Power [kg]	239.8	719.4	52.2	+667.2
Total Mass [kg]	852.4	2557.2	2132.4	+424.8

The ETCS line pumping power is unchanged. The power values include penalties for the pressure drops associated with the condenser and the evaporator. The condenser power penalty is 50% of the power to pump fluid through the radiators designed for use with the heat pump (or 0.5 × 0.12 kW). The evaporator power penalty is 50% of the power to pump fluid through the baseline radiator configuration (or 0.5 × 0.47 kW/3). As the tabulation above indicates, a continuously operating vapor compression heat pump will be more massive than the baseline ETCS for ML.

Specific Assessments:

Equipment Mass Savings	242 kg
Power Savings	-6.01 kW
Power Savings as Mass	-667 kg
Overall Mass Savings	-425 kg
Composite Qualitative Score	+1

4.3.4.5　Solar Vapor Compression Heat Pump

The single greatest drawback of a TCS continuously using a vapor compression heat pump is the power requirement. For the vapor compression heat pump presented in the previous section, the power accounts for about a quarter of the total ETCS mass. On Mars it is only necessary to operate a vapor compression heat pump while the vehicle or

---

[219]　See the footnotes in Section 3.1.5.4 for the heat pump sizing correlation.

habitat is in sunlight. Heat can be rejected at night using only radiators. Thus, to reduce overall system mass for ML using a vapor compression heat pump, the heat pump is bypassed after the Sun sets to allow the ETCS working fluid to flow directly to the radiators. During the day, the heat pump radiator loop operates normally with the radiator working fluid flowing only between the heat pump condenser and the radiators. Here the heat pumps will only operate while sunlight is available using dedicated photovoltaic solar arrays and the assumed power mass penalty is 25 kg/kW for energy consumed only in this mode [220]. As above, the continuous power mass penalty is 111 kg/kW.

A two parameter parametric study (Figure 4.22) indicates that the ETCS mass per loop is minimized for this option when the heat pump temperature lift is 28.1 K and the radiator fluid mass flowrate is increased to 0.82 kg/s per ETCS loop. The controlling limitation is the radiator area required while the heat pump is not available, which is 78.0 m^2 per loop. This is the radiating area required to reject the nominal heat load at sunset under the least favorable environmental conditions. (See Section 4.3.3) Therefore:

|	
Cold Source Temperature, T_C (evaporator temperature)	274.0 K
Temperature Lift, $T_H - T_C$	28.1 K
Hot Source Temperature, T_H (condenser temperature)	302.1 K
Radiator Inlet Temperature, T_{in}	298.1 K
Environmental Temperature, T_{sink}	243.14 K
Total Cooling Load per Loop, Q_C	10.0 kW
Ideal Coefficient of Performance, COP_{Carnot}	9.75
Heat Pump Efficiency, η [221] (Ewert, 1991)	0.50
Necessary Input Power, W_{real}	2.05 kW

The vertical radiators are simulated by the model developed for the parametric study. Vertical radiators, compared to comparable horizontal units, have better heat rejection under their worst-case conditions [222].

Emissivity	0.80
Solar Absorptivity	0.20
Fin Efficiency	0.85
Radiator Mass Flowrate of Ammonia (per ETCS loop)	0.82 kg/s
Average Ammonia Temperature	295.8 K
Average Panel Surface Temperature	294.3 K
Heat Rejection per Unit Area	0.154 kW/m^2

---

[220] This study has not addressed the issue of whether sufficient power can be generated by a photovoltaic solar array if a dust storm is present. This is significant because midday on Mars is thermally the hottest diurnal environment even when a dust storm is present. As such, if heat pumping is not available, the radiators alone may not be able to reject the full heat load by themselves during the entire Martian day. See Section 2.2.2 for additional information on solar vapor compression heat pumps.

[221] Percentage of Carnot coefficient of performance (COP).

[222] This occurs for a vertical radiator facing east and west on a clear day during the late afternoon.
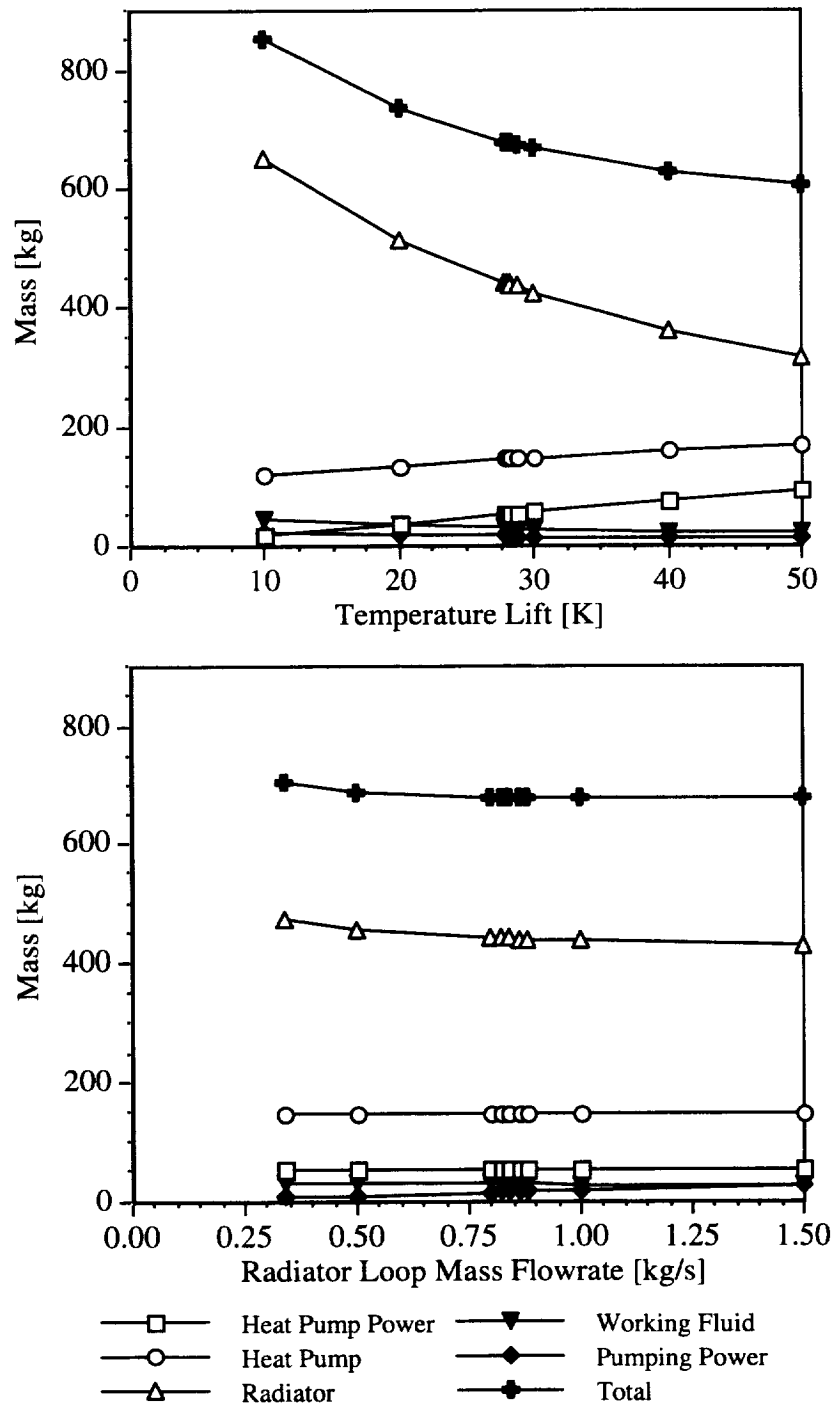
Figure 4.22 Variation of the Mars Lander external thermal control system mass per loop as a function of the solar vapor compression heat pump temperature lift and the radiator loop mass flowrate. The baseline mission from Section 4.3.2 forms the basis for this study. The external thermal control system mass was optimized with respect to both variables mentioned above.

Total Heat Rejected per Loop by the Radiators, $Q_{H,real}$　　12.05 kW
Radiator Mass Per Unit Area　　5.625 kg/m^2
Radiator Working Fluid Mass Per Unit Area　　0.269 kg/m^2
Necessary Radiator Surface Area during the Day (per loop)　　78.05 m^2
Necessary Radiator Surface Area at Night (per loop)　　78.00 m^2

Here the radiator design is constrained by the radiating area necessary to reject the nominal load at sunset (Figure 4.23). The power may be grouped according to its applicable power mass penalty.

Power Mass Penalties:
Heat Pump Power　　　　　　　　　　　　Daytime Only
Evaporator Pumping Power　　　　　　　　Daytime Only
Condenser Pumping Power　　　　　　　　Daytime Only
Radiator Pumping Power　　　　　　　　　Continuous

Mass Gained by Using a Solar Vapor Compression Heat Pump	Mars Lander ETCS Loop With Solar Heat Pump	Total ML ETCS With Solar Heat Pump	Total Baseline Mars Lander TCS	Change for Mars Lander ETCS
Radiator Mass [kg]	439.0	1317.0	1985.3	-668.3
Working Fluid [kg]	21.0	63.0	94.9	-31.9
Heat Pump Mass [223] [kg]	144.3	432.9	--	+432.9
Radiator, Fluid, and Heat Pump Mass [kg]	604.3	1812.9	2080.2	-267.3
Power: Heat Pump [kW]	2.05	6.15	--	
Evaporator Pumping Power [kW]	0.08	0.24	--	
Condenser Pumping Power [kW]	0.04	0.12	--	
Radiator Pumping Power [kW]	0.09	0.27	0.47	
Total Power [kW]	2.26	6.78	0.47	
Mass due to Power [kg]	64.2	192.6	52.2	+140.4
Total Mass [kg]	668.5	2005.5	2132.4	-126.9

The ETCS line pumping power is unchanged. As in the previous section, the power values include penalties for the pressure drops associated with the condenser and the evaporator.

As anticipated, the heat pump using solar power generation is less massive than a continually operating heat pump. Further, the reduction in mass also allows the solar heat pump to be less massive than the baseline ETCS configuration.

---

[223] See the footnotes for Section 3.1.5.4 for the heat pump sizing correlation.
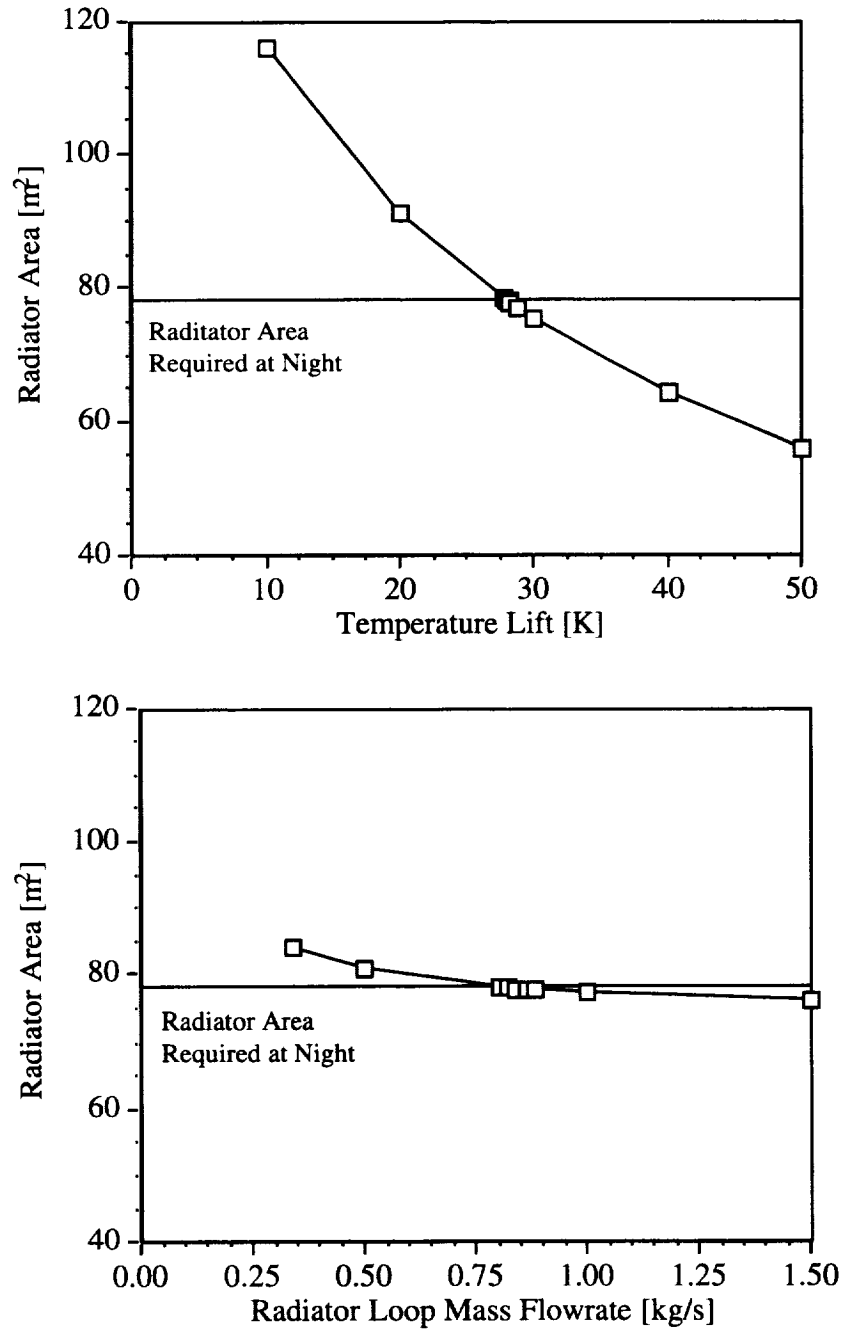
Figure 4.23 Variation of radiator area per ETCS loop for the Mars Lander ETCS as a function of the solar vapor compression heat pump temperature lift and the radiator loop mass flowrate. The solar heat pump option is constrained by the radiator area required for rejection of the ATCS heat load at night without the heat pump operating.

Specific Assessments:

Equipment Mass Savings	267 kg
Power Savings	-6.31 kW
Power Savings as Mass	-140 kg
Overall Mass Savings	127 kg
Composite Qualitative Score	+2

4.3.4.6 Lightweight Radiators

To identify potential mass savings from using lighter materials for portions of the ML radiator assembly, a parametric study is presented below. As with several previous vehicles, the ML ETCS is in an early design stage and is not well defined, so the components and categories listed here are estimates.

Category Within Mars Lander Radiator Assembly [224]	Mass [kg]	Mass Percentage
Structure and Deployment:		29.3
Base Radiator Support Structure	211.8	
Deployment Mechanism	397.1	
Radiator Panels	1376.4	66.1
Radiator Panel Working Fluid (ammonia)	94.9	4.6
Total	2080.2	100.0

This study varies the component ML radiator assembly masses linearly based on the original total mass in each category. The structure and deployment masses are reduced by up to 20% when the radiator panel mass is reduced by up to 40%. The radiator panel working fluid volume will be unchanged, so the working fluid mass will also be unchanged [225].

The most important underlying assumption is that composites and other advanced materials are most likely to offer a significant mass reduction for only some components of the radiator panels such as the honeycomb and the facesheets. Because the radiator panels are the single most massive item of the ML radiator assembly, such savings would constrain the remainder of the design. A less significant mass reduction is assumed for the structures and deployment because the sizes of these components are primarily dictated by the dimensions of the radiator array and the deployment scheme. However, composites should allow comparable components to replace some of the structure and deployment with lighter parts.

---

[224] The overall mass per radiating area excluding fluids is 5.625 kg/m² for the dry radiator panel assembly. The assumed component composition is: 3.9 kg/m² for radiator panels, 0.6 kg/m² for the base support structure, and 1.125 kg/m² for deployment. As presented above, the radiator panel working fluid mass is 0.269 kg/m² of radiating area.

[225] See Section 2.4 for additional general background on lightweight radiators plus specific examples of proposed lightweight radiators.
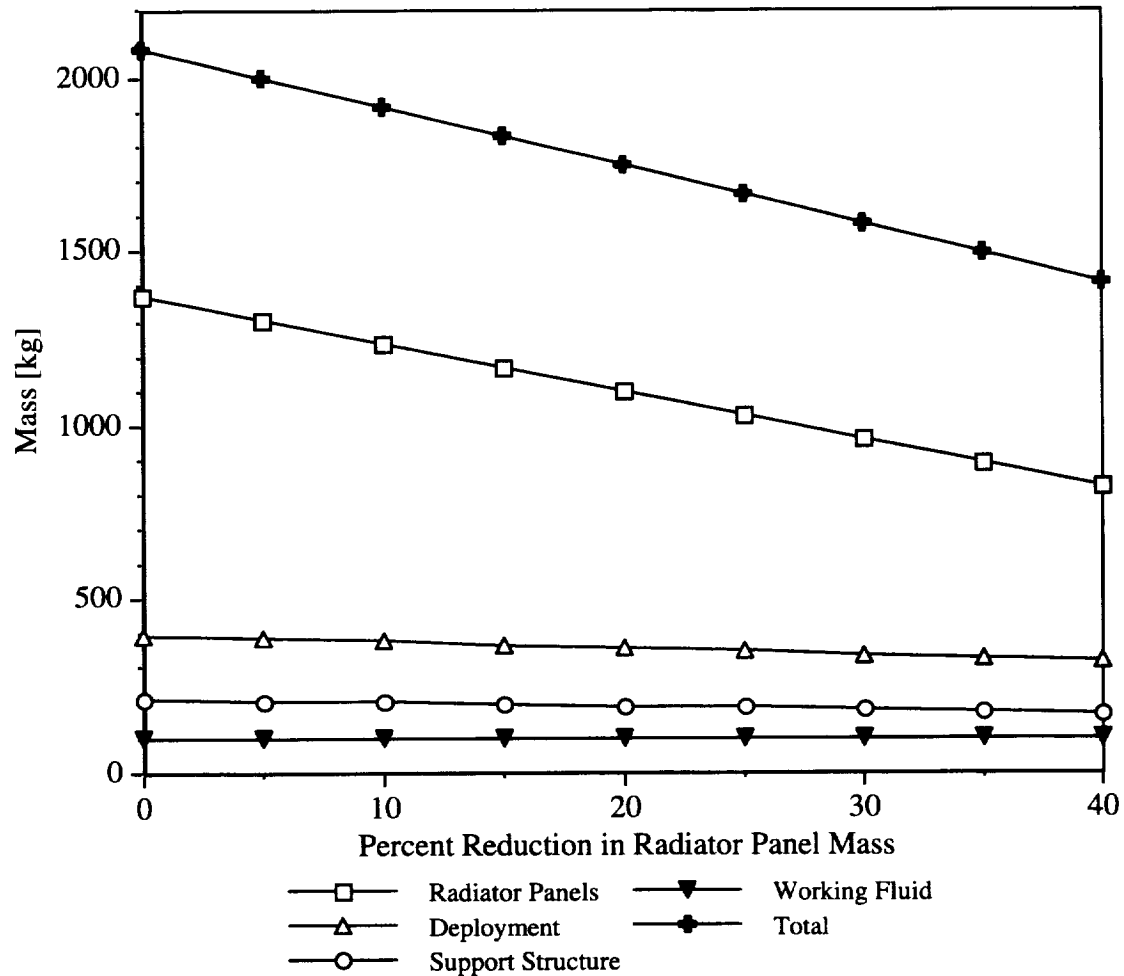
Figure 4.24 ML radiator mass as a function of mass reduction within the radiator panel set. Study Assumption: For each 10% mass reduction in the radiators the masses for the support structure and the deployment decrease by 5%.

Category Within Mars Lander Radiator Assembly	Percent Reduction in Radiator Panel Mass 20%	40%
Structure and Deployment [kg]	548.0	487.1
Radiator Panels [kg]	1101.1	825.8
Radiator Working Fluid [kg]	94.9	94.9
Overall Radiator Mass [kg]	1744.0	1407.8
Overall Mass Reduction in Radiators [kg]	336.2	672.4
Mass Reduction as a Percentage of the Original ML Radiator Assembly	16.2	32.3
Radiator Mass Per Surface Area [kg/m^2]	4.94	3.99

Considering the available lightweight radiators presented in Section 2.4, an overall mass reduction of 20.0% was selected as a representative value. Thus, the mass savings for ML is 416.0 kg for the reference mission (Figure 4.24). The power requirements will be unchanged because the internal fluid dynamics and, therefore, the pumping power are functions of the working fluid material properties.

Because ML is a planetary mission, any of the lightweight radiator concepts may be used. All of the radiators presented in Section 2.4 can be deployed vertically. Unlike the lunar missions, vertical radiators may be used without additional equipment. Again, the composite flow-through radiators could also be oriented horizontally.

Specific Assessments:

Equipment Mass Savings	416 kg
Power Savings as Mass	none
Overall Mass Savings	416 kg

4.3.5 Summary

The various advanced technologies and their estimated benefits are summarized in the table below for ML. From Section 4.3.2, the mass of the baseline ETCS is 2,171.5 kg. Again, assuming the mass determinations throughout this study have associated uncertainties on the order of 10%, a complete TCS with an advanced technology would need to show a savings of at least 217 kg to ensure a mass savings. Further, because design and development costs are not trivial, a mass savings of 25%, or 543 kg, is desirable. Using these criteria, the TCSs with advanced technologies proposed for ML may be divided into five categories:

- TCSs using advanced technologies requiring a mass penalty greater than 10% of the overall baseline ETCS mass: vapor compression heat pump.

- TCSs using advanced technologies requiring a mass penalty less than 10% of the overall baseline ETCS mass: none.

- TCSs using advanced technologies with a mass savings less than 10% of the overall baseline ETCS mass: LP two-phase TCS, capillary pumped loops, and solar vapor compression heat pump.

- TCSs using advanced technologies with a mass savings between 10 and 25% of the overall baseline ETCS mass: lightweight radiators.

- TCSs using advanced technologies with a mass savings greater than 25% of the overall baseline ETCS mass: none.

A continuously operated vapor compression heat pump is not appropriate for ML. The technologies in the third category will produce an ETCS which is comparable to the baseline ETCS. The technology in the fourth category is promising for this mission.

Table 4.13 Advanced Active Thermal Control System Architecture for Mars Lander

Summary of Advanced Active Thermal Control System Architecture for Mars Lander	Overall Mass Savings [kg]	Qualitative Score
4.3.4.1 Low-Power Two-Phase Thermal Control System	45	-1
4.3.4.2 Two-Phase Thermal Control System With Electrohydrodynamic Pumping	unknown	+2
4.3.4.3 Capillary Pumped Loops	58	0
4.3.4.4 Vapor Compression Heat Pump	-425	+1
4.3.4.5 Solar Vapor Compression Heat Pump	127	+2
4.3.4.6 Lightweight Radiators	416	--

5.0 CONCLUSIONS

Each section above provides conclusions within the summary highlighting the most promising set of thermal control technologies for each reference mission. This section presents conclusions concerning the mass savings, or general appropriateness, of each advanced thermal technology across the spectrum of missions examined in this study. Table 5.1 summarizes the mass savings for each technology as it applies to the various missions.

**Table 5.1 Mass Savings [kg] of Advanced Technologies
Applied to Reference Missions**

	Reference Vehicles and Habitats				
	ISS	STS	FLO	PLB	ML
Baseline ETCS Architecture Masses [226]	15,568	201,306	2,101	10,948	2,172
Advanced Technologies					
Two Phase Thermal Control Systems (TCSs):					
1. Two-Phase TCS With Mechanical Pump/Separator	1,203			456	
2. Low-Power Two-Phase TCS	1,366	8,176	286	751	45
3. Two-Phase TCS with Electrohydrodynamic Pumping			unknown	unknown	unknown
4. Capillary Pumped Loops	1,535		370	917	58
Heat Pumps:					
5. Vapor Compression Heat Pump	-250			7,017	-425
6. Solar Vapor Compression Heat Pump	5,021		259	7,321	127
7. Complex Compound Heat Pump				4,241	
8. Zeolite Heat Pump				3,818	
Heat Pipe Radiators:					
9. Arterial Heat Pipe Radiators	-154				
10. Axial-Groove Heat Pipe Radiators	-309				
11. Arterial Heat Pipes With Electrohydrodynamic Pumping	490				
Lightweight Radiators [227]:	1,661	22,904	584	3,306	416
12. Composite Flow-Through Radiators	x	x	x	x	x
13. Composite Heat Pipe Radiators	x		x	x	x
14. Composite Reflux Boiler Tube Radiators			x	x	x
15. Unfurlable Radiators			x	x	x
Other Heat Rejection Technologies:					
16. Phase-Change Thermal Storage		11,875			
17. Parabolic Radiator Shade				642	7,416
Additional Technologies:					
18. Rotary Fluid Coupler	444				
19. Plant Chamber Cooling Improvements				2,867	
20. Carbon Brush Heat Exchanger	118			154	

---

[226]   See reference missions in Sections 3.0 and 4.0 for details.

[227]   The listed mass savings comes from the generic lightweight radiator assessment while the lightweight radiator technologies which appear appropriate are marked with an 'x'. Actual lightweight radiators may offer a greater or lesser mass savings than the figure listed here.

Qualitative assessments for these technologies are presented with discussion in Section 2.0 and the assessments are summarized in Table 2.1.

From the information above, the radiator masses per radiating area for the individual reference mission architectures are summarized in Table 5.2. These values are based on the total radiator mass, including any working fluid, divided by the radiating surface area.

Table 5.2 Summary of Masses per Radiating Area for Reference Mission Baseline Thermal Control System Architectures

Reference Mission	Mass per Radiating Area [kg/m^2]	Fin Efficiency	Effective Mass per Radiating Area [228] [kg/m^2]
3.1.2 International Space Station Evolution	8.51	0.88	9.67
3.2.2 Space Transportation System Upgrade (6-Panel Configuration) [229]			5.01
Space Transportation System Upgrade (8-Panel Configuration)			5.30
4.1.2 First Lunar Outpost Lander	7.37	0.85	8.67
4.2.2 Permanent Lunar Base [230]	7.86	0.85	9.25
4.3.2 Mars Lander	5.89	0.85	6.93

5.1 General

Over the spectrum of missions presented above, solar vapor compression heat pumps and lightweight radiators are the most generally applicable advanced thermal control technologies. The vapor compression heat pump suffers from high power consumption. Offsetting this drawback, vapor compression heat pumps drastically reduce the required thermal control radiator area for thermal environments where rejection of life support heat loads would normally be difficult. The solar vapor compression heat pump concept attempts to deal with the compressor's power requirement using a systems engineering approach to integrate the heat pump with its power source in one package. In addition to comparing favorably in terms of mass to the baseline architecture, the solar vapor compression heat pump is applicable to a wide range of duties, including both planetary and orbital missions. Likewise, lightweight radiators also apply to a wide range of planetary and orbital missions. Specific lightweight radiators may be mission-specific or mission-type-specific. For example, composite reflux boiler tube radiators require a gravitational force to operate and are inappropriate for orbital missions.

The qualitative assessments are independent of the quantified mass savings. The qualitative assessments represent a conglomeration of expert opinions dealing with volume, ease of deployment, reliability, development cost, and terrestrial use potential of the various technologies. Several technologies which did not offer large mass savings

---

[228] The effective mass per radiating area is the mass per radiating area divided by the fin efficiency.

[229] Jaax (1978) provides the effective radiator area, not the actual radiator area.

[230] These values reflect a single set of radiator panels. For the entire 15-year reference mission, assuming two sets of radiator panels, the mass per radiating area is 15.36 kg/m^2.

scored high in the qualitative assessments. These include the rotary fluid coupler, the carbon brush heat exchanger, and electrohydrodynamic pumping. Thus, these assessments indicate that these technologies may offer other benefits and, therefore, reasons for developing them other than their potential for saving mass.

5.2   Two-Phase Thermal Control Systems

Two-phase thermal control systems offer greater promise for larger systems with long flow lines. With the exception of International Space Station and Permanent Lunar Base, the vehicles here are too small to make adequate use of this technology. Additionally, retrofitting International Space Station with a two-phase thermal control system may be difficult. For Permanent Lunar Base, however, a two-phase thermal control system may be a wise investment, especially if the base will be expanded sometime in the future. As flow lines lengthen and heat loads increase, the mass saved by a two-phase thermal control system could be significant. Capillary pumped loops provide a two-phase thermal control architecture which can be economical even for smaller vehicles. The only major disadvantage of this specific two-phase thermal control system is the relatively low pressure rise generated by capillary forces. As such, care is required when designing a capillary pumped loop for use on a planetary surface and this technology is probably inappropriate for a thermal control system while a vehicle is accelerating during a launch or re-entry maneuver.

5.3   Heat Pumps

In general, heat pumps are extremely versatile. They depend on elevating waste heat to relatively high temperatures. High rejection temperatures in turn reduce the thermal control system's sensitivity to radiator surface properties by increasing the driving temperature difference between the radiator and the environment. Further, heat pumps are not sensitive to planetary surface conditions except as those conditions affect the radiator surface properties. Design of heat pumps for use in microgravity environments is an unsettled issue.

Vapor compression heat pumps suffer from high power consumption. However, provided with a sufficiently inexpensive power source, such as a dedicated solar photovoltaic power array, vapor compression heat pumps offer one of the least massive options for many thermal control systems.

For some missions, heat-driven heat pumps also appear to offer mass savings compared with the baseline architectures using only metal flow-through radiators. Coupled with a source of high-temperature waste heat, such as from an industrial process, they may provide economical cooling. However, they are not as efficient as the vapor compression heat pumps.

5.4   Heat Pipe Radiators

Due to their extra mass, metal heat pipes appear to be justified for human missions only when thermal control system flow loop punctures from external debris are expected to be a serious problem. When a mission flies in such an environment, mass savings become secondary to the reliability of the heat-rejection system. Longer heat pipe units

exhibit lower mass per radiating area ratios than shorter units. As such, longer heat pipes are preferred. Mass predictions for systems augmented with electrohydrodynamic pumps are lower than for systems which are not augmented because the pumps increase the heat pipe's transport limit over that derived from capillary forces alone. Current predictions for the missions here do not consider flow loop punctures from micrometeroids and on-orbit debris to be a significant problem except possibly for the International Space Station evolution mission. For International Space Station evolution, the thermal control system mass assuming metallic heat pipe radiators will be comparable to that of the baseline flow-through radiator technology. Additionally, the operational benefit of greater resistance to thermal control flow loop punctures is gained with this architecture. Table 5.3 presents the mass per radiating area for the arterial heat pipe concepts along with a similar value from the baseline architecture for International Space Station evolution.

**Table 5.3 Summary of Masses per Radiating Area
for Arterial Heat Pipe Radiators**

	Mass per Radiating Area $[kg/m^2]$	Fin Efficiency	Effective Mass per Radiating Area $[kg/m^2]$
3.1.2 International Space Station Evolution	8.51	0.88	9.67
2.3 Heat Pipe Radiators			
2.3.1 13.11-m Arterial Heat Pipe Radiators	8.80	0.925	9.51
6.71-m Arterial Heat Pipe Radiators	9.88	0.925	10.68
2.3.2 Arterial Heat Pipe Radiators			
With Electrohydrodynamic Pumping	7.64	0.763	10.01

5.5   Lightweight Radiators

Lightweight radiators, though not rigorously defined here, offer the hope of directly reducing the radiator mass, which is the single greatest mass within the external thermal control system. Additionally, lightweight flow-through radiators can be used regardless of the other external thermal control system elements.

To add a more concrete basis to this approach, four different lightweight radiator concepts are presented under this category. These include composite flow-through radiators and composite heat pipe radiators which may be applied for either planetary or orbital missions. Composite reflux boiler tube radiators and unfurlable radiators both depend on working fluid density differences for internal heat transport and therefore require gravity to operate. Table 5.4 presents the mass per radiating area for each of these concepts along with the corresponding values from the baseline architectures of the reference missions for comparison.

Table 5.4 Summary of Masses per Radiating Area
for Lightweight Radiators

	Mass per Radiating Area [kg/m^2]	Fin Efficiency	Effective Mass per Radiating Area [kg/m^2]
Reference Missions			
3.1.2 International Space Station Evolution	8.51	0.88	9.67
3.2.2 Space Transportation System Upgrade (6-Panel Configuration) [231]			5.01
Space Transportation System Upgrade (8-Panel Configuration)			5.30
4.1.2 First Lunar Outpost Lander	7.37	0.85	8.67
4.2.2 Permanent Lunar Base	7.86	0.85	9.25
4.3.2 Mars Lander	5.89	0.85	6.93
2.4 Lightweight Radiators			
2.4.1 Composite Flow-Through Radiators (Single-Sided Rejection)	8.21	~1.00	8.21
Composite Flow-Through Radiators (Double-Sided Rejection)	4.67	~1.00	4.67
2.4.2 Composite Reflux Boiler Tube Radiators	3.44	1.00	3.44
2.4.3 Composite Heat Pipe Radiators [232]	1.91	0.97	1.96
2.4.4 Unfurlable Radiators	4.62	1.00	4.62

5.6　Other Heat Rejection Technologies

The technologies listed under this category have more limited applicability than some of the other technologies presented above. Phase-change thermal storage is useful for orbital missions where the time during which the vehicle must endure its maximum heat load is less than the orbital period. This allows the phase-change thermal storage device to provide supplemental cooling while the vehicle is under its maximum heat loading and to solidify the phase-change material while the vehicle experiences its minimum heat loading.

The parabolic radiator shade operates well on airless planetary bodies with small planetary inclinations. For a lunar mission, these devices offer the greatest mass savings of the technologies analyzed. While a parabolic shade could be adapted for other environments, this would require additional equipment, including a rigid shade assembly and tracking equipment. For a planetary body with an atmosphere, additional equipment or techniques would be needed to keep dust and other debris off of the shade surface.

---

[231] Jaax (1978) provides the effective radiator area, not the actual radiator area.

[232] The fin efficiency listed for the composite heat pipe radiator is estimated based on an analysis using the Thermal Synthesizer System (TSS) and SINDA/FLUINT. The actual value is unknown.

5.7   Additional Technologies

The heat transfer technologies presented under this heading are all enhancing technologies. While individually they are not usually expected to yield large mass savings for their respective missions, the listed mass savings is independent of the architecture of the remainder of the thermal control system. Thus, these technologies are extremely useful in a supporting role to reduce the overall mass of the thermal control system.

6.0   RECOMMENDATIONS

While this study is a good start, it fails to answer all questions one might have about advanced thermal control system technology. Some answers are unknowable using the preliminary analysis format presented here. However, other areas could be more adequately addressed by additional study. The recommendations which follow focus on additional analysis which could extend and improve the current study without relying on extensive input from future research and development. As technologies mature and data become available, the study estimates could be updated and refined. Further, additional reference mission scenarios could be added and examined as future missions are contemplated.

6.1   Additional Mission Scenarios

- **Human Lunar Return** - Consider a small lunar habitat with room for a crew of two to four and a very limited mission length of 3 to 14 days.

- **Permanent Lunar Base at a Lunar Pole** - Consider Permanent Lunar Base located at a lunar pole instead of an equatorial site. Some scientific missions, such as a telescope located on Luna, would prefer a polar site to an equatorial site (Burke, 1989). Further, finding water on Luna, if it exists, is deemed more likely at one of the poles. Such a discovery could reduce the mass of supplies sent from Earth for human operations.

- **Extended Presence on Mars** - Consider a base at an equatorial latitude on the martian surface built up over several missions from remotely placed vehicles. A single thermal control system will be used for both the transit and surface phases of the mission. A common thermal control architecture should be employed for all vehicles.

- **Generic Transfer Vehicles** [233]:

  - **Interplanetary Vehicle for Transfer to Luna** - Consider a vehicle with a capacity of three or four crew members for a transfer mission from Earth to Luna.
  - **Orbit to Surface Transfer Vehicle for Luna** - Consider a vehicle for the transfer of two to three crew members to the surface of Luna and back again from lunar orbit.
  - **Combined Transfer Vehicle to Luna** - Consider a vehicle which would carry a crew of three or four to the surface of Luna from Earth orbit and back again.
  - **Interplanetary Vehicle for Transfer to Mars** - Consider a vehicle with a capacity of three or four crew members for a transfer mission from Earth to Mars.

---

[233] A basic study of thermal control technologies for transfer vehicles might identify heat rejection technologies which are more generally applicable to not only the surface or orbital stages of a mission, but also to the transit stages.

- **Orbit to Surface Transfer Vehicle for Mars** - Consider a vehicle for the transfer of two to three crew members to the surface of Mars and back again from martian orbit.
- **Combined Transfer Vehicle to Mars** - Consider a vehicle which would carry a crew of three or four to the surface of Mars from Earth orbit and back again.

6.2 Additional Thermal Control Technology Studies

- **General:**

  - Perform conceptual design studies for aluminum, flow-through radiators to determine more accurately the associated equipment mass per radiating area for various radiator deployments. In particular, look at vertical and horizontal radiator deployments on planetary surfaces such as Luna and Mars.

- **Two-Phase Thermal Control Systems:**

  - Determine the variation in mass savings as a function of assumed power mass penalty for two-phase thermal control systems. Because the two-phase thermal control system's greatest overall benefit is to reduce thermal control system power requirements, the mass savings for these systems are dependent on the price of power for a mission.
  - Conduct a more in-depth analysis for the two-phase thermal control systems similar to the analysis in Ungar (1995) instead of the more simplistic approach used. These studies, like Ungar (1995), would assume and analyze a base or vehicle architecture including flow line lengths, mass flowrates, and pumping power. This, in turn, would permit estimates for the ETCS lines and fittings.

- **Heat Pumps:**

  - Determine the variation in mass savings as a function of assumed power mass penalty for the vapor compression heat pumps.
  - Develop estimates based on more in-depth heat pump models.
  - Consider distributed heat pumping versus centralized heat pumping.

- **Lightweight Radiators:**

  - As more detailed information becomes available for individual lightweight radiator concepts, assess these concepts individually, when appropriate, for each of the reference missions.

- **Combining Technologies:**

  - Combine a parabolic radiator shade with a solar vapor compression heat pump and determine the least massive system. This technology would apply to missions on the lunar surface.

- Combine a parabolic radiator shade with a solar vapor compression heat pump using lightweight radiators in place of vertical flow-through radiators and determine the least massive system. This technology would apply to missions on the lunar surface.
- Combine the carbon brush heat exchanger and arterial heat pipes with electrohydrodynamic pumping.
- Combine the carbon brush heat exchanger with composite heat pipes.

6.3   Additional Mission Specific Work for Current Study

- **International Space Station Evolution:**

  - Determine the variation in mass savings for various advanced heat-rejection technologies as a function of assumed environmental temperature.
  - Conduct a transient analysis for the option using a solar vapor compression heat pump. Check to ensure that adequate heat rejection can be maintained while ISS is within the planetary shadow.
  - Add phase-change thermal storage.

- **Lunar Planetary Missions:**

  - Determine the thermal control system mass as a function of radiator surface temperature.
  - Determine the thermal control system mass as a function of latitude on the lunar surface.
  - Consider the effect of vertical radiators in place of the horizontal radiators.
  - Measure the frequency and distribution of micrometeoroid impacts and dust accumulation on the lunar surface.

- **Permanent Lunar Base:**

  - Conduct an in-depth parametric study for a system using a solar vapor compression heat pump. Consider vertical and horizontal radiators and vary both the surface properties and the assumed radiator mass per radiating area.
  - Determine the variation in heat pump mass as a function of heat pump efficiency and power mass penalty.
  - Determine the variation in thermal control system mass as a function of surface latitude. Use a combined system with a parabolic radiator shade and a solar vapor compression heat pump.

- **Mars Lander:**

  - Replace the assumed external and internal thermal control systems with a single thermal control loop using a non-toxic working fluid. Possible working fluids might include air, carbon dioxide, or water. The system might use a Brayton gas cycle heat pump or a standard flow loop.

- Consider the case where the radiator rejection temperature is allowed to rise to that assumed for First Lunar Outpost Lander.
- Measure the frequency and distribution of micrometeoroid impacts and dust accumulation on the martian surface.

7.0   REFERENCES

Andish, K. K. (1995) Lockheed Martin Engineering and Science Services, Houston, Texas. Private conversation.

Barta, D. J., Dominick, J. S., and Kallberg, M. (1995) "Early Human Testing of Advanced Life Support Systems, Phase I," SAE Paper 951490, 25th Intersociety Conference on Environmental Systems, San Diego, California, 1995, Society of Automotive Engineers, Warrendale, Pennsylvania.

Binder, A. B. (1990) "Lunar Data Base (Preliminary)," Lockheed Engineering and Sciences Company, Houston, Texas. Document dated 21 February, 1990.

Blades, B. (1996) Lockheed Martin Engineering and Science Services, Houston, Texas. Private conversation via C. Cross of the National Aeronautics and Space Administration, Lyndon B. Johnson Space Center, Houston, Texas.

Brown, R., Ungar, E., and Cornwell, J. (1992) "Flight Test Results of the SHARE II Monogroove Heat Pipe," AIAA Paper 92-2886, AIAA 27th Thermophysics Conference, Nashville, Tennesee, American Institute of Aeronautics and Astronautics, Washington, D.C.

Bryan, J. (1995) Texas A&M University, College Station, Texas. Private conversation at the National Aeronautics and Space Administration, Lyndon B. Johnson Space Center, Houston, Texas.

Burke, J. D. (1989) "Lunar Observatories," Spaceflight, Volume 31, pp. 308-309.

Cataldo, R. (1989) Lewis Research Center, National Aeronautics and Space Administration, Cleveland, Ohio. Private communication.

Chambliss, J., and Ewert, M. (1990) "Modular, Thermal Bus-to-Radiator Integral Heat Exchanger for Space Station Freedom," SAE paper 901435.

Christiansen, E. (1992) "SSF Flow-Through Radiator Meteoroid/Debris Penetration Probabilities," SN3-92-144, National Aeronautics and Space Administration, Lyndon B. Johnson Space Center, Houston, Texas. An internal memorandum to P. Petete and M. Ewert on August 6, 1992.

Cross, C. (1995) "Reusable Launch Vehicle Passenger Module ATCS Impact Study," JSC 33429 (CTSD-ADV-186), National Aeronautics and Space Administration, Lyndon B. Johnson Space Center, Houston, Texas.

Cross, C. (1996) "Chamber E EVA Composite Radiator and Lunar Radiator Technology Test Part II, Test Plan Document," JSC 38451, National Aeronautics and Space Administration, Lyndon B. Johnson Space Center, Houston, Texas.

Cullimore, B. A. (1993) "Capillary Pumped Loop Application Guide," SAE Paper 932156, 23rd International Conference on Environmental Systems, Colorado Springs, Colorado, 1993, Society of Automotive Engineers, Warrendale, Pennsylvania.

Dzenitis, J. M. (1992) "The Thermal Environment on the Surface of Mars," JSC 37632 (CTSD-ADV-055), National Aeronautics and Space Administration, Lyndon B. Johnson Space Center, Houston, Texas.

Ewert, M. (1991) National Aeronautics and Space Administration, Lyndon B. Johnson Space Center, Houston, Texas. Constants used for an unpublished trade study examining a lunar heat pump thermal control system versus a pumped shade thermal control system.

Ewert, M. (1993) "Investigation of Lunar Base Thermal Control System Options," SAE Paper 932112, Society of Automotive Engineers, Warrendale, Pennsylvania.

Ewert, M. K., and Clark, C. S. (1991) "Analysis and Conceptual Design of a Lunar Radiator Parabolic Shade," 26th Intersociety Energy Conversion Engineering Conference, Boston, Massachusetts, 1991.

Ewert, M. K., Graf, J.P., and Keller, J. P. (1995) "Development of a Lunar Radiator Parabolic Shading System," SAE Paper 951524, 25th Intersociety Conference on Environmental Systems, San Diego, California, 1995, Society of Automotive Engineers, Warrendale, Pennsylvania.

Ewert, M. K., Keller, J. R., and Hughes, B. (1996) "Conceptual Design of a Solar Powered Heat Pump for Lunar Base Thermal Control System," SAE Paper 961535, 26th International Conference on Environmental Systems, Monterey, California, 1996, Society of Automotive Engineers, Warrendale, Pennsylvania.

Ewert, M. K., Paul, T. H., and Barta, D. J. (1995) "Design, Analysis and Testing of a Thermal Control System for Plant Growth Lighting Using Coldplate Technology," SAE Paper 951663, 25th Intersociety Conference on Environmental Systems, San Diego, California, 1995, Society of Automotive Engineers, Warrendale, Pennsylvania.

Ewert, M. K., Petete, P. A., and Dzenitis, J. (1990) "Active Thermal Control Systems for Lunar and Martian Exploration," SAE Paper 901243, Advanced Environmental/Thermal Control and Life Support Systems, SP-831, 20th Intersociety Conference on Environmental Systems, Williamsburg, Virginia, 1990, Society of Automotive Engineers, Warrendale, Pennsylvania.

Farner, D. (1995) Lockheed Martin Engineering and Science Services, Houston, Texas. From the results of a SINDA/FLUINT model for ISS ETCS.

Gernert, N. J., and Donovan, K. G. (1994) "Unfurlable Radiator for Lunar Base Heat Rejection," SAE Paper 941326, 24th International Conference on Environmental Systems and 5th European Symposium on Space Environmental Control Systems, Friedrichshafen, Germany, 1994, Society of Automotive Engineers, Warrendale, Pennsylvania.

Green, S. T. (1991) "Models of Energy Transport System Components for Space Applications," Southwest Research Institute, San Antonio, Texas.

Harwell, W. D. (1992) "Rotary Fluid Transfer Technology Presentation," B3-A1-107, Crew and Thermal Systems Division, Boeing. Presented to the National Aeronautics and Space Administration, Lyndon B. Johnson Space Center, on July 20, 1992.

Henson, R. A. (1995) "Conceptual Thermal and Mass Analysis for a Mars Lander Thermal Control System," Lockheed Martin Engineering and Science Services. CTSD report in preparation.

Howell, H., *et al.* (1992) "Heat Rejection Subsystem Radiator Assembly, Technical Review No. 5," SDRL Item No. MR 04.1 LT, Loral Vought Systems, Dallas, Texas. Presented to McDonnell Douglas Aerospace on June 17, 1992.

Howell, H., *et al.* (1994) "Heat Rejection Subsystem Radiator Assembly, Technical Review No. 13," SDRL Item No. MR 04.1 LT, Loral Vought Systems, Dallas, Texas. Presented to McDonnell Douglas Aerospace on March 30, 1994.

Hughes, M. B. (1995) "Lunar Base Power System for Solar Heat Pumps," LMES-31919 (HDID-E-96-191) Lockheed Martin Engineering and Science Services.

Hurlbert, K. M., Ewert, M. K., Graf, J. P., Keller, J. R., Pauley, K. A., Guenther, R. J., and Antoniak, Z. I. (1996) "Final Report for the Ultralite Fabric Reflux Tube Thermal Vacuum Test," NASA TM 104815, National Aeronautics and Space Administration, Lyndon B. Johnson Space Center, Houston, Texas.

Jaax, J. R. (1978) Orbiter Active Thermal Control Subsystem Description and Test History, CSD-SH-126, Crew Systems Division, National Aeronautics and Space Administration, Lyndon B. Johnson Space Center, Houston, Texas, July 20, 1978.

Jerng, L. T. (1991) "Weight Comparison Study Between LCELSS Conceptual Design and JSC-10ft Chamber," CTSD-1155 (LESC-29711), Lockheed Engineering and Sciences Company, Houston, Texas.

Juhasz, A. J. (1996) National Aeronautics and Space Administration, Lewis Research Center, Cleveland, Ohio. Private communication.

Juhasz, A. J., and Bloomfield, H. S. (1994) "Development of Lightweight Radiators for Lunar Based Power Systems," NASA TM 106604, National Aeronautics and Space Administration, Lewis Research Center, Cleveland, Ohio.

Juhasz, A. J., and Rovang, R. D. (1995) "Composit Heat Pipe Development Status: Development of Lightweight Prototype Carbon-Carbon Heat Pipe With Integral Fins and Metal Foil Liner," NASA TM 106909, National Aeronautics and Space Administration, Lewis Research Center, Cleveland, Ohio.

Kantara, J. J. (1989) "CTB Radiator Weight and Size Assessment Using 43' Long Radiator Panels," CTSD-00299 (LESC-27157), Lockheed Engineering and Sciences Company, Houston, Texas.

Keller, J. R. (1994) "Full and Partial Parabolic Shade Modeling Using the Thermal Synthesizer System (TSS)," CTSD-1829 (LESC-31341), Lockheed Engineering and Sciences Company, Houston, Texas.

Keller, J. R. (1995 a) Lockheed Martin Engineering and Science Services, Houston, Texas. Private conversation.

Keller, J. R. (1995 b) "Lunar Dust Contamination Effects on Lunar Radiator Shade Systems," Lockheed Martin Engineering and Science Services, Houston, Texas. Presented to Crew and Thermal Systems Department, National Aeronautics and Space Administration, Lyndon B. Johnson Space Center, Houston, Texas, June 2, 1995.

Knowles, T. R. (1995) "Carbon Brush Heat Exchanger," Energy Sciences Laboratories, Incorporated, San Diego, California. Presentation to the Crew and Thermal and Systems Division, National Aeronautics and Space Administration, Lyndon B. Johnson Space Center, Houston, Texas, May 1995.

Ku, J. (1996) National Aeronautics and Space Administration, Goddard Space Flight Center, Greenbelt, Maryland. Private communication.

LTV (1990) "Space Station Freedom Heat Rejection Subsystem Preliminary Design Review," DRD Item No. MR-04 (DRLI Item No. 021-02), Missiles Division, LTV Missiles and Electronics Group, Dallas, Texas. Presented to Lockheed Missiles and Space Company on April 3-4, 1990.

Lucas, G. W. (1996) Lockheed Martin Engineering and Science Services, Houston, Texas. Private conversation.

Mistrot, J. W. (1994) Shuttle Operational Data Book, Volume I, Shuttle Systems Performance and Constraints Data, NSTS-08934, Revision E, Amendment 275, Flight Data Office, Flight Data and Evaluation Office, Orbiter and GFE Projects Office, National Aeronautics and Space Administration, Lyndon B. Johnson Space Center, Houston, Texas, August 4, 1994.

NASA (1991) 1991 Integrated Technology Plan for Civil Space Program, Office of Aeronautics and Space Technology, National Aeronautics and Space Administration, Washington, D. C..

NASA (1994) "International Station Assembly Flights Equipment List/Weight," National Aeronautics and Space Administration, Lyndon B. Johnson Space Center, Houston, Texas, September 28, 1994.

Nguyen, T. M. (1992) "Summary Report for Heat Pipe Radiator Concept for the Space Station Freedom," OAO Corporation, Greenbelt, Maryland, November 10, 1992.

Oren, J. (1995) Loral Vought Systems, Dallas, Texas. Private communication.

Paul, T. (1995) Lockheed Martin Engineering and Science Services, Houston, Texas. Private conversation.

Peck, S. (1990) "Radiator Panel Coating Comparisons," LDEF Test Results, LTV Corporation. Presented to National Aeronautics and Space Administration, Lyndon B. Johnson Space Center, Houston, Texas, August 3, 1990.

Pekrul, P. J., *et al.* (1989) "Thermal Control System Single-Phase / Two-Phase Trade Study Interim Status Report (CEI: Photovoltaic System)," Revision B, TSR-00051, National Aeronautics and Space Administration, Lewis Research Center, Cleveland, Ohio.

Pollack, J. B., Colburn, D. S., Flasar, F. M., Kahn, R., Carlston, C. E., and Pidek, D. (1979) "Properties and Effects of Dust Particles Suspended in the Martian Atmosphere," Journal of Geophysical Research, Volume 84, Number B6.

Reich, G., and Scoon, G. E. N. (1993) "Thermal Environment and Thermal Control Aspects for Mars Landers," SAE Paper 932111, 23rd Intersociety Conference on Environmental Systems, Colorado Springs, Colorado, 1993, Society of Automotive Engineers, Warrendale, Pennsylvania.

Rotter, H. A. (1987) "Active Thermal Control Subsystem (ATCS)," Crew and Thermal Systems Division, National Aeronautics and Space Administration, Lyndon B. Johnson Space Center, Houston, Texas. A lecture presented on December 9, 1987.

Rotter, H. A. (1996) National Aeronautics and Space Administration, Lyndon B. Johnson Space Center, Houston, Texas. Private communication via E. K. Ungar on January 9, 1996.

Simon, A. L. (1994) Space Shuttle Systems Handbook, Volume 1, Section 7, Revision E, DCN-4, Mission Operations Directorate, Systems Division, National Aeronautics and Space Administration, Lyndon B. Johnson Space Center, Houston, Texas, October 28, 1994.

STS-41 (1990) Flight Data from Discovery during Mission STS-41, October 6-10, 1990, National Aeronautics and Space Administration, Lyndon B. Johnson Space Center, Houston, Texas.

Swanson, T. D., Sridhar, K. R., and Gottmann, M. (1993) "Moderate Temperature Control Technology for a Lunar Base," SAE Paper 932114, Society of Automotive Engineers, Warrendale, Pennsylvania.

Swerdling, B. (1993) "OAO HP Radiator Efficiency Calculation Error," ATSM-93-057, Electronics Programs, Grumman Aerospace and Electronics. From an interoffice memorandum to J. Alario, April 23, 1993.

Thermacore (1995 a) "Ultra-Lightweight Heat Pipe Radiator for Lunar Based Heat Rejection," Summary Progress Report No. 22, Thermacore, Inc., Lancaster, Pennsylvania, March 1995.

Thermacore (1995 b) "Titanium-Lined Lunar Radiator Heat Pipes," SBIR Phase I Final Report, Contract NAS9-19280, Thermacore, Inc., Lancaster, Pennsylvania. Submitted to National Aeronautics and Space Administration, Lyndon B. Johnson Space Center, Houston, Texas, on August 10, 1995.

Thermacore (1996) "Component and overall weight of lunar radiator heat pipe," Thermacore, Inc., Lancaster, Pennsylvania. This is a facsimile message to Mike Ewert on September 4, 1996.

Ungar, E. K. (1995) "Single Phase vs. Two-Phase Active Thermal Control Systems for Space Applications: A Trade Study," AIAA Paper 95-0634.

Ungar, E. K. (1996) National Aeronautics and Space Administration, Lyndon B. Johnson Space Center, Houston, Texas. Private communication.

Woodcock, G. R. (1993) "Space Transfer Concepts and Analyses for Exploration Missions; Phase 3, Final Report, June 1993," D615-10062-2, Boeing Defense and Space Group, Civil Space Product Development, Huntsville, Alabama.

Wuestling, M. (1994) "Preliminary Accumulator Concept Selection and Design Optimization," MDA-ATCS, McDonnell Douglas. From a presentation to the National Aeronautics and Space Administration, Lyndon B. Johnson Space Center, Houston, Texas, in January 1994.

Yerushalmi, S. (1992) "Preliminary Comparison of Heat Pump Cycles," CTSD-01268 (LESC-30011), Lockheed Engineering and Sciences Company, Houston, Texas.

REPORT DOCUMENTATION PAGE

Public reporting burden for this collection of information is estimated to average 1 hour per response, including the time for reviewing instructions, searching existing data sources, gathering and maintaining the data needed, and completing and reviewing the collection of information. Send comments regarding this burden estimate or any other aspect of this collection of information, including suggestions for reducing this burden, to Washington Headquarters Services, Directorate for information Operations and Reports, 1215 Jefferson Davis Highway, Suite 1204, Arlington, VA 22202-4302, and to the Office of Management and Budget, Paperwork Reduction Project (0704-0188), Washington , DC 20503.

1. AGENCY USE ONLY (Leave Blank)	2. REPORT DATE October 1996	3. REPORT TYPE AND DATES COVERED NASA Technical Memorandum

4. TITLE AND SUBTITLE

Advanced Active Thermal Control Systems Architecture Study

5. FUNDING NUMBERS

6. AUTHOR(S)

Michael K. Ewert; Anthony J. Hanford*

7. PERFORMING ORGANIZATION NAME(S) AND ADDRESS(ES)

Lyndon B. Johnson Space Center
Crew and Thermal Systems Division
Houston, Texas 77058

8. PERFORMING ORGANIZATION REPORT NUMBERS

TM-104822

9. SPONSORING/MONITORING AGENCY NAME(S) AND ADDRESS(ES)

National Aeronautics and Space Administration
Washington, D. C. 20546-0001

10. SPONSORING/MONITORING AGENCY REPORT NUMBER

S-817

11. SUPPLEMENTARY NOTES

*Lockheed Martin Engineering and Science Services, Houston, Texas

12a. DISTRIBUTION/AVAILABILITY STATEMENT
Unclassified/Unlimited
Available from the NASA Center for AeroSpace Information (CASI)
800 Elkridge Landing Road
Linthicum Heights, MD 21090-2934
(301) 621-0390   Subject Category: 34

12b. DISTRIBUTION CODE

13. ABSTRACT *(Maximum 200 words)*

The Johnson Space Center (JSC) initiated a dynamic study to determine possible improvements available through advanced technologies (not used on previous or current human vehicles), identify promising development initiatives for advanced active thermal control systems (ATCSs), and help prioritize funding and personnel distribution among many research projects by providing a common basis to compare several diverse technologies. Some technologies included were two-phase thermal control systems, light-weight radiators, phase-change thermal storage, rotary fluid coupler, and heat pumps. JSC designed the study to estimate potential benefits from these various proposed and under-development thermal control technologies for five possible human missions early in the next century. The study compared all the technologies to a baseline mission using mass as a basis. Each baseline mission assumed an internal thermal control system; an external thermal control system; and aluminum, flow-through radiators.

Solar vapor compression heat pumps and light-weight radiators showed the greatest promise as general advanced thermal technologies which can be applied across a range of missions. This initial study identified several other promising ATCS technologies which offer mass savings and other savings compared to traditional thermal control systems. Because the study format compares various architectures with a commonly defined baseline, it is versatile and expandable, and is expected to be updated as needed.

14. SUBJECT TERMS
two-phase systems, heat pumps, heat pipes, heat radiators, radiators, heat exchangers, missions, lunar bases, space transportation system, thermal analysis

15. NUMBER OF PAGES
216

16. PRICE CODE

17. SECURITY CLASSIFICATION OF REPORT	18. SECURITY CLASSIFICATION OF THIS PAGE	19. SECURITY CLASSIFICATION OF ABSTRACT	20. LIMITATION OF ABSTRACT
Unclassified	Unclassified	Unclassified	Unlimited